



HAL
open science

Impact de la matière organique sur le comportement des terres rares en solution: étude expérimentale et modélisation

Olivier Pourret

► To cite this version:

Olivier Pourret. Impact de la matière organique sur le comportement des terres rares en solution: étude expérimentale et modélisation. Géochimie. Université Rennes 1, 2006. Français. NNT: . tel-00135155

HAL Id: tel-00135155

<https://theses.hal.science/tel-00135155>

Submitted on 6 Mar 2007

HAL is a multi-disciplinary open access archive for the deposit and dissemination of scientific research documents, whether they are published or not. The documents may come from teaching and research institutions in France or abroad, or from public or private research centers.

L'archive ouverte pluridisciplinaire **HAL**, est destinée au dépôt et à la diffusion de documents scientifiques de niveau recherche, publiés ou non, émanant des établissements d'enseignement et de recherche français ou étrangers, des laboratoires publics ou privés.

N° ordre : 3401

THESE
présentée
DEVANT L'UNIVERSITE DE RENNES 1
pour obtenir
le grade de **DOCTEUR DE L'UNIVERSITE DE RENNES 1**
Mention Sciences de la Terre
PAR
Olivier POURRET
Equipe d'accueil: Géosciences Rennes
Ecole Doctorale Sciences de la Matière
Composante universitaire: UFR Structure et Propriétés de la Matière

Impact de la matière organique sur le comportement des terres
rares en solution: étude expérimentale et modélisation

Soutenue le 6 octobre 2006 devant la commission d'examen composée de

Rapporteurs	Marc Benedetti	IPGP Université Paris VII
	Bernard Dupré	LMTG Toulouse
Examineurs	Michael Bau	International University Bremen (Allemagne)
	Françoise Elbaz-Poulichet	Université Montpellier II
Directeurs de thèse	Gérard Gruau	Université Rennes 1
	Mélanie Davranche	Université Rennes 1
Membre invité	Aline Dia	Université Rennes 1

"These elements perplex us in our researches, baffle us in our speculations, and haunt us in our very dreams. They stretch like an unknown sea before us - mocking, mystifying and murmuring strange revelations and possibilities."

Williams Crookes (1887) talking about Rare Earths (in Elderfield, 1988).

Avant-Propos

Ce mémoire de thèse est le résultat d'un travail réalisé au sein du groupe de Biogéochimie de l'équipe Transfert de Géosciences Rennes (UMR CNRS 6118). Cette thèse a été encadrée par Gérard Gruau et Mélanie Davranche, en collaboration avec Aline Dia. Le travail expérimental et analytique a été réalisé au sein de l'atelier de Géochimie Analytique de Géosciences Rennes avec le soutien technique de Martine Bouhnik-Le Coz, Patrice Petitjean et Odile Hénin.

Cette thèse s'inscrit dans le cadre du projet intitulé "Développement de la recherche sur la maîtrise de la qualité de l'eau en Bretagne" financé par le Contrat de Plan Etat-Région 2000-2006.

Remerciements

Je tiens à vous remercier en tout premier lieu Gérard et Mélanie d'avoir dirigé cette thèse dans la continuité de mon stage de DEA. Tout au long de ces années, vous avez su éveiller ma curiosité et orienter mes recherches aux bons moments en me faisant découvrir l'expérimentation et la modélisation au travers de vos regards de géochimiste et chimiste, et la dualité qui peut exister entre ces deux domaines, tout en tirant partie de ma formation de géologue curieux et observateur. Je tiens aussi à te remercier Aline pour tes conseils et ton avis notamment sur mes "questions du vendredi" comme tu les as surnommées! Vous avez été, tous les trois, toujours disponibles (parfois à tour de rôle) pour des discussions passionnées, parfois animées, mais toujours profitables. Pour tout cela, votre confiance, votre soutien et vos conseils, je vous remercie vivement. C'est grâce à vous, à vos compétences et approches différentes que j'ai pu avancer dans ma réflexion!

Merci Martine, Patrice et Odile de m'avoir initié aux techniques analytiques et de m'avoir permis de travailler dans de bonnes conditions au labo! Merci aussi d'avoir répondu à mes nombreuses questions techniques!

Je remercie les rapporteurs (Bernard Dupré et Marc Benedetti) et examinateurs (Françoise Elbaz-Poulichet et Michael Bau) de cette thèse d'avoir accepté de juger mon travail et pour l'intérêt que vous y avez porté.

Merci aux (choisissez ce qui vous correspond) bio-geo/geol-phys-chim/iciens-istes-ogues que j'ai rencontré ou côtoyé, en particulier (c'est pas un ordre chronologique mais presque!):

- Philippe pour son coup pouce! Non le Rock'n Roll n'est pas mort!
- Eric, Sam, on en a fait des kilomètres pour aller fouiner dans des carrières! J'en ai des cartons de cailloux de stockés chez moi!
- les vétérans du DEUG Guitch, Charles & Yder, avec qui j'ai fait un bon bout de chemin et c'est pas fini! toujours plus à l'Ouest!
- les anciens de licences, maîtrise, DEA (Julie, David, Fabieng, Carlos, Youl, Odile, Nathalie, Cécile, Francous, Caroline ...), eh oui je sais je suis pas toujours très expressif! C'est toujours sympa de se croiser, qui à un congrès, qui à une formation CIES, qui à une soutenance de thèse!
- les colloqs de bureau ou de labo, de passage ou de longue durée (Gosia, Fanny, Bruno, Maxime, Raul, Selva, Géraldine, Léa, Dominique, Emilie², Mohamad, Lucile, Jessy, Emmanuel, Mathieu et ceux que j'oublie), c'est bon j'ai fini d'hiver(rédiger)ner!
- les djeuns du labo qui m'ont précédé ou à qui il reste encore du boulot (Flo, Ben, Nico, Nico, Chrystelle, Erwan, Fabien, Nolwenn, Laure, Olivier, Tanguy, Nuno, Sebi "Bulle d'eau", Eric, Jérôme, Vincent, Céline, Cécile, Loic, Cédric, Raymi, Oskar, Karen là encore je dois en oublier...) avec qui j'ai partagé des pauses cafés, le RU de midi moins le quart, et de nombreuses happy hours! Il s'est passé plein de choses au labo ces dernières années, des poissons d'avril à la journée de la moustache en passant par les geolympiques et son 110 mètres haies virtuelles mémorable, on aura eu quelques occaz de se détendre! On a même réussi à sortir du labo, eh oui, le terrain me manquait! on a pris le grand air avec initiation à l'escalade! Vive la descente en rappel! ski "Dans mon Jura, il y a des sapins..." et randonnées dans les Pyrénées! Merci aux participants et organisateurs pour ces bons moments dans la bonne humeur!

Et " puisqu'on est jeune et con" ...maintenant vous savez comment me représenté à Dessiné c'est gagné! Et là chui vraiment pas fier!

"There was nothing to fear and nothing to doubt"!

Merci pour tous ces bons moments et bon courage pour la suite surtout aux ptits nouveaux qui prennent la suite! Au milieu de tous je n'oublie ni Géocontact et ses causeries, apéros, week ends, ni les pots du LIGHT pour bien terminer la semaine! et comme dirait Sean: "tiens vlà les Daltons!"

Je tiens aussi à remercier les amis non-géologues qui m'ont permis de penser à d'autres choses! mais pas tout le temps! Vous aussi vous êtes curieux!

- les joueurs de 7 à 77 ans de la MdQ La Touche et en particulier la Team Chouchen José, Stef & Moorf (il faut qu'on se le fasse tous ensemble au moins une fois le CE!), les "BOC"s de Dinan, les valentinois, les nordistes et les parisiens! On se refait un stand "galettes saucisses"! J'ai pas trop eu le temps ces derniers temps, comme vous je crois aussi! à quand une de ces nuits de jeu endiablées comme au bon vieux temps? May the force be with you!

- les basketteurs en herbe de la West Coast Team: Antoine, Lolo, Ludo, Katy, Jujute & Charles! C'est quand qu'on se le fait tous ensemble ce ptit match NBA? Votre "docteur cayoux" connaît le chemin, j'aurai pas besoin de GPS!

And last but not least, j'adresse un grand merci à mes parents et à toute ma famille qui ont toujours été présents lorsque j'en ai eu besoin. Et non, je n'ai pas écrit trop de fois le mot terres rares dans ma thèse! Et là c'est sûr je suis plus étudiant!

Merci...

Sommaire

Résumé	1
Mots clés	1
Abstract	2
Keywords	2
Introduction	3
Première Partie. Impact de la complexation humique sur l'adsorption-oxydation des terres rares à la surface d'oxydes de fer et de manganèse	11
I.1. Impact of humate complexation on the adsorption of REE onto Fe oxyhydroxide	13
Résumé	15
Abstract	15
1.1. Introduction	15
1.2. Materials and methods	16
1.2.1. HFO: hydrous ferric oxide	16
1.2.2. REE(III)-humate complexes	17
1.2.3. Adsorption procedure	17
1.3. Results and discussion	18
1.3.1. Description of $\log K_d^{\text{REE}}$ and $\log K_d^{\text{DOC}}$ patterns	18
1.3.2. Description of mechanisms	19
1.3.3. Consequences on using the Ce anomaly as a paleo-redox proxy	22
1.4. Summary	23
Appendix	24
I.2. Adsorption of REE(III)-humate complexes onto MnO₂: Experimental evidence for cerium anomaly and lanthanide tetrad effect suppression	29
Résumé	31
Abstract	31
2.1. Introduction	32
2.2. Experimental procedure	33
2.2.1. Manganese Oxide	33
2.2.2. REE(III)-Humate Complexes	34
2.2.3. Adsorption Procedure	37
2.2.4. REE Measurements	38
2.3. Results	40
2.3.1. Inorganic Experiments at pH 5	40
2.3.2. Organic Experiments at pH 5	40
2.3.3. Organic Experiments at pH 7.5	44
2.4. Discussion	44
2.4.1. Mechanism of Reduction/Suppression of Ce Anomaly and Tetrad Effect	44
2.4.2. Comparison with Natural Waters and Inferences on the Use of Ce Anomaly as a Redox Proxy in Paleosols	48
2.5. Summary	50
Deuxième Partie. Modélisation	51
II.1. Organic complexation of rare earth elements in natural waters: evaluating model calculations from ultrafiltration data	53
Résumé	55
Abstract	55

1.1. Introduction	56
1.2. Material and methods	57
1.2.1. Model description	57
1.2.1.1. Humic Ion Binding Model VI (Model VI)	57
1.2.1.2. Stockholm Humic Model (SHM)	58
1.2.1.3. Model differences	59
1.2.2. Estimation of models constant values for the REE	59
1.2.3. Ultrafiltration set up and chemical analyses	65
1.3. Comparing the predicting ability of SHM and Models V and VI	66
1.3.1. World Average River Water	66
1.3.2. Mengong and Mar 2 samples	67
1.3.3. Kervidy-Naizin and Petit Hermitage groundwater samples	70
1.3.3.1. Ultrafiltration data	70
1.3.3.2. REE speciation modelling	76
1.4. Discussion	76
1.4.1. Effect of HM proton dissociation	78
1.4.2. Effect of major competing cations (Fe, Al and Ca)	79
1.4.3. Effect of major competing anions	79
1.4.4. Validity fields	80
1.5. Conclusion	80
II.2. Rare Earth Elements complexation with humic acid.	83
Résumé	85
Abstract	85
2.1. Introduction	86
2.2. Materials and Method	87
2.2.1. Experimental Binding of Rare Earth Elements by Humic Acid	87
2.2.1.1. Humic acid	87
2.2.1.2. Experimental set-up description	87
2.2.2. Humic Ion Binding Model VI	88
2.3. Results	89
2.3.1. Experimental results	89
2.3.2. Calculating log K_{MA} values	90
2.4. Discussion	91
2.4.1. Comparison with published results	91
2.4.2. REE speciation in natural river and soil waters	97
2.5. Conclusions	101
Troisième Partie. Complexation compétitive entre acides humiques et carbonate vis-à-vis des terres rares	103
III.1. Competition between humic acid and carbonates for rare earth elements complexation	105
Résumé	107
Abstract	107
1.1. Introduction	107
1.2. Materials and Methods	108
1.2.1. Experimental Binding of Rare Earth Elements by Humic Acid and Carbonates	108
1.2.1.1. Humic acid	108
1.2.1.2. Experimental set-up	109
1.2.2. WHAM 6 and Humic Ion Binding Model VI	110
1.3. Experimental Results	110

1.4. Discussion	113
1.4.1. Lack of evidence of ternary complexe formation	113
1.4.2. Competition between humic acid and carbonates for REE complexation	113
1.5. Conclusions	115
III.2. A new insight of cerium anomaly	117
Résumé	119
Abstract	119
2.1. Introduction	119
2.2. Experimental Binding of Rare Earth Elements by Humic Acid and Carbonates	120
2.2.1. Humic acid	121
2.2.2. Experimental set-up description	121
2.3. Experimental results	122
2.4. Discussion	125
2.4.1. Cerium Anomaly	125
2.4.2. Inferences on the understanding of Ce anomaly in natural waters	126
2.4.3. Implications on the understanding of cerium anomaly in natural water	128
2.5. Conclusions	128
Conclusions et Perspectives	129
1. Conclusions	131
2. Implications	135
3. Perspectives	139
Annexes	143
Bibliographie	163

Résumé

Les objectifs de cette thèse ont été principalement de comprendre l'impact de la matière organique sur le comportement des terres rares en solution et notamment: (i) de comprendre pourquoi le développement d'anomalie de cérium négative dans des eaux organiques oxydantes ne se produit pas; (ii) de tester la capacité des modèles à prédire la spéciation des terres rares dans des eaux organiques; (iii) d'évaluer les réactions compétitives de complexation des terres rares avec les acides humiques et les carbonates.

La première partie a été consacrée à deux études expérimentales de l'impact de la complexation organique sur le comportement redox du cérium et l'adsorption des terres rares à la surface d'oxydes de fer et de manganèse. La complexation des terres rares par la matière organique inhibe à la fois, l'oxydation du Ce(III) en Ce(IV) et le développement d'un effet tetrad visible sur les spectres de terres rares des eaux. Cette inhibition est due au développement d'un écran organique entre les terres rares et les surfaces oxydantes/adsorbantes que représentent les oxydes de fer et de manganèse.

La deuxième partie présente une évaluation de deux modèles, Model VI et SHM, quant à leur faculté à prédire la spéciation organique dans les eaux naturelles. La comparaison entre les résultats calculés et les expériences d'ultrafiltration a permis de valider Model VI dans sa capacité à prédire la spéciation des terres rares dans les eaux organiques. Par contre, la divergence entre les résultats obtenus avec SHM et les résultats expérimentaux indique que SHM, dans l'état actuel du programme, n'est pas apte à décrire précisément la spéciation des terres rares dans une eau naturelle. Dans un deuxième temps, cette étude a permis de fournir un jeu de constantes terres rares - acides humiques spécifiques à Model VI, fiables et cohérentes.

La troisième partie de ce travail a été consacrée aux réactions de compétitions entre ligands, acides humiques et carbonates, pour la complexation des terres rares. En fonction du pH et du rapport entre acide humique et carbonate, les terres rares vont se répartir entre ces deux ligands. La compétition entre les deux ligands induit également la formation d'une anomalie positive de cérium sur les acides humiques et négative dans la solution. Un nouveau mécanisme capable de développer sans surface oxydante ou bactérie, une anomalie négative de Ce dans les eaux naturelles a ainsi été mis en évidence.

La matière organique est responsable d'une forte complexation des terres rares dans les eaux naturelles. Une plus grande attention doit donc être portée à cette forme complexée pour étudier le transport des terres rares dans les eaux. Cette étude remet également en cause l'utilisation de l'anomalie de Ce comme témoin des conditions redox dans des eaux riches en matières organiques.

Mots clés: géochimie, terres rares, acide humique, oxyde de fer et de manganèse, modélisation, Model VI, SHM, spéciation, eaux naturelles, ultrafiltration, oxydation - adsorption, complexation, carbonate, anomalie de cérium.

Abstract

The objectives of this thesis were mainly to understand the impact of organic matter on the rare earth elements behavior in solution and in particular: (i) to understand why the development of negative cerium anomaly in oxidizing organic water does not occur; (ii) to test models capacity to predict rare earth elements speciation in organic-rich water; (iii) to evaluate competitive reactions between humic acids and carbonate towards rare earth elements complexation.

The first part was devoted to two experimental studies on the impact of organic complexation on the redox behavior of cerium and adsorption of rare earth elements on manganese and iron oxide surface. Rare earth elements complexation by organic matter inhibits at the same time, the oxidation of Ce(III) in Ce(IV) and the development of a tetrad effect displayed by rare earth elements pattern. This inhibition is due to the development of an organic screen between rare earth elements and oxidizing/adsorbant surfaces which represent manganese and iron oxides. The second part presents an evaluation of two models, Model VI and SHM, in their capacity of rare earth elements with natural organic matter in natural water. The comparison between calculated results and ultrafiltration experiments made it possible to validate Model VI in its capacity to predict the speciation of rare earth elements in organic water. On the other hand, the divergence between the results obtained with SHM and experimental results indicates that SHM, in the current state of the program, is not ready to precisely describe the speciation of rare earth elements in natural water. In a second time, this study made it possible to provide a reliable and coherent set of Model VI specific rare earth elements - humic acids complexation constants. The third part of this work was devoted to competitive reactions between humic acids and carbonates, toward rare earth elements complexation. According to the pH and relationship between humic acid and carbonate, rare earth elements will be distributed between these two ligands. The competition between both ligands also induces formation of a positive cerium anomaly onto humic acids and negative in the solution. A new mechanism able to develop a negative Ce anomaly in natural water, without oxidizing surface or bacterium, was thus highlighted.

Organic matter is responsible for strong complexation of rare earth elements in natural water. A greater attention must thus be paid to this complexed form to study the transport of rare earth elements in water. This study also calls into question the use of the Ce anomaly as redox proxy of the conditions in organic-rich waters.

Keywords: geochemistry, rare earth elements, humic acid, Fe and Mn oxide, modelling, Model VI, SHM, speciation, natural waters, ultrafiltration, Oxidation/scavenging, competitive binding, carbonate cerium anomaly.

Introduction

Les terres rares ou lanthanides, forment une famille de 15 éléments chimiques (du La au Lu) du groupe IIIA dans la classification périodique des éléments, du numéro atomique 57 au 71. Conventionnellement, les terres rares légères (de La à l'Eu) sont distinguées des terres rares lourdes (du Gd au Lu). Les terres rares peuvent aussi être subdivisées en trois groupes les terres rares légères (du La au Nd), les terres rares intermédiaires (du Sm au Tb) et les terres rares lourdes (du Dy au Lu). Les terres rares sont caractérisées par une structure électronique de type $[Xe]4f^n$ [$0(La) < n < 14(Lu)$] et forment des composés qui présentent des liaisons à caractère ionique dominant. Le remplissage de la couche électronique 4f depuis le La jusqu'au Lu, génère une augmentation de l'attraction du noyau sur les électrons, ce qui entraîne une diminution des rayons ioniques et atomiques le long de la série, classiquement nommée contraction des lanthanides. Cette diminution reste cependant faible, ce qui explique les propriétés chimiques très voisines des lanthanides. La chimie des terres rares est caractérisée par la prédominance du degré d'oxydation +III. Deux exceptions existent cependant: l'euporium qui peut passer à l'état d'oxydation +II dans des conditions réductrices typiques de fluides hydrothermaux ou métamorphiques (e.g., Sverjensky, 1984; Bau, 1991), et le cérium qui peut être oxydé en Ce(IV) dans des conditions de pression et de température supergènes (e.g., De Baar et al., 1988; Elderfield, 1988).

Les propriétés chimiques intrinsèques des terres rares ont permis d'utiliser leur abondance et leur fractionnement dans les roches comme traceurs des processus cosmochimiques, géodynamiques et pétrogénétiques (e.g., Henderson, 1984; Taylor et McLennan, 1985). Ces travaux ont permis de mieux contraindre les processus de différenciation et d'évolution chimique de la Terre. Ce n'est cependant que depuis une vingtaine d'années, grâce à la mise au point des techniques ICP-MS et à l'abaissement des limites de quantification, que les terres rares sont utilisées, et notamment leur fractionnement, dans les différents réservoirs de l'hydrosphère que sont les océans et les mers (Goldberg et al., 1963; Martin et al., 1976; Elderfield et Greaves, 1982; De Baar et al., 1983; Hoyle et al., 1984; De Baar et al., 1985; De Baar et al., 1988; Elderfield, 1988; Byrne et Kim, 1990; German et al., 1991; German et al., 1995; Bau et al., 1996; Byrne et Sholkovitz, 1996; Bau et al., 1997; Duncan et Shaw, 2004; Lawrence et Kamber, 2006), les fleuves et les rivières (Goldstein et Jacobsen, 1988; Elderfield et al., 1990; Sholkovitz, 1993; Sholkovitz, 1995; Bau et Dulski, 1996; Dupré et al., 1996; Gaillardet et al., 1997; Viers et al., 1997; Dupré et al., 1999; Elbaz-Poulichet et Dupuy, 1999; Tricca et al., 1999; Ingri et al., 2000; Deberdt et al., 2002; Shiller et al., 2002; Gerard et al., 2003; Gaillardet et al., 2004; Andersson et al., 2006), les lacs (Fee et al., 1992; Möller et Bau, 1993; Johannesson et Lyons, 1994; 1995; Johannesson et Zhou, 1999; De Carlo et Green, 2002; Gammons et al., 2003; Shacat et al., 2004) et les eaux souterraines (Smedley, 1991; Johannesson et al., 1995; 1996b; 1997; Viers et al., 1997; Braun et al., 1998; Johannesson et al., 1999; Dia et al., 2000; Johannesson et Hendry, 2000; Johannesson et al., 2000; Aubert et al., 2001; Janssen et Verweij, 2003; Duncan et Shaw, 2004; Gruau et al., 2004; Johannesson et al., 2004; Nelson et al., 2004). Dans ce cadre, les terres rares sont utilisées pour tracer les circulations d'eau et de matière et/ou contraindre les mécanismes de l'altération.

Les terres rares dans les eaux superficielles se distribuent entre deux composantes principales traditionnellement séparées par filtration à 0,2 μm . La composante supérieure à 0,2 μm correspond à la fraction particulaire, tandis que la composante inférieure regroupe les fractions colloïdales (organiques et minérales) et le "dissous vrai" (Sholkovitz, 1995; Viers et al., 1997; Braun et al., 1998). Les terres rares liées aux colloïdes¹ peuvent être distinguées des terres rares en solution grâce à des techniques d'ultrafiltration. Afin de corriger des variations d'abondances systématiques entre terres rares de numéros atomiques pairs et impairs, les teneurs

¹ Les colloïdes sont de petites particules, organiques ou inorganiques, de taille comprise entre 1 μm et 1 nm (Stumm et Morgan, 1996).

en terres rares des eaux sont normalisées par rapport à celles de réservoirs de références et représentées sous forme de spectres. Les terres rares des eaux proviennent de l'altération des enveloppes superficielles de la Terre, de ce fait les réservoirs de référence utilisés sont des réservoirs "rocheux" de surface. Deux types de réservoirs sont généralement utilisés: (i) la croûte continentale supérieure et (ii) les "Shales" (Haskin et al., 1968; Taylor et McLennan, 1985; McLennan, 1989). La puissance des spectres de terres rares en tant que marqueur de mélange d'eau ou des processus d'altération tient de la diversité des spectres de terres rares rencontrés dans les eaux.

Les terres rares libres en solution sont peu abondantes, du fait de leur faible hydrosolubilité. De nombreuses études s'accordent pour attribuer un rôle majeur à la chimie des solutions et des interfaces dans le contrôle des concentrations en terres rares des eaux de surface, comparé à celui joué par les teneurs dans les roches mères (Goldstein et Jacobsen, 1988; Elderfield et al., 1990; Sholkovitz, 1995). La forme des spectres de terres rares des eaux et la teneur en terres rares en solution résultent de la conjonction d'un ensemble de processus susceptibles d'induire leur fractionnement. Ces processus sont eux-mêmes sous le contrôle d'un certain nombre de facteurs environnementaux (pH, température, potentiel redox, force ionique...). Parmi ces processus, quatre processus majeurs peuvent ainsi être distingués (Fig. 1): (i) la complexation avec les anions inorganiques (e.g., carbonates, sulfates) et les anions organiques simples de bas poids moléculaire (e.g., acide acétique, acide lactique), (ii) la complexation avec les colloïdes organiques (e.g., substances humiques), (iii) les processus d'adsorption/désorption avec la surface des minéraux et les colloïdes inorganiques (e.g., oxyhydroxydes de Fe, Mn et Al, argiles) et (iv) les processus de précipitation (e.g., CeO_2). Ainsi le spectre d'une eau filtrée correspondant au spectre du matériau source modifié des constantes de complexation/adsorption des terres rares vis à vis des particules, des colloïdes et des divers ligands en solution. Il en résulte une diversité de formes de spectres de terres rares, s'exprimant soit par des degrés d'enrichissement ou d'appauvrissement relatifs en terres rares lourdes variables, soit par la présence ou l'absence d'anomalies négatives en cérium.

Elderfield et al. (1990) classent les eaux continentales en deux groupes en fonction de leurs spectres de terres rares (Fig. 2). Le premier correspond aux spectres qui montrent un enrichissement en terres rares légères et intermédiaires (Fig. 2a). Le deuxième groupe est caractérisé par des spectres montrant un enrichissement continu du La au Lu (Fig. 2b). Le premier type de spectre serait caractéristique des eaux à pH acide contenant de fortes concentrations en terres rares, tandis que le deuxième serait plutôt associé à des eaux présentant des pH alcalins et des teneurs en terres rares plus faibles. Ces auteurs expliquent le premier type de spectre par une complexation préférentielle des terres rares légères à intermédiaires par les colloïdes et le deuxième par une complexation préférentielle par des ligands inorganiques en solution des terres rares lourdes, associée à une adsorption préférentielle des terres rares légères sur la fraction particulaire. Goldstein et Jacobsen (1988) précisent que la présence de matière organique dans les eaux pourrait expliquer les spectres convexes observés, tandis que les spectres enrichis en terres rares lourdes seraient contrôlés par la formation de complexes carbonatés et hydroxylés. Sholkovitz (1995) propose un contrôle des concentrations en terres rares dans les eaux de rivières par les réactions avec les surfaces minérales. A la vue de ces interprétations, il semble important de comprendre la spéciation des terres rares en solution. En effet, leur liaison à des colloïdes peut avoir un rôle prépondérant dans la mesure où la spéciation des terres rares peut dépendre des changements de propriétés. Il peut donc en résulter des différences d'adsorption, des variations de la chimie redox du Ce, des différences de transport et/ou de mélange...

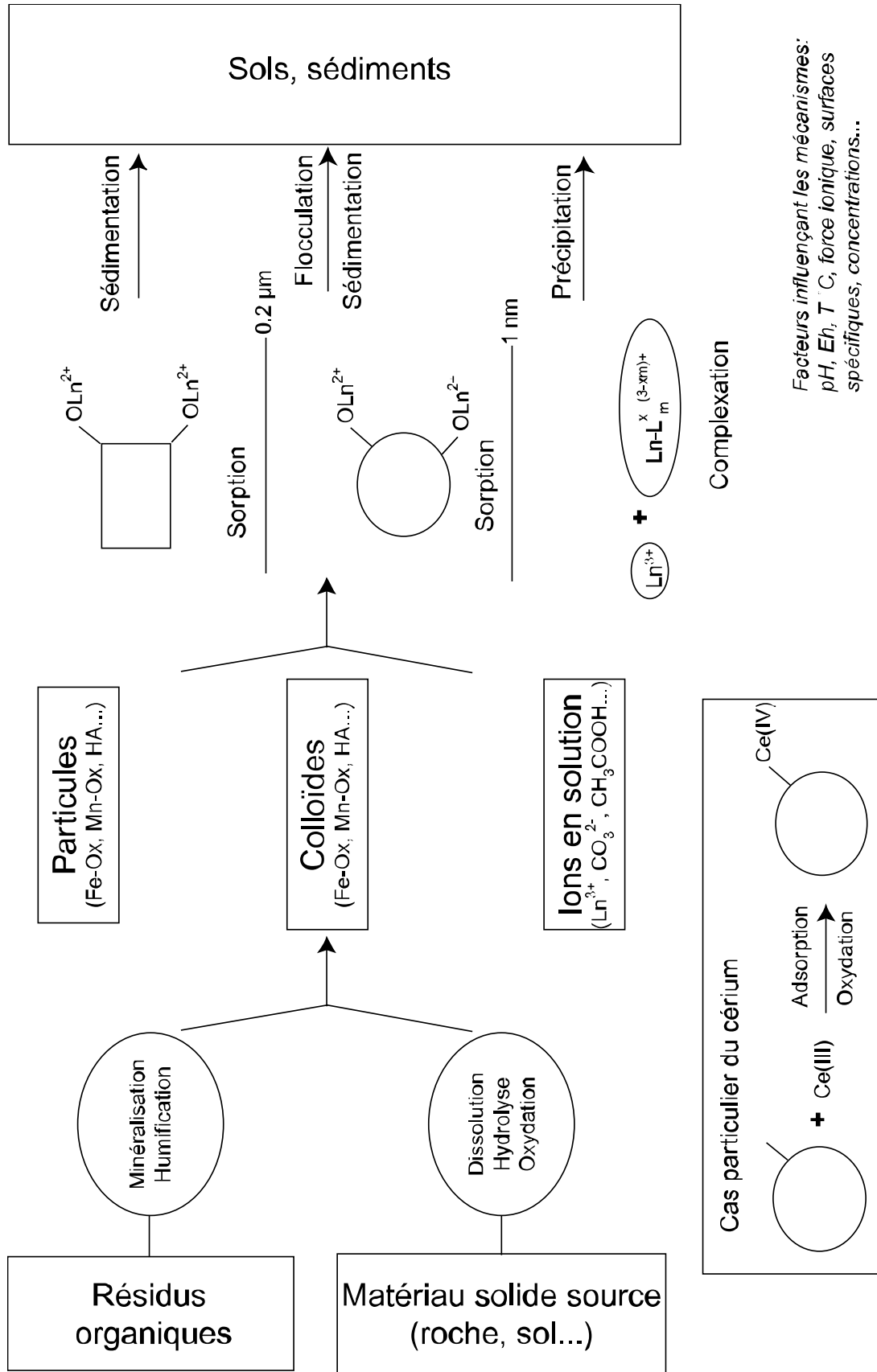


Fig. 1. Schéma des différents processus et facteurs contrôlant l'hydrochimie des terres rares.

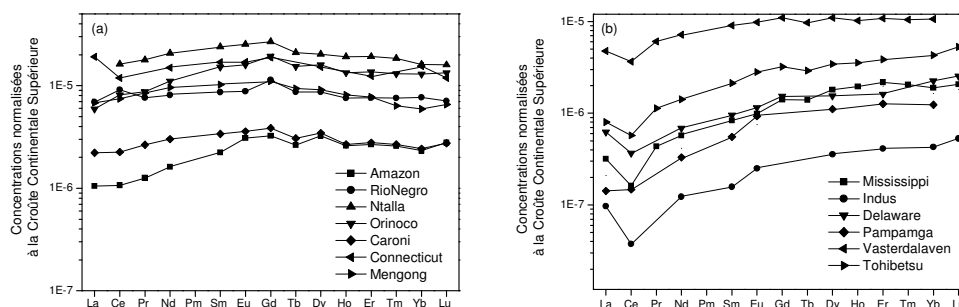


Fig. 2. Spectres de terres rares normalisés à la Croûte Continentale Supérieure d'eaux de rivières montrant (a) un enrichissement en terres rares légères à intermédiaires et (b) un enrichissement en terres rares lourdes (Goldstein et Jacobsen, 1988; Elderfield et al., 1990; Sholkovitz, 1995; Deberdt et al., 2002).

La compréhension et la modélisation de l'information portée par la très large variété de spectres de terres rares rencontrée dans l'hydrosphère nécessite de connaître parfaitement les propriétés thermodynamiques des complexes aqueux de terres rares avec les ligands organiques simples (e.g., acide acétique, acide lactique) et inorganiques (e.g., sulfates, carbonates). Actuellement, comme l'ont souligné Wood (1990; 1993) et Byrne et Li (1995), les conditions expérimentales dans lesquelles les constantes de complexation ont été déterminées manquent de cohérence. Par ailleurs, le rôle des complexes organiques comme vecteur de mobilité des terres rares n'a été mis en évidence que depuis une dizaine d'années (Dupré et al., 1996; Viers et al., 1997; Dia et al., 2000) dans des eaux continentales. Le manque de données expérimentales fiables concernant les complexes organiques de terres rares a suscité l'utilisation de codes de calculs théoriques ou empiriques (Wood, 1990; Lee et Byrne, 1992; Millero, 1992; Wood, 1993; Fairhurst et al., 1995; Tang et Johannesson, 2003). Néanmoins, l'acquisition de données expérimentales reste nécessaire afin de valider ces prédictions (Fairhurst et al., 1995; Lead et al., 1998; Tang et Johannesson, 2003).

Les travaux, à l'origine de cette thèse, ont permis de montrer que l'hydrogéochimie des terres rares (formes des spectres et niveaux de concentration) dans les eaux du sol était principalement contrôlée par la nature des ligands en solution et notamment par la concentration en matières organiques colloïdales. Ainsi, Viers et al. (1997) et Dia et al. (2000) ont montré la même distribution spatiale des terres rares entre les eaux inorganiques de versants drainés (spectres enrichis en terres rares légères; présence d'une anomalie négative marquée en Ce) et les eaux riches en matière organique de bas-fonds hydromorphes (spectres de terres rares plats; absence d'anomalie négative de Ce) dans deux contextes différents, (i) un bassin versant agricole sur schiste en zone tempérée et (ii) un bassin versant semi naturel sur granite en zone tropicale. Aucun effet lié à la différence de substrat, au régime hydroclimatique, ou aux apports anthropiques (terres rares associées aux engrais phosphatés) n'a été mis en évidence (Gruau et al., 2004). Le développement de l'anomalie de Ce semble également être étroitement lié à la spéciation en solution des terres rares. En effet, un suivi temporel des concentrations en terres rares dans l'eau d'un sol subissant des oscillations des conditions redox n'a pas montré d'anomalies de Ce (Dia et al., 2000; Gruau et al., 2004).

Dans ce cadre, les objectifs de cette thèse sont principalement de comprendre l'impact de la spéciation organique sur le comportement des terres rares en solution et notamment:

(i) de comprendre pourquoi le développement d'anomalie de cérium négative dans des eaux organiques oxydantes ne se produit pas: s'agit-il d'un effet complexant? le proxy Ce est-il remis en cause?

(ii) de tester, valider (par des travaux expérimentaux) et améliorer (détermination de constantes) les modèles de complexation des éléments traces par la matière organique quant à leur capacité à prédire le comportement des terres rares dans des eaux riches en matière organique;

(iii) d'évaluer les réactions compétitives de complexation des terres rares avec les acides humiques et les carbonates: ligands fortement répandus dans le milieu naturel potentiels compétiteurs de la matière organique (Byrne et Sholkovitz, 1996; Tang et Johannesson, 2003).

La démarche de ce travail s'est construite autour de trois axes complémentaires (Fig. 3):

(i) Analyse d'échantillons naturels (par ultrafiltration), (ii) Expérimentation (réacteurs fermés) et (iii) Modélisation (Model VI principalement).

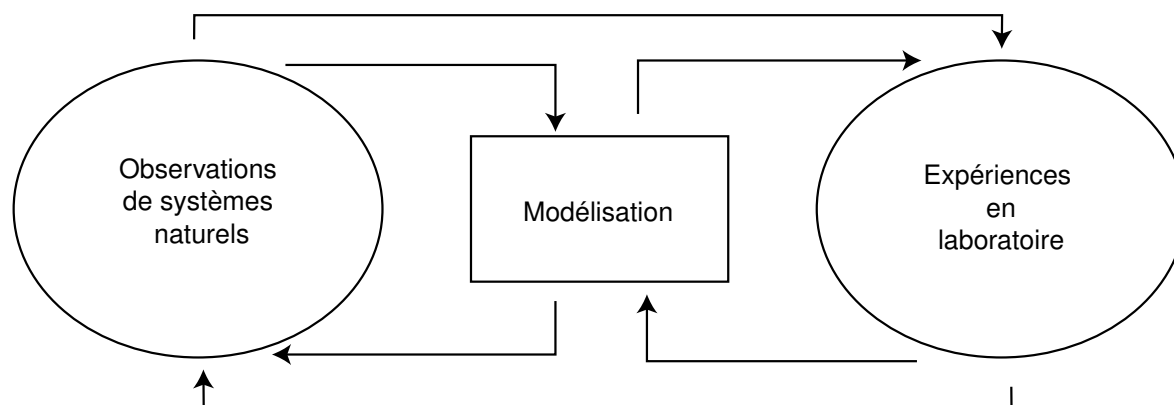


Fig. 3. Schéma de la démarche (modifié d'après Stumm et Morgan, 1996).

Ce manuscrit, qui se présente comme une succession d'articles rédigés en anglais publiés ou soumis dans des revues scientifiques internationales, est organisé de la manière suivante:

La **première partie** est consacrée à deux études expérimentales sur l'impact de la complexation organique des terres rares sur leur adsorption à la surface d'oxyde de fer amorphe et d'oxyde de manganèse et sur le comportement redox du cérium. Ces expériences ont pour objectif d'établir le mécanisme par lequel les matières organiques en solution empêchent l'expression de la chimie redox du Ce. La **deuxième partie** présente une évaluation de deux modèles de calculs de spéciations (Model VI et SHM) des terres rares avec la matière organique naturelle dans les eaux naturelles (Tipping, 1998; Gustafsson, 2001a). La capacité à prédire la spéciation des terres rares dans les eaux naturelles riches en matière organique des deux modèles est évaluée en considérant des constantes de complexation terres rares - matière organique estimées. Les constantes matière organique - terres rares spécifiques aux modèles sont obtenues à partir de relations linéaires entre les constantes de complexation ligands organiques simples - métaux, de la littérature, et les constantes de complexation ligands organiques simples - métaux spécifiques à chaque modèles. La validation des modèles est effectuée par confrontation des calculs de spéciation avec des expériences d'ultrafiltration effectuées sur des échantillons d'eaux riches en matières organiques. Dans un deuxième temps, cette étude est complétée par une modélisation inverse de données expérimentales de complexation des terres rares par des acides humiques afin de déterminer des constantes spécifiques à Model VI. Les données calculées avec ce nouveau jeu de constantes sont ensuite confrontées aux résultats obtenus avec les constantes extrapolées. La **troisième partie** de ce travail est consacrée aux réactions de compétitions entre ligands, acides humiques et carbonates, pour la complexation des terres rares.

Enfin, les **conclusions** et les **implications** des principaux résultats sont synthétisées et des **perspectives** sont proposées.

Première Partie
Impact de la complexation humique sur
l'adsorption-oxydation des terres rares à la surface
d'oxydes de fer et de manganèse

1. Impact of humate complexation on the adsorption of REE onto Fe oxyhydroxide.

Cette partie est extraite de Journal of Colloid and Interface Science, Davranche M., Pourret O., Gruau G., and Dia A. (2004) Impact of humate complexation on the adsorption of REE onto Fe oxyhydroxide. 277, 271-279.

Résumé- Des expériences d'adsorption de terres rares (REE) sur des oxydes de fer (HFO) ont été réalisées afin d'évaluer les effets de la complexation organique des terres rares sur le taux d'adsorption des REE(III) et l'oxydation du Cérium(III). Les expériences d'adsorption ont été réalisées à pH 5.2 dans des solutions de NaCl et NaNO₃ contenant soit des REE(III) libres soit des complexes REE(III)-humate. Les spectres des $\log K_d^{REE}$ obtenus à partir des suspensions de HFO montrent une légère anomalie de Ce positive lorsque les terres rares sont introduites sous forme libre. Au contraire le mélange complexe REE(III)-humate et HFO produit des spectres complètement plats. Les expériences organiques montrent un rapport $\log K_d^{REE} / \log K_d^{COD}$ (COD = carbone organique dissous) proche de 1.0, les REE(III) et les humates restent donc liés entre eux au cours des expériences d'adsorption. L'absence d'anomalie de Ce positive ou d'effet tétrad de type M dans les expériences organiques semble refléter une adsorption anionique du complexe REE-humate. L'adsorption s'effectue du côté humique du complexe REE(III)-humate. L'oxydation du Ce(III) par le Fe(III) et la proportion de groupements hydroxyliques de surfaces liés aux REE(III) à la surface des HFO sont les deux processus les plus communément invoqués pour expliquer le développement d'une anomalie de Ce positive et l'effet tétrad des lanthanides de type M. Cependant, de tels processus ne peuvent pas se mettre en place car les REE ne sont pas en contact direct avec la surface des HFO, étant eux-mêmes écrantés par les substances humiques. Les résultats de cette étude porte un doute sur l'utilisation de l'anomalie de Cérium comme témoin des conditions paleoredox dans les précipités naturels. Ils montrent également que la matière organique peut inhiber l'effet tétrad des lanthanides dans des échantillons géologiques.

Abstract- Adsorption experiments of rare-earth elements (REE) onto hydrous ferric oxide (HFO) were performed to evaluate the impact of organic complexation on both REE(III) adsorption and the Ce(III) oxidation rate. Scavenging experiments were performed at pH 5.2 with NaCl and NaNO₃ solutions containing either free REE (III) or REE(III)-humate complexes. The $\log K_d^{REE}$ patterns obtained from HFO suspensions exhibit a slight positive Ce anomaly and an M-type lanthanide tetrad effect, in contrast with the partitioning between REE(III)-humate complexes and HFO, which yields completely flat distribution patterns. The "organic" partitioning runs yield $\log K_d^{REE} / \log K_d^{DOC}$ ratios (DOC=dissolved organic carbon) close to 1.0, implying that the REE(III) and humate remain bound to each other during the adsorption experiment. The lack of any positive Ce anomaly or M-type lanthanide tetrad effect in the organic experiments seems to reflect an anionic adsorption of the REE-humate complex. Adsorption onto HFO takes place via the humate side of the REE(III)-humate complexes. The oxidation of Ce(III) by Fe(III) and the proportion of surface hydroxyl groups coordinated to REE(III) at the HFO surface are the two most commonly invoked processes for explaining the development of positive Ce anomalies and the M-type tetrad lanthanide effect. However, such processes cannot proceed since the REE are not in direct contact with the HFO suspensions, the latter being shielded by PHA. The present results further complicate the use of Ce anomalies as reliable paleoredox proxies in natural precipitates. They are also further demonstration that organic matter may inhibit the lanthanide tetrad effect in geological samples.

1.1. Introduction

Hydrous ferric oxides (HFO) are often thought to control the mobility of trace elements in aqueous systems (Davis and Kent, 1990). Due to their large specific surface area, these mineral phases are indeed very effective scavengers of trace elements, and hence they exert a key control on the concentration and migration of trace metals in aqueous systems (Dzombak and Morel, 1990). Interactions between trace elements and Fe oxyhydroxides depend upon various processes such as adsorption, surface precipitation, and, in the particular case of the REE (rare earth elements), oxidation/scavenging (Koeppenkastrop and De Carlo, 1992; Bau, 1999; Ohta and Kawabe, 2001).

Understanding the REE distribution between Fe oxyhydroxides and aqueous solutions continues to be a major issue in REE studies on geochemical processes (Elderfield et al., 1990). Marine ferromanganese crusts are fairly enriched in REE and some of them exhibit large positive Ce anomalies (Piper, 1974; Elderfield et al., 1981; De Carlo and McMurtry, 1992; Bau et al., 1996; Ohta et al., 1999). Deep-sea ferromanganese nodules, banded iron formations, and Fe and Mn concretions in paleosols are geological deposits of major geochemical importance, because they can record the REE signatures of ancient marine and fresh waters (Goldberg et al., 1963; Rankin and Childs, 1976; Elderfield et al., 1981; Shimizu et al., 1990; Alibert and McCulloch, 1993; Braun et al., 1998).

Several authors have examined the adsorption processes of REE onto Fe oxyhydroxides and Mn oxides (Koeppenkastrop et al., 1991; Koeppenkastrop and De Carlo, 1992; Bau, 1999; De Carlo et al., 1998; Ohta and Kawabe, 2001). Koeppenkastrop and De Carlo (1992) presented the available data on sorption of REE from seawater, noting the close similarity between their experimentally determined K_d^{REE} values and those estimated from REE analyses of marine Mn-Fe deposits and seawater samples. More recently, Bau (1999) and Ohta and Kawabe (2001) reported experimental investigations of the sorption of REE from low-salinity solutions. These authors showed that (i) Fe and Mn oxyhydroxides can both oxidize Ce(III) into Ce(IV), even though the resulting preferential enrichment of Ce as compared to its trivalent REE neighbors (the so-called positive Ce-anomaly) is much larger with Mn oxide than with Fe oxyhydroxide, and (ii) at $\text{pH} \geq 5$, the M-type lanthanide tetrad effect appears on patterns of apparent REE distribution coefficients between Fe and Mn oxyhydroxides and aqueous solutions.

However, very little is known about the influence of organic matter on the sorptive properties of REE on Fe oxyhydroxides. The speciation of the REE partitioning between Fe oxyhydroxide and solution governs the REE behavior in natural waters, as well as the oxidative scavenging of Ce(III). This behavior has possible major implications on the use of Ce anomalies as paleo-redox proxies (Wright et al., 1987; MacLeod and Irving, 1996; Gallet et al., 1996; Holser, 1997; Morad and Felitsyn, 2001). The aim of this article is (i) to compare apparent K_d^{REE} between hydrous ferric oxide (HFO) suspensions and synthetic solutions in which the REE(III) occurs alternatively as free REE(III) and REE(III)-humate complexes and (ii) to examine the effect of organic complexation on Ce(III) oxidation and tetrad lanthanide effects in the presence of HFO.

1.2. Materials and methods

All chemicals used in this study were of analytical grade, and the solutions were all prepared with doubly deionized water (Milli-Q system, Millipore). Polyethylene containers used in the adsorption experiments were soaked in 10 % Ultrapur HNO_3 for 48 h at 60 °C and then rinsed with Milli-Q water for 24 h at 60 °C to remove all possible REE contamination sources. Synthetic REE solutions were prepared from nitrate REE standards (10 ppm, Accu Trace Reference Standard). REE concentrations were determined by ICP-MS—HP 4500, Agilent Technologies at Rennes University (France) (see Appendix A).

1.2.1. HFO: hydrous ferric oxide

The HFO was synthesized according to Schwertmann and Cornell (1996). A quantity of 1.5 mol of NaOH (pellets) was added slowly to 1 L of a solution containing 0.5 M $\text{Fe}(\text{NO}_3)_3$. The solution was continuously bubbled with nitrogen to avoid carbonate precipitation. The HFO precipitate was centrifuged and washed several times with Milli-Q water, dried at 20 °C, sieved for homogenization, and, finally, stored in a dessicator. The crystallographic structure of the HFO was checked by X-ray diffraction (XRD). Analyses revealed a two-line ferrihydrite and traces of poorly crystallized goethite. The total number of surface sites of the solid phase was

estimated using the solid cation exchange capacity (CEC) determined from the cobalthexammine method, ISO 11260 (AFNOR, 1994). Ions bound to the solid surface were exchanged with cobalthexammine ions, the CEC being taken as equal to the concentration of cobalthexammine ions removed from solution. Five grams of HFO were mixed with 10 mL of 0.017 M cobalthexammine solution for 3 h. The suspension was then centrifuged and the concentration of cobalthexammine ion remaining in solution was measured at 470 nm with a Shimadzu 160 A UV spectrophotometer. The CEC of the HFO used in this study is 24.5 meq/100 g.

The surface acidity constants were determined from potentiometric titrations of suspensions of 5 g L⁻¹ HFO with NaOH (0.1 M) or HNO₃ (0.1 M), with a 0.1 M NaCl solution as the supporting electrolyte (Davranche et al., 2003). Titrations were carried out with a Metrohm 794 DMS Titrino apparatus equipped with a Metrohm combined (3 M KCl) glass electrode. The HFO acidity constants obtained were $pK_{a1} = 6.77$ and $pK_{a2} = 8.56$, while pH_{zpc} was 7.7.

1.2.2. REE(III)-humate complexes

Humate, referred to below as PHA (purified humic acid), was obtained from the synthetic Aldrich humic acid (Aldrich, H1, 675-2) according to the process described by Vermeer et al. (1998). The PHA obtained in this way is ash-free and in its protonated form, with the following elemental composition (in weight percent): C = 55.8 %, O = 38.9 %, H = 4.6 %, N = 0.6 %. Purified humic acid has a mean molecular weight of 23,000 Da (Vermeer et al., 1998). Prior to use, the freeze-dried PHA was resuspended overnight in a NaOH solution (pH 10) to ensure complete dissolution of the sample.

Rare earth element-humate complexes were prepared as follows. Twenty mg of dissolved PHA were enclosed in a 250 mL sodium acetate dialysis bag with a pore size of 12,000-14,000 Da. The bag was introduced into 1000 mL of a 5 ppb REE solution (corresponding to a molar concentration range of 36 to 29 nM depending on the REE considered), the ionic strength being buffered at 10⁻³ M with NaCl or NaNO₃, and the pH at 7 with HNO₃. Both NaCl and NaNO₃ were used as neutral electrolytes (see below). The suspension was stirred for 48 h (equilibrium time determined from preliminary kinetic experiments), to allow equilibration and partitioning of the REE between the aqueous solution and the PHA suspension. The dialysis bag was then removed and the REE-PHA complexes recovered. The concentrations of REE in solution both inside and outside the dialysis bag were monitored versus time to quantify the amount of REE complexed to PHA. Possible REE adsorption onto the dialysis bag was checked by analyzing the REE content of the membrane (dissolved by acidic digestion with HNO₃ 14 N). The results show that around 95 % (~ 4.75 ppb REE, with NaCl) or 60 % (~ 3 ppb REE, with NaNO₃) of the REE initially present in the solution were complexed to the PHA. The remaining 5 or 40 % were left in solution outside the membrane or adsorbed onto the dialysis bag. Moreover, complexation rates are found to increase slightly but regularly from the heavy to the light REE, which is consistent with the constant stability order determined by Takahashi et al. (1999) for REE(III)-humate complexes.

1.2.3. Adsorption procedure

Four time-series experiments were carried out - two with the REE occurring as REE(III)-humate complexes and two with the REE occurring as free aqueous species - to assess the effects of organic complexation during REE(III) adsorption onto HFO. All suspensions were made up from 100 mg L⁻¹ HFO left to equilibrate with a 0.001 M NaCl or NaNO₃ aqueous solution at pH 5.2. Experiments were carried out at room temperature. The pH was monitored periodically with a pH meter and adjusted to 5.2 by addition of HNO₃ (4.6 N) or NaOH (4 N). The pH value of 5.2 was chosen because it was sufficiently basic to promote adsorption processes, but low enough to avoid total REE sorption that might mask any eventual development of Ce anomaly. In the

inorganic experiment, a solution of 5 ppb REE was used, and in the organic experiment, concentrations were 20 mg L⁻¹ for PHA, ~ 4.75 ppb with NaCl, and ~ 3 ppb with NaNO₃ for REE, respectively.

The first set of experiments carried out with free REE(III) was essentially conducted to validate the experimental and analytical protocol used in this study. In the second and third series of experiments, the equilibration was made with the REE(III)–PHA complexes described above. We can describe the adsorption behavior of the REE using the apparent partition coefficient K_d , expressed as

$$K_d = \frac{\mu\text{g REE adsorbed/g HFO}}{\mu\text{g mL}^{-1} \text{ REE in solution}} \quad (1.1)$$

Suspension aliquots of about 10 ml were sampled at predetermined time intervals and filtered in-line through 0.2 μm cellulose acetate membranes (Sartorius). The REE concentrations were then measured to determine the K_d^{REE} variations. Sample aliquots used for REE determination in organic experiments were all immediately digested with sub-boiled nitric acid (HNO₃ 14 N) at 100 °C and then resolubilized in 0.4 N HNO₃ after complete evaporation in order to avoid interference with organic matter during mass analysis.

REE concentrations were determined by ICP-MS at Rennes University. Precision of individual REE concentrations and log K_d values is estimated at ± 2 % (see Appendix A).

The adsorption behavior of the REE(III)–humate complexes was also monitored by measuring the dissolved organic carbon (DOC) content. DOC measurements can be converted into apparent partition coefficients using the equation

$$K_d = \frac{\mu\text{g DOC adsorbed/g HFO}}{\mu\text{g mL}^{-1} \text{ DOC in solution}} \quad (1.2)$$

Dissolved organic carbon concentrations were determined at Rennes University using a Shimadzu 5000 TOC analyzer. The precision on DOC contents and log K_d^{DOC} are better than ± 1.5 %.

1.3. Results and discussion

1.3.1. Description of log K_d^{REE} and log K_d^{DOC} patterns

The time dependence of the sorption of free REE(III) and REE-PHA complexes onto HFO is presented in Fig. 1.1 and Fig. 1.2, respectively. Both the organic and inorganic experiments exhibit a faster adsorption in runs conducted with NaCl solutions as compared with those conducted with NaNO₃. However, the composition of the neutral electrolyte has no effect on the equilibrium log K_d^{REE} inorganic values. Adsorption kinetics were slowed down by a factor of 2 in organic experiments compared with runs where REE(III) occurred as free species. The values of equilibrium log are more closely grouped than the log K_d^{REE} inorganic equilibrium data. Ratios of log K_d^{REE} organic / log K_d^{DOC} are close to 1.0, indicating that the REE(III) and humate remain bound to each other during interaction of the REE(III)–humate complexes with the HFO surface. Log K_d^{REE} inorganic equilibrium data between HFO and solutions containing free REE(III) are comparable to earlier values reported by Ohta and Kawabe (2001) at similar pH conditions.

All inorganic patterns exhibit slight positive Ce anomalies and a clear M-type lanthanide tetrad effect (Fig. 1.3). The tetrad effect often corresponds to a very small discrete feature in the REE patterns of geological samples (McLennan, 1994). However, in the present study, the total uncertainty on the REE and log K_d^{REE} is estimated at 2 %. In NaNO₃ inorganic experiment, the difference between log K_d^{Eu} inorganic and log K_d^{Gd} inorganic is 0.2, which corresponds to 5.5 % of the

$\log K_d^{\text{Gd}}_{\text{inorganic}}$ value. This relative error of 5.5 % is far higher than the uncertainty determined for analytical measures, confirming that the observed tetrad effect reflects a true feature rather than an analytical artifact.

Positive Ce anomalies and a clear M-type lanthanide tetrad effect were already apparent in the $\log K_d^{\text{REE}}$ patterns obtained by Bau (1999) and Ohta and Kawabe (2001) under similar experimental conditions. $\text{Ce}_{\text{inorganic}}$ anomaly values (Ce/Ce^*) as calculated by $\log K_d^{\text{Ce}} - [(\log K_d^{\text{Pr}} + \log K_d^{\text{La}})/2]$ range from 0.11 to 0.15. However, organic patterns differ markedly from the former in showing no positive Ce anomaly ($\text{Ce}/\text{Ce}^* = 0.01$) and no M-type lanthanide tetrad effect (Fig. 1.4). The general lack of a conspicuous M-shaped lanthanide tetrad effect in the organic patterns is very interesting and probably highly significant for the mechanism(s) of adsorption of the REE(III)–PHA complexes onto HFO.

The complexation of REE(III) by humic acid has a large effect on K_d^{REE} equilibrium values. Time-series variations of $\log K_d^{\text{REE}}_{\text{organic}}$ indicate that equilibrium is modified, 60 h under organic conditions vs 40 h in inorganic experiments (Fig. 1.1 and Fig. 1.2).

1.3.2. Description of mechanisms

The complexes are bound to the HFO surface on their humate side:



This process accounts for the modification of $\log K_d^{\text{REE}}_{\text{organic}}$ values in the organic experiment as compared with the inorganic runs (Fig. 1.1 and Fig. 1.2 and Fig. 1.3 and Fig. 1.4).

Moreover, the tetrad effect expresses the differences in Racah parameters for 4f electron repulsion between the pair of REE complexes. Ohta and Kawabe (2001) suggested that Racah parameters in REE^{3+} ions decrease with increasing covalence of bonding of REE^{3+} with ligands. If the REE–PHA complex is adsorbed onto HFO as $\equiv\text{S-O-ML}$ (cationic adsorption), the Racah parameters are smaller and, consequently, a conspicuous M-type tetrad effect can be observed. Thus, the lack of tetrad effect in $K_d^{\text{REE}}_{\text{organic}}$ suggests that REE are bound solely to PHA, confirming the chemical mechanism of Eq. (3).

The distribution of REE in the presence of organic complex is determined by the distribution of humate at the HFO surface. Takahashi et al. (2002) obtained the same result in their study of the adsorption of Cm(III) fulvate onto an acid montmorillonite, even when using relatively low concentrations of organic matter.

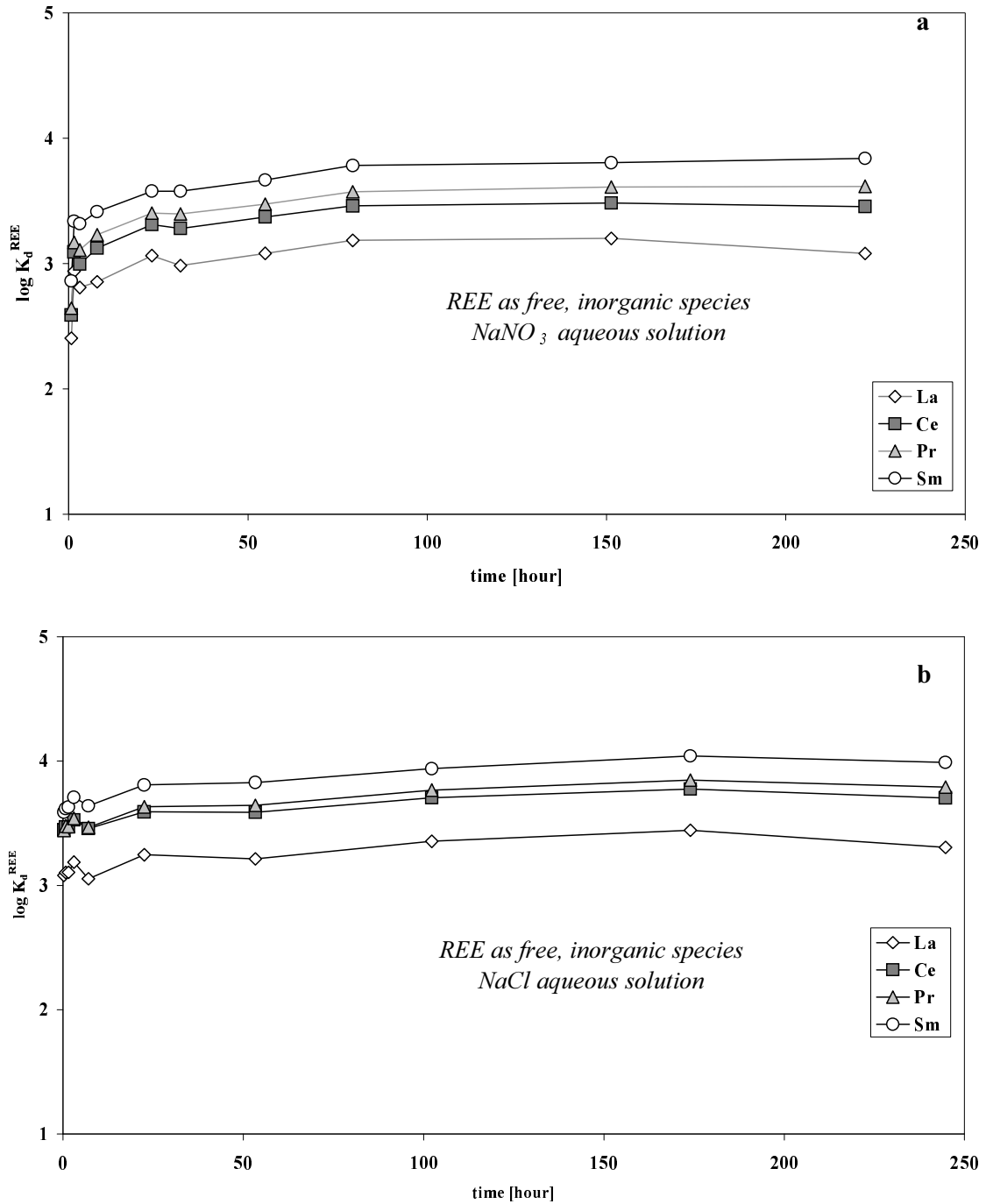


Fig. 1.1. $\log K_d^{\text{REE}}$ values between HFO suspensions and (a) NaCl and (b) NaNO₃ aqueous solutions, plotted vs equilibrium time.

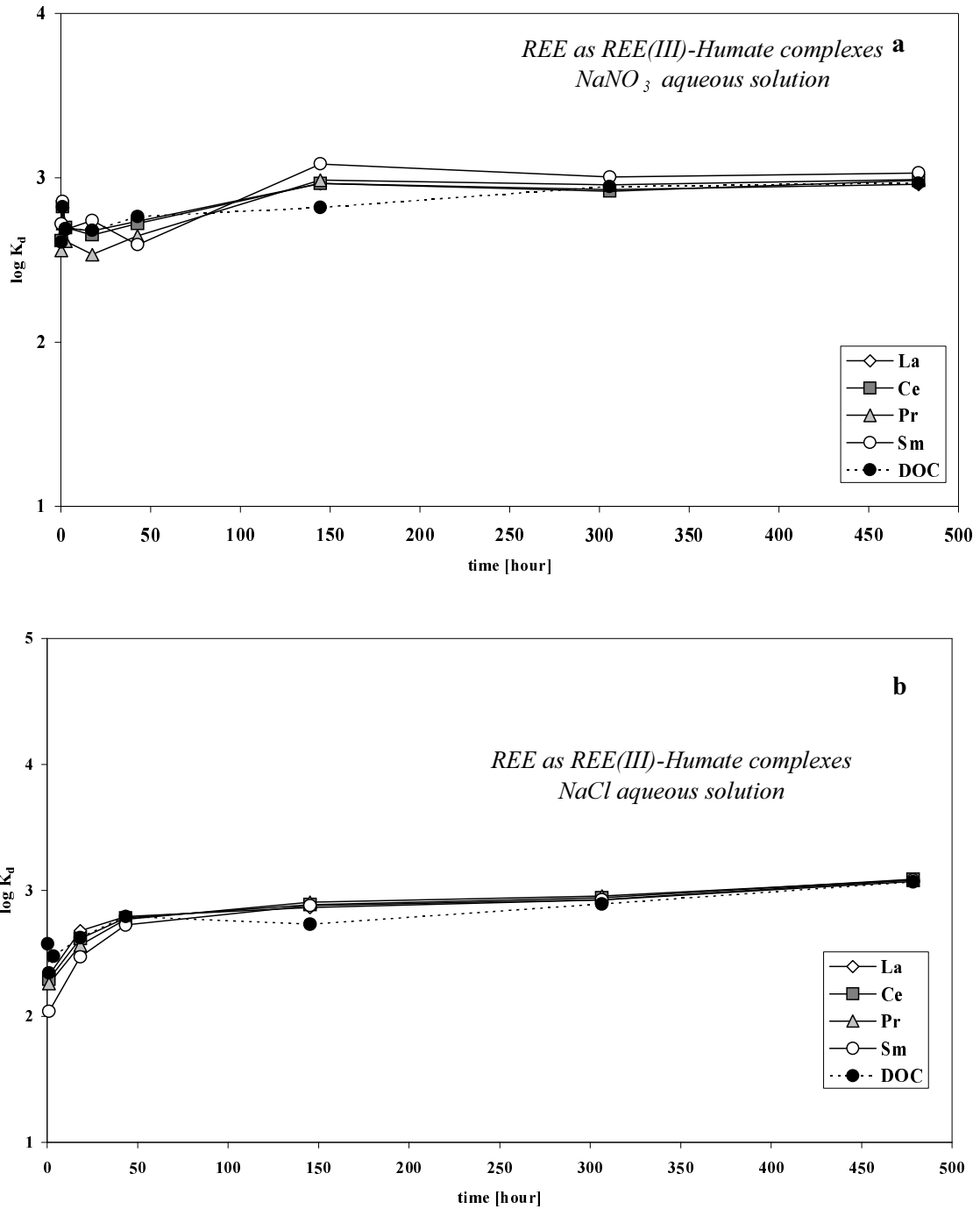


Fig. 1.2. $\log K_d^{\text{REE inorganic}}$ and $\log K_d^{\text{DOC}}$ values between HFO suspensions and (a) NaCl and (b) NaNO₃ aqueous solutions, plotted vs equilibrium time.

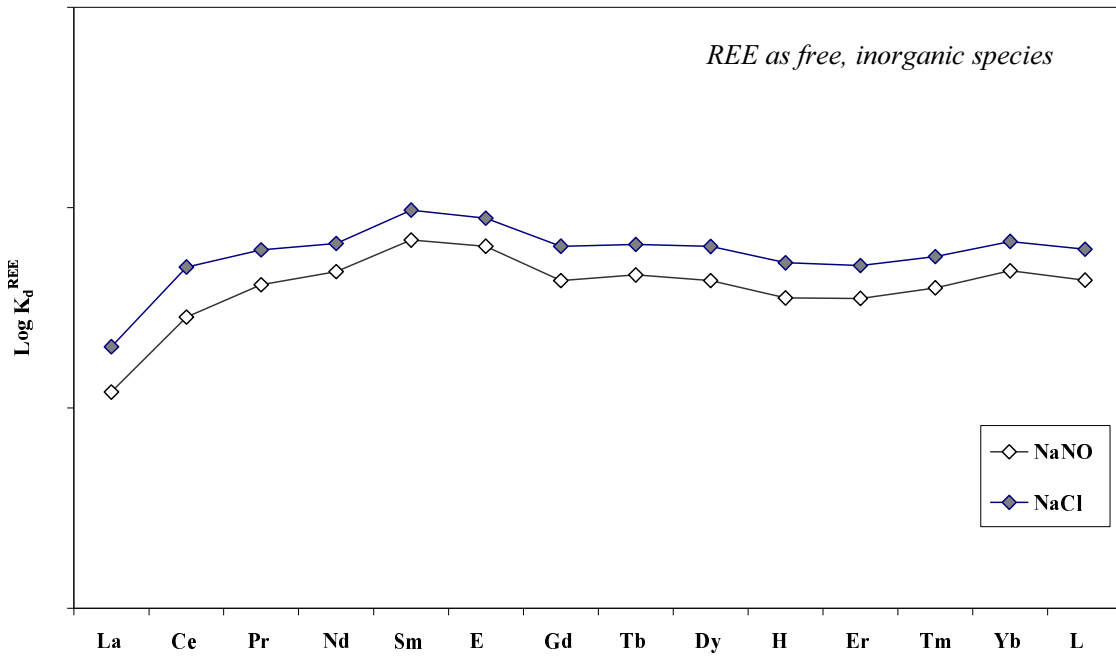


Fig. 1.3. Patterns of equilibrium $\log K_d^{REE}$ values derived from time-series experiments with aqueous solutions of NaNO_3 (open symbols) and NaCl (full symbols). Note the slight positive Ce anomaly and the conspicuous lanthanide tetrad effect.

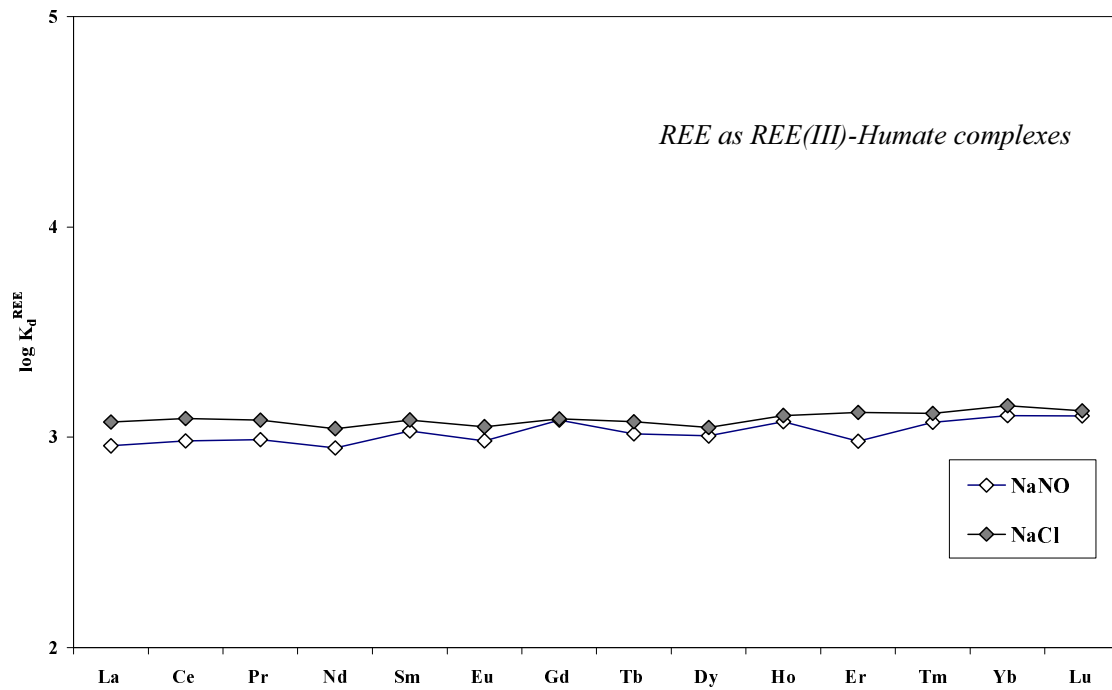


Fig. 1.4. Patterns of equilibrium $\log K_d^{REE}$ derived from time-series experiments with solutions of NaNO_3 (open symbols) and NaCl (full symbols). Note the flatness of the $\log K_d^{REE}$ patterns.

1.3.3. Consequences on using the Ce anomaly as a paleo-redox proxy

The present study shows that the Ce anomaly can hardly be used as a paleo-redox proxy in organic-rich environments. This particularly applies to paleosols, where Ce anomalies have often been reported (Rankin and Childs, 1976; Gallet et al., 1996; Braun et al., 1998) and authors have explored the possibility of using Ce depletions to reconstruct the redox state of paleosols at the time of their formation (e.g., MacLeod and Irving, 1996). From a paleoclimatic point of view, we may consider that wet periods lead to the dominance of oxidizing conditions in paleosols - due to the continuous recharge of the soil solutions by oxygen-rich rainwater - a process that would stabilize both Mn and Fe oxyhydroxide phases in the weathering front. Just considering the inorganic experimental results of Bau (1999) and Ohta and Kawabe (2001), we would expect the development of either negative or positive Ce anomalies in paleosols formed under such conditions. However, these experimental results lead us to suppose that organic complexation can severely inhibit Ce(III) oxidation. This calls into question the validity of using Ce anomalies as a *reliable* paleo-redox proxy in paleosols. The interplay between variable redox conditions and the REE(III) organic speciation is expected to lead to complex Ce anomaly patterns in paleosols. The behavior of Ce might not unambiguously reflect the redox conditions at time of the soil genesis.

1.4. Summary

Scavenging of dissolved REE(III)-PHA complexes by HFO was experimentally studied to elucidate further the role played by humate ligands in REE(III) adsorption and Ce(III) oxidation produced by Fe oxyhydroxides. The apparent $\log K_d^{\text{REE}}$ patterns in HFO suspensions exhibit slight positive Ce anomalies and an M-type lanthanide tetrad effect. This is in contrast with the distribution patterns obtained between REE(III)-humate complexes and HFO, which are completely flat. These modifications are believed to reflect an anionic adsorption of the organic complex. The ternary complexes formed at the surface of the HFO represent structures in which the binding of the REE(III)-PHA with the HFO surface takes place on the humate side. Consequently, the humate ligand physically separates Ce(III) ions from the HFO catalysis surface, thus preventing their oxidation by Fe(III) and stopping the development of an M-type tetrad effect. The distribution of REE at the HFO surface is then governed by the behavior of humic substances.

These data add further limitations to the use of Ce anomalies in reconstructing redox conditions in ancient geological systems. The present results strongly suggest that use of this proxy could be rendered impossible in organic-rich systems such as paleosols.

Appendix A. REE analyses

Rare earth concentrations were determined by ICP-MS (Agilent Technologies HP4500) at the Rennes University (France). Normal plasma conditions were used, with the instrumental parameters reported in Table 1.1.

Quantitative analyses were performed using a conventional external calibration procedure. Three external standard solutions having REE concentrations corresponding to the samples were prepared from a multi-REE standard solution (Accu Trace reference, 10 mg L⁻¹, USA). Indium was added to all samples as an internal standard at a concentration of 0.87 μM (100 ppb) to correct for instrumental drift and possible matrix effects. Indium was also added to the external standard solutions. Calibration curves were calculated from measured REE/indium intensity ratios.

Detection limits (DL in pmol L⁻¹) of the Agilent Technologies ICP-MS set up at Rennes University (Table 1.2) were calculated using the following equation:

$$DL = \frac{3SD.C}{S - B}$$

SD is the standard deviation obtained during instrumental blank measurements, *C* the REE concentration of a standard solution (between 29 and 36 pM depending on the REE), and *S* and *B* the ion counts measured during standard solution and instrumental blank analyses, respectively. Chemical blanks of individual REE were all lower than 10 pM, which is a negligible value (Table 1.2), three to four orders of magnitude lower than the concentrations measured in the synthetic solutions used in the adsorption experiments.

Isobaric interferences due to the formation and ionization of oxides and/or hydroxides in the ICP-MS can modify the determination of Sm, Eu, Gd, and Tb concentrations. The interference list is given in Table 1.3, along with the equations used at Rennes to correct REE concentrations from this potential source of error. Note that Ce and its neighbors La and Pr - and thus the calculated value of the Ce anomaly as well - are unaffected by isobaric interference problems. There was no need to correct Eu and Sm for BaO and/or BaOH interference because our synthetic solutions did not contain any Ba.

The amplitude and efficiency of the Gd and Tb corrections can be evaluated from Table 1.4, where we present measured and corrected concentrations of Gd and Tb measured for the SLRS-4 water geostandard along with reference data (Yeghicheyan et al., 2002). The correction amplitudes are moderate, being 6 % for Gd and only 2 % for Tb. The corrected values in both cases show relative discrepancies of ≤ 2.5 %, thus lying within the range of the reference values published for the SLRS-4 water geostandard (Yeghicheyan et al., 2002). These values should be regarded as maximum values for the results presented here, since the ratios of [Interfering Element]/[Interfered Element] are close to unity in our synthetic solutions, as against 10-65 in the SLRS-4 geostandard.

Finally, we can check the overall validity of the results using Table 1.5, which reports duplicate analyses of the synthetic solutions. Table 1.6 reports the concentrations of the SLRS-4 standard compared with published reference values (Yeghicheyan et al., 2002). From these two tables, and from an analysis of the efficiency of the correction procedure used to correct the REE results for oxide and hydroxide isobaric interferences, we estimate the total uncertainty on the REE results presented here at ± 2 %.

RF Power	1360 W
Plasma gas	15 L/min
Auxiliary gas	1.0 L/min
Carrier gas	1.13 L/min
Nebulizer type	Cross-flow
Spray chamber T°	2°C
Integration time	3 s/mass
CeO ⁺ /Ce ⁺	0.6 %
Ce ⁺⁺ /Ce ⁺	1 %

Table 1.1. Instrumental and data acquisition parameters.

Isotope	DL	Chemical Blanks
La 139	1.15	4.37
Ce 140	3.21	5.71
Pr 141	0.64	2.35
Nd 146	3.54	7.28
Sm 147	5.52	0.64
Eu 153	0.92	0.76
Gd 158	2.67	2.07
Tb 159	0.38	1.50
Dy 163	1.29	2.76
Ho 165	0.49	1.08
Er 166	1.26	0.88
Tm 169	0.59	1.27
Yb 174	1.44	1.14
Lu 175	0.51	0.85

Table 1.2. Detection limits (DL) and chemical blanks (in pM) measured during the course of the study.

Isotope	Interference	Correction
$^{147}\text{Sm}^+$	$^{130}\text{BaOH}^+$	negligible
$^{153}\text{Eu}^+$	$^{137}\text{BaO}^+$; $^{136}\text{BaOH}^+$	$\text{Eu}[153] = \text{Int}[153] - \frac{^{153}(\text{BaO}, \text{BaOH})}{^{137}\text{Ba}} \times \text{Int}[137]$
$^{158}\text{Gd}^+$	$^{142}\text{CeO}^+$; $^{142}\text{NdO}^+$; $^{141}\text{PrOH}^+$	$\text{Gd}[158] = \text{Int}[158] - \frac{^{158}(\text{PrOH})}{^{141}\text{Pr}} \times \text{Int}[141] - \frac{^{158}(\text{CeO})}{^{140}\text{Ce}} \times \text{Int}[140] - \frac{^{158}(\text{NdO})}{^{142}\text{Nd}} \times \text{Int}[142]$
$^{159}\text{Tb}^+$	$^{143}\text{NdO}^+$	$\text{Tb}[159] = \text{Int}[159] - \frac{^{159}(\text{NdO})}{^{143}\text{Nd}} \times \text{Int}[143]$

Table 1.3. Summary of isobaric interferences encountered during REE analysis and correction equations used at Rennes University to correct measured concentrations for this effect.

Isotope	Reference Values	Measured Values	Corrected Values	Correction (%)	Δ (%)
Gd 158	0.210	0.228	0.213	6.4	-1.5
Tb 159	0.026	0.026	0.026	2.4	2.4

Table 1.4. Amplitude and efficiency of oxide and hydroxide interference correction on Gd and Tb concentrations of the SLRS-4 water geostandard (concentrations expressed in nM)

Note. Δ : Relative discrepancy between corrected and reference values. Reference concentrations are from Yeghicheyan et al. (2002).

Isotope	NaNO ₃			NaCl		
	Average (n=2)	SD	RSD %	Average (n=2)	SD	RSD %
La 139	35.07	0.16	0.46	37.41	0.06	0.17
Ce 140	34.24	0.10	0.29	36.37	0.13	0.35
Pr 141	34.85	0.09	0.24	37.22	0.10	0.28
Nd 146	33.87	0.06	0.19	36.66	0.01	0.02
Sm 147	32.62	0.07	0.22	35.08	0.02	0.06
Eu 153	31.64	0.04	0.12	34.49	0.00	0.00
Gd 158	30.91	0.03	0.08	33.63	0.04	0.11
Tb 159	31.19	0.03	0.09	34.11	0.03	0.08
Dy 163	29.60	0.02	0.06	32.34	0.04	0.11
Ho 165	29.58	0.04	0.14	32.62	0.04	0.12
Er 166	28.81	0.02	0.07	31.58	0.03	0.09
Tm 169	28.67	0.07	0.26	31.78	0.04	0.14
Yb 174	28.25	0.04	0.14	31.41	0.08	0.24
Lu 175	27.41	0.03	0.13	30.41	0.04	0.13

Table 1.5. Duplicate analyses of the synthetic solutions used in the inorganic adsorption experiments (concentrations expressed in nM)

Note. SD: standard deviation; RSD (%): relative standard deviation = (SD/mean value)×100.

Isotope	Average Concentrations (n=13)	Reference Concentrations ^a
La 139	2.069	2.066
Ce 140	2.548	2.569
Pr 141	0.493	0.492
Nd 146	1.842	1.865
Sm 147	0.371	0.382
Eu 153	0.055	0.053
Gd 158	0.219	0.217
Tb 159	0.027	0.027
Dy 163	0.143	0.149
Ho 165	0.028	0.028
Er 166	0.081	0.080
Tm 169	0.011	0.010
Yb 174	0.068	0.069
Lu 175	0.011	0.011

Table 1.6. Comparison of the analytical accuracy of the Agilent Technology HP4500 ICP-MS setup at Rennes University against published reference values of the SLRS-4 water geostandard (concentrations expressed in nM).

^a From Yeghicheyan et al. (2002).

2. Adsorption of REE(III)-humate complexes onto MnO₂: Experimental evidence for cerium anomaly and lanthanide tetrad effect suppression

Cette partie est extraite de Geochimica et Cosmochimica Acta, Davranche M., Pourret O., Gruau G., Dia A., and Le Coz-Bouhnik M. (2005) Adsorption of REE(III)-humate complexes onto MnO₂: Experimental evidence for cerium anomaly and lanthanide tetrad effect suppression, 69, 4825-4835.

Résumé- L'impact de la complexation organique sur le développement de l'anomalie de Cérium et sur l'effet tetrad des lanthanides a été évalué expérimentalement lors de réactions d'adsorption de terres rares (REE) sur des oxydes de manganèse (MnO₂). Deux types de solutions aqueuses - NaCl et NaNO₃ - ont été testés à pH 5 et 7.5. Les études cinétiques montrent qu'un état d'équilibre est atteint au bout de 10 h quand les REE sont présentes sous formes inorganiques, alors que cet état d'équilibre n'est atteint qu'au bout de 10 j quand les REE sont présentes sous formes complexées à des substances humiques. Les coefficients de partage (K_d^{REE}) entre MnO₂ et la solution montrent peu ou pas d'anomalie positive de Cerium ou d'effet tetrad des lanthanides sur le solide quand les REE sont présentes sous forme de complexes humiques contrairement aux expériences où les REE sont sous formes inorganiques. De plus, les rapports $K_d^{REE\text{ organique}}/K_d^{COD}$ (COD : carbone organique dissous) sont proches de 1.0, les REE et les humates restent donc liés entre eux pendant l'adsorption. La réduction/suppression de l'anomalie de Ce dans les expériences organiques est le résultat d'une combinaison de deux processus: (i) l'incapacité du MnO₂ à oxyder le Ce(III) due à l'écrantage des surfaces du MnO₂ par les substances humiques et (ii) le Ce(IV) ne peut pas être préférentiellement adsorbé et extrait de la solution puisque la totalité des REE est complexée à la matière organique. L'absence d'effet tetrad des lanthanides peut être due à l'adsorption anionique du complexe REE-Humate sur MnO₂. L'adsorption du complexe se produit par le côté humique du complexe, prévenant ainsi l'expression des différences du paramètre Racah par la répulsion des électrons 4f entre les REE et la surface des oxydes. Les résultats présentés dans cette étude expliquent pourquoi, aucune anomalie négative de Ce n'est observée dans des eaux riches en matière organique malgré la présence de MnO₂ et des conditions oxydantes. Cette étude remet également en cause l'utilisation de l'anomalie de Ce comme témoin des conditions redox dans des eaux riches en matières organiques ou dans des précipités formés à l'équilibre avec de telles eaux.

Abstract- Experiments were conducted to evaluate the impact of organic complexation on the development of Ce anomalies and the lanthanide tetrad effect during the adsorption of rare-earth elements (REE) onto MnO₂. Two types of aqueous solutions - NaCl and NaNO₃ - were tested at pH 5 and 7.5. Time-series experiments indicate that a steady-state is reached within less than 10 h when REE occur as free inorganic species, whereas steady state is not reached before 10 d when REE occur as REE-humate complexes. The distribution coefficients (K_d^{REE}) between suspended MnO₂ and solution show no or only very weak positive Ce anomaly or lanthanide tetrad effect when REE occur as humate complexes, unlike the results obtained in experiments with REE occurring as free inorganic species. Monitoring of dissolved organic carbon (DOC) concentrations show that $\log K_d^{REE\text{ organic}}/K_d^{DOC}$ ratios are close to 1.0, implying that the REE and humate remain bound to each other upon adsorption. Most likely, the Ce anomaly reduction/suppression in the organic experiments arises from a combination of two processes: (i) inability of MnO₂ to oxidize Ce(III) because of shielding of MnO₂ surfaces by humate molecules and (ii) Ce(IV) cannot be preferentially removed from solution due to quantitative complexation of the REE by organic matter. We suggest that the lack of lanthanide tetrad effect arises because the adsorption of REE-humate complexes onto MnO₂ occurs dominantly via the humate side of the complexes (anionic adsorption), thereby preventing expression of the differences in Racah parameters for 4f electron repulsion between REE and the oxide surface. The results presented here explain why, despite the development of strongly oxidizing conditions and the presence of MnO₂ in the aquifer, no (or insignificant) negative Ce anomalies are observed in organic-rich waters. The present study demonstrates experimentally that the Ce anomaly cannot be used as a reliable proxy of redox conditions in organic-rich waters or in precipitates formed at equilibrium with organic-rich waters.

2.1. Introduction

Studies focused on the behaviour of the rare-earth elements (REE) have recently become a major issue in aqueous trace-element chemistry. The REE are a highly coherent group of elements whose chemical properties vary gradually along the series. REE are highly sensitive to pH changes and adsorption/desorption reactions, being also strongly influenced by the redox chemistry of Fe and Mn. Thus, REE have been used as tracers in many studies on the geochemistry of rivers, lakes, seawater, groundwater and geothermal fluids (Elderfield and Greaves, 1982; De Baar et al., 1983; De Baar et al., 1985; De Baar et al., 1988; Elderfield, 1988; Elderfield et al., 1990; Smedley, 1991; Gosselin et al., 1992; Johannesson and Lyons, 1994; Johannesson and Lyons, 1995; Johannesson et al., 1995; Braun et al., 1998; van Middlesworth and Wood, 1998; Elbaz-Poulichet and Dupuy, 1999; Dia et al., 2000; Leybourne et al., 2000; Yan et al., 2001; Aubert et al., 2002; Biddau et al., 2002; De Carlo and Green, 2002; Möller et al., 2002; Shacat et al., 2004).

Rare-earth elements exhibit a trivalent (+III) oxidation state in natural waters. However, among the REE, Ce is the only element that can be oxidized to the (+IV) state. Ce oxidation can either occur abiotically through oxidation/scavenging of dissolved Ce(III) by Mn and Fe oxyhydroxides (Koeppenkastrup and De Carlo, 1992; De Carlo et al., 1998; Bau, 1999; Ohta and Kawabe, 2001), or biotically. In the latter case, either bacteria oxidize Ce(III) directly into Ce (IV), or they catalyze the oxidation of Mn(II) into Mn(IV). The Ce(III) is then oxidized abiotically by the MnO₂ so formed (Moffet, 1990). Since Ce(IV) is adsorbed more strongly than the other trivalent REE, the Ce oxidation/scavenging reaction may result in solutions displaying a negative Ce anomaly, whereas the solids exhibit positive Ce anomalies. In fact, negative Ce anomalies are widespread in both oceanic and fresh waters. Seawater, for example, shows a strong negative Ce anomaly mirrored by a positive anomaly in hydrogenic ferromanganese nodules (Piper, 1974; Elderfield et al., 1981; De Carlo and McMurtry, 1992). Groundwaters also often show negative Ce anomalies (Smedley, 1991; Braun et al., 1998; Dia et al., 2000; Leybourne et al., 2000).

The development of negative Ce anomalies in waters has been widely used for geochemical fingerprinting of redox conditions and notably in the study of marine environments (De Baar et al., 1983; De Baar et al., 1985; De Baar et al., 1988; Elderfield, 1988; Smedley, 1991; Johannesson and Lyons, 1994; Johannesson and Lyons, 1995; Braun et al., 1998; Leybourne et al., 2000; Kuss et al., 2001). In recent years, much attention has also been paid to the potential application of Ce anomaly as a paleoceanographic indicator of widespread marine anoxia, as well as a redox proxy in paleosols (Wright et al., 1987; MacLeod and Irving, 1996; Gallet et al., 1996; Holser, 1997; Morad and Felitsyn, 2001; Picard et al., 2002). However, many oxidizing waters do not exhibit negative Ce anomalies. In fact, evidence exists that the occurrence of organic ligands in the solutions could prevent the development of Ce anomalies. Such evidence was provided by Dia et al. (2000), who reported time series data for REE, dissolved organic carbon (DOC), Fe, and Mn concentrations for shallow groundwaters rich in organic matter (DOC contents 7–32 mg L⁻¹) from a small catchment in western France. Despite the occurrence of temporary oxidizing conditions and neof ormation of Mn oxides, no (or insignificant) negative Ce anomalies were observed in these waters. Similar results were reported by Viers et al. (1997) who investigated the major, trace element and REE chemistry of organic-rich (DOC contents 4–24 mg L⁻¹) shallow groundwaters from a small tropical catchment in western Africa. In such organic-rich, shallow groundwaters, the so-called "dissolved" REE pool generally occurs as REE(III)-humate complexes (Sholkovitz, 1995; Viers et al., 1997). This observation is consistent with the high conditional stability constants of these complexes (Byrne and Li, 1995; Takahashi et al., 1999; Tang and Johannesson, 2003).

Another specific feature of the aqueous chemistry of REE is the frequent occurrence of a lanthanide tetrad effect in the REE patterns of aqueous samples or in the patterns of mineral

precipitates formed at equilibrium with aqueous solutions. The term "lanthanide tetrad effect" was initially used to describe the behaviour of the trivalent lanthanides during liquid-liquid extraction experiments (Peppard et al., 1969), and refers to the apparent subdivision of La and the fourteen *4f* REE elements into four "groups" or "tetrads": 1: La-Nd; 2: Pm-Gd; 3: Gd-Ho; 4: Er-Lu. This effect is known from seawater and marine precipitates (e.g., Bau, 1996). It is also frequently met during experimental adsorption of REE onto Fe-hydroxide or MnO₂ as shown by Bau (1999) and Ohta and Kawabe (2001), among others. To our knowledge, the impact of organic complexation on the development of a lanthanide tetrad effect has not been so far investigated.

It is especially important to understand the influence of REE speciation on REE sorption properties and Ce anomaly development because this latter has often been proposed as a paleoredox proxy, both in the ocean and in soils. Although this application clearly has some potential, a more thorough understanding is required of the processes that control Ce/REE fractionation in both the marine and continental environments. In a recent paper, Davranche et al. (2004) demonstrated experimentally that the complexation of REE by dissolved humic substances prevents Ce anomaly development during REE partitioning between Fe oxyhydroxides and solution. In the present study, we focus on MnO₂, which has a much stronger oxidizing potential with respect to Ce(III) than Fe hydroxide (e.g., Koeppenkastrop and De Carlo, 1992; Koeppenkastrop and De Carlo, 1993; Ohta and Kawabe, 2001). In the following, we examine the impact of organic matter on the development of Ce anomalies and lanthanide tetrad effect during adsorption onto MnO₂ particles, by comparing apparent REE distribution coefficients between MnO₂ suspensions and solutions. In the adsorption experiments, REE(III) occurred in solution either as humate complexes or as free inorganic species.

2.2. Experimental procedure

All chemicals used in this study were of analytical grade. All solutions were prepared with doubly de-ionized water (Milli-Q system, Millipore). The polyethylene containers used in the adsorption experiments were soaked in 10 % ultrapure HNO₃ for 48 h at 60 °C, then rinsed with Milli-Q water for 24 h at 60 °C, to remove all possible REE contamination sources.

2.2.1. Manganese Oxide

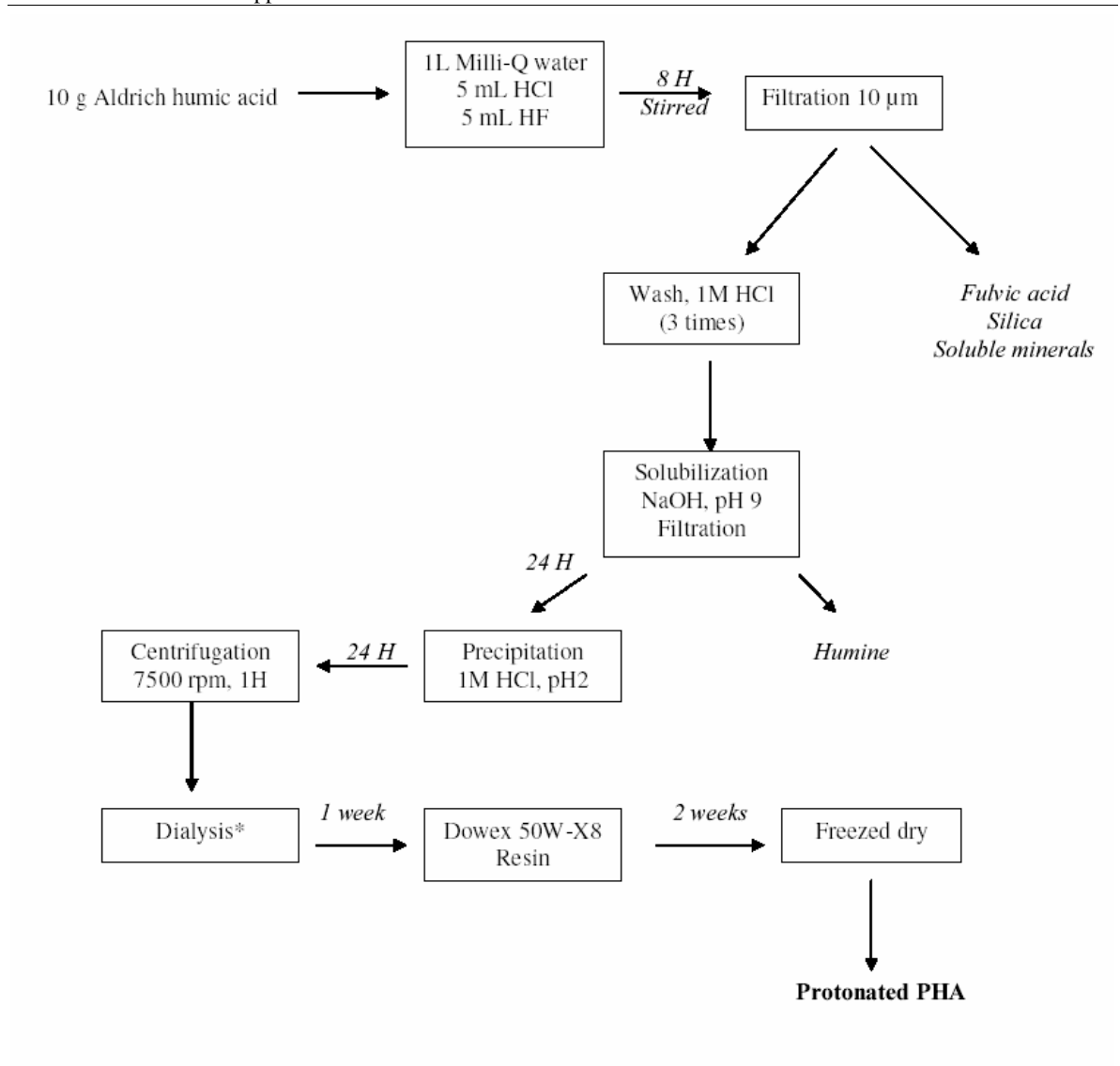
Synthetic MnO₂ (Aldrich) was used in the adsorption experiments. The solid structure was analyzed by X-Ray diffraction (XRD) on a Siemens D5000 diffractometer. The principal *d* spacing indicated a pyrolusite (MnO₂) structure. The total surface site number of MnO₂ was estimated using the solid CEC (Cation Exchange Capacity) and determined following the cobalthexammine method, ISO 11260 (AFNOR, 1994). Ions bound with the solid surface are exchanged with cobalthexammine ions, and the CEC is the concentration of cobalthexammine ions eliminated from the solution. Five g of solid MnO₂ were mixed with 10 mL of 0.017 M cobalthexammine solution for 3 h. The suspension was then centrifuged and the concentration of cobalthexammine ion remaining in the solution was measured at 470 nm with a Shimadzu-160 A U.V.-spectrophotometer. These analyses indicate that the MnO₂ used in this study has a CEC of 70 mEq/100 g.

Surface acidity constants were determined from potentiometric titrations of 5 g L⁻¹ of solid with NaOH (0.1 M) and HNO₃ (0.1 M), in 0.1 M NaCl solution as the supporting electrolyte (Davranche et al., 2003). Titrations were carried out with a Metrohm 794 DMS Titrino apparatus equipped with a Metrohm combined (3 M KCl) glass electrode. Measured acidity constants ($pK_{a1} = 7.89$ and $pK_{a2} = 3.65$) yielded a pH_{zpc} equal to 5.8, a value that falls within the reported pH_{zpc} range for MnO₂ (i.e., 4.5 to 7.8; Langmuir, 1997).

2.2.2. REE(III)-Humate Complexes

Humate was obtained from the synthetic Aldrich humic acid (Aldrich, H1, 675-2) according to the procedure described by Vermeer et al. (1998) (Fig. 2.1). The humate obtained in this way is ash free and in a protonated form, with the following elemental composition (in weight percent): C = 55.8 %, O = 38.9 %, H = 4.6 % and N = 0.6 %. Purified humic acid has a mean molecular weight of 23 kDa (Vermeer et al., 1998). Prior to use, the freeze-dried humate was resuspended overnight in a NaOH solution (pH 10) to ensure complete dissolution of the sample.

Rare-earth element(III)-humate complexes were prepared as follows. Twenty mg of dissolved humate were enclosed in a 250 mL sodium-acetate dialysis bag with a pore size of 12–14 kDa. The bag was introduced into 1000 mL of a 5 ppb REE solution, the ionic strength being fixed at 10^{-3} M with either NaCl or NaNO₃, and the pH adjusted to 7 with HNO₃. The suspension was stirred for 48 h (equilibrium time determined from preliminary kinetic experiments) to allow equilibration and partitioning of the REE between the aqueous solution and the humate suspension. The dialysis bag was then removed and the REE-humate complexes recovered. The concentrations of REE in solution both inside and outside the dialysis bag were monitored vs. time in order to quantify the amount of REE complexed to humate. Moreover, an aliquot of the REE-humate suspension inside the dialysis bag was ultrafiltrated at the end of a NaNO₃ complexation experiment. Ultrafiltrations were carried out with a new Amicon Ultra cell (Millipore) equipped with a filter of 5 kDa pore size. The performed analyses evidenced that REE were effectively complexed to humate within the bag allowing less than 0.7 % of total REE concentration to be as free inorganic species. Possible REE adsorption onto the dialysis bag was also checked by analyzing the whole REE content of the dialysis membrane (dissolved by acidic digestion with HNO₃ 14 N). REE measurements showed that REE complexation yields were between 75 and 50 % in solution using NaCl as neutral electrolyte, and between 95 and 90 % in those using NaNO₃. Measurements also suggested that complexation increased regularly from the heavy to the light REE (Fig. 2.2), which is consistent with the stability constant order determined by Takahashi et al. (1999) and Tang and Johannesson (2003) for REE(III)-organic complexes.



*: until the solution resistance equals before and after dialysis

Fig. 2.1. Purification procedure of Aldrich humic substances.

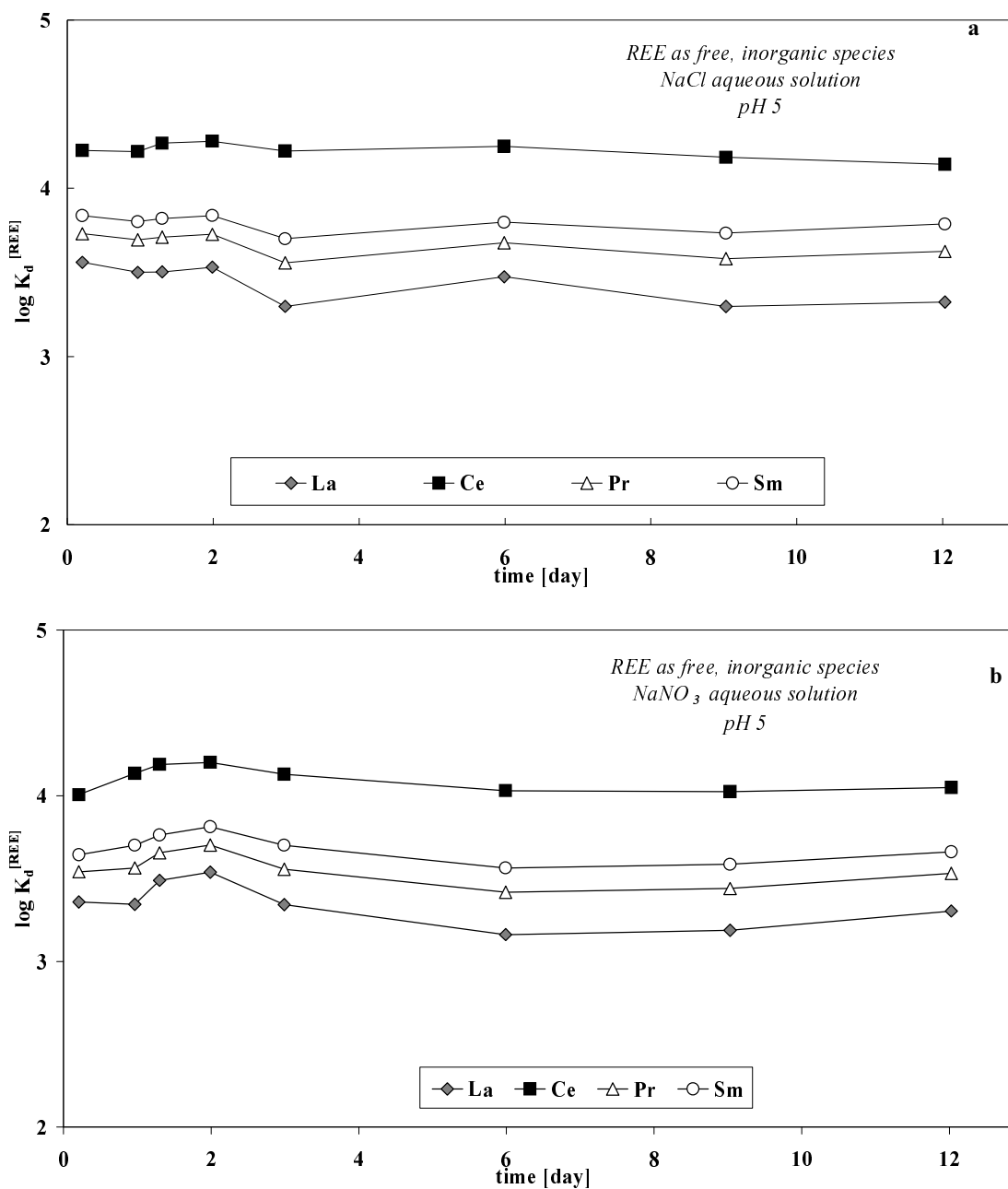


Fig. 2.2. REE patterns between humate suspension and NaNO₃ aqueous solution plotted vs. increasing atomic number within REE series. Initial concentration of each REE was 5 ppb and humate concentration was 20 mg L⁻¹. Errors bars correspond to σ for three replicates.

2.2.3. Adsorption Procedure

Five time-series experiments - three with NaCl and two with NaNO₃ as neutral electrolyte - were performed to assess the effects of organic complexation on REE(III) adsorption by MnO₂. The choice of NaNO₃ as one of the two tested neutral electrolytes was imposed by the occurrence of high NO₃⁻ concentrations (up to 5.10⁻³ M) in some of the organic-rich shallow groundwaters showing no development of negative Ce anomalies, despite the presence of strongly oxidizing conditions (Dia et al., 2000). In all five cases, we used 1 L of 10⁻³ M NaCl or 10⁻³ M NaNO₃ solution containing 100 mg MnO₂ in suspension. We tested pH conditions of 5 and 7.5. A pH of 7.5 was used to promote adsorption of REE(III)-humate complexes onto MnO₂ via the cationic side of the complexes, which could eventually favor Ce oxidation. The pH value of 5 was chosen because published results on the adsorption of free, inorganic REE(III) by MnO₂ show that Ce anomalies are easier to detect when REE(III) concentrations in the precipitates are low (Ohta and Kawabe, 2001). Such a situation occurs when the pH is close to or lower than the pH_{zpc} value of the oxide used (5.8 in the present study). The pH was monitored periodically with a pH-meter and adjusted to 5 and 7.5 by addition of HNO₃ (4.6 N) or NaOH (4 N). All experiments were carried out at room temperature, 20 °C ± 2.

In two of the experiments (each performed in duplicate), we used free inorganic REE(III) species. These two experiments are termed the "inorganic experiments". They were carried out essentially to provide the inorganic reference baseline necessary to interpret the organic results. However, they were also carried out to validate the experimental and analytical protocol used in our laboratory by comparing our results with published work on the adsorption of inorganic REE(III) onto MnO₂ (Koeppenkastrop and De Carlo, 1992; Koeppenkastrop and De Carlo, 1993; Ohta and Kawabe, 2001). The concentration of each REE was 5 ppb in the inorganic experiments, which corresponds to molar concentrations ranging from 36 to 29 nM, depending on the respective REE. In the remaining three experiments (each performed in triplicate), adsorption was carried out using the REE(III)-humate complexes described above. These experiments are termed the "organic experiments".

Here, we quantify the adsorption behaviour of the REE by using the apparent partition coefficient K_d , expressed as:

$$K_d = \frac{\mu\text{g REE adsorbed/g Mn oxide}}{\mu\text{g L}^{-1} \text{ REE in solution}} \quad (2.1)$$

Ce anomalies of K_d^{REE} are quantified as follows:

$$Ce/Ce^* = \frac{\log(K_d^{Ce})}{\frac{1}{2} [\log(K_d^{La}) + \log(K_d^{Pr})]} \quad (2.2)$$

Suspension aliquots of about 10 mL were regularly sampled and filtered through 0.2 μm cellulose acetate filters (Sartorius) and the REE concentration of the filtrate analyzed to determine the concentration of REE in solution. The amount of REE adsorbed onto MnO₂ was obtained by subtracting REE concentrations left in solution from initial REE concentrations taking into account sampling-induced volume variations. Sample aliquots used for REE determination were all immediately digested with subboiled nitric acid (HNO₃ 14 N) at 100 °C, then resolubilized in HNO₃ 0.4 N after complete evaporation, in order to avoid interferences with organic matter during mass analysis for the organic experiments.

The adsorption behaviour of the REE(III)-humate complexes was also monitored by measuring the dissolved organic carbon (DOC) content of the experimental solutions. DOC measurements can be converted into apparent partition coefficients using Eqn. 2.3:

$$K_d = \frac{\mu\text{g DOC adsorbed/g Mn oxide}}{\mu\text{g mL}^{-1} \text{ DOC in solution}} \quad (2.3)$$

Dissolved organic carbon concentrations were determined at Rennes University using a Shimadzu 5000 TOC analyzer. The accuracy of DOC concentration measurements is estimated at $\pm 5 \%$ as determined by repeated analyses of freshly prepared standard solutions (potassium biphtalate). Experimental reproducibility obtained on $\log K_d^{\text{DOC}}$ values as determined from triplicate runs is better than $\pm 10 \%$ (Table 2.1).

	A	B	C	Mean	RSD ^a
NaCl, pH 5	3.46	3.53	3.56	3.52	1.4
NaNO₃, pH 5	3.56	3.74	3.52	3.61	3.2
NaCl, pH 7.5	3.36	3.00	2.96	3.11	7.2

^aRSD = *relative standard deviation*

Table 2.1. Reproducibility of $\log K_d^{\text{DOC}}$ at pH 5 and 7.5.

2.2.4. REE Measurements and Reproducibility of Adsorption Experiments

REE concentrations were determined at Rennes University using an Agilent Technologies HP4500 ICP-MS instrument. Quantitative analyses were performed using a conventional external calibration procedure. Three external standard solutions with REE concentrations similar to the samples analyzed in this study were prepared from a multi-REE standard solution (Accu Trace Reference, 10 mg L⁻¹, USA). Indium was added to all samples as an internal standard at a concentration of 0.87 μM (100 ppb) to correct for instrumental drift and possible matrix effects. Indium was also added to the external standard solutions. Calibration curves were calculated from measured REE/indium intensity ratios. The instrumental error on REE analysis in our laboratory as established from repeated analyses of multi-REE standard solution (Accu Trace Reference, USA) and of the SLRS-4 water standard is $< \pm 2 \%$. Chemical blanks of individual REE were all lower than 10 pM, which is negligible since they are three to four orders of magnitude lower than concentrations measured in the synthetic solutions used in the adsorption experiments.

Equilibrium $\log K_d^{\text{REE}}$ values obtained during duplicate and triplicate experiments conducted in order to determine the overall experimental reproducibility of the method used in this study are presented in Table 2 (REE(III) occurring as free, inorganic species) and Table 3 (REE(III) as REE(III)-humate complexes). The two tables show that the overall experimental reproducibility on the $\log K_d^{\text{REE}}$ values discussed in this paper is better than $\pm 10 \%$.

	Inorganic, NaCl, pH 5				Inorganic, NaNO ₃ , pH 5			
	A	B	Mean	RSD ^a	A	B	Mean	RSD ^a
La	3.15	3.50	3.32	7.46	3.32	3.29	3.30	0.45
Ce	4.07	4.22	4.14	2.62	4.14	3.96	4.05	3.23
Pr	3.54	3.71	3.63	3.48	3.55	3.51	3.53	0.71
Nd	3.57	3.73	3.65	3.16	3.55	3.53	3.54	0.43
Sm	3.71	3.86	3.79	2.85	3.67	3.66	3.66	0.19
Eu	3.73	3.86	3.80	2.54	3.68	3.68	3.68	0.02
Gd	3.59	3.76	3.68	3.40	3.58	3.56	3.57	0.38
Tb	3.58	3.75	3.67	3.35	3.55	3.55	3.55	0.03
Dy	3.60	3.76	3.68	3.07	3.56	3.57	3.56	0.28
Ho	3.49	3.70	3.59	4.15	3.49	3.49	3.49	0.14
Er	3.50	3.71	3.61	4.07	3.52	3.50	3.51	0.26
Tm	3.52	3.73	3.62	3.98	3.53	3.51	3.52	0.40
Yb	3.57	3.75	3.66	3.55	3.57	3.56	3.56	0.25
Lu	3.56	3.76	3.66	3.77	3.56	3.55	3.56	0.07

^aRSD: relative standard deviation

Table 2.2. Reproducibility of log K_d^{REEinorganic} at pH 5.

2.3. Results

2.3.1. Inorganic Experiments at pH 5

The variations of log K_d for La, Ce, Pr and Sm with run duration are presented in Figure 2.3. The values were almost constant from 10 h to 12 d, with NaCl runs exhibiting faster adsorption rates compared to NaNO₃ runs. Thus, the inorganic experiments point to the same conclusion reached earlier by Ohta and Kawabe (2001) and Koeppenkastrop and De Carlo (1992, 1993); namely, that steady state is attained in less than 1 d (<10 h, here) when REE are present in the MnO₂ suspension as free inorganic species. The equilibrium K_d values obtained here (3.3 on average) are within error of the results reported by Ohta and Kawabe (2001) (3.2 on average) for comparable pH conditions, thus validating the experimental and analytical protocol used in our laboratory.

All the Log K_d patterns exhibit large positive Ce anomalies (Fig. 2.4 and Fig. 2.5), as well as convex tetrad curves (or "M" shaped), two features that were already apparent in De Carlo et al. (1998) and Ohta and Kawabe (2001) results. In the present case, we consider that the observed tetrad effect is real rather than an analytical artifact. This is because of the low analytical uncertainty on log K_d^{REE} values, combined with the large amplitude variation of log K_d^{REE} values between REE families defining the different tetrad groups (e.g., 8.2 % between log $K_d^{Eu}_{inorganic}$ and log $K_d^{Gd}_{inorganic}$ for the NaNO₃ adsorption experiment).

Cerium anomalies, expressed as Ce/Ce* values, are all greater than one and nearly constant over the duration of the adsorption experiments, ranging from 1.16 to 1.23 (Fig. 2.5). These values are slightly lower than those obtained by Ohta and Kawabe (2001) under similar pH conditions.

2.3.2. Organic Experiments at pH 5

Figure 2.6 reports the experimental results of log $K_d^{REE}_{organic}$ for La, Ce, Pr, and Sm. The data show that the complexation of REE(III) by humic acid has a large effect on both REE adsorption kinetics and K_d^{REE} equilibrium values. Time-series variations of log $K_d^{REE}_{organic}$ values reveal that equilibrium was not reached before about 10 d when REE is present as REE(III)-humate complexes (Fig. 2.6). This compares with 10 h in experiments where REE occurred as free metal ions (Fig. 2.1; Ohta and Kawabe, 2001). The REE partition coefficient values at pH 5 are comparable between organic and inorganic experiments, except for the higher Ce values in the inorganic experiments (see Fig. 2.5 and Fig. 2.7). Ratios of log $K_d^{REE}_{organic}/K_d^{DOC}$ are close to 1.0, indicating that the REE(III) and the humic acid remain bound to each other during adsorption of the REE(III)-humate complexes onto the MnO₂ surface.

Patterns of log $K_d^{REE}_{organic}$ differ markedly from those obtained during the inorganic experiments (compare Fig. 2.5 and Fig. 2.7). Firstly, the organic patterns do not show the same conspicuous tetrad effect or "M" shape as in the inorganic patterns (Fig. 2.4). The general lack of a conspicuous "M" shape in the organic patterns is highly significant with regard to the mechanism of adsorption of the REE(III)-humate complexes onto MnO₂. We note that all the experimental data so far obtained yield log K_d^{REE} patterns with invariably convex tetrad effects for adsorption between REE(III)_(aq) and either MnO₂ or Fe oxyhydroxides (De Carlo et al., 1998; Bau, 1999; De Carlo et al., 2000; Ohta and Kawabe, 2001; and Davranche et al., 2004; Fig. 2.4). Secondly, unlike the inorganic experiments, log K_d^{REE} patterns corresponding to the REE(III)-humate adsorption show no, or only very weak positive Ce anomalies (Fig. 2.5 and Fig. 2.7).

	Organic, NaCl, pH 5					Organic, NaCl, pH 7,5					Organic, NaNO ₃ , pH 5				
	A	B	C	mean	rsd	A	B	C	mean	rsd	A	B	C	mean	rsd
La	3.26	3.25	3.29	3.27	0.70	3.12	3.15	3.14	3.14	0.48	3.52	3.36	3.47	3.45	2.45
Ce	3.49	3.37	3.41	3.42	1.70	3.21	3.20	3.17	3.19	0.68	3.64	3.45	3.53	3.54	2.67
Pr	3.37	3.29	3.33	3.33	1.10	3.20	3.17	3.16	3.18	0.61	3.56	3.41	3.46	3.47	2.28
Nd	3.28	3.26	3.29	3.28	0.55	3.20	3.22	3.08	3.17	2.47	3.52	3.38	3.41	3.44	2.14
Sm	3.31	3.26	3.26	3.28	0.85	3.15	3.21	3.11	3.15	1.70	3.51	3.36	3.40	3.42	2.38
Eu	3.27	3.21	3.31	3.27	1.53	3.13	3.22	3.19	3.18	1.33	3.52	3.32	3.42	3.42	2.88
Gd	3.31	3.25	3.34	3.30	1.44	3.15	3.25	3.20	3.20	1.55	3.49	3.33	3.41	3.41	2.36
Tb	3.25	3.22	3.31	3.26	1.45	3.13	3.23	3.10	3.15	2.13	3.45	3.32	3.39	3.39	1.91
Dy	3.25	3.19	3.32	3.25	1.90	3.14	3.31	3.12	3.16	1.59	3.43	3.33	3.36	3.37	1.55
Ho	3.21	3.23	3.32	3.25	1.67	3.18	3.24	3.13	3.19	1.75	3.41	3.35	3.32	3.36	1.40
Er	3.21	3.24	3.31	3.25	1.65	3.16	3.23	3.16	3.18	1.27	3.42	3.32	3.31	3.35	1.82
Tm	3.24	3.25	3.35	3.28	1.81	3.14	3.15	3.13	3.14	0.31	3.43	3.28	3.32	3.35	2.31
Yb	3.27	3.28	3.41	3.32	2.29	3.06	3.22	3.16	3.14	2.65	3.47	3.27	3.37	3.37	2.99
Lu	3.29	3.29	3.41	3.33	2.05	3.07	3.21	3.12	3.13	2.21	3.45	3.27	3.38	3.36	2.65

^aRSD = relative standard deviation

Table 2.3. Reproducibility of log K_d^{REEorganic} at pH 5 and 7.5.

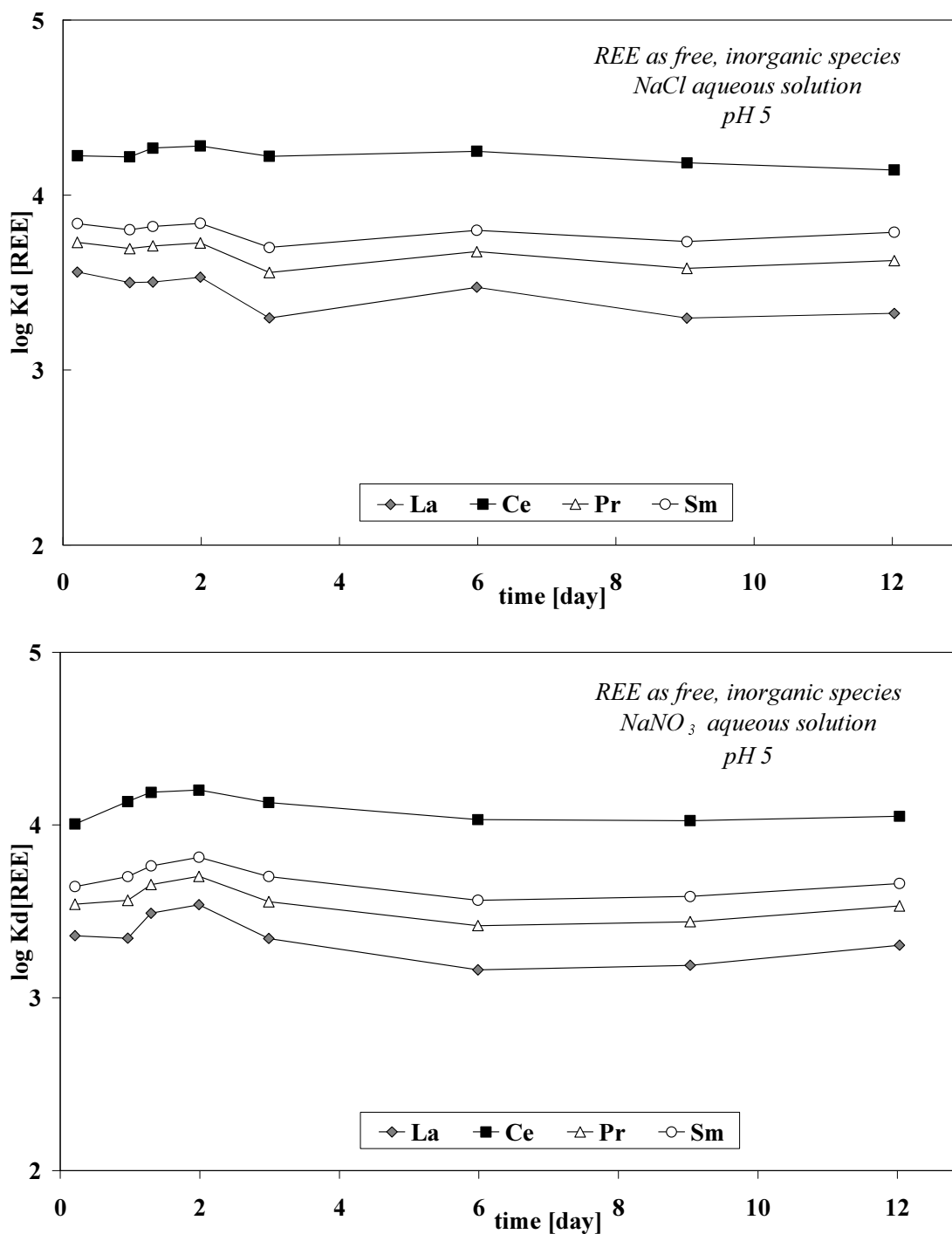


Fig. 2.3. Equilibrium time of $\log K_d^{\text{REE inorganic}}$ in the suspension of MnO₂ and NaCl (a) or NaNO₃ (b) at pH 5, expressing the partitioning of 5 ppb REE between 100 mg MnO₂ and 1000 mL water within 2 weeks.

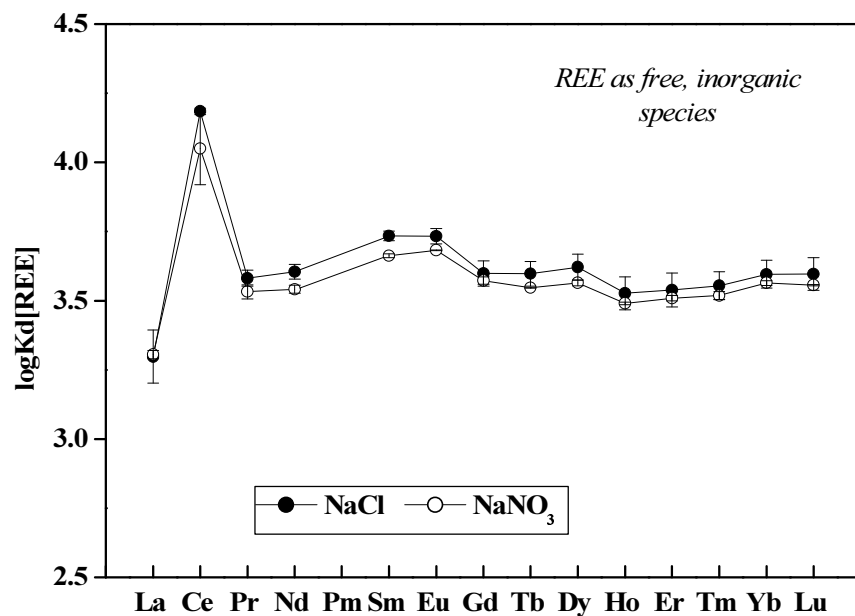


Fig. 2.4. Log K_d^{REE} patterns between MnO₂ suspension and NaCl or NaNO₃ aqueous solution at pH 5 plotted vs. increasing atomic number within REE series, obtained after 12 d. Initial concentration of each REE was 5 ppb and solid phase concentration was 100 mg L⁻¹. Errors bars correspond to σ for two replicates, some errors bars are within the symbol size.

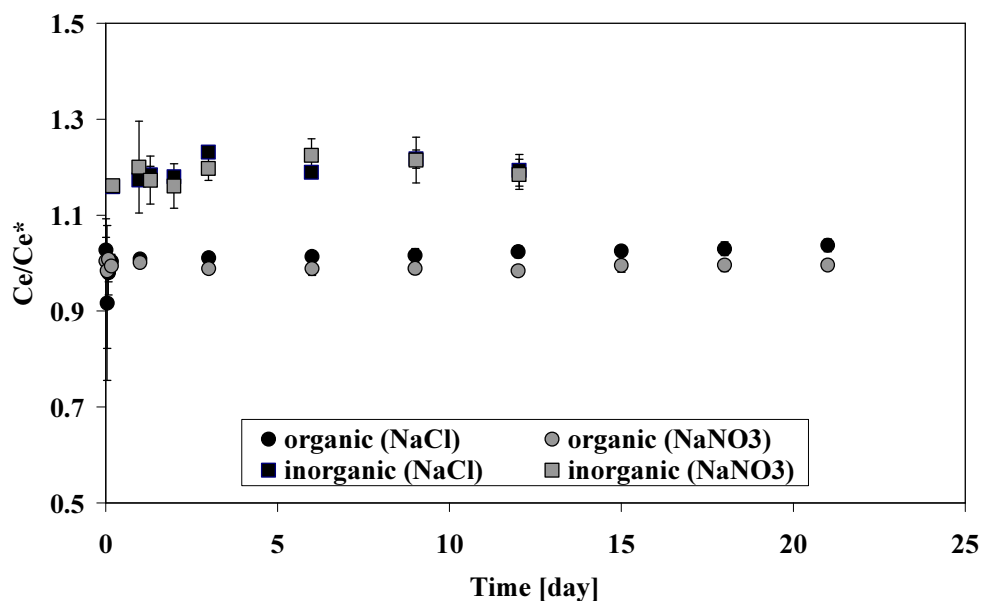


Fig. 2.5. Time variation of Ce-anomaly in the suspension of MnO₂ and NaCl or NaNO₃ at pH 5 expressing the Ce anomaly development. Errors bars corresponds to σ for two replicates in inorganic and three replicates in organic experiments, some errors bars are within the symbol size.

Cerium anomalies, expressed as Ce/Ce* values, are all greater than one and nearly constant over the duration of the adsorption experiments, ranging from 1.16 to 1.23 (Fig. 2.5). These values are slightly lower than those obtained by Ohta and Kawabe (2001) under similar pH conditions.

2.3.3. Organic Experiments at pH 7.5

Figure 2.6 presents the results of sorption experiments of REE(III)-humate complexes onto MnO₂ at pH 7.5. Adsorption kinetics are faster at pH 7.5 (equilibrium reached after 4 d) than at pH 5 (equilibrium reached only after 10 d), while equilibrium $\log K_d^{\text{REE}}_{\text{organic}}$ values are lower than at pH 5. As with the experiments at pH 5, we observe no positive Ce anomaly or tetrad effect at pH 7.5. In addition, ratios of $\log K_d^{\text{REE}}_{\text{organic}}/K_d^{\text{DOC}}$ remain close to 1.0, suggesting that the rise in pH has essentially no effect on the stability of the REE(III)-humate complexes upon adsorption.

2.4. Discussion

2.4.1. Mechanism of Reduction/Suppression of Ce Anomaly and Tetrad Effect

Rare-earth adsorption experiments onto MnO₂ with REE(III) present as REE(III)-humate complexes yield the same trends when compared with inorganic runs, that is (i) slowing down of REE adsorption kinetics, and (ii) suppression or strong reduction of tetrad effect and Ce anomaly development. The trends seem to be essentially independent on the nature of the neutral electrolyte used, since comparable results are obtained in both NaNO₃ and NaCl suspensions even though the final equilibrium $\log K_d^{\text{REE}}_{\text{organic}}$ values appear to be slightly higher in the former (3.40 on average) than in the latter electrolyte (3.23 on average). Thus, although MnO₂ is more oxidizing than ferrous hydroxide with respect to Ce(III) (e.g., Ohta and Kawabe, 2001), adsorption of REE(III)-humate complexes onto MnO₂ leads to reduction/suppression of positive Ce anomaly development in the same way as adsorption of REE(III)-humate onto hydrous ferric oxide (Davranche et al., 2004). In this context, the key question is: how does complexation of REE(III) by humic acid reduce or suppress the development of a positive Ce anomaly at the surface of the MnO₂ oxide?

From the outset, we should stress that the strong reduction or suppression of positive Ce anomaly, as observed in the present organic experiments, does not necessarily mean that all the adsorbed Ce occurs as Ce(III). In fact, the situation regarding Ce oxidation state encountered in these experiments might resemble that obtained during high-pH adsorption of inorganic REE species onto Mn or/and Fe oxyhydroxides. In Mn or Fe oxyhydroxide suspensions where REE occur as inorganic species, the development of a positive Ce anomaly is due to the oxidative scavenging of Ce by MnO₂ (Ohta and Kawabe, 2001). Such a process can be viewed as the combination of (i) oxidation of Ce(III) into Ce(IV) and (ii) preferential sorption of Ce(IV) compared to Ce(III) and the other REE(III) (De Carlo et al., 1998; Bau, 1999; Ohta and Kawabe, 2001). This decoupling of Ce(IV) from the REE(III) during adsorption is due to the change in ionic charge and ionic radius imposed by the oxidation process. However, it is well known that cationic adsorption onto oxides and hydroxides increases with increasing pH. Thus, above a given pH, dissolved REE are quantitatively removed from the solution (Figure 6 in Ohta and Kawabe, 2001). Under such conditions, Ce(IV) may be present on the oxyhydroxide surface, but is masked by the large amount of REE(III) scavenged [no development of a positive Ce anomaly despite the occurrence of Ce(IV)]. This effect of pH on Ce anomaly was studied by De Carlo et al. (1998) and by Ohta and Kawabe (2001) for Fe hydroxide and MnO₂, and by Bau (1999) for Fe hydroxide. According to De Carlo et al. (1998) and Bau (1999) data, the amount of extra Ce scavenged onto Fe hydroxide due to oxidation of Ce(III) to Ce(IV) could not be detected above a pH of ca. 5 (no occurrence of measurable positive Ce anomaly), while Ohta and Kawabe (2001) observed a small but significant positive Ce anomaly in the Fe-OOH-inorganic REE system even above a pH of 5. In the case of MnO₂, a positive Ce anomaly was still present at pH 7 - the highest pH investigated by Ohta and Kawabe (2001) - even though a decrease in the Ce anomaly development was noted above pH of 6.5.

I.2: Adsorption of REE(III)-humate complexes onto MnO₂: Experimental evidence for cerium anomaly and lanthanide tetrad effect suppression

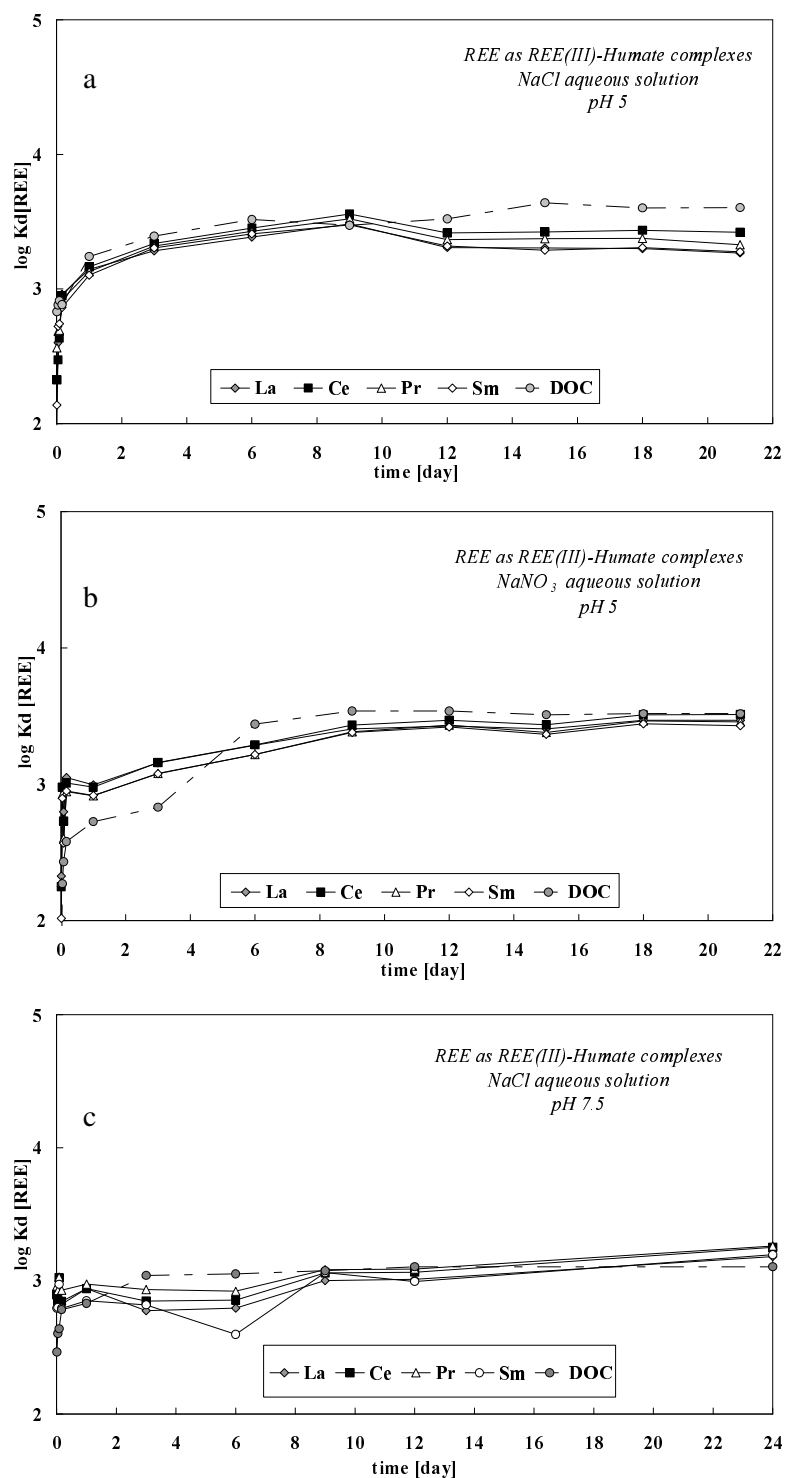


Fig. 2.6. Equilibrium time of $\log K_d^{\text{REE}}_{\text{inorganic}}$ in the suspension of MnO₂ and NaCl (a), NaNO₃ (b) at pH 5 and NaCl (c) at pH 7.5 aqueous solutions, expressing the partitioning of REE-humate complexes between 100 mg solid and 1000 mL water within 3.5 weeks.

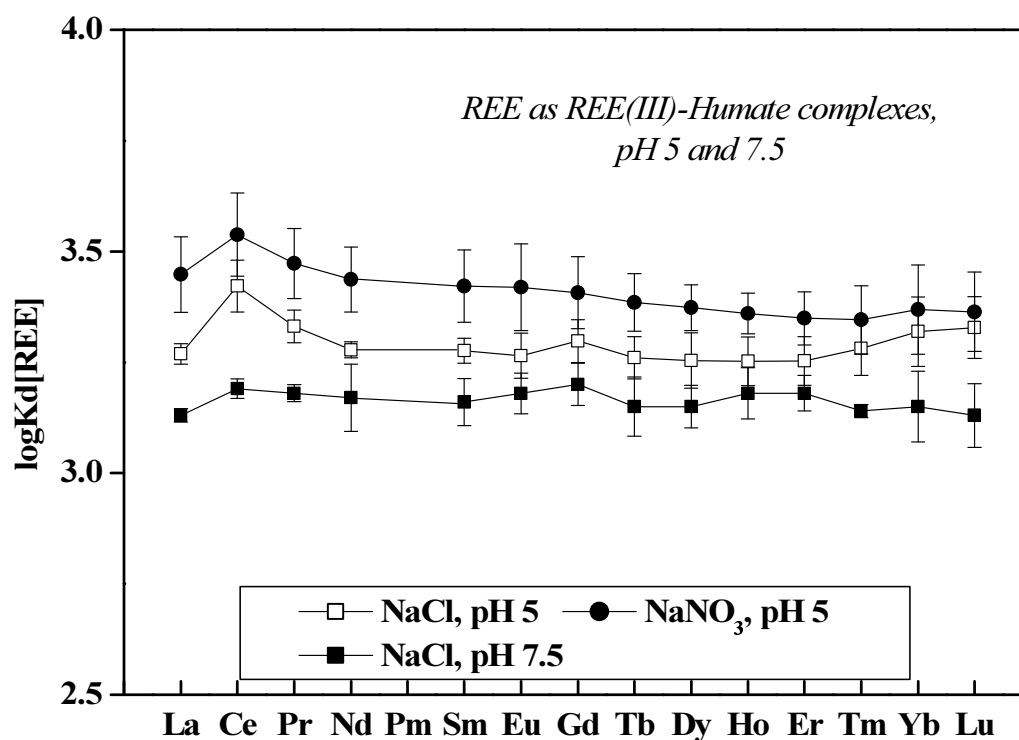


Fig. 2.7. Log K_d^{REE} pattern in the suspension of MnO₂ and NaCl or NaNO₃ at pH 5 and 7.5. Errors bars correspond to σ for three replicates; some errors bars are within the symbol size.

The adsorption of REE(III)-humate complexes is complicated by the fact that the REE, and the high molecular weight organic molecules (humate) to which they are bound, have opposite responses to changes in pH. Humate is adsorbed more strongly at low pH (e.g., Avena and Koopal, 1999), while adsorption of REE is stronger at high pH (Ohta and Kawabe, 2001). Moreover, humate does not selectively complex Ce as compared with the other REE. This is consistent with the regular $\log K_d^{\text{REE}}$ patterns obtained during preparation of the REE(III)-humate complexes (no sign of any preferential Ce complexation). The lack of selectivity in Ce complexation prevents preferential Ce(IV) adsorption, but selectivity is required for the development of a positive Ce anomaly in REE patterns. This may explain (rather than inhibition of Ce(III) oxidation) why positive Ce anomalies were not observed in experiments where REE are present as REE(III)-humate complexes.

The "inhibiting" effect of humate on Ce/REE fractionation is confirmed by comparing results from organic experiments performed at pH 5 and 7.5. Cation or metal ligand complexes, denoted as ML (with M and L representing the cation and the ligand, respectively) can adsorb onto a solid ($\equiv\text{S}$) in two ways to form ternary surface complexes: (i) $\equiv\text{S-LM}$ (cation linked to the mineral surface through the ligand) or (ii) $\equiv\text{S-O-ML}$ (ligand linked to the surface through the cation) (Schindler, 1990; Nowack and Sigg, 1996). The formation of both types of complexes depends on whether the surface groups of the oxide can participate in exchanging their OH^- with the cation-ligand complex, as well as the nature of the complex effectively formed. The reaction depends strongly on pH. When pH is lower than the solid pH_{zpc} (pH at which positive and negative charges occur in equal numbers) adsorption is of anionic type ($\equiv\text{S-LM}$). In the organic experiments performed at pH 5, pH was slightly lower than the pH_{zpc} of the MnO₂ used (5.8). Consequently, anionic adsorption likely prevailed in these experiments:



In such a situation, Ce is not in direct contact with the oxidative MnO₂ surface, so Ce(III) is unlikely to be oxidized into Ce(IV). In the second series of organic experiments, however, pH rises to 7.5, i.e., a value well above the pH_{zpc} of the MnO₂ used. Under such a situation, cationic adsorption could occur, as follows:



In this case, Ce(III) could become oxidized, and Ce/REE fractionation could theoretically develop. However, it appears from Figure 2.5 that no Ce/REE fractionation takes place in the pH-7.5 organic experiments. Unlike the inorganic runs, in which Ce and REE can be adsorbed onto MnO₂ surfaces independently of each other, REE [including Ce(IV)] cannot behave independently from each other in the organic experiments being all collectively bound to humate molecules. Even if Ce is oxidized by the MnO₂ surface, a positive anomaly cannot develop, simply because the process of preferential Ce(IV) sorption cannot proceed due to binding of the entire REE pool to humate.

Comparable suppression of Ce anomaly was noted by Kawabe et al. (1999) and Ohta and Kawabe (2000) for adsorption experiments upon FeOOH in which REE occurred as REE(III)-carbonate complexes. The experimental Ce anomaly was greatly reduced as compared to baseline experiments in which REE occurred as REE(III) aqueous species. These authors suggested that a Ce anomaly could not develop because the Ce(III) complexation kinetics by carbonate are faster than the Ce(III) oxidation kinetics. Thus, according to these authors, the key of "inhibition of Ce anomalies" might be how rapidly Ce(III) is transformed into stable Ce(III) complexes in solution. In the case of REE(III)-humate complexes, the kinetic effect could be added to the above "anionic adsorption" effect to suppress Ce anomaly development. However, the present study does not allow to quantify precisely the role of complexation kinetics since the REE were introduced in the MnO₂ experimental suspensions directly as REE(III)-humate complexes.

Finally, we should point out the lack of any tetrad effect in the log K_d^{REE}_{organic} patterns. We suggested that the appearance of a convex tetrad effect might express a change of coordination state of the REE(III) adsorbed onto either MnO₂ or Fe oxyhydroxide surfaces (Bau, 1999; Ohta and Kawabe, 2001). De Carlo et al. (1998) and Ohta and Kawabe (2001) proposed that REE(III) adsorbed onto MnO₂ are bound to the oxide surface by means of hydroxyl ions, water molecules and oxygen bridges. According to these authors, this coordination would explain the increase of a convex tetrad effect with pH, by increasing the proportion of hydroxyl ions bonding REE(III) to the MnO₂ surface. When REE(III) are complexed by humic acid, the ternary complex thus formed interacts with the MnO₂ surface predominantly via the humate side. This implies that a large part of the REE(III) pool (particularly when pH < pH_{zpc}) is probably not directly bound to the MnO₂ surface. The presence of the lanthanide tetrad effect shows that, during the interaction of dissolved REE(III) with MnO₂, the behaviour of these elements cannot fully be described by differences between their ionic radii, requiring instead changes of the coordination state of the REE(III) adsorbed onto MnO₂. The latter mechanism would be hardly activated in organic experiments, because REE(III) seem less likely to interact directly with the MnO₂ surface owing to the humate complexation.

Moreover, the tetrad effect expresses the differences in Racah parameters for 4f electron repulsion between REE and the oxide surface. Ohta and Kawabe (2001) suggested that Racah parameters in REE(III) ions decrease with increasing covalence of bonding of REE(III) with ligands. If REE-humate complexes are adsorbed onto MnO₂ as ≡S-O-ML (Eqn. 2.5), cationic adsorption), Racah parameters are smaller and, consequently, a conspicuous M-type tetrad effect should be observed. However, the lack of tetrad effect in the log K_d^{REE}_{inorganic} patterns at pH 7.5

suggests that REE(III)-humate complexes are still bound to MnO₂ via the humate side of the complexes under relatively high pH condition, thus favoring the chemical mechanism of Eqn. 2.4. The distribution of REE in humic environments appears to be controlled by the distribution of humate at the solid surface, at least in the pH range investigated here (5 to 7.5).

2.4.2. Comparison with Natural Waters and Inferences on the Use of Ce Anomaly as a Redox Proxy in Paleosols

Shallow organic-rich waters from several continental areas (e.g., western Europe and Africa) have been reported to display small negative Ce anomalies - or no anomaly at all - despite the occurrence of strongly oxidizing conditions and Mn oxides in the associated aquifers (Viers et al., 1997; Braun et al., 1998; Dia et al., 2000; Gruau et al., 2004). Figure 2.8 presents Ce/Ce* vs. Mn and Ce/Ce* vs. DOC plots that illustrate both of these characteristics. The data from the Kervidy-Naizin and Pleine-Fougère catchments in western France are particularly interesting (Dia et al., 2000; Gruau et al., 2004). As can be seen, the hydrochemical data set from these catchments show clear evidence of Mn oxidation and MnO₂ precipitation at the soil-water interface, as reflected by the marked decrease of dissolved Mn concentrations and Eh increase. Nevertheless, Ce/Ce* values remain constant during the Mn oxidation/precipitation process (Fig. 2.8).

In their paper, Dia et al. (2000) stated that "*it is clear that the lack of Ce anomaly development is a rather surprising feature given the redox sensitive chemistry of this element and the occurrence of seasonal redox variations*" in the Kervidy-Naizin catchment. Taking into account the fact that Ce and REE do not occur as free metal ions in these waters, but occur predominantly as dissolved and colloidal organic complexes, Dia et al. (2000) put forward two hypotheses to account for this lack of Ce anomalies: (i) either Ce precipitation and oxidation become impossible because of the complexation of Ce(III) by organic matter or, (ii) CeO₂ are precipitated onto colloids then considered as part of the solution. The experimental data reported in this study favor the first hypothesis, while suggesting that the ultimate cause of the lack of Ce anomalies in these waters is likely to be inhibition of preferential Ce(IV) sorption rather than actual inhibition of the Ce oxidation reaction.

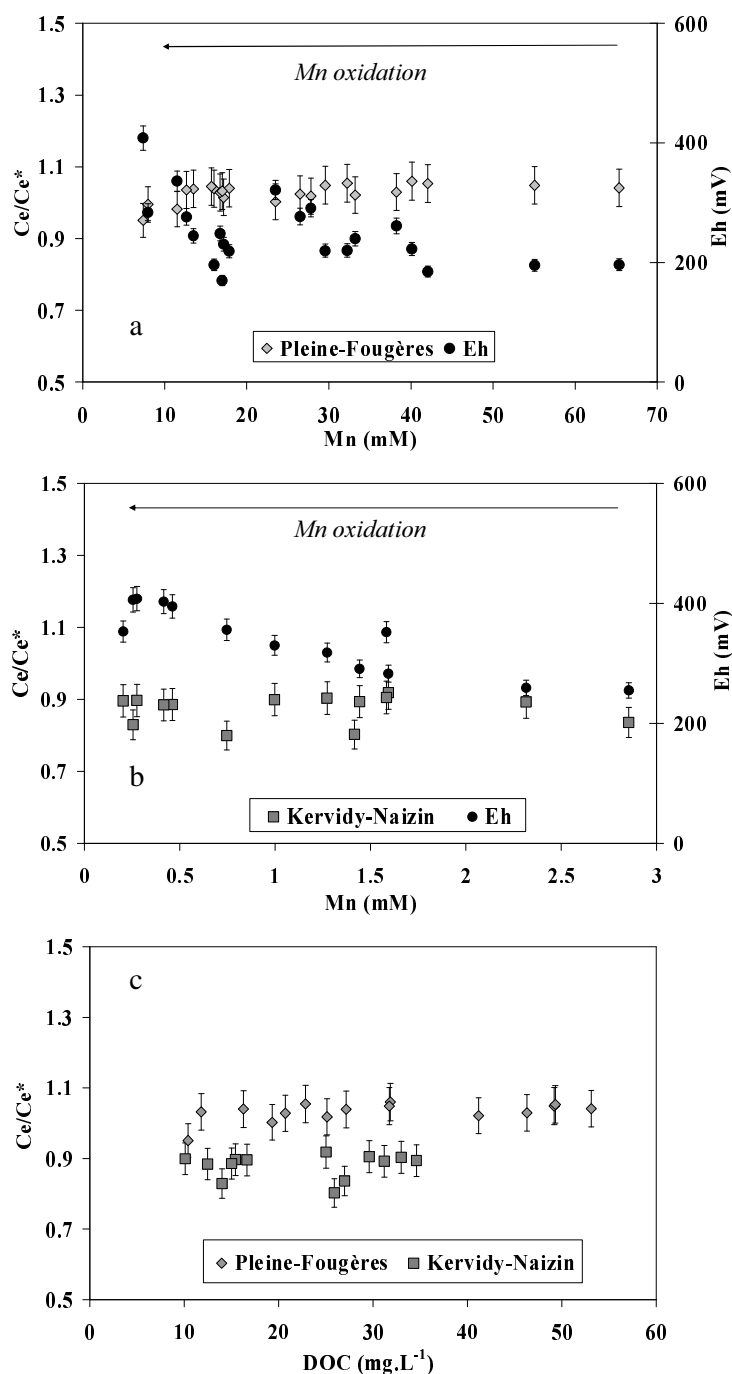


Fig. 2.8. Relationships between Ce/Ce* values, DOC, Mn concentrations, and redox potential (Eh) in organic-rich soil waters from the Pleine-Fougères and Kervidy-Naizin catchments, western France. The data set from the Kervidy-Naizin catchment is particularly meaningful as Ce/Ce* values remain constant in these waters despite the evidence of Mn oxidation and precipitation as shown by the marked decrease of dissolved Mn concentrations and marked Eh increase. Data sources: Dia et al. (2000) and Gruau et al. (2004).

The results of this study have implications on the use of Ce anomalies as paleoclimatic proxies in paleosols. Over the last two decades, many environmental proxies have been investigated in paleosol sequences, including Ce anomalies (Rankin and Childs, 1976; Gallet et al., 1996; Braun et al., 1998). It was considered that the redox state of a paleosol at the time of its formation should correlate with climatic factors such as rainfall intensity or/and ambient atmospheric temperature. From a paleoclimatic point of view, it is indeed possible that wet

periods may lead to the predominance of oxidizing conditions in paleosols due to the continuous recharge of the soil solution by oxygen-rich rainwater, a process that would stabilize Mn oxide phases in the weathering front. Considering solely the inorganic experimental results of Ohta and Kawabe (2001), we would then expect the occurrence of both negative and positive Ce anomalies in paleosols formed under such conditions. However, this would depend on whether the paleosol incorporated the stabilized Mn oxide phases (positive Ce anomaly) or contained secondary mineral phases precipitated from fluids in equilibrium with the Mn oxide (negative Ce anomaly). The present experimental results, on the other hand, show that the complexation of REE(III) by humic substances - a process likely to occur during formation of organic-rich paleosols - could possibly destroy such a pattern by partially inhibiting the development of a positive Ce anomaly on soil Mn oxides. In such a way, this would mean that Ce anomalies are a poor paleo(redox)climatic proxy in paleosols. In previous studies testing the validity of paleoclimatic proxies in the loess-paleosol sequences of China, Gallet et al. (1996) and Jahn et al. (2001) showed that the soils from these sequences yielded variable Ce anomalies, uncorrelated with well-established climatic proxies such as magnetic susceptibility or the chemical alteration/weathering index. In their 2001 paper, Jahn and coworkers failed to find any satisfactory explanation for this discrepancy in terms of climatic variability or differences in pedogenetic or weathering intensity. Thus, the interplay between variable redox conditions and REE(III) organic speciation may lead to complex REE patterns in paleosols that may not unambiguously reflect the climatic conditions at the time of their genesis.

2.5. Summary

The behaviour of free REE(III) species and REE(III)-humate complexes during adsorption onto MnO₂ shows that humate complexation strongly modifies the sorptive properties of REE. Time-series experiments indicate that a stationary exchange equilibrium is reached within less than 10 h when dissolved REE(III) are present as inorganic species and about 10 d when present as REE(III)-humate complexes. Humate complexation also strongly reduces or even suppresses the development of positive Ce anomalies and M-type lanthanide tetrad effects. Humates have a strong REE complexation capacity, but this is coupled with their inability to form complexes preferentially with Ce, thus preventing the preferential adsorption of Ce(IV) necessary to develop positive Ce anomalies during adsorption of the REE onto MnO₂. The inhibition of the lanthanide tetrad effect is attributed to sorption of REE humate complexes where the REE(III)-humate moiety is bound to MnO₂ surface through the humate side of complexes, thereby precluding any change in the REE coordination number necessary for observation of tetrad effect. Ce(III) may also be separated physically from direct interaction with the MnO₂ surface, such that Ce oxidation is inhibited.

The new experimental data presented here show that Ce anomalies may not be a reliable proxy of redox conditions in organic-rich waters or in precipitates formed in equilibrium with waters rich in humic substances. These data also help to explain the insignificant negative Ce anomalies or total absence of anomalies observed in shallow organic-rich groundwaters, despite the development of strongly oxidizing conditions in these waters and the presence of MnO₂ in the aquifer.

Deuxième Partie
Modélisation

1. Organic complexation of rare earth elements in natural waters: evaluating model calculations from ultrafiltration data

Cette partie est extraite d'un article soumis à Geochimica et Cosmochimica Acta, Pourret O., Davranche M., Gruau G. and Dia A. (2006) Organic complexation of rare earth elements in natural waters: evaluating model calculations from ultrafiltration data.

Résumé- Les modèles Stockholm Humic Model (SHM) et Humic Ion-Binding Models V et VI ont été comparés quant à leur capacité à prédire le rôle de la matière organique dans la spéciation des terres rares (REE) dans les eaux naturelles. A la différence de Models V et VI, SHM fait partie d'un modèle plus complet permettant de tenir compte des phénomènes de dissolution/précipitation, adsorption/désorption et oxydation/réduction. Trois séries de données ont été utilisées pour cette comparaison: (i) une eau de rivière mondiale moyenne, précédemment étudiée avec Model V, (ii) deux eaux naturelles riches en matières organiques, dont la spéciation des REE a précédemment été déterminée avec Model V et par ultrafiltration, et (iii) des expériences d'ultrafiltration effectuées sur des eaux de nappes de sols de pH neutres ($6.2 < \text{pH} < 7.1$), riches en matières organiques ($7 < \text{Carbone Organique Dissous (COD)} < 20 \text{ mg L}^{-1}$) provenant des bassins-versants de Kervidy-Naizin et du Petit-Hermitage (France). Ces trois séries ont été réexaminées en utilisant SHM et Model VI. Model VI et SHM ont donné des résultats comparables pour l'eau de rivière mondiale moyenne confirmant les résultats déjà publiés. La comparaison des résultats modélisés avec les données calculées et d'ultrafiltration déjà publiées suggèrent que Model VI est capable de prédire de façon fiable la spéciation des REE avec la matière organique dans des eaux de nappes et de rivières acides ($4.5 < \text{pH} < 5.5$) et riches en COD ($\sim 20 \text{ mg L}^{-1}$). Cependant, SHM prédit une complexation organique des REE plus faible que l'ultrafiltration et peut donc être remis en cause. De plus, les résultats fournis par Model VI sont plus proches des données d'ultrafiltration que SHM, pour des eaux de nappes riches en matières organiques ($7 < \text{COD} < 20 \text{ mg L}^{-1}$), de pH neutres ($6.2 < \text{pH} < 7.1$). La correction électrostatique de SHM induit une déprotonation des substances humiques (HM) plus faible que Model VI. Cette faible déprotonation est couplé à une plus forte concurrence entre les REE et les cations majeurs en solution (Fe, Al et Ca) et entre les matières organiques et les carbonates. La complexation organique des REE calculée par SHM est donc plus faible. De façon générale, SHM doit être amélioré pour concurrencer Models V et VI quant à leur capacité à calculer la spéciation organique des REE dans les eaux naturelles. De plus, les données présentées dans cette étude montrent qu'un grand soin doit être apporté dans l'utilisation des données d'ultrafiltration pour valider les modèles de spéciation. La présence possible de colloïdes inorganiques riches en REE et/ou de molécules organiques non-humiques sont aussi à prendre en considération.

Abstract- Stockholm Humic Model (SHM) and Humic Ion-Binding Models V and VI were compared for their ability to predict the role of organic matter in the speciation of rare earth elements (REE) in natural waters. Unlike Models V and VI, SHM is part of a wider model also allowing for dissolution/precipitation, sorption/desorption, and oxidation/reduction reactions, which makes this model particularly interesting. Three datasets were used for the comparison purposes: (i) World Average River Water, previously investigated using Model V, was reinvestigated using SHM and Model VI; (ii) two natural and organic-rich waters, whose REE speciation have already been determined with both Model V and ultrafiltration, were also reinvestigated using these two models; and (iii) ultrafiltration experiments were carried out at circumneutral-pH ($6.2 \leq \text{pH} \leq 7.1$), and organic-rich ($7 \leq \text{Dissolved Organic Carbon (DOC)} \leq 20 \text{ mg L}^{-1}$) groundwaters from the Kervidy-Naizin and Petit-Hermitage catchments, western France. The results obtained were compared with those from the same waters using both Model VI and SHM. Model VI and SHM yielded comparable results for World Average River Water confirming earlier finding that a large fraction of the REE carried in solution by circumneutral, low DOC rivers occurs as organic complexes. Comparisons of the model results with published and newly obtained ultrafiltration data suggest that Model VI is reliable in calculating the speciation of REE with organic matter in acidic ($4.5 \leq \text{pH} \leq 5.5$), DOC-rich ($\text{DOC} \sim 20 \text{ mg L}^{-1}$) ground- and river waters. However, SHM predicts lowest REE organic complexation than ultrafiltration and is thus less reliable. Moreover, Model VI is a closer model from ultrafiltration data than SHM for DOC-rich ($7 \leq \text{DOC} \leq 20 \text{ mg L}^{-1}$), circumneutral pH ($6.2 \leq \text{pH} \leq 7.1$)

groundwaters. In SHM, electrostatic correction implies lower Humic Material (HM) deprotonation than in Model VI. This is coupled to stronger REE competition with major cations (Fe, Al and Ca) and stronger competition between HM and carbonates, and led to predict lower REE organic complexation. Overall, SHM needs to be improved to become a reliable alternative to Model V and Model VI for establishing the organic speciation of REE in natural waters. Moreover, the data reported here show that great care should be exercised in the use of ultrafiltration data to validate or invalidate speciation models. Possible presence of REE-rich inorganic colloid and/or of non-humic organic molecules are indeed unable to complex the REE in the ultrafiltered waters.

1.1. Introduction

The aquatic geochemistry of rare earth elements (REE) has been the subject of numerous studies in the past two decades (Elderfield and Greaves, 1982; De Baar et al., 1988; Elderfield et al., 1990; De Baar et al., 1991; Sholkovitz, 1995; Byrne and Sholkovitz, 1996; Johannesson et al., 2000; Nelson et al., 2004). The identical trivalent charge among the REE series results in comparable chemical behaviour, allowing these elements to be used as tracers of geochemical processes in natural waters (Smedley, 1991; Gosselin et al., 1992; Johannesson et al., 1997; Johannesson and Hendry, 2000; Janssen and Verweij, 2003). REE come from the dissolution of rock-forming minerals and there have been reported cases in which the REE patterns of the waters closely resemble those of their source rocks (Smedley, 1991; Johannesson et al., 1997). However, the extent to which the REE patterns in natural waters are controlled by that of the source rocks is not fully assessed (Johannesson et al., 1999; Dia et al., 2000; Aubert et al., 2001). Processes such as REE complexation by inorganic ligands, or REE adsorption onto solid mineral phases can fractionate the REE. As an example, Johannesson et al. (1999) showed that both the preferential complexation of the heavy REE (HREE) by carbonate ligands and the larger affinity of minerals for the light REE (LREE) resulted in strong HREE enrichments in the groundwaters of a tuffaceous alluvial aquifer. It is also well established that REE adsorption onto Fe- and Mn-oxides may result in negative Ce anomalies in waters due to the oxidative scavenging onto these metallic oxides (Viers et al., 1997; Dupré et al., 1999; Dia et al., 2000; Davranche et al., 2004; Gruau et al., 2004; Davranche et al., 2005). Finally and most importantly, it is now well established that complexation of REE with natural organic ligands is of prime importance for REE speciation in natural waters. This importance has for the most part been deduced from recent ultrafiltration studies or electrochemical measurements of organic rich waters (Tanizaki et al., 1992; Viers et al., 1997; Dupré et al., 1999; Dia et al., 2000; Ingri et al., 2000; Johannesson et al., 2004).

Consequently, it is essential to develop models to predict the REE complexation with organic matter in natural waters. For that purpose, intrinsic equilibrium constants for REE-proton exchange with humic substances are needed. A few REE binding constants to humic material (HM) have been published either for individual REE (e.g., Bidoglio et al., 1991; Moulin et al., 1992; Lead et al., 1998; Lippold et al., 2005) or for the whole REE series (Yamamoto et al., 2005; Sonke and Salters, 2006). However, datasets may be difficult to homogenize and do not allow to obtain sufficiently good fit for a direct use in an number of speciation models. To circumvent this problem, authors have estimated REE intrinsic equilibrium constants using published complexation constants for REE with lactic and acetic acid. These estimated constants were integrated in thermodynamics models dealing with metal complexation by HM to test their ability to predict REE organic complexation. The most succeeded attempt made in this way was done by Tang and Johannesson (2003). They used a modified version of the metal-ion speciation model Humic Ion-Binding Model V (Tipping, 1994) to predict REE complexation with HM. Comparison between model calculation and ultrafiltration studies of REE speciation in six natural water samples (Tang and Johannesson, 2003) were made to validate Model V. However,

Model V is not a widespread model which takes into account dissolution/precipitation, adsorption/desorption, oxidation/reduction reactions absolutely necessary to determine the speciation of REE in natural waters.

In this study, the ability of the Stockholm Humic Model (SHM) to predict REE complexation by organic matter was tested (Gustafsson, 2001a; Gustafsson et al., 2003). This model was selected because it is included in a full chemical equilibration model allowing a complete set of complex reactions to be modelled (Visual MINTEQ; Gustafsson, 2001b). The aim of this study is also to compare SHM with Model VI, which is the latest version of Humic Ion Binding Model (Tipping, 1998). The same method of the REE constants estimation necessary to run both models as that developed by Tang and Johannesson (2003) was used. For the comparison purpose, the following three-step approach was used: firstly, World Average River Water, previously investigated using Model V by Tang and Johannesson (2003), was reinvestigated using Model VI and SHM. Secondly, two of the six ultrafiltered, organic-rich natural waters used by Tang and Johannesson (2003) to validate Model V, were reinvestigated using SHM and Model VI. Finally, new ultrafiltration experiments were carried out for circumneutral-pH ($6.2 < \text{pH} < 7.1$), organic-rich ($7 < \text{Dissolved Organic Carbon (DOC)} < 20 \text{ mg L}^{-1}$) groundwaters from the Kervidy-Naizin and Petit-Hermitage catchments, western France. These were compared to speciation results obtained using both Model VI and SHM. The present work is thus also a new step in the evaluation and in the understanding of the ability of models to predict REE complexation by organic matter because such models have been compared so far to only a limited number of ultrafiltration results (Tang and Johannesson, 2003). In this paper, the term *organic matter-bound REE solution complex* is used in the same way as in Tang and Johannesson (2003), namely to include REE complexed to both low- and high-molecular weight (MW) organic matter.

1.2. Material and methods

1.2.1. Model description

1.2.1.1. Humic Ion Binding Model VI (Model VI)

Humic Ion-Binding Model VI (hereafter denoted as Model VI) is the latest version of a model developed by Tipping and co-workers in the early 1990s (Tipping and Hurley, 1992; Tipping, 1994; Tipping, 1998). Model VI is a discrete site/electrostatic model for proton and metal ion interactions with fulvic and humic acids. The thermodynamic basis of the model has been further presented and discussed elsewhere (e.g. Tipping, 1998). Briefly, the model assumes that proton and metal complexation by organic matter takes place by way of two types of discrete sites (Type A and Type B sites) having strong and weak binding affinities, respectively. Each type of site is defined by (i) an intrinsic proton binding constant (pK_A and pK_B), (ii) a "spread factor" (ΔpK_A and ΔpK_B), describing proton binding constant variability, and (iii) a numerical constant (n_A and n_B), referring to the number of sites. Model VI accounts for most of the binding capacity by considering metal complexation with single H^+ sites (monodentate) or with pairs of H^+ sites (bidentate), whose proportion is described by the proximity factor (f_{pr}). In the model, n_A (mol g^{-1}) stands for the number of Type A sites (associated with carboxylic groups) and $n_B = n_A/2$ (mol g^{-1}) for the number of Type B sites (commonly associated with weaker groups such as phenolic sites).

Type A and Type B sites have separate intrinsic binding constants for metals ($\log K_{MA}$ and $\log K_{MB}$) - each associated with a parameter ΔLK_1 - defining the spreads of values around the medians. A second parameter, ΔLK_2 , takes into account a small number of stronger sites (bidentate and tridentate sites). By considering results from many data sets, a universal average value of ΔLK_1 is obtained, and a correlation established between $\log K_{MB}$ and $\log K_{MA}$ (Tipping,

1998). Thus, only one single adjustable parameter ($\log K_{MA}$) is necessary to fully describe metal binding in Model VI. Moreover, all the above parameters can be derived and fixed separately for fulvic (FA) and humic acids (HA). This allows the model to be used for investigating metal interactions with both the more soluble, lower MW FA fraction and the less soluble, higher MW HA fraction. The model parameters necessary to run Model VI are presented in Table 1.1 (based on Tipping, 1998).

As shown by Tipping (1998) and Tipping et al. (2002), updating Model V to Model VI resulted in an overall improvement of the predictive abilities of the model in many cases. The main difference between the two models is a better account of the binding site heterogeneity by Model VI than by Model V. This is achieved both by allowing complexation with tridentate sites to occur in Model VI and by introduction in Model VI of two new adjustable parameters, ΔLK_1 and ΔLK_2 , to describe the distribution of binding strength.

Parameter	Description	Values
n_A	Amount of type A sites (mol g^{-1})	$4.8 \cdot 10^{-3}$ (FA), $3.3 \cdot 10^{-3}$ (HA)
n_B	Amount of type B sites (mol g^{-1})	$0.5 \times n_A$
pK_A	Intrinsic proton dissociation constant for type A sites	3.2 (FA), 4.1 (HA)
pK_B	Intrinsic proton dissociation constant for type B sites	9.4 (FA), 8.8 (HA)
ΔpK_A	Distribution terms that modifies pK_A	3.3 (FA), 2.1 (HA)
ΔpK_B	Distribution terms that modifies pK_B	4.9 (FA), 3.6 (HA)
$\log K_{MA}$	Intrinsic equilibrium constant for metal binding at type A sites	Fitted from experimental data
$\log K_{MB}$	Intrinsic equilibrium constant for metal binding at type B sites	$3.39 \log K_{MA} - 1.15$
ΔLK_1	Distribution term that modifies $\log K_{MA}$	2.8 (REE)
ΔLK_2	Distribution term that modifies the strengths of bidentate and tridentate sites	$0.55 \log K_{NH3} = 0.29$ (REE)
P	Electrostatic parameter	-115 (FA), -330 (HA)
K_{sel}	Selectivity coefficient for counterion accumulation	1
f_{prB}	Fraction of proton sites that can make bidentate sites	Calculated from geometry
f_{prT}	Fraction of proton sites that can make tridentate sites	Calculated from geometry
M	Molecular weight	1500 (FA), 15000 (HA)
r	Molecular radius	0.8 nm (FA), 1.72 nm (HA)

Table 1.1. Model VI parameters (Tipping, 1998).

1.2.1.2. Stockholm Humic Model (SHM)

The Stockholm Humic Model (SHM) is an integrated part of the chemical equilibrium model Visual MINTEQ (Gustafsson, 2001b), which enables solution speciation to be modelled along with adsorption/desorption, dissolution/precipitation and redox reactions. The principles of SHM have been fully presented and discussed elsewhere by Gustafsson (2001a) and Gustafsson et al. (2003). Where applicable, Gustafsson (2001a) gave to SHM parameters the same acronyms as those of corresponding parameters in Models VI, for sake of consistency.

SHM is a discrete-ligand model in which the FA and HA are assumed to have eight proton-binding sites with distinct acid-base characteristics. In this model, seven adjustable parameters (n_A , n_B , $\log K_A$, $\log K_B$, ΔpK_A , ΔpK_B and g_f) are required to describe the proton dissociation reaction. As with Model VI, these parameters can be derived and fixed separately for FA and HA, allowing investigation of metal interactions with both the FA and HA fractions. Table 1.2 lists the fixed values derived for these seven parameters by Gustafsson (2001a) for FA and HA. In this study, we select for these parameters the generic values listed in the "shmgeneric.mdb" database as they are average values obtained from a large number of aquatic FA and HA samples (Gustafsson, 2001b). In SHM, three parameters are required to model the complexation of metals with organic matter, i.e. the monodentate complexation constant K_{Mm} , the bidentate complexation constant K_{Mb} , and the ΔLK_2 parameter, which determines the degree of binding site heterogeneity.

Parameter	Description	Values
n_A	Amount of type A sites (mol g^{-1})	$5.4 \cdot 10^{-3}$ (FA), $3.55 \cdot 10^{-3}$ (HA)
n_B	Amount of type B sites (mol g^{-1})	$1.62 \cdot 10^{-3}$ (FA), $1.78 \cdot 10^{-3}$ (HA)
$\log K_A$	Intrinsic proton dissociation constant for type A sites	-3.51 (FA), -4.13 (HA)
$\log K_B$	Intrinsic proton dissociation constant for type B sites	-8.81 (FA), -8.99 (HA)
ΔpK_A	Distribution term that modifies $\log K_A$	3.48 (FA), 3.03 (HA)
ΔpK_B	Distribution term that modifies $\log K_B$	2.49 (FA), 3.03 (HA)
$\log K_{Mm}$	Intrinsic equilibrium constant for monodentate complexation of metal M	Fitted from experimental data
$\log K_{Mb}$	Intrinsic equilibrium constant for bidentate complexation of metal M	Fitted from experimental data
ΔLK_2	Distribution term that modifies the strengths of complexation sites	0.29 (REE)
r	Molecular radius	0.75 nm (FA), 1.8 nm (HA)
C	Stern layer capacitance	2 F m^{-2}
N_s	Site density of HS functional groups	1.2 sites nm^{-2}
A_s	Specific surface area of HS	Calculated from geometry using r and N_s
g_f	Gel fraction parameters	0.72 (FA) 0.78 (HA)
K_c	Intrinsic equilibrium constant for the accumulation of screening counterions	universal value: $10^{0.8}$

Table 1.2. SHM parameters (Gustafsson, 2001b).

However, the $\log K_{Mm}$ and $\log K_{Mb}$ dataset - reported by Milne et al. (2001; 2003) for a large number of trace metals - show these two constants to be much the same for HA and FA. Thus, a single set of $\log K_{Mm}$ and $\log K_{Mb}$ values can be introduced into SHM to describe metal complexation by both HA and FA (Gustafsson, personal communication). Moreover, as HA and FA have different proton-binding and electrostatic properties, the overall metal affinity is thus different.

1.2.1.3. Model differences

Besides the fact that SHM may use two complexation constants (K_{Mm} and K_{Mb}) against only one for Model VI, the main difference between the two models is the electrostatic term. Model VI considers that humic compounds can be represented as rigid spheres of homogenous size, carrying metal-humic binding sites on their surface with different binding strength and allowing bidentate and tridentate binding configuration to occur. Electrostatic effects are corrected in this model with equations based on the Debye-Hückel and Gouy-Chapman theories, assuming a homogeneous electrical double layer at the surface of each sphere (Tipping, 1998). In SHM, a discrete-site approach is employed in which eight sites of different acid strength are considered. The bulk of the humic substances is considered to form gels. These are primarily treated as impermeable spheres and electrostatic interactions on the surfaces are modelled using equations based on the Basic Stern Model (see Gustafsson (2001a) for further details).

1.2.2. Estimation of models constant values for the REE

To simulate REE complexation with humic substances, constant values must be known for each REE to be input in Model VI and SHM, respectively. The REE complexed with humic substances will be denoted as LnHM thereafter. Gustafsson (2001a) displayed that trivalent cation (e.g. Al) organic complexation are better fitted if only bidentate binding are involved. Thus, $\log K_{Mb}$ is only needed to calculate LnHM in SHM. Some datasets can be fitted but they generally provide poor fits as indicated by their high root mean square (rms) errors (e.g. Sonke and Salters, 2006). Existing experimental data provide representative $\log K_{MA}$ values only for EuFA, EuHA, DyFA and DyHA complexation (Lead et al., 1998; Tipping, 1998), and $\log K_{Mb}$ value only for EuHa complexation (Gustafsson, 2001b). Therefore, a method is required to estimate REE $\log K_{MA}$ and $\log K_{Mb}$ necessary to run the models. The constants are estimated by the same extrapolation method used by Tang and Johannesson (2003). The method is based on Tipping's observation (Tipping, 1994; Tipping, 1998) that a linear free-energy relationship exists

between $\log K_{MA}$ and $\log K$ for metal-lactic acid (LA) and metal-acetic acid (AA) complexation or the first hydrolysis (OH) constant of metal (thereafter denoted as $\log K(AA)$, $\log K(LA)$ and $\log K(OH)$). The same approach is applied for $\log K_{Mb}$ in SHM. Tables 1.3 and 1.4 list $\log K_{MA}$ and $\log K_{Mb}$ values describing the complexation of numerous metals with HA and FA (data from Tipping, 1998, and Gustafsson, 2001b). In addition, $\log K(AA)$, $\log K(LA)$, $\log K(OH)$, $\log K_2(AA)$, $\log K_2(LA)$ and $\log K_2(OH)$ (bidentate constants) for the same metals are listed in these tables (values are from NIST Database; Martell and Smith, 1998).

Metals	$\log K(LA)$	$\log K(AA)$	$\log K(MOH)$	$\log K_{MA}(HA)$	$\log K_{MA}(FA)$	ΔLK_2
Mg ²⁺	1.37	1.27	2.60	0.70	1.10	0.12
Ca ²⁺	1.45	1.18	1.30	0.70	1.30	0.0
Sr ²⁺	0.97	1.14	0.82	1.11	1.20	0.0
Mn ²⁺	1.43	1.4	3.40	0.60	1.70	0.58
Co ²⁺	1.90	1.46	4.35	1.10	1.40	1.22
Ni ²⁺	2.22	1.43	4.14	1.10	1.40	1.57
Cu ²⁺	3.02	2.22	6.50	2.00	2.10	2.34
Zn ²⁺	2.22	1.57	5.00	1.50	1.60	1.28
Cd ²⁺	1.70	1.93	3.09	1.30	1.60	1.48
Pb ²⁺	2.78	2.68	6.40	2.00	2.20	0.93
Al ³⁺	3.30	2.57	9.00	2.60	2.50	0.46

Table 1.3. Log K for metal complexation with lactic acid (LA), acetic acid (AA), and the first hydrolysis (OH), and $\log K_{MA}$ for HA and FA (from Tipping, 1998), used to obtain linear free-energy relationship equations between the $\log K_{MA}$ and $\log K$ for each ligand. Log K for AA, LA and OH are from NIST Database (Martell and Smith, 1998) at 25°C and zero ionic strength.

Metals	$\log K_2(LA)$	$\log K_2(AA)$	$\log K_2(OH)$	$\log K_{Mb}$
Ca ²⁺	2.45	-	-	-11.30
Mn ²⁺	2.10	-	5.8	-
Cu ²⁺	4.84	3.63	11.8	-5.80
Zn ²⁺	3.75	1.36	10.2	-9.00
Cd ²⁺	2.74	2.86	7.7	-9.30
Pb ²⁺	3.61	4.08	10.9	-6.15
Al ³⁺	5.97	4.55	17.9	-4.20
Co ²⁺	3.07	1.10	9.2	-10.10

Table 1.4. Log K for metal complexation with lactic acid (LA), acetic acid (AA), and hydrolysis (OH), and $\log K_{Mb}$ for HA and FA (from Gustafsson and van Schaik, 2003), used to obtain linear free-energy relationship equations between $\log K_{Mb}$ and $\log K$ for each ligand. Log K for LA, AA and OH are from NIST Database (Martell and Smith, 1998) at 25°C and zero ionic strength.

Studentized residuals (i.e. the residual divided by its standard error; Ramsey, 1969) were used to detect and remove outliers cations (Cd and Th). Good linear correlations exist between the $\log K_{MA}$ and $\log K_{Mb}$, and their hydrolysis constant, or constants with LA and AA (Figs. 1.1 and 1.2).

The linear regression curves and correlation coefficients describing these relationships are as follows:

$$\log K_{MA}(HA) = 0.76 \log K(LA) - 0.21 \quad R^2 = 0.80 \quad (1.1)$$

$$\log K_{MA}(FA) = 0.52 \log K(LA) + 0.58 \quad R^2 = 0.78 \quad (1.2)$$

$$\log K_{MA}(HA) = 1.03 \log K(AA) - 0.43 \quad R^2 = 0.80 \quad (1.3)$$

$$\log K_{MA} (FA) = 0.75 \log K (AA) + 0.36 \quad R^2 = 0.87 \quad (1.4)$$

$$\log K_{MA} (HA) = 0.24 \log K (OH) + 0.32 \quad R^2 = 0.78 \quad (1.5)$$

$$\log K_{MA} (FA) = 0.17 \log K (OH) + 0.91 \quad R^2 = 0.83 \quad (1.6)$$

$$\log K_{Mb} = 1.89 \log K_2 (LA) - 15.13 \quad R^2 = 0.81 \quad (1.7)$$

$$\log K_{Mb} = 1.49 \log K_2 (AA) - 11.80 \quad R^2 = 0.82 \quad (1.8)$$

$$\log K_{Mb} = 0.57 \log K_2 (OH) - 13.86 \quad R^2 = 0.73 \quad (1.9)$$

These equations are subsequently used to estimate $\log K_{MA}$ (Table 1.5), and $\log K_{Mb}$ (Table 1.6) for REE complexation with HA and FA. $\log K(AA)$, $\log K(LA)$ and $\log K(OH)$ used for REE are from the NIST Database (Martell and Smith, 1998). The 95 % confidence intervals are reported along with the range of published $\log K(LA)$, $\log K(AA)$ and $\log K(OH)$ for REE on Figs. 1.1 and 1.2. However, as Tables 1.5 and 1.6 show, there are differences in the estimated $\log K_{MA}$ and $\log K_{Mb}$ depending on the equation. The difficulty in estimating $\log K_{MA}$ (Table 1.5) and $\log K_{Mb}$ (Table 1.6) using the linear free-energy relationships method was already encountered by Tang and Johannesson (2003). Therefore, the estimated values listed in Tables 1.5 and 1.6 are compared to the few stability $\log K_{MA}$ and $\log K_{Mb}$ obtained by fitting available experimental dataset using either Model VI and SHM (Tipping 1998; Gustafsson, 2001b). For the reasons already outlined, only "best-fit" $\log K_{MA}$ and $\log K_{Mb}$ (rms errors < 0.1) are considered for the comparison purpose, which limits the comparison solely to Eu and Dy. The $\log K_{MA}$ estimated from the first hydrolysis constants (Eqn. 1.5 and 1.6) are too low: e.g., $\log K_{MA} = 1.78$ for EuHA and $\log K_{MA} = 1.97$ for EuFA, against 2.1 and 2.4 determined by Tipping (1998). The same is true for DyHA and DyFA complexation: i.e., $\log K_{MA} = 1.74$ and 1.93, respectively, as obtained from Eqn. 1.5 and 1.6, against 2.9 and 2.5 obtained by Tipping (1998). By contrast, $\log K_{MA}$ estimated from Eqn. 1.1 and 1.3 for EuHA and DyHA complexes, and from Eqn. 1.2 and 1.4 for EuFA and DyFA complexes, better fit the literature data (e.g., 2.47 and 2.44 for EuFA, respectively, from Eqn. 1.2 and 1.4, against 2.36). $\log K_{MA}$ estimated from Eqn. 1.1 and 1.3, and Eqn. 1.2 and 1.4 for LREE are close (standard deviation are less than 0.16). By contrast, $\log K_{MA}$ estimated from Eqn. 1.1 and 1.3, and Eqn. 1.2 and 1.4 for HREE are different (standard deviation increasing with atomic number from 0.14 to 0.41). Consequently, selected $\log K_{MA}$ could not be averages of estimated $\log K_{MA}$ using Eqn. 1.1 and 1.3 for HA and Eqn. 1.2 and 1.4 for FA (Table 1.5). According to Yamamoto et al. (2005) complexation experiments of REE with fulvic acid, the characteristics of $\log K$ of the REE-fulvate complex is similar to that of diacetate. Carboxylic group seems to be the major binding site of REE in fulvic acid (Yamamoto et al., 2005). Moreover, acetate represents a model molecule of simple carboxylic sites on complex organic matter, such as humic and fulvic acids (Wood, 1993). Thus, adopted $\log K_{MA}$ are $\log K_{MA}$ estimated from Eqn. 1.3 and 1.4, for HA and FA, respectively (Table 1.5).

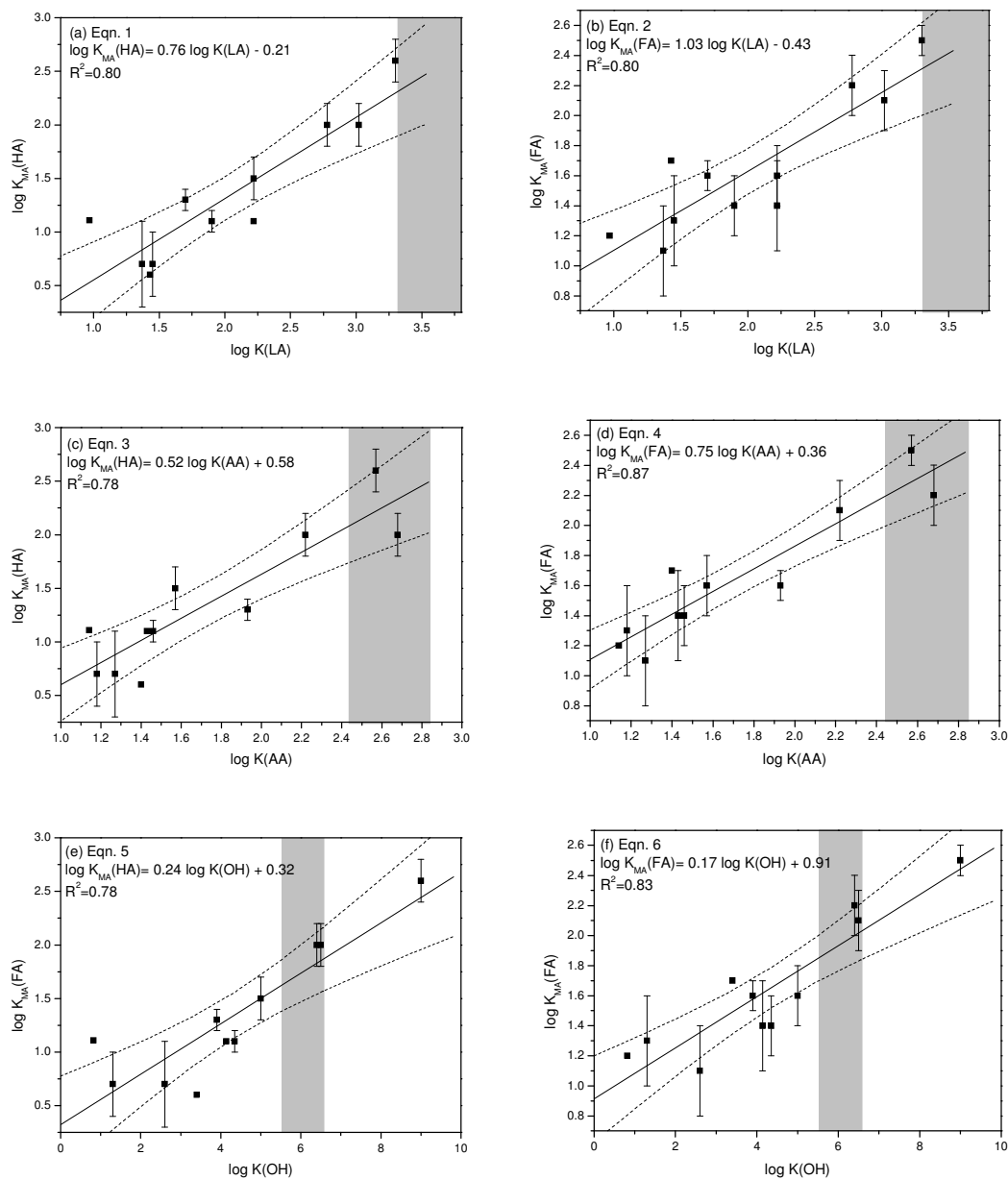


Fig. 1.1. Linear free-energy relationships between $\log K_{MA}$ and $\log K(LA)$, $\log K(AA)$ and $\log K(OH)$ listed in Table 1.2. $\log K(LA)$, $\log K(AA)$ and $\log K(OH)$ are from NIST Database (Martell and Smith, 1998), and $\log K_{MA}$ are from Tipping (Tipping, 1998). Dash lined represent 95 % confidence intervals and shaded area represents REE field (see text for details). Standard deviation are plotted when available.

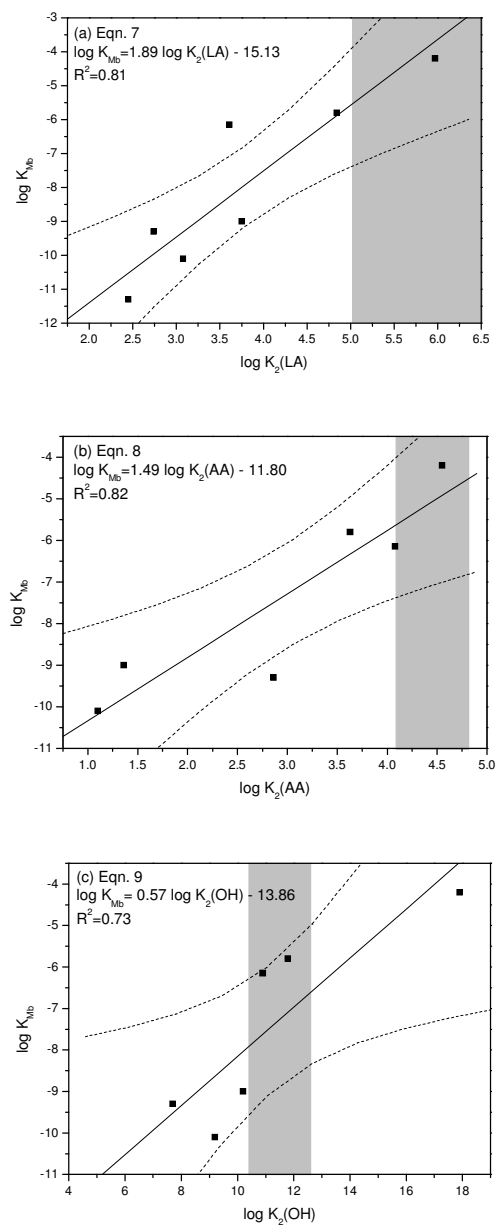


Fig. 1.2. Linear free-energy relationships between $\log K_{Mb}$ and $\log K_2(LA)$, $\log K_2(AA)$ and $\log K_2(OH)$ listed in Table 1.5. The AA, LA and OH constants values are from NIST Database (Martell and Smith, 1998), and the values of $\log K_{Mb}$ are from "shmgeneric" Database (Gustafsson, 2001b). Dash lined represent 95 % confidence intervals and shaded area represents REE field (see text for details).

REE	log K_{MA} (HA)				log K_{MA} (FA)			
	From LA (Eqn. 1.1)	From AA (Eqn. 1.3)	From OH (Eqn. 1.5)	Adopted estimated values	From LA (Eqn. 1.2)	From AA (Eqn. 1.4)	From OH (Eqn. 1.6)	Adopted estimated values
La	2.30	2.20	1.62	2.20	2.30	2.27	1.85	2.27
Ce	2.45	2.25	1.66	2.25	2.40	2.31	1.88	2.31
Pr	2.46	2.30	1.71	2.30	2.40	2.35	1.92	2.35
Nd	2.47	2.32	1.74	2.32	2.41	2.37	1.93	2.37
Sm	2.53	2.50	1.76	2.50	2.45	2.49	1.95	2.49
Eu	2.56	2.42	1.78	2.42	2.47	2.44	1.97	2.44
Gd	2.54	2.31	1.74	2.31	2.46	2.36	1.93	2.36
Tb	2.56	2.20	1.76	2.20	2.47	2.27	1.95	2.27
Dy	2.55	2.13	1.74	2.13	2.47	2.23	1.93	2.23
Ho	2.59	2.09	1.74	2.09	2.49	2.20	1.93	2.20
Er	2.60	2.07	1.76	2.07	2.50	2.18	1.95	2.18
Tm	2.62	2.11	1.81	2.11	2.51	2.21	1.98	2.21
Yb	2.64	2.21	1.81	2.21	2.53	2.28	1.98	2.28
Lu	2.72	2.13	1.83	2.13	2.58	2.23	2.00	2.23

 Table 1.5. Summary of estimated log K_{MA} for the REE.

REE	log K_{Mb}			
	From LA (Eqn. 1.7)	From AA (Eqn. 1.8)	From OH (Eqn. 1.9)	Adopted estimated values
La	-5.74	-5.66	-10.73	-5.66
Ce	-5.02	-5.60	-10.63	-5.60
Pr	-4.68	-5.13	-10.62	-5.13
Nd	-4.55	-5.04	-10.44	-5.04
Sm	-4.32	-4.65	-10.34	-4.65
Eu	-4.15	-4.79	-10.32	-4.79
Gd	-4.41	-5.04	-10.32	-5.04
Tb	-4.11	-5.40	-10.21	-5.40
Dy	-3.83	-5.50	-10.21	-5.50
Ho	-3.70	-5.57	-10.15	-5.57
Er	-3.32	-5.65	-10.15	-5.65
Tm	-3.15	-5.71	-10.10	-5.71
Yb	-2.94	-5.30	-10.10	-5.30
Lu	-2.83	-5.50	-10.10	-5.50

 Table 1.6. Summary of estimated log K_{Mb} for the REE.

This choice is supported by the fact that the field of estimated REE log K_{MA} with AA is within the 95 % confidence intervals whereas the field with LA is outside those intervals. This is illustrated by the shaded zones on Figs. 1.1 and 1.2.

Estimates of log K_{Mb} , constants calculated with Eqn. 1.7, 1.8 and 1.9 strongly differ, ca. four orders of magnitude for the LREE and ca. seven orders of magnitude for the HREE (Table 1.6). The log K_{Mb} for EuHM complex estimated from the first hydrolysis constants (-10.32; Eqn. 1.9) is lower than the literature value (-4.65; Gustafsson, 2001b). By contrast, log K_{Mb} estimated from Eqn. 1.7 and 1.8 for EuHM complexation, is close to the literature value (-4.15 and -4.79 for EuHM from Eqn. 1.7 and 1.8, respectively, against -4.65 in Gustafsson, 2001b). Moreover, log K_{Mb} estimated from Eqn. 1.7 and 1.8 for LREE and HREE are different (standard deviation

increasing with atomic number from 0.06 to 1.89). Therefore, adopted $\log K_{Mb}$ could not be an average of estimated $\log K_{Mb}$. By analogy with $\log K_{MA}$, $\log K_{Mb}$ use in SHM, are $\log K_{Mb}$ estimated with the metal-AA constants (Eqn. 1.8). However, due to a fewer number of data, the confidence intervals are wider and thus estimated constants are less constrained as compared to that recovered with Model VI.

1.2.3. Ultrafiltration set up and chemical analyses

To further test the ability of SHM and Model VI to predict REE complexation with organic matter, new ultrafiltration experiments were performed on four circumneutral-pH ($6.2 < \text{pH} < 7.1$), organic-rich ($7 < \text{DOC} < 20 \text{ mg L}^{-1}$) groundwater samples (PF1, PF3, F7 and F14). These samples were taken from two wetlands located in the Kervidy-Naizin and Petit-Hermitage catchments, in western France. These groundwaters have already been intensively studied for their DOC and REE chemistry (Dia et al., 2000; Olivié-Lauquet et al., 2001; Gruau et al., 2004).

Samples were collected in November 2004 from shallow piezometers (0.5 to 1.5 m deep). The pH was measured in the field with a combined Sentix 50 electrode. The accuracy of pH measurements is estimated at ± 0.05 pH unit. About 60 mL of each sample were immediately filtered on site, through 0.2 μm cellulose acetate filter (Sartorius Minisart). An aliquot of 30 mL was acidified on site and subsequently used to measure major and trace cation concentrations. The remaining 30 mL were not acidified and used to measure alkalinity, major anions and DOC concentrations. For each sample, an extra 1 L aliquot was collected. This extra aliquot was filtered through 0.2 μm cellulose acetate membrane using a Sartorius Teflon filtration unit. Thirty mL of the filtrate were acidified and used to re-measure major and trace cation concentrations (including REE), while 10 mL were used to re-measure the major anions and DOC content. Ultrafiltration experiments were performed with the remaining filtrate. Ultrafiltrations were carried out with 15 mL centrifugal tubes equipped with permeable membranes of decreasing pore size cut off (Millipore Amicon Ultra-15): 30 kDa (Da = Dalton), 10 kDa and 5 kDa. Each centrifugal filter device was washed and rinsed with HCl 0.1 N and MilliQ water two times before use. Centrifugations were performed using a Jouan G4.12 centrifuge equipped with swinging bucket at 3000 g for 20 minutes and 30 minutes, for 30 kDa and 10 kDa, and 5 kDa devices, respectively. Each of the four investigated samples (PF1, PF3, F7 and F14) was ultrafiltered in duplicate. All experiments were performed at room temperature: 20 ± 2 °C. For further details about ultrafiltration experiments see Pourret et al. (2006a).

Alkalinity was determined by potentiometric titration with an automatic titrator (794 Basic Titrino Methrom). Major anions (Cl^- , SO_4^{2-} and NO_3^-) concentrations were measured by ionic chromatography (Dionex DX-120). Major cations and trace elements concentrations were determined by ICPMS (Agilent 4500), using indium as an internal standard. Dissolved organic carbon (DOC) was analysed on a total organic carbon analyzer (Shimadzu TOC-5050A). Typical uncertainties on anion and cation measurements as established from repeated analyses of standard solutions (SLRS 4 geostandard water solution for cations; K-biphtalate solutions for DOC; Dionex seven anions standard solutions for anions) are estimated at $< \pm 4$ % for anions and at $< \pm 5$ % for all other measured species.

All procedures (sampling, filtration, storing and analysis) were carried out in order to minimize contamination. Samples were stored in acid-washed Nalgene polypropylene containers before analyses. Blank concentrations for DOC and REE were $< 0.5 \text{ mg L}^{-1}$ and $< 1 \text{ ng L}^{-1}$, respectively. All presented DOC concentrations are blank corrected (maximum correction = 8 %). For the REE, there was no need for blank corrections, the sample concentrations being systematically two to three orders of magnitude higher than blank levels. The instrumental error on REE analysis in our laboratory as established from repeated analyses of multi-REE standard solution (Accu TraceTM Reference, USA) and of the SLRS-4 water standard is $< \pm 2$ % (Dia et al., 2000; Davranche et al., 2004; Gruau et al., 2004; Davranche et al., 2005).

1.3. Comparing the predicting ability of SHM and Models V and VI

Speciation calculations were performed using the computer programs WHAM 6 (Version 6.0.13) and Visual MINTEQ (Version 2.40) which includes Model VI and SHM, respectively. Each model was modified by integrating a database, which included our adopted $\log K_{MA}$, and $\log K_{Mb}$ for REE complexation with humic substances and well-accepted, infinite dilution (25°C) stability constants for REE inorganic (sulphate and carbonate) complexes (Lee and Byrne, 1992; Millero, 1992; Lee and Byrne, 1993; Klungness and Byrne, 2000; Luo and Byrne, 2004). Up-to-date default values of $\log K_{MA}$, $\log K_{Mm}$ and $\log K_{Mb}$ are used for competing cations (Tipping, 1998; Gustafsson, 2001b).

To test the validity of SHM for predicting REE complexation with organic matter, and to compare SHM to Models V and VI, three water samples, previously investigated by Tang and Johannesson (2003) using Model V, were selected and re-analyzed with Model VI and SHM. These include (i) a modelled, moderately organic-rich ($DOC \sim 5 \text{ mg L}^{-1}$) sample of World Average River Water composition; and (ii) two acidic, organic-rich ($18 < DOC < 24 \text{ mg L}^{-1}$) water samples from the Nsimi-Zoetele catchment, Cameroon, Africa (Viers et al., 1997). The former was selected because the REE speciation for World Average River Water is expected to control some key features of REE cycling in the hydrosphere, such as the REE pattern of seawater or the processes of REE transport and REE fractionation in rivers and estuaries (e.g. Sholkovitz, 1995). The latter were selected because they are acidic, DOC-rich waters on which ultrafiltration data are available (Viers et al., 1997), providing thus a reference basis to interpret "modelled" data on low pH, DOC-rich waters. The four newly ultrafiltered water samples from the Kervidy-Naizin and Petit Hermitage catchments (France), were then, chosen to provide a reference basis for the case of circumneutral pH, DOC-rich waters.

1.3.1. World Average River Water

The same mean concentrations of major ions, Fe and Al such as those used by Tang and Johannesson (2003) were adopted for re-calculating the REE speciation (see Table 11 in Tang and Johannesson, 2003). The same value of 5 mg L^{-1} for DOC was used. It was also assumed that 80 % and 20 % of humic material is made up of FA and HA, respectively. Moreover, because pH is crucial to REE speciation, the REE speciation calculations were performed in the same way these authors (op. cit.) did, i.e. holding the major solute composition constant (except HCO_3^- and CO_3^{2-}) and varying pH. The results obtained are shown for La, Eu, and Lu in Figs. 1.3 (Model VI) and 1.4 (SHM), respectively.

Model VI results show that REE occur as free species (Ln^{3+}) and complexed to sulphate (LnSO_4^+) at acidic pH and complexed to carbonates (LnCO_3^+ and $\text{Ln}(\text{CO}_3)_2^-$) at alkaline pH (Fig. 1.3). In circumneutral pH, REE will occur in solution as a bulk (i.e. > 50 %) complexed to HM. Model VI predicts that LREE (e.g. La) predominantly occur in solution as organic complexes in the pH range between 5.2 and 9.5, MREE (e.g. Eu) in the pH range between 4.3 and 9.5, whereas HREE (e.g. Lu) occur complexed to HM for pH between 5.4 and 7. The pH value at which the proportion of LnHM species is maximum decreases from La (7) to Lu (6). LREE and MREE are more complexed to HM (maximum of 95 %) than HREE (60 %). These results are consistent with earlier investigations performed using Model V (Tang and Johannesson, 2003). The only noticeable difference as regards to Model V is that Model VI calculates significantly higher proportions of REE complexed with organic matter under high pH conditions (Model VI predicts, for example, LaHM ~ 60 % at pH 9, whereas Model V predicts only 10 % of LaHM).

SHM results show that REE occur as free species (Ln^{3+}) and complexed to sulphate (LnSO_4^+) at acidic pH and complexed to carbonates (LnCO_3^+ and $\text{Ln}(\text{CO}_3)_2^-$) at alkaline pH (Fig. 1.3). In circumneutral pH, LREE and MREE will occur in solution as a bulk (i.e. > 50 %) complexed to HM whereas HREE occur as complexed to HM only for minor fraction (maximum

of 35 %). SHM predicts that LREE (e.g. La) predominantly occur in solution as organic complexes in the pH range between 6.3 and 9.1, MREE (e.g. Eu) in the pH range between 5.6 and 8.9, whereas HREE (e.g. Lu) occur complexed to HM (> 30 %) for pH between 6 and 7.5. The pH value at which the proportion of LnHM species is maximum decreases from La (7.75) to Lu (6.75). LREE and MREE are more complexed to HM (maximum of 95 %) than HREE (35 %). However, three important differences are noted with respect to Models V and VI: (i) the pH at which LnHM is maximum is about 0.75 pH unit higher with SHM (Fig. 1.4) than with Model VI (Fig. 1.3); (ii) the range of LnHM as predominant species is larger with Model VI than with SHM. LaHM is > 50 % for 4.3 pH unit with Model VI whereas it is only the major species for 2.8 pH unit with SHM; finally (iii) the proportion of LnHM species calculated for alkaline pH is larger with Models VI than with SHM (Figs. 1.3 and 1.4 of this study; see Fig. 4 in Tang and Johannesson, 2003).

At any rate, the results of our REE speciation calculations using Model VI and SHM for World Average River Water confirm the earlier conclusion of Tang and Johannesson (2003) that a bulk of REE dissolved in rivers are carried to the oceans as dissolved organic ligand complexes. The major consequence is that dissolved organic ligand complexes of the REE are, at least, as important as carbonate complexes in circumneutral to alkaline river waters. However, determining which of Models V and VI or SHM gives the most reliable description of REE speciation in natural waters is clearly difficult on the basis of modelled data alone. Experimental studies involving direct measurement of the REE speciation is needed.

1.3.2. Mengong and Mar 2 samples

Mengong and Mar 2 samples are two samples of organic-rich, acidic waters whose REE speciation was firstly investigated by ultrafiltration (Viers et al., 1997), and subsequently modelled with Model V (Tang and Johannesson, 2003). Because most of DOC is distributed in larger MW size fractions in these waters (Viers et al., 1997), Tang and Johannesson (2003) assumed that 80 % of DOC is composed of high MW HA, the remaining 20 % being composed of low MW FA. The same assumption is used in the model calculations. The pH values (Mengong = 4.62 and Mar 2 = 5.5) and the major solutes, DOC, Fe and Al concentrations reported in Viers et al. (1997), used in calculations are the same as those used by Tang and Johannesson (2003). Table 1.7 lists proportions of organic REE complexation obtained here with Model VI and SHM, and by Tang and Johannesson (2003) with Model V.

Speciation calculations performed with Model VI suggest that between 46 and 90 % and > 98 % of the REE dissolved in Mengong and Mar 2 samples, respectively, occur as organic complexes. The remainder of each REE occurs as free species (Ln^{3+}). These results are in good agreement with Model VI, although some differences appeared between the models for HREE in the more acidic sample Mengong (see Table 1.7; Table 8 in Tang and Johannesson, 2003).

SHM calculations confirm these high proportions for Mar 2 sample. Nevertheless, SHM predicts a lower REE organic complexation (between 69 and 86 %; Table 1.7) than model VI. Calculations for Mengong sample are more contrasted. SHM indicates much lower proportions of organic-REE complexes (27 % to 36 %, depending on the REE against 46 to 90 % in Model VI; Table 1.7). The remainder of each REE occurs as free species (Ln^{3+}).

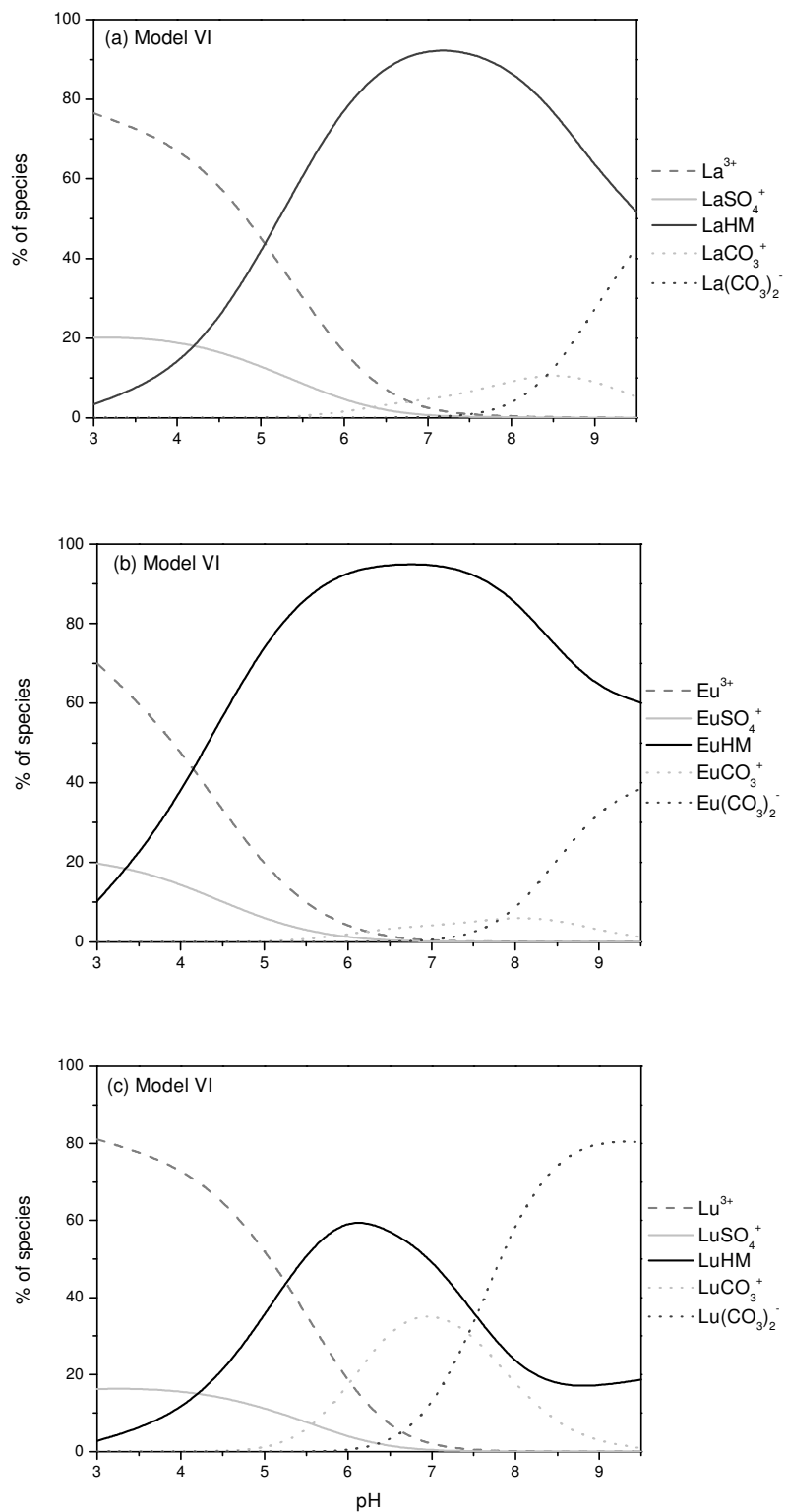


Fig. 1.3. Model VI speciation calculations for (a) La, (b) Eu and (c) Lu in World Average River Water as a function of pH.

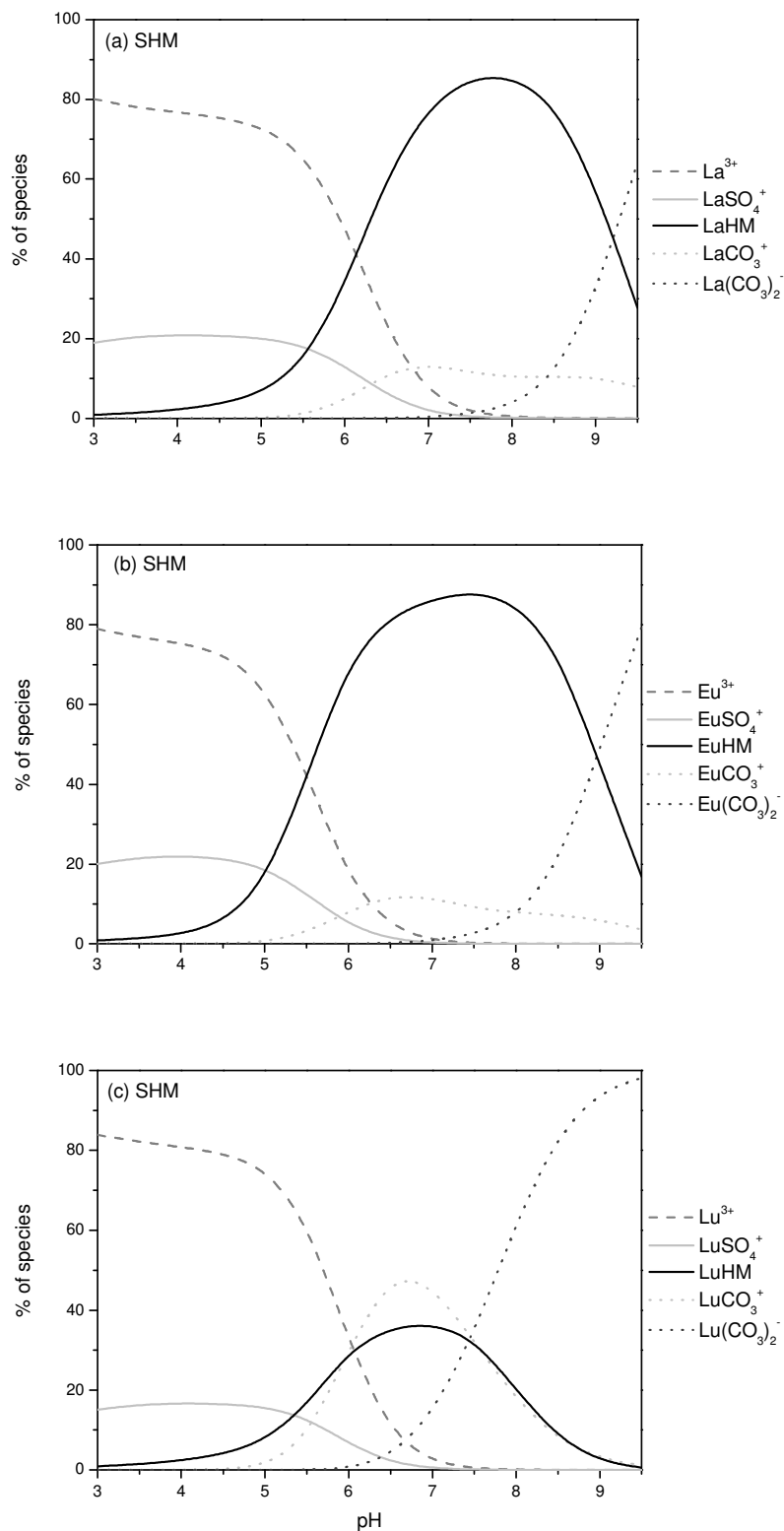


Fig. 1.4. SHM speciation calculations for (a) La, (b) Eu and (c) Lu in World Average River Water as a function of pH.

	Mengong				Mar 2			
	Ultrafiltration	Model V	Model VI	SHM	Ultrafiltration	Model V	Model VI	SHM
	% LnHM	% LnHM	% LnHM	% LnHM	% LnHM	% LnHM	% LnHM	% LnHM
La	100	63	60	27	100	87	99	70
Ce	100	72	65	27	100	91	99	70
Pr	100	76	71	30	100	92	100	77
Nd	100	77	74	31	100	93	100	79
Sm	100	86	90	36	100	96	100	86
Gd	100	80	73	31	100	94	100	78
Tb	100	77	60	28	100	93	99	72
Dy	100	75	52	28	100	92	99	71
Ho	100	75	48	28	100	92	98	70
Er	100	75	46	27	100	93	98	69
Tm	100	77	50	27	100	93	98	69
Yb	100	78	61	29	100	93	99	73
Lu	100	81	52	28	100	95	99	71

Table 1.7. Proportions of LnHM complexes calculated with Model V (Tang and Johannesson, 2003), Model VI and SHM for Mengong and Mar 2 waters. Fraction of LnHM complexes previously estimated for these two samples by ultrafiltration experiments are shown for comparison (Viers et al., 1997).

Proportions of REE organic complexes measured by ultrafiltration for Mengong and Mar 2 samples are reported in Table 1.7 (Viers et al., 1997). Comparison of these proportions with those calculated by the models shows that Models V and VI are closer from ultrafiltration results than SHM. This is particularly well evidenced by Mar 2 results. The difference between the ultrafiltration data and model results is less than 5 % when Models V and VI are used, while a ~ 25 % deviation is observed with SHM (Table 1.7). For Mengong sample (the more acidic sample), Model VI predictions slightly differ from ultrafiltration (between 10 and 54 %) whereas SHM calculations strongly differ from ultrafiltration (between 64 and 73 %).

Consequently, only Model VI might be a valuable speciation model in predicting REE speciation in low-pH, organic-rich natural waters. Note, however, that for the more acidic sample (Mengong) Models VI calculates weaker complexation proportions, as regards to ultrafiltration data.

1.3.3. Kervidy-Naizin and Petit Hermitage groundwater samples

1.3.3.1. Ultrafiltration data

Concentrations of major anions, and of major and trace cations (including REE) and DOC in the 0.2 μm filtrates, are presented in Table 1.8, along with alkalinity and pH data. Concentrations of REE, Fe, Mn and DOC in the three ultrafiltrated fractions (i.e. < 30 kDa, < 10 kDa, < 5 kDa) are presented in Table 1.9 (mean of two analyses). These results are further displayed in REE (Fe) vs. DOC variation diagrams in Fig. 1.5.

	PF1	PF3	F7	F14
T (°C)	10.6	10.7	10.6	10.4
pH	7.08	6.93	6.19	6.4
Cl	47507	36871	69133	52825
SO ₄	10234	8569	61710	35020
NO ₃	2091	45939	570	430
DOC	17.25	7.66	11.12	21.49
Na	14440	12760	35090	19960
Mg	17930	12470	11180	6476
Al	107	73	16	107
K	492	321	548	301
Ca	8567	6454	28960	24440
Fe	955	99	1431	2462
Mn	31	10	1193	512
La	0.176	0.804	0.518	1.389
Ce	0.365	1.889	1.299	3.105
Pr	0.055	0.255	0.175	0.426
Nd	0.239	1.105	0.812	1.828
Sm	0.0502	0.194	0.202	0.441
Eu	0.0104	0.0368	0.0406	0.0923
Gd	0.0401	0.135	0.206	0.43
Tb	0.0048	0.0135	0.0287	0.0606
Dy	0.0256	0.0669	0.182	0.363
Ho	0.0049	0.0126	0.04	0.0708
Er	0.0147	0.035	0.128	0.204
Tm	0.0021	0.0048	0.0185	0.029
Yb	0.0149	0.0304	0.123	0.182
Lu	0.0027	0.0052	0.0203	0.0284
Alkalinity	1867	385	1318	623

Table 1.8. Major solute REE concentrations (in ppb) except for DOC concentrations (in mg L⁻¹) and alkalinity (in μmol L⁻¹) for studied groundwaters.

The fact that the positive correlations displayed in Fig. 1.5 yield negative Y axis intercepts strongly suggest that the bulk of the REE is linked to the colloidal phase in these waters. However, interpreting ultrafiltration data is not a trivial task and caution must be exercised before using this type of data to validate speciation models. A recurrent problem of ultrafiltration studies is that mineral colloids (e.g. Fe and Mn oxyhydroxides) can be present in the waters along with organic colloids, some of them being potentially strong competitors of organic matter for REE complexation (e.g. Fe oxyhydroxides; Bau, 1999; Dupré et al., 1999). The presence of mineral colloids may lead to an overestimation of the proportion of REE that are effectively complexed by humic substances. Thus, it is especially important to carefully evaluate whether the REE decrease - which occurs when PF1, PF3, F7 and F14 waters are ultrafiltered - is accompanied solely by a decrease of the DOC content, or whether this decrease also occurs with a decrease in Fe concentrations.

Three of the four investigated waters (i.e. PF1, F7 and F14) present a significant decrease in their Fe content upon ultrafiltration. However, the decrease in Fe content concerns only the 30 kDa ultrafiltration step (Fig. 1.5) After this step, the Fe content of the four samples is equally very low. This decrease corresponds to a marked change in the slope of the REE vs. DOC linear relationships otherwise observed in the REE vs. DOC variation diagrams (Fig. 1.5). This behaviour is particularly well illustrated by sample PF1 in which ca. 80 % of the REE and 96 % of the Fe, but only 9 % of the DOC, are removed during the first ultrafiltration step. Moreover, it appears that the magnitude of the change in the slope of the REE-DOC linear relationships is correlated to the Fe/ΣREE ratio of the waters. The Fe/ΣREE ratio of PF1 before ultrafiltration is

950, whereas the Fe/ Σ REE ratios of F7, F14 and PF3 are 377, 285 and 22 respectively. Such a relationship strongly suggests that the "colloidal" REE budget of samples PF1, F7 and F14 is controlled, in part, by REE-bearing Fe colloids and that the Fe-colloid/organic-colloid ratio varies in these samples as follows: PF1 \gg F7 > F14 \gg PF3.

The REE colloidal pool of PF1, F7 and F14 samples was corrected for the contribution of the Fe-colloid fraction. The Fe colloid-free REE budget of these waters can be estimated by extrapolating linearly the relationship defined by the < 5 kDa, < 10 kDa and < 30 kDa results at the DOC content of the < 0.2 μ m fraction (point A in Fig. 1.5). The linear correlation defined by the DOC and REE contents of the four ultrafiltered fractions of PF3 (i.e. the water sample clearly depleted in Fe colloid) is a confirmation that the organic fractions must define a linear correlation in the REE vs. DOC variation plots. This interpretation is supported by the fact that the angle in the slope of the REE vs. DOC correlations defined by the three Fe colloid-bearing waters (i.e. PF1, F7 and F14) decreases when the Fe/REE ratio of the raw waters decreases. This indicates that the REE and DOC contents have to be linearly correlated in the Fe-free waters.

Another problem encountered during ultrafiltration studies of organic-rich waters appears when the Y axis intercept of the REE vs. DOC correlations is negative (Fig. 1.5). The likely interpretation for this, is that (i) 100 % of the REE present in the waters are bound to organic molecules and (ii) the organic pool is not solely composed of humic substances, but also contains a significant proportion of low MW organic molecules that do not complex REE. In such waters, the key question is: can the amplitude of the REE-free organic fraction be estimated? In other words, how much DOC must be removed from the waters to estimate the amount of HA and FA that effectively complex the REE? Considering the PF3 results, there is a possibility that this amount could correspond to the Y = 0 intercept on the X axis obtained by linearly extrapolating the REE vs. DOC relationships (points B in Fig. 1.5). Moreover, such an observation can be validated by both previously published ultrafiltration data (Tanikazi et al., 1992; Sholkovitz, 1995; Ingri et al., 2000) and Johannesson et al. (2004) observations that all of the "dissolved" La in organic rich waters of a swamp in south-eastern Virginia, was "complexed" with organic ligands.

In the following, ultrafiltration corrections were performed as earlier mentioned. It was assumed that all the REE left in the < 5 kDa fraction are complexed with the low molecular FA fraction. This amount is obtained by subtracting the DOC content of point B in Fig. 1.5, from the < 5 kDa fraction. The initial REE concentration of the sample that can be partitioned between the humic molecules and the true dissolved fraction (i.e. free REE species and the carbonate and sulphate complexes) is considered to correspond to the REE content given by point A in Fig. 1.5 (i.e. the REE content of the < 0.2 μ m fraction of the samples minus the fraction linked to the Fe colloid). Thus, the amount of REE complexed with the HA fraction is assumed to correspond to the REE content of point A minus the < 5 kDa fraction. Proportions of calculated LnHA complexes are listed in Table 1.10 for each REE. Proportions are minimum for PF3 and F7 (65 and 76 %, respectively, on average), but maximum for PF1 and F14 (77 and 83 %, respectively, on average). Given the correlations shown in Fig. 1.5, the assumption can be made that the remaining REE are linked to the low MW FA fraction. LnFA calculated fractions are, on average: 23 % for PF1, 35 % for PF3, 24 % for F7 and 17 % for F14. Thus, the LnFA/LnHA ratios of the four ultrafiltered samples were estimated to be: 0.30 for PF1; 0.54 for PF3, 0.31 for F7 and 0.21 for F14 (Table 1.10).

However, the hereabove calculations are strongly dependent on the validity of the correction/estimation procedures used to remove the contribution of Fe colloids and calculate the FA/HA ratio of the waters. A test of this validity is shown below, where the "corrected/estimated" ultrafiltration data were compared with the modelled results. If the results of this test are positive - i.e. the modelling and ultrafiltration approaches yield convergent results - this will confirm the ability of the models to predict the speciation of REE in the four

investigated water samples. Taking into account that the correction procedures of ultrafiltration data are independent of the modelling approach.

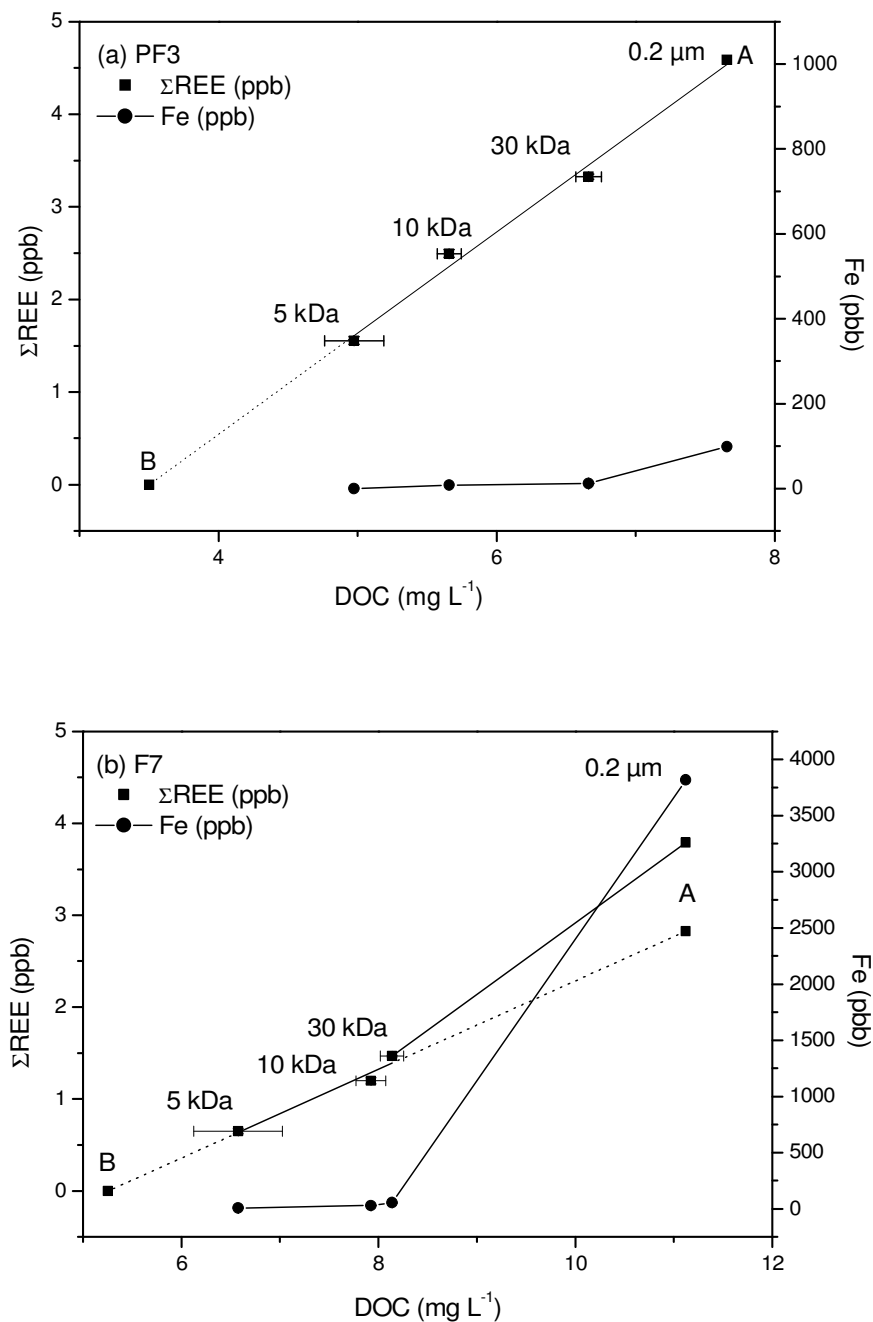


Fig. 1.5. Σ REE and Fe concentrations as a function of DOC concentrations in the successive filtrates ($< 0.2 \mu\text{m}$, $< 30 \text{ kDa}$, $< 10 \text{ kDa}$, $< 5 \text{ kDa}$) for (a) PF3, (b) F7, (c) F14, (d) PF1. Errors bars correspond to standard deviation for two replicates, some errors bars are within the symbol size. Point A represents the extrapolated REE bound only to humic substances point and point B is the projection of 0 REE point (see text for details) (to be continued).

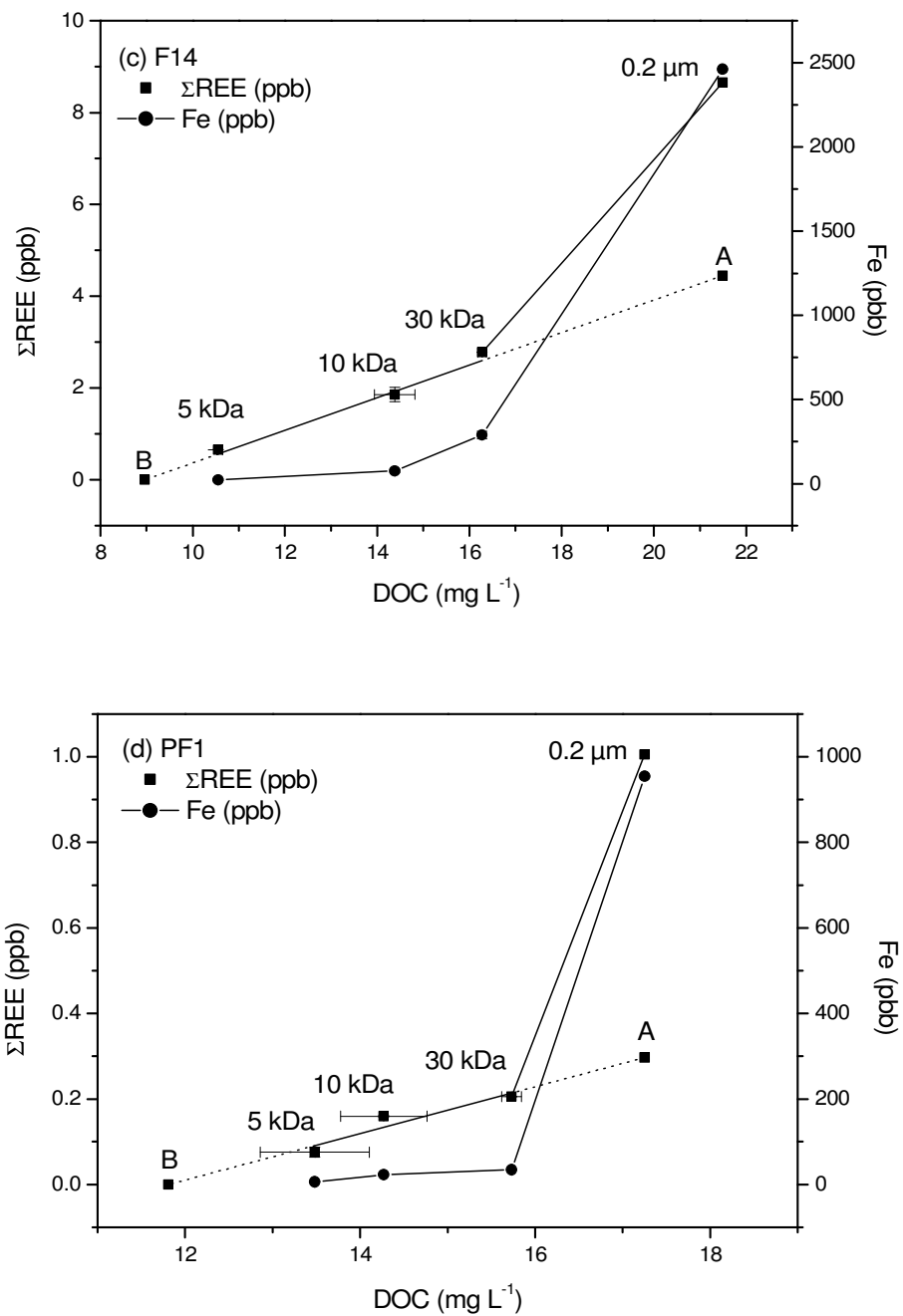


Fig. 1.5. Σ REE and Fe concentrations as a function of DOC concentrations in the successive filtrates ($< 0.2 \mu\text{m}$, $< 30 \text{ kDa}$, $< 10 \text{ kDa}$, $< 5 \text{ kDa}$) for (a) PF3, (b) F7, (c) F14, (d) PF1. Errors bars correspond to standard deviation for two replicates, some errors bars are within the symbol size. Point A represents the extrapolated REE bound only to humic substances point and point B is the projection of 0 REE point (see text for details).

II.1: Organic complexation of REE in natural waters: evaluating model calculations from ultrafiltration data

	PF3				F7				F14				PF1			
	0.2 μm	30 kDa	10 kDa	5 kDa	0.2 μm	30 kDa	10 kDa	5 kDa	0.2 μm	30 kDa	10 kDa	5 kDa	0.2 μm	30 kDa	10 kDa	5 kDa
La	0.8040	0.5755	0.4330	0.2791	0.5180	0.1825	0.1515	0.0833	1.3890	0.4120	0.2461	0.1104	0.1760	0.0285	0.0211	0.0112
Ce	1.8890	1.3495	1.0115	0.5886	1.2990	0.4320	0.3525	0.1820	3.1050	0.8790	0.4977	0.1338	0.3650	0.0594	0.0445	0.0243
Pr	0.2550	0.1845	0.1390	0.0930	0.1750	0.0623	0.0512	0.0270	0.4260	0.1310	0.0757	0.0340	0.0550	0.0107	0.0076	0.0040
Nd	1.1050	0.8260	0.6240	0.4107	0.8120	0.3155	0.2610	0.1440	1.8280	0.6005	0.3600	0.1632	0.2390	0.0515	0.0417	0.0178
Sm	0.1940	0.1420	0.1020	0.0685	0.2020	0.0837	0.0677	0.0361	0.4410	0.1520	0.0916	0.0405	0.0502	0.0130	0.0102	0.0045
Eu	0.0368	0.0265	0.0190	0.0122	0.0406	0.0163	0.0130	0.0048	0.0923	0.0321	0.0188	0.0079	0.0104	0.0030	0.0024	0.0005
Gd	0.1350	0.0954	0.0727	0.0449	0.2060	0.0939	0.0761	0.0431	0.4300	0.1630	0.0982	0.0448	0.0401	0.0121	0.0096	0.0034
Tb	0.0135	0.0096	0.0071	0.0042	0.0287	0.0121	0.0100	0.0055	0.0606	0.0233	0.0140	0.0062	0.0048	0.0016	0.0012	0.0005
Dy	0.0669	0.0480	0.0363	0.0214	0.1820	0.0844	0.0645	0.0368	0.3630	0.1415	0.0875	0.0389	0.0256	0.0085	0.0065	0.0030
Ho	0.0126	0.0095	0.0072	0.0043	0.0400	0.0204	0.0166	0.0091	0.0708	0.0309	0.0197	0.0088	0.0049	0.0019	0.0017	0.0007
Er	0.0350	0.0265	0.0196	0.0129	0.1280	0.0665	0.0557	0.0319	0.2040	0.0926	0.0612	0.0271	0.0147	0.0066	0.0055	0.0023
Tm	0.0048	0.0039	0.0028	0.0018	0.0185	0.0106	0.0085	0.0049	0.0290	0.0136	0.0092	0.0040	0.0021	0.0010	0.0008	0.0003
Yb	0.0304	0.0242	0.0182	0.0119	0.1230	0.0733	0.0602	0.0357	0.1820	0.0913	0.0616	0.0287	0.0149	0.0065	0.0056	0.0024
Lu	0.0052	0.0044	0.0034	0.0022	0.0203	0.0132	0.0108	0.0064	0.0284	0.0149	0.0099	0.0050	0.0027	0.0013	0.0011	0.0005
ΣREE	4.5871	3.3255	2.4958	1.5558	3.7931	1.4667	1.1993	0.6506	8.6491	2.7776	1.6511	0.6533	1.0054	0.2056	0.1593	0.0753
DOC	7.66	6.66	5.66	4.97	11.12	8.14	7.93	6.58	21.49	16.28	14.38	10.55	17.25	15.73	14.27	13.48
Al	72.6	18.02	15.44	10.53	15.53	7.43	6.05	3.56	107	42.72	31.4	16.26	25.21	11.64	10.32	6.47
Mn	10	9	9	3	1193	1257	1239	1153	512	427	424	13	31	25	25	10
Fe	99	12	27	0	1431	54	27	6	2462	290	76	23	955	35	23	6

Table 1.9. Trace metal (in ppb) and DOC (in mg L^{-1}) concentrations of the ultrafiltrates.

1.3.3.2. REE speciation modelling

REE contents corresponding to point A in Fig. 1.5 are used to model the REE speciation of PF3, PF1, F7 and F14 waters using alternatively SHM and Model VI (note that for PF3 sample, point A corresponds to the 0.2 μm point). The HA and FA contents necessary to run both models are assumed to be equal to the difference between the DOC content of the $< 0.2 \mu\text{m}$ fraction and that of the $< 5 \text{ kDa}$ fraction for HA, and to the difference between the DOC content of the $< 5 \text{ kDa}$ fraction and that corresponding to point B in Fig. 1.5 for FA. The model results are presented in Table 1.10 where they are compared to ultrafiltration corrected values. The "modelled" complexation proportions displayed in Table 1.10 include the REE partitioning between the high MW HA fraction ($> 5 \text{ kDa}$) and the low MW FA fraction ($< 5 \text{ kDa}$). Remember that 100 % of REE are supposed to be complexed by the sum of HA and FA in the four ultrafiltered waters.

Table 1.10 shows good convergence between Model VI and ultrafiltration results. LnHM proportions calculated with Model VI are all higher than 97 %, indicating that nearly all of the REE are complexed by organic matter in PF1, PF3, F7 and F14 waters. By contrast, the convergence is of poor quality with SHM, LnHM proportions vary between 24 and 99 % depending of the samples. The remainder of REE is present under carbonate, sulphate or free ions species (e.g. for Tm: in PF3: 49 % ($\text{TmCO}_3^+ + \text{Tm}(\text{CO}_3)_2^-$) and 10 % Tm^{3+} ; in F7: 33 % ($\text{TmCO}_3^+ + \text{Tm}(\text{CO}_3)_2^-$), 30 % Tm^{3+} and 18 % TmSO_4^+ ; in F14: 28 % ($\text{TmCO}_3^+ + \text{Tm}(\text{CO}_3)_2^-$), 23 % Tm^{3+} and 10 % TmSO_4^+ ; in PF1: 40 % ($\text{TmCO}_3^+ + \text{Tm}(\text{CO}_3)_2^-$) and 4 % Tm^{3+}).

Ultrafiltration data are independent of the modelling data, the strong convergences between ultrafiltered and Model VI results could thus not be fortuitous. These convergences provide further support for the ability of Model VI to accurately predict the speciation of REE in organic-rich circumneutral-pH, waters. However, non-convergence between SHM and ultrafiltration results highlights some limitations in the use of this model in the present circumstances.

1.4. Discussion

Based on available data, $\log K_{MA}$ and $\log K_{Mb}$ adopted in section 1.2 look like the best overall estimated values for REE complexation by HM. Comparison of speciation calculations results from Model VI and SHM with published (Viers et al, 1997) and new ultrafiltration data, allow us to define the fields in which the tested models could accurately calculate the REE speciation. Modelling of the World Average River Water (Tang and Johannesson, 2003) shows that both Models VI and SHM yield comparable results for circumneutral pH, low-DOC waters. Nevertheless, a detailed inspection of model results reveals that SHM predicts significantly lower complexation for HREE than Models V and VI. By contrast, results are divergent for alkaline waters, with SHM predicting an out-competition of the organic complexes over the carbonate complexes. However, these results do not really question the ability of SHM and Models V and VI to give realistic speciation of REE with organic matter, remembering the fact that the majority of world rivers is characterized by circumneutral pH values (Brownlow, 1996). Comparisons of the model results with the ultrafiltered data suggest that Model VI could be more accurate than SHM in acidic and circumneutral-pH, DOC-rich ground- and river waters. These differences might be due to intrinsic model thermodynamics hypothesis like HM proton dissociation and how REE competition with others cations and HM competition with others anions are taken into account.

II.1: Organic complexation of REE in natural waters: evaluating model calculations from ultrafiltration data

	PF3									F7								
	Ultrafiltration			SHM			Model VI			Ultrafiltration			SHM			Model VI		
	% LnHA	% LnFA	% LnHM	% LnHA	% LnFA	% LnHM	% LnHA	% LnFA	% LnHM	% LnHA	% LnFA	% LnHM	% LnHA	% LnFA	% LnHM	% LnHA	% LnFA	% LnHM
La	65	35	100	53	22	76	74	26	100	76	24	100	15	11	26	69	30	100
Ce	69	31	100	51	21	72	74	26	100	79	21	100	15	12	27	71	29	100
Pr	64	36	100	61	25	86	73	27	100	78	22	100	29	21	50	72	28	100
Nd	63	37	100	62	26	88	74	26	100	76	24	100	31	23	54	73	26	100
Sm	65	35	100	66	27	93	66	34	100	78	22	100	42	31	72	70	30	100
Eu	67	33	100	64	27	91	71	29	100	87	13	100	37	28	65	73	27	100
Gd	67	33	100	60	25	85	73	27	100	76	24	100	30	22	52	73	27	100
Tb	69	31	100	49	20	69	72	27	99	76	24	100	18	14	31	69	31	99
Dy	68	32	100	43	18	61	75	23	98	77	23	100	15	12	27	71	28	99
Ho	66	34	100	40	18	58	74	23	98	76	24	100	14	11	25	70	28	98
Er	63	37	100	36	15	51	73	24	97	75	25	100	12	9	20	68	30	98
Tm	63	38	100	31	14	44	72	25	97	74	26	100	10	8	18	69	30	98
Yb	61	39	100	43	18	61	71	27	98	71	29	100	18	13	31	69	30	99
Lu	58	42	100	37	15	52	72	26	97	68	32	100	14	11	24	70	29	99
	F14									PF1								
	Ultrafiltration			SHM			Model VI			Ultrafiltration			SHM			Model VI		
	% LnHA	% LnFA	% LnHM	% LnHA	% LnFA	% LnHM	% LnHA	% LnFA	% LnHM	% LnHA	% LnFA	% LnHM	% LnHA	% LnFA	% LnHM	% LnHA	% LnFA	% LnHM
La	83	17	100	32	21	53	61	38	100	73	27	100	66	20	86	80	20	100
Ce	91	9	100	33	21	53	62	38	100	71	29	100	63	19	82	81	19	100
Pr	83	17	100	47	28	75	62	38	100	75	25	100	70	21	91	81	19	100
Nd	83	17	100	49	29	78	64	36	100	76	24	100	71	21	92	82	18	100
Sm	83	17	100	56	33	89	57	43	100	75	25	100	77	22	99	78	22	100
Eu	84	16	100	53	32	85	61	39	100	89	11	100	72	21	94	81	19	100
Gd	82	18	100	48	29	76	63	37	100	81	19	100	70	21	90	81	18	100
Tb	83	17	100	36	22	58	61	38	99	83	17	100	60	18	77	78	22	100
Dy	83	17	100	32	20	52	64	35	99	75	25	100	54	16	70	80	20	99
Ho	82	18	100	29	19	49	63	35	98	77	23	100	53	15	68	78	21	99
Er	82	18	100	26	17	43	62	36	98	78	22	100	46	14	60	75	23	99
Tm	81	19	100	23	15	38	62	37	98	82	18	100	42	12	53	75	24	99
Yb	80	20	100	35	21	56	61	38	99	76	24	100	53	16	68	77	23	100
Lu	79	21	100	29	18	47	63	36	99	64	36	100	46	14	60	74	25	99

Table 1.10. Comparison between the proportions of LnFA and LnHA complexes in PF1, PF3, F7 and F14 samples obtained by ultrafiltration experiments and modelling calculation using Model VI and SHM.

1.4.1. Effect of HM proton dissociation

As previously described (section 1.2.1.3), the electrostatics hypotheses made in both models are different. This leads to a shift, in the area where REE-organic complexes are predicted to dominate the REE speciation towards more or less alkaline conditions. The larger affinity of REE for humic substances obtained with Model VI than with SHM is a direct consequence of the proton dissociation of the humic substances surface sites. The proton dissociation of HA and FA are illustrated on Fig. 1.6 for both models. Model VI predicts that HA and FA are more electronegative than in SHM. The amount of surface site available for REE complexation are thus higher on the pH range in Model VI than in SHM. The larger affinity of REE for humic substances obtained with Model VI in acidic waters is thus a direct consequence of the humic substances proton dissociation. Deprotonation of HA and FA modelled by Model VI occurred at more acidic pH (about 0.5 pH unit) than SHM (Fig. 1.6). It results in a higher LnHM calculation by Model VI than SHM from acidic to alkaline pH.

This proton dissociation effect is well illustrated by the three sets of studied samples: (i) the World Average River Water modelling shows that there is a shift of about 0.75 pH unit between Model VI and SHM prediction (Figs. 1.3 and 1.4); (ii) this "pH effect" explains why the proportions of REE complexed with organic matter in Mengong (pH = 4.62) and Mar 2 (pH = 5.5) samples are predicted to be significantly higher with Model VI than SHM; (iii) REE speciations of the four organic-rich circumneutral pH waters (i.e. PF1, PF3, F7 and F14) show that the differences between models are maximum at acidic pH (i.e. F7 pH = 6.19) and minimum at higher pH (i.e. PF1 pH = 7.08).

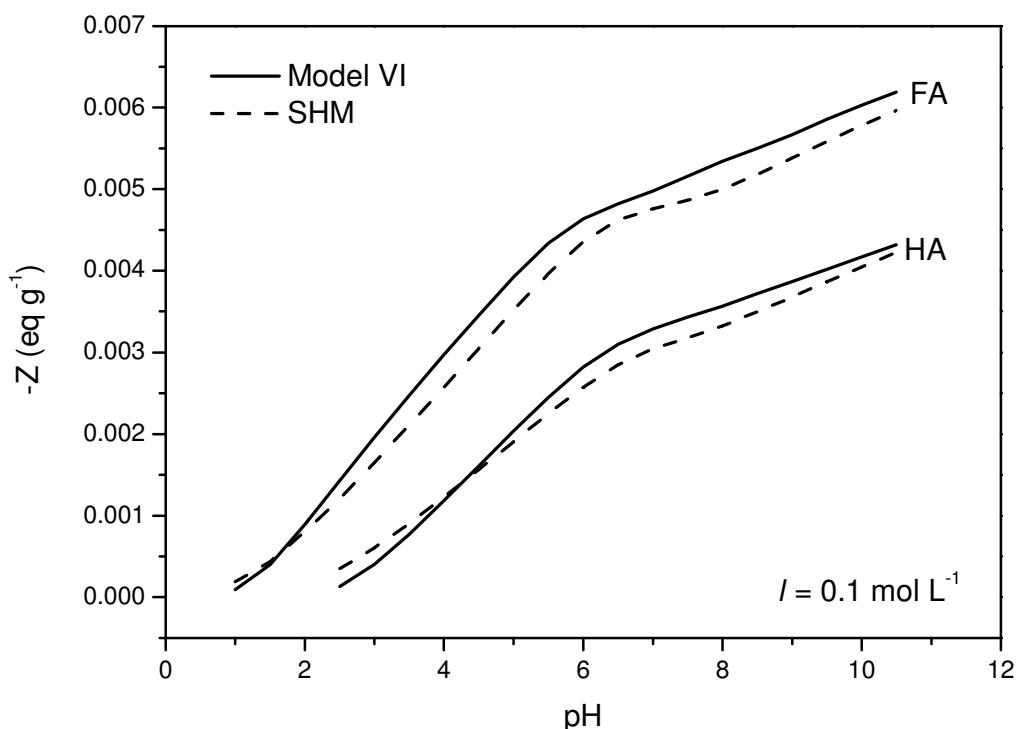


Fig. 1.6. Proton dissociation of HA and FA.

Moreover, REE speciation being closest to ultrafiltration results with Model VI than SHM, it seems that proton dissociation is better described by Model VI than SHM. The only difference on the way how proton dissociation are calculated in both models is the electrostatic

correction. A better definition of the value of the "gel-fraction" parameter should thus increase the quality of the HM proton dissociation in SHM.

1.4.2. Effect of major competing cations (Fe, Al and Ca)

Fe, Al and Ca are known for their strong complexation with HM (Dupré et al., 1999; Tipping et al., 2002), resulting in competition with REE for complexation with HM. As previously shown by Tang and Johannesson (2003), competition with Fe and Al can decrease the amount of REE bound to HM in a range of about 10 %. In Model VI, fraction of iron and aluminium bound to HM are lower than in SHM. If less HM are bound to Fe or Al as in Model VI, high LnHM complex could be then produced and inversely if high proportion of HM is bound to Fe as in SHM. The higher the competitor concentration is, the more important the discrepancy between both models will be. Impact of competing cations (Fe, Al and Ca) is well illustrated by speciation of World Average River Water (Table 1.11). At acidic pH, prediction of FeHM is higher in SHM than in Model VI and at circumneutral pH prediction of AlHM is higher in SHM than in Model VI. Moreover, if competition with Fe, Al and Ca is not at all taken into account, both models will predict similar speciation for the four ultrafiltered samples (i.e. PF1, PF3, F7 and F14), namely 100 % of LnHM.

pH	% Fe-HM		% Al-HM		% Ca-HM	
	Model VI	SHM	Model VI	SHM	Model VI	SHM
3	10	31	19	1	0	0
3.5	15	41	38	2	0	0
4	16	45	56	7	1	0
4.5	15	42	71	26	1	0
5	13	34	81	64	1	0
5.5	12	25	82	85	1	1
6	10	16	75	90	2	1
6.5	10	9	53	85	2	1
7	10	5	17	62	2	1
7.5	9	3	2	27	2	1
8	7	2	0	8	2	2
8.5	4	1	0	2	3	2
9	2	0	0	0	3	2
9.5	1	0	0	0	3	2

Table 1.11. Model VI and SHM speciation calculations for Fe, Al and Ca in World Average River Water as a function of pH.

Moreover, REE speciation being closest to ultrafiltration results with Model VI than SHM, it seems that competing cations complexation is better described by Model VI than SHM. The values of $\log K_{Mm}$ and $\log K_{Mb}$ with Fe, Al and Ca in SHM is thus questionable. As an example, $\log K_{MA}$ for Al rely on numerous literature values whereas $\log K_{Mb}$ is based on an empirical relationship taken from a restricted number of samples of Swedish sites (Cory and Andrén, 2004). Improvement in the quality of $\log K_{Mm}$ and $\log K_{Mb}$ for competing cations (i.e. Fe, Al and Ca) in SHM are thus required to improve the reliability of this model.

1.4.3. Effect of major competing anions

As a consequence of the two previous effect (i.e. deprotonation and competing cations), if less HM surface sites are available for REE complexation as in SHM, competition between anionic ligands (sulphates and carbonates) and HM could occur. As an example in alkaline waters, in World Average River Water REE are more complexed to humic substances in Model VI calculations than in SHM. This might be a direct consequence of a competition with anionic

ligands, like carbonates. These differences are more significant for HREE, since $\log K_{MA}$ and $\log K_{Mb}$ are of the same order than for LREE whereas $\log K$ with carbonates increase of 1 and 2 $\log K$ unit for carbonates and bicarbonates, respectively. This phenomenon is well evidenced in Figs. 1.3 and 1.4. Moreover, the proportion of LnHM at $\text{pH} \geq 8$ decreases faster in SHM than in Model VI when $\log K_{Mb}$ strongly decreases ($\log K_{Mb}$ decreasing of about 2 % versus a $\log K_{MA}$ decreasing of 1 %). This indicates that $\log K_{Mb}$ in SHM become weaker competitor of carbonate for REE at $\text{pH} \geq 8$, than $\log K_{MA}$ in Model VI. This is probably the reason why Models VI predicts much higher proportions of REE organic complexes at $\text{pH} \geq 8$ than SHM.

1.4.4. Validity fields

Determining which of Models V and VI or SHM gives the most reliable description of REE speciation in natural waters is clearly difficult on the basis of modelled data alone. Direct comparison with measurement of the REE speciation in acidic to circumneutral pH waters using ultrafiltration techniques led us to validate the reliability of Model VI to predict REE speciation in such samples. However, SHM could not be considered reliable considering the previously cited needed improvement of this model. Moreover, experimental studies involving direct measurement of the REE speciation in alkaline waters using ultrafiltration techniques or other analytical techniques (e.g., electrochemical; Johannesson et al., 2004) are clearly needed to validate any of these models in such conditions.

Although, it is important to stress that differences in the model calculations may result from the use of different stability constants. A 0.1 $\log K$ unit variation leads to speciation calculation results that differ ca. 4-5 % with Model VI and 7-8 % with SHM at pH 7 for the World Average River Water. This sensitivity analysis shows that the values of $\log K_{MA}$ and $\log K_{Mb}$ are critical in expanding the stability field of REE organic complexes towards high pH values. The determination of validity fields for the models is strongly subordinated to the knowledge of the stability constants. The lack of experimentally determined $\log K_{Mb}$ is clearly one of the major limitation preventing the validation of SHM. Consequently, it is critical that additional experimental and laboratory studies be systematically conducted to obtain more reliable values for each REE.

Another difficulty is the presence of REE-bearing inorganic colloids in the ultrafiltered waters which are used to validate the speciation models. Neither Model V and VI, nor SHM account for the complexation of REE by inorganic colloids. Some of these colloids can be important REE carriers, as evidenced by the role of Fe-rich colloids in the ultrafiltered waters. It is critical that stability constants be determined for the complexation of REE by inorganic colloid and be systematically introduced in the speciation models. The last difficulty relies upon the need to know the composition of the dissolved organic matter fraction in waters. The ultrafiltered waters analyzed during this study have an important fraction of their DOC (between 40 and 70 %; Fig. 1.5) which does not complex the REE. Strong differences in model calculations depend on the presence and concentration of this non-complexing organic matter. The lack of knowledge of the composition of the dissolved organic matter pool could be a major limitation in applying models to these waters.

1.5. Conclusion

The scope of this study was to increase our understanding of how to describe REE-organic complexation in equilibrium speciation models. For this purpose SHM and Models V and VI were compared for their ability to assess the role of dissolved organic matter in the speciation of REE in organic-rich groundwaters. The interest in testing SHM is that this model is part of a wider equilibrium model (Visual MINTEQ), that allows as well dissolution/precipitation, sorption/desorption and oxidation/reduction modelling. A comparison

of the three models using World Average River Water shows that Models V and VI and SHM yield comparable results for circumneutral pH, low-DOC waters, confirming earlier findings that a large fraction of the REE carried in solution by rivers occurs as organic complexes. Comparison of the model results with published and new ultrafiltration data suggests that Model VI could be reliable in acidic, DOC-rich ground- and river waters, whereas SHM is unadapted. The same is true for circumneutral pH, DOC-rich groundwaters, where Model VI appears closest to ultrafiltration data than SHM. Lower HM deprotonation coupled to stronger REE competitions with other cations such as Fe, Al and Ca, as well as stronger HM competition with carbonates in SHM led to lower REE organic complexation than in Model VI. Model VI calculation are thus closer to ultrafiltration data than SHM for this type of waters. Overall, the obtained results indicate that SHM needs some improvement to become a reliable alternative to Models V and VI. After that, the speciation program including this model could become a valuable tool to explore the bulk of the processes that control the distribution of REE in natural waters. The data reported in this study show that great care should be exercised in the use of ultrafiltration data to validate or invalidate modelled data. The possible occurrence - in the ultrafiltrates of REE/Fe-rich inorganic colloids and/or non-humic organic molecules unable to complex REE - also suggest that more experimental studies should be conducted to obtain reliable complexation constants of REE and humic substances.

2. Rare earth elements complexation with humic acid

Cette partie est extraite d'un article soumis à Chemical Geology, Pourret O., Davranche M., Gruau G., and Dia A. (2006) Rare Earth Elements complexation with humic acid.

Résumé– La complexation des terres rares (REE) par des acides humiques (HA) a été étudiée en combinant des techniques d'ultrafiltration et ICP-MS. Les expériences de complexation de REE-HA ont été réalisées à différents pH (2 à 10.5) en utilisant une méthode standard d'équilibre en batchs. Les résultats montrent que la quantité de REE liées aux HA augmente fortement avec le pH. De plus, à pH acide les spectres des coefficients de partage des REE sont concaves, enrichis en REE intermédiaires (MREE). La modélisation inverse des données expérimentales par Humic Ion Binding Model VI a fourni une série de valeurs de $\log K_{MA}$ (i.e., les constantes de complexation REE - HA spécifiques à Model VI) pour l'ensemble de la série des REE. La distribution des $\log K_{MA}$ obtenus montre une concavité centrée sur les MREE. Les $\log K_{MA}$ ont des valeurs comprises entre 2.42 et 2.79. Ces constantes de complexation sont en accord avec les quelques séries de données quantifiant la complexation des REE par les substances humiques. Elles sont cependant en désaccord avec une étude récemment publiée qui met en évidence une contraction des lanthanides (i.e. un accroissement continu de la constante du La au Lu). Cependant, la concavité centrée sur les MREE mise en évidence par notre étude a également été mise en évidence dans des études de complexation REE - acides fulviques et REE - acides acétiques. Cette similitude dans les formes de spectres des constantes de complexation des REE suggère que les groupements carboxyliques sont les sites complexants principaux des HA vis-à-vis des REE. Cette conclusion est confortée par une étude détaillée des eaux de nappes et de rivières riches en matières organiques, qui ne présentent de spectre typiques des effets contraction des lanthanides. En conclusion, l'application du Model VI et des nouvelles constantes, $\log K_{MA}$, à l'étude de la spéciation de l'eau de rivière moyenne mondiale confirme la spéciation organique des REE (> 60 %) dans la gamme de pH entre 5-5.5 et 7-8.5 (i.e., dans les eaux de pH neutres). La seule différence significative entre les résultats obtenus avec des constantes estimées est que la proportion de REE légères sous forme organique est sensiblement supérieure pour des conditions de pH plus alcalines. D'une façon plus générale, les nouveaux résultats expérimentaux mettent en avant l'impact que peut avoir la matière organique sur les formes des spectres de REE dans les eaux naturelles riches en matières organiques.

Abstract - The binding of rare earth elements (REE) to humic acid (HA) was studied by combining Ultrafiltration and Inductively Coupled Plasma Mass Spectrometry techniques. REE-HA complexation experiments were performed at various pH conditions (ranging from 2 to 10.5) using a standard batch equilibration method. Results show that the amount of REE bound to HA strongly increase with increasing pH. Moreover, a Middle REE (MREE) downward concavity is evidenced by REE distribution patterns at acidic pH. Modelling of the experimental data using Humic Ion Binding Model VI provided a set of $\log K_{MA}$ values (i.e. the REE-HA complexation constants specific to Model VI) for the entire REE series. The $\log K_{MA}$ pattern obtained displays a MREE downward concavity. $\log K_{MA}$ values range from 2.42 to 2.79. These binding constants are in good agreement with the few existing datasets quantifying the binding of REE with humic substances except a recently published study which evidence a lanthanide contraction effect (i.e. continuous increase of the constant from La to Lu). The MREE downward concavity displayed by REE-HA complexation pattern determined in this study compares well with results from REE-fulvic acid (FA) and REE-acetic acid complexation studies. This similarity in the REE complexation pattern shapes suggests that carboxylic groups are the main binding sites of REE in HA. This conclusion is further supported by a detailed review of published studies for natural, organic-rich, river- and ground-waters which show no evidence of a lanthanide contraction effect in REE pattern shape. Finally, application of Model VI using the new, experimentally determined $\log K_{MA}$ values to World Average River Water confirms earlier suggestions that REE occur predominantly as organic complexes ($\geq 60\%$) in the pH range between 5-5.5 and 7-8.5 (i.e. in circumneutral pH waters). The only significant difference as compared to earlier model predictions made using estimated $\log K_{MA}$ values is that the experimentally determined $\log K_{MA}$ values predict a significantly higher amount of Light REE

bound to organic matter under alkaline pH conditions. Taken as a whole, the new experimental results shed additional light on the processes that govern REE pattern shapes in natural, organic-rich waters.

2.1. Introduction

Rare Earth Elements (REE) are commonly used as tracers for geochemical processes in natural waters (Elderfield and Greaves, 1982; Henderson, 1984; Elderfield et al., 1990; Smedley, 1991; Sholkovitz, 1995; Johannesson et al., 1997; Johannesson et al., 2000). Ground- and river-waters do not exhibit uniform REE patterns (Goldstein and Jacobsen, 1988; Elderfield et al., 1990; Sholkovitz, 1995). Systematic variations in REE pattern shapes occur which have been attributed, in part, to the presence of two REE pools - so-called "dissolved" and "colloidal" pools - having different REE pattern shapes. For example, it is often suggested that REE patterns of rivers result from the mixing between (i) a low REE concentration, dissolved pool, Light-REE (LREE) depleted, but Heavy-REE (HREE) enriched related to Upper Continental Crust (UCC) (Taylor and McLennan, 1985) and (ii) a REE-rich colloidal phase having a Middle-REE (MREE) downward concavity pattern, namely a pattern that exhibits both $(La/Sm)_N$ ratio below 1 and $(Gd/Yb)_N$ ratio above 1 (Goldstein and Jacobsen, 1988; Elderfield et al., 1990; Sholkovitz, 1995). Humic substances constitute a significant part of the colloidal phase in both ground- and river-waters (Thurman, 1985). Consequently, interpreting and understanding the significance of REE pattern shape variability in these waters rely, for a large part, on a better description of the binding of REE to humic materials (HM) and of the fractionation in REE pattern shape that may occur during this binding.

Models based on thermodynamics principles offer an interesting perspective in order to predict the complexation of REE with HM and thus to explore the extent to which the shape of ground- and river-water REE patterns depends on REE fractionation by HM. Modelling calculations were already performed in seawater (Cantrell and Byrne, 1987; Byrne and Kim, 1990; De Baar et al., 1991) and groundwaters (Wood, 1990; Lee and Byrne, 1992; Johannesson et al., 1996b). They evidence that hydroxides and carbonates (Cantrell and Byrne, 1987; Lee and Byrne, 1993; Liu and Byrne, 1998; Luo and Byrne, 2004) are the major inorganic complexing ligands of REE. However, organic complexation is often not taken into account in these calculations. Studies on REE - dissolved organic material (DOM) interactions and in particular humic and fulvic acids (HA and FA) are sparse in all respect (Dupré et al., 1999; Tang and Johannesson, 2003; Johannesson et al., 2004). Natural organic molecules contain numerous and chemically different binding sites, and thus it is difficult to define discrete equilibrium constants for each complexation reaction (Crawford, 1996). Thus, addressing complexation with DOM in existing aqueous speciation models is not obvious. Until recently, REE-FA or -HA complexation constants were generally determined for a single REE (e.g. for HA: Sm-HA, Eu-HA, Tb-HA and Dy-HA) (Maes et al., 1988; Bidoglio et al., 1991; Moulin et al., 1992; Dierckx et al., 1994; Fairhurst et al., 1995; Franz et al., 1997; Lead et al., 1998; Lippold et al., 2005) while accurate stability constants are needed for the 14 naturally occurring REE to model speciation of natural water. Only two studies reporting REE-humate binding constants for the 14 naturally occurring REE have been so far published. They have unfortunately yielded to strongly different results. Yamamoto et al. (2005) studied complexation of REE with Suwannee River FA (SRFA) using a solvent extraction method. Pattern of REE-FA complexation constants obtained by these authors shows a MREE downward concavity similar to that obtained for REE-diacetic acid complexation. By contrast, Sonke and Salters (2006) studied complexation of REE with SRFA, Leonardite coal HA (LHA) and Elliot soil HA (EHA) using an EDTA-ligand competition method. Complexation patterns obtained by these authors are markedly different from those reported by Yamamoto et al. (2005) exhibiting a lanthanide contraction effect, i.e. a regular and progressive increase of the constants from La to Lu.

In this contribution, in order to both assess the discrepancy between both studies (Sonke and Salters, 2006; Yamamoto et al., 2005) and provide a more accurate REE-HA complexation dataset, experiments of REE-Aldrich HA complexation were performed for the 14 naturally occurring REE simultaneously. This new dataset was obtained using a third experimental method which combines an ultrafiltration technique and the Inductively Coupled Plasma Mass Spectrometry method. Humic Ion Binding Model VI (hereafter denoted as Model VI) was used to model the experimental results (Tipping, 1998). Therefore, the constants reported are not intrinsic equilibrium constants but Model VI specific equilibrium constants (i.e. $\log K_{MA}$ values). Considering the key role played by organic colloids in natural terrestrial waters, the new results were also used to revisit the significance of REE pattern shapes in organic-rich, ground- and river-waters. Finally, the new constants were input in Model VI to reinvestigate World Average River Water (Tang and Johannesson, 2003) and further constrain the speciation of REE in river waters.

2.2. Materials and Method

2.2.1. Experimental Binding of Rare Earth Elements by Humic Acid

All chemicals used in this study were of analytical grade, and all the experimental solutions used prepared with doubly deionized water (MilliQ system, Millipore™). REE-HA complexes were prepared in polyethylene containers previously soaked in 10 % Ultrapure HNO₃ for 48 h at 60 °C, then rinsed with MilliQ water for 24 h at 60 °C to remove all possible REE contamination sources. Synthetic REE solutions were prepared from nitrate REE standards (10 ppm, Accu Trace™ Reference Standard). All experiments were carried out at room temperature, i.e. 20 °C ± 2.

2.2.1.1. Humic acid

Purified humate, referred to below as HA (humic acid), was obtained from synthetic Aldrich™ humic acid (Aldrich™, H1, 675-2) following the protocol described by Vermeer et al. (1998). HA sample was freeze-dried and stored in a glass container at room temperature. HA obtained was ash free and in its protonated form, with the following elemental composition (in weight percent): C = 55.8 %, O = 38.9 %, H = 4.6 %, N = 0.6 %. REE concentrations REE in HA were below the detection limit of ICP-MS measurement (i.e. < 1 ppt). HA has a mean molecular weight of 23 kDa (Vermeer et al., 1998). Prior to use, the freeze-dried humate was resuspended overnight in an 0.001 mol L⁻¹ NaCl electrolyte solution at pH = 10, to ensure complete dissolution of the sample (Davranche et al., 2004; Davranche et al., 2005).

2.2.1.2. Experimental set-up description

REE complexation with HA was investigated using a standard batch equilibration technique. REE (50 ppb of each REE) and HA (5, 10 and 20 mg L⁻¹) were placed together in solution, at an ionic strength of 0.001 mol L⁻¹ and at pH values ranging from 2.18 to 10.44. The pH was measured with a combined Radiometer Red Rod electrode. The electrode was calibrated with WTW standard solutions (pH 4, 7 and 10). The accuracy of the pH measurement was ± 0.05 pH unit. Experimental solutions were stirred for 48 h (equilibrium time determined from preliminary kinetic experiments) to allow equilibration and partitioning of REE between the aqueous solution and the humate suspension. Solution aliquots of about 10 mL were sampled twice: first at the beginning of the experiment; then after 48 h at equilibrium state. REE complexed by the HA were separated from the remaining inorganic REE by ultrafiltration. Ultrafiltrations were carried out by centrifugating the 10 mL solution samples

through 15 mL centrifugal tubes equipped with permeable membranes of 5 kDa pore size (Millipore Amicon Ultra-15). All centrifugal filter devices used were washed and rinsed with 0.1 mol L⁻¹ HCl and MilliQ water two times before use in order to minimize contamination. Centrifugations were performed using a Jouan G4.12 centrifuge with swinging bucket rotor at 3000 g for 30 minutes. This allowed the REE-HA complexes to be quantitatively separated from inorganic REE species. REE-HA complexes have a mean molecular weight of 23 kDa, and are therefore caught up by the 5 kDa membrane whereas inorganic REE species went through it. The selectivity of the 5 kDa membrane regards to the REE-HA complexes was verified by monitoring the Dissolved Organic Carbon (DOC) contents of the ultrafiltrates. Results show that the latter were systematically lower or equal to blank values (≤ 1 ppm). Possible adsorption of inorganic REE species onto the membrane or onto cell walls was also monitored. Inorganic REE solutions of known REE concentration were ultrafiltered several times. Results showed that 100 % of the REE present in solution was recovered in the ultrafiltrates, demonstrating that no REE was adsorbed on the membranes nor on the walls of the cell devices used.

In the following, REE complexation with HA is described by quantifying the amount of REE that remains into the < 5 kDa ultrafiltrates after equilibration of the REE-bearing aqueous solutions with HA and by comparing this amount to the amount of REE which has been introduced initially into the experimental solutions. All the removed REE are assumed to have been complexed by the 23 kDa HA. REE concentrations were determined at Rennes 1 University using an Agilent TechnologiesTM HP4500 ICP-MS instrument. Quantitative analyses were performed using a conventional external calibration procedure. Three external standard solutions with REE concentrations similar to the analyzed samples were prepared from a multi-REE standard solution (Accu TraceTM Reference, 10 mg L⁻¹, USA). Indium was added to all samples as an internal standard at a concentration of 0.87 $\mu\text{mol L}^{-1}$ (100 ppb) to correct for instrumental drift and possible matrix effects. Indium was also added to the external standard solutions. Calibration curves were calculated from measured REE/indium intensity ratios. The instrumental error on REE analysis in our laboratory as established from repeated analyses of multi-REE standard solution (Accu TraceTM Reference, USA) and of the SLRS-4 water standard is $< \pm 2$ % (Dia et al., 2000; Davranche et al., 2005). Chemical blanks of individual REE were all lower than detection limit (1 ppt), which is negligible since they are three to four orders of magnitude lower than the concentrations measured in the synthetic solutions used in the complexation experiments.

DOC concentrations were determined at Rennes 1 University using a Shimadzu 5000 TOC analyzer. The accuracy of DOC concentration measurements is estimated at ± 5 % as determined by repeated analyses of freshly prepared standard solutions (potassium biphtalate).

2.2.2. Humic Ion Binding Model VI

Humic Ion Binding Model VI (Model VI) has been described in detail by Tipping (Tipping, 1998). The model is a discrete binding site model which takes into account electrostatic interactions. There is an empirical relation between net humic charge and an electrostatic interaction factor. The discrete binding sites are represented by two types of sites (types A and B), each comprising four different site subtypes present in equal amounts. Types A and B sites are described by intrinsic proton binding constants (pK_A and pK_B) and spreads of the values (ΔpK_A and ΔpK_B) within each type. There are n_A (mol g⁻¹) Type A sites (associated with carboxylic type groups) and $n_B = n_A/2$ (mol g⁻¹) Type B sites (often associated with phenolic type groups). Metal binding occurs at single proton binding sites (monodentate complexation) or by bidentate complexation between pairs of sites. A proximity factor is introduced that quantifies whether pairs of proton binding groups are close enough to form bidentate sites. Type A and Type B sites have separate intrinsic binding constants ($\log K_{MA}$ and $\log K_{MB}$), together associated with a parameter, ΔLK_1 , defining the spreads of values around the medians. A further parameter,

ΔLK_2 , takes into account a small number of stronger sites (bidentate and tridentate sites). By considering results from many datasets, a universal average value of ΔLK_1 is obtained, and a correlation established between $\log K_{MB}$ and $\log K_{MA}$ (Tipping, 1998). Then, a single adjustable parameter ($\log K_{MA}$) is necessary to fully describe metal complexation with HA in Model VI. Model VI parameters for HA are presented in Table 2.1. Model VI was preferentially selected because this model is a widely accepted metal-organic matter speciation code whose capability to model REE complexation with HM has been already tested and proved to perform reasonably well (Lead et al., 1998).

Parameter	Description	Values
n_A	Amount of type A sites (mol g ⁻¹)	$3.3 \cdot 10^{-3}$
n_B	Amount of type B sites (mol g ⁻¹)	$0.5 \times n_A$
pK_A	Intrinsic proton dissociation constant for type A sites	4.1
pK_B	Intrinsic proton dissociation constant for type B sites	8.8
ΔpK_A	Distribution terms that modifies pK_A	2.1
ΔpK_B	Distribution terms that modifies pK_B	3.6
$\log K_{MA}$	Intrinsic equilibrium constant for metal binding at type A sites	Fitted from experimental data
$\log K_{MB}$	Intrinsic equilibrium constant for metal binding at type B sites	$3.39 \log K_{MA} - 1.15$
ΔLK_1	Distribution term that modifies $\log K_{MA}$	2.8 (REE)
ΔLK_2	Distribution term that modifies the strengths of bidentate and tridentate sites	$0.55 \log K_{NH_3} = 0.29$ (REE)
P	Electrostatic parameter	-330
K_{sel}	Selectivity coefficient for counterion accumulation	1
M	Molecular weight	15000 Da
r	Molecular radius	1.72 nm

Table 2.1. Model VI parameters for humic acid (Tipping, 1998).

2.3. Results

2.3.1. Experimental results

Experimental data are reported in Table 2.2. and illustrated for three REE (La, Eu, Lu) in Fig. 2.1. REE complexation by HA is examined by considering the proportion of REE-HA complexes formed as a function of pH. As shown in Fig. 2.1, the proportion of REE-HA complexes increases with increasing pH. It also depends on the HA concentration of the experimental solution. More specifically, the pH at which 100 % of the REE are complexed by HA decreases with increasing HA concentration: $pH \approx 4, 5.5$ and 7 for HA concentrations of 20, 10 and 5 mg L⁻¹, respectively (see Fig. 2.1). These results are in good agreement with previously published data (Maes et al., 1988; Dierckx et al., 1994; Franz et al., 1997; Lippold et al., 2005). The observed pH-dependence of REE complexation by HA can be explained by the deprotonation of the HA carboxylic and phenolic surface groups at increasing pH, which is a classical feature of metal ion complexation by humic acid (Fairhurst et al., 1995; Lippold et al., 2005). Interestingly, patterns of the proportions of REE-HA exhibits a MREE downward concavity (i.e. $\log K_{MA}(\text{La-HA})/\log K_{MA}(\text{Sm-HA}) < 1$ and $\log K_{MA}(\text{Gd-HA})/\log K_{MA}(\text{Yb-HA}) > 1$) when the amount of REE complexed with HA is sufficiently low to evidence possible fractionation among the REE series (i.e. under acidic pH conditions; patterns not shown, see Table 2.2.). The same feature was already observed in complexation experiments of the REE with Aldrich HA using the dialysis method (Davranche et al., 2005).

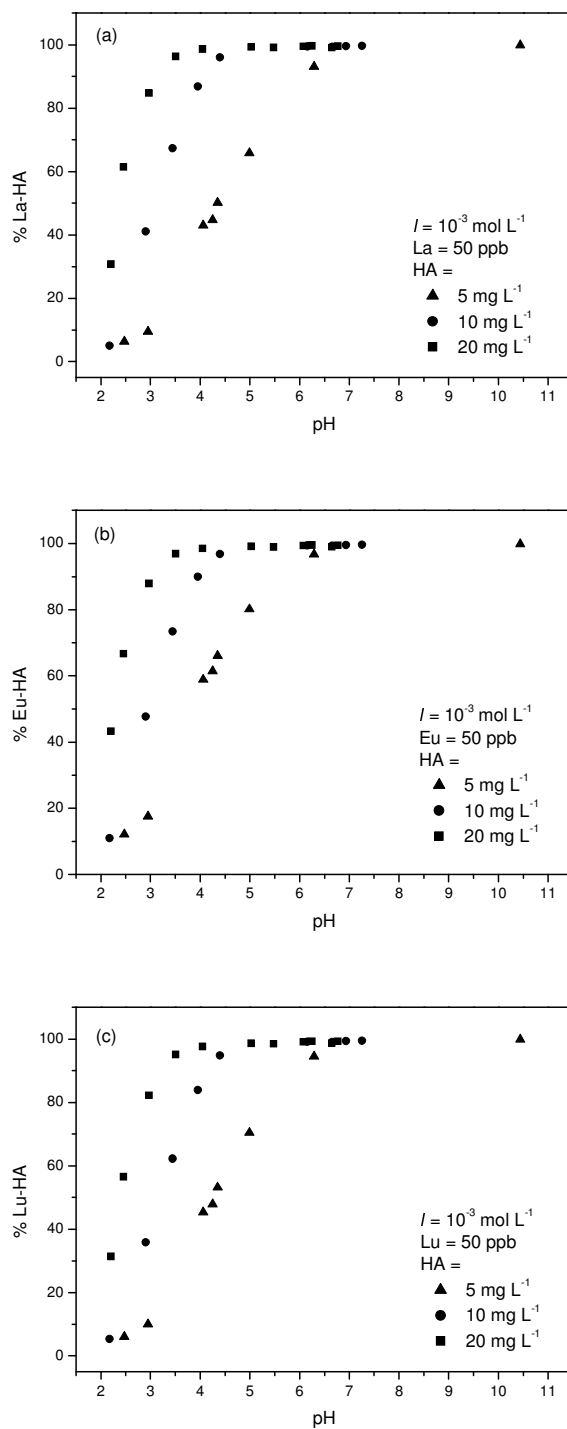


Fig. 2.1. Proportions of (a) La-HA, (b) Eu-HA and (c) Lu-HA complexes as a function of pH for various HA concentrations.

2.3.2. Calculating log K_{MA} values

Calculations were performed using the computer program WHAM 6 (Version 6.0.13) which includes Model VI. The three datasets corresponding to the three different HA concentrations used were separately modelled. A classical strategy that consists in adjusting log K_{MA} for each REE simultaneously until a reasonable fit is achieved was used. Values of $[REE^{3+}]$

(i.e. the amount of REE left in the < 5 kDa ultrafiltrates) and v (moles of REE bound per gram of humic acid; i.e. the difference between the amount of REE left in the < 5 kDa ultrafiltrates and the amount of REE initially present in the experimental solutions) are derived from the experimental data. The best fit is obtained when the root mean square error of the regression ($\text{rmse} = \text{sum of the squares of the differences between observed and calculated } \log v$) is minimised. The three sets of optimised $\log K_{\text{MA}}$ values thus obtained are reported in Table 2.3 for the 14 analyzed REE and illustrated in Fig. 2.2 for the case of La. As indicated by rmse values (< 0.07), fits could be considered of good quality. The main characteristics of the REE-HA experiments to be reproduced by Model VI are a high proportion of REE-HA complexes at relatively low pH and a marked increase of this proportion with increasing pH. $\log K_{\text{MA}}$ values increase with HA concentration of experimental solutions. The overall difference is of ca. 0.3 for all REE, which corresponds to a difference of ca. 12 % on estimated $\log K_{\text{MA}}$ values. As can be seen in Fig. 2.2, a 12 % difference on $\log K_{\text{MA}}$ values may result in a difference of up to 20 % on the calculated proportion of REE-HA complex if the pH and the HA concentration are low. The default value is easily computed by taking the mean between the three sets of values. This procedure means that equal weight is given to all the data sets obtained for different HA concentration levels. It implies that differences in $\log K_{\text{MA}}$ for a given type of humic material are due to variations from one sample to another (Tipping, 1998). The adopted values are listed in Table 2.3. $\log K_{\text{MA}}$ values increase from La (2.58) to Eu (2.65), then decreasing from Gd (2.63) to Lu (2.59). It follows a $\log K_{\text{MA}}$ pattern showing a MREE downward concavity.

2.4. Discussion

2.4.1. Comparison with published results

Data from previous studies (Moulin et al., 1992; Fairhurst et al., 1995; Lippold et al., 2005; Sonke and Salters, 2006) were modelled using Model VI to compare them with the newly obtained set of $\log K_{\text{MA}}$. Previous studies (Moulin et al., 1992; Fairhurst et al., 1995; Lippold et al., 2005) provide data for only a limited number of REE, namely Tb, Dy and Eu. Experimental conditions and fit results for these three studies are presented in Table 2.4. Modelled $\log K_{\text{MA}}$ values for Tb (2.57) and Eu (2.73 and 2.77) are within the error range of the average $\log K_{\text{MA}}$ values obtained here for these two REE (2.62 ± 0.16 and 2.65 ± 0.15 , respectively; see Table 2.3). Only results for Dy are statistically different: 3.19 against 2.61 ± 0.16 in the present study. The present results have also been compared to recently published results for the complexation of the 14 naturally occurring REE by Leonardite HA (LHA), a coal derived HA (Sonke and Salters, 2006). Complexation of the REE by LHA was experimentally studied at four different pH (6, 7, 8 and 9) using an EDTA-ligand competition method (Sonke and Salters, 2006). The corresponding modelled $\log K_{\text{MA}}$ values are reported in Table 2.5. Even if $\log K_{\text{MA}}$ values calculated for the LHA are of the same order of magnitude that $\log K_{\text{MA}}$ values calculated for the Aldrich HA, a marked difference is noted in the shape of the pattern of $\log K_{\text{MA}}$ values. REE-LHA complexation constants do not evidence the same MREE downward concavity as compared to that obtained with Aldrich HA, showing instead a progressive and continuous increase of $\log K_{\text{MA}}$ values from La to Lu (i.e. $\log K_{\text{MA}}(\text{La-HA})/\log K_{\text{MA}}(\text{Sm-HA}) < 1$ and $\log K_{\text{MA}}(\text{Gd-HA})/\log K_{\text{MA}}(\text{Yb-HA}) < 1$). This continuous increase of $\log K_{\text{MA}}$ values from La to Lu as obtained for the LHA as been ascribed to a lanthanide contraction effect, defined as the numerical difference between the Lu and La binding constants ($\Delta_L \beta_{\text{Lu-La}}$ in Sonke and Salters, 2006).

II.2: Rare earth elements complexation with humic acid

[HA]	5 mg L ⁻¹										
pH	2.47	2.95	4.06	4.25	4.35	4.99	6.29	10.44			
La	6.34	9.44	43.01	44.74	50.20	65.83	93.05	99.86			
Ce	9.23	13.66	50.65	52.92	57.97	72.98	95.15	99.83			
Pr	10.33	15.83	54.59	56.81	61.77	76.13	95.89	99.85			
Nd	11.33	15.77	55.44	57.98	62.81	77.37	96.08	99.84			
Sm	12.61	19.05	60.12	62.84	67.27	80.96	96.86	99.84			
Eu	12.10	17.55	58.86	61.45	66.06	80.13	96.70	99.83			
Gd	9.18	14.12	53.04	55.78	60.87	76.16	95.80	99.83			
Tb	9.07	13.52	52.01	54.94	59.90	75.47	95.58	99.83			
Dy	7.87	12.48	49.95	52.99	58.07	73.94	95.22	99.83			
Ho	6.93	10.79	46.92	49.66	54.99	71.50	94.60	99.83			
Er	5.99	9.97	45.74	48.11	53.55	70.22	94.28	99.82			
Tm	6.39	10.35	45.73	48.16	53.62	70.38	94.33	99.82			
Yb	6.16	10.49	46.89	49.16	54.53	71.39	94.61	99.82			
Lu	6.07	9.99	45.35	47.89	53.17	70.40	94.47	99.82			
[HA]	10 mg L ⁻¹										
pH	2.18	2.91	3.45	3.96	4.40	6.16	6.66	6.94	7.26		
La	4.31	34.55	60.55	82.92	94.94	99.44	99.35	99.60	99.69		
Ce	5.00	41.08	67.34	86.81	96.05	99.46	99.36	99.58	99.66		
Pr	10.12	44.49	70.32	88.32	96.45	99.45	99.34	99.56	99.64		
Nd	11.27	45.61	71.33	88.67	96.50	99.41	99.32	99.53	99.61		
Sm	12.2	49.31	74.69	90.25	96.90	99.42	99.30	99.53	99.59		
Eu	10.95	47.67	73.40	89.89	96.78	99.41	99.28	99.52	99.59		
Gd	7.52	42.00	68.91	87.63	96.15	99.36	99.24	99.49	99.57		
Tb	7.5	41.10	67.93	87.33	96.02	99.36	99.22	99.49	99.57		
Dy	5.91	39.21	66.30	86.50	95.71	99.31	99.19	99.47	99.56		
Ho	5.79	36.82	63.87	85.07	95.27	99.27	99.15	99.44	99.53		
Er	5.17	35.88	62.69	84.33	95.01	99.22	99.10	99.41	99.51		
Tm	5.68	36.13	62.77	84.22	94.87	99.18	99.08	99.38	99.48		
Yb	5.15	37.02	63.70	84.75	94.97	99.17	99.07	99.36	99.47		
Lu	5.32	35.77	62.21	83.92	94.77	99.15	99.05	99.34	99.45		
[HA]	20 mg L ⁻¹										
pH	2.21	2.46	2.97	3.51	4.05	5.03	5.48	6.08	6.25	6.65	6.77
La	26.03	57.24	81.73	95.76	98.52	99.44	99.28	99.57	99.67	99.16	99.60
Ce	30.79	63.60	85.09	96.65	98.62	99.38	99.19	99.52	99.63	99.11	99.57
Pr	41.25	67.06	88.39	97.06	98.58	99.31	99.10	99.47	99.59	99.08	99.54
Nd	41.81	67.94	88.83	97.06	98.49	99.22	99.01	99.41	99.54	99.01	99.50
Sm	45.53	70.12	89.96	97.32	98.50	99.20	98.94	99.40	99.54	98.97	99.47
Eu	43.31	68.40	89.34	97.19	98.46	99.18	98.93	99.39	99.54	98.97	99.47
Gd	36.32	63.18	86.97	96.65	98.38	99.16	98.93	99.38	99.52	98.91	99.46
Tb	35.14	61.70	86.46	96.55	98.38	99.17	98.97	99.39	99.53	98.93	99.47
Dy	33.68	60.04	85.65	96.35	98.32	99.12	98.94	99.38	99.52	98.88	99.46
Ho	31.34	57.42	84.34	95.98	98.18	99.04	98.86	99.31	99.47	98.83	99.41
Er	30.33	56.94	83.87	95.74	98.02	98.96	98.77	99.25	99.42	98.77	99.36
Tm	31.41	57.32	84.02	95.70	97.91	98.87	98.69	99.21	99.37	98.73	99.34
Yb	32.64	59.02	84.81	95.76	97.80	98.81	98.59	99.16	99.35	98.73	99.32
Lu	31.37	57.32	83.81	95.41	97.63	98.70	98.48	99.07	99.27	98.62	99.26

Table 2.2. Proportion of REE-HA.

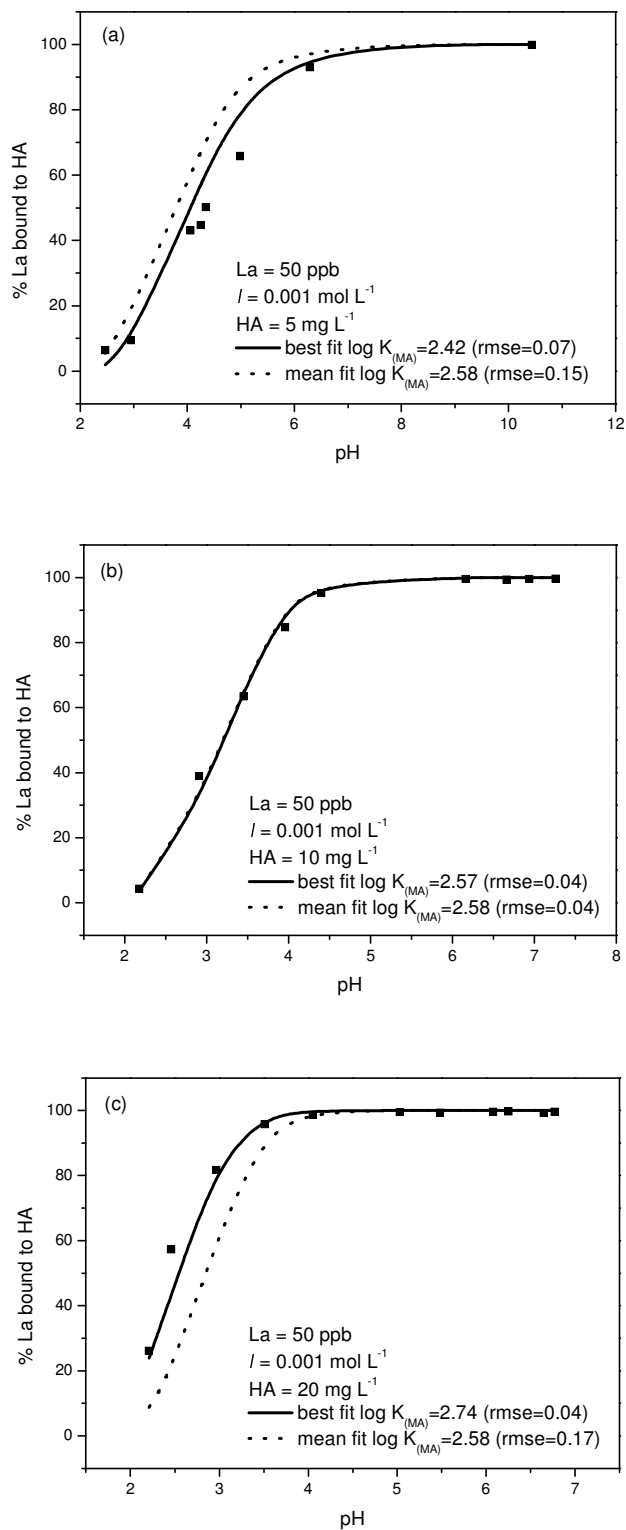


Fig. 2.2. Binding of La by HA. Dependence on pH of % La bound, measured by ultrafiltration; the solid line is the best fit and the dash line represents the calculated binding for the overall average $\log K_{\text{MA}}$ (2.58) for various HA concentrations (a) 5 mg L^{-1} , (b) 10 mg L^{-1} , (c) 20 mg L^{-1} .

[HA] (mg L ⁻¹)	5	(rmse)	10	(rmse)	20	(rmse)	mean	sd
La	2.42	0.07	2.57	0.04	2.74	0.04	2.58	0.16
Ce	2.44	0.05	2.60	0.04	2.77	0.03	2.60	0.17
Pr	2.45	0.05	2.61	0.03	2.78	0.01	2.61	0.17
Nd	2.47	0.06	2.63	0.02	2.79	0.02	2.63	0.16
Sm	2.50	0.05	2.65	0.03	2.81	0.01	2.65	0.16
Eu	2.50	0.05	2.64	0.04	2.80	0.02	2.65	0.15
Gd	2.48	0.07	2.62	0.05	2.79	0.02	2.63	0.16
Tb	2.47	0.07	2.61	0.04	2.78	0.02	2.62	0.16
Dy	2.46	0.06	2.59	0.04	2.78	0.02	2.61	0.16
Ho	2.45	0.07	2.58	0.05	2.77	0.02	2.60	0.16
Er	2.45	0.07	2.57	0.02	2.77	0.02	2.60	0.16
Tm	2.44	0.07	2.56	0.02	2.76	0.02	2.59	0.16
Yb	2.45	0.06	2.57	0.01	2.77	0.03	2.60	0.16
Lu	2.44	0.07	2.56	0.04	2.76	0.02	2.59	0.16
La/Sm	0.97		0.97		0.98		0.97	
Gd/Yb	1.01		1.02		1.01		1.01	

Table 2.3. Log K_{MA} values obtained for the three datasets using Model VI. rmse refers to root mean square error of the regression analysis (see text for details) while sd refers to standard deviation on the mean.

REE	[REE] ($\mu\text{mol L}^{-1}$)	I (mol L^{-1})	[HA] mg L ⁻¹	pH	technique	log K_{MA}	rmse	n	References
Eu	0.001	0.05	10	2 to 10	IE	2.73	0.01	7	Fairhurst et al., 1995
Eu	0.001	0.05	2	2 to 10	IE	2.77	0.04	7	Fairhurst et al., 1995
Tb	0.100	0.10	5	2 to 7	IE	2.57	0.06	7	Lippold et al., 2005
Dy	2.000	0.10	0.5 to 9	5	S	3.19	0.03	13	Moulin et al., 1992

Table 2.4. Experimental conditions and fit of literature data (IE: ion exchange; S: spectrofluorometry). rmse corresponds to root mean square error of the regression analysis (see text for detail).

The major difference between the results obtained here and the only dataset so far published for the 14 naturally occurring REE with HA is thus in the shape of the log K_{MA} values: MREE downward concavity here against linear increase from La to Lu for data published by Sonke and Salters (2006). They compared the constants they found for REE-LHA complexation with those found for 101 organic ligands (Byrne and Li, 1995). They further suggested that the lanthanide contraction effect they observed for LHA was in fact shared by a large number of organic ligands and could thus be a general feature of REE complexation by organic compounds. In addition to LHA, Sonke and Salters (2006) also determined REE complexation constants for two other organic ligands – namely, fulvic acid from the Suwannee River and Elliot soil humic acid – using the same ligand-ligand technique as that used for LHA. They also evidenced a lanthanide contraction effect of their constant pattern. These authors also compared their experimental data with REE patterns of river and soil waters. They argued that organic-rich waters usually exhibit HREE enriched patterns and that this enrichment is a natural verification that a lanthanide contraction effect should exist in the organic matter mediated REE complexation constant pattern (i.e. preferential complexation of the HREE over the LREE). In the present study, no justification was found that a lanthanide contraction effect should exist in the complexation constants of REE by organic matter. Instead, the existing databank (Wood, 1993; Byrne and Li, 1995) points to a MREE downward concavity of the constant pattern, as obtained in the present study.

pH	6	7	8	9
La	2.57	2.44	2.22	2.16
Ce	2.56	2.44	2.25	2.20
Pr	2.53	2.44	2.26	2.23
Nd	2.51	2.40	2.26	2.22
Sm	2.52	2.42	2.30	2.28
Eu	2.54	2.46	2.31	2.25
Gd	2.54	2.45	2.31	2.23
Tb	2.59	2.45	2.34	2.30
Dy	2.59	2.48	2.37	2.37
Ho	2.60	2.45	2.39	2.38
Er		2.47	2.41	2.41
Tm	2.64	2.51	2.46	2.46
Yb		2.51	2.47	2.44
Lu	2.67	2.54	2.50	2.48
La/Sm	1.02	1.01	0.97	0.95
Gd/Yb		0.98	0.94	0.91

Table 2.5. Log K_{MA} values obtained for the four Sonke and Salters' datasets (2006) using Model VI (pH 6 to 9, 0.1 mol L⁻¹ NaNO₃, 100 nmol L⁻¹ REE, 10 mg L⁻¹ LHA and 500 nmol L⁻¹ EDTA).

Complexation constants of REE with SRFA were also determined by Yamamoto et al. (2005) using a solvent extraction technique (Fig. 2.3a; see also Fig. 1 in Yamamoto et al., 2005). Pattern of log β (REE-FA) looks very much like that found in the present study for REE-HA, being characterized by a MREE downward concavity shape (i.e. $\log K_{MA}(\text{La-HA})/\log K_{MA}(\text{Sm-HA}) < 1$ and $\log K_{MA}(\text{Gd-HA})/\log K_{MA}(\text{Yb-HA}) > 1$). Binding of the REE to humic substances occurs mainly through carboxylic functions (Yamamoto et al., 2005). In this respect, simple organic compounds possessing carboxylic functional groups such as acetate can be regarded as analogue of complex organic matter, such as HA and FA (Wood, 1993). Thus, log K_{MA} pattern of REE complexation with FA, HA and acetic acid can be together compared (Fig. 2.3) (Wood, 1993; Byrne and Li, 1995). As can be seen, patterns of log K_{MA} values for acetic and diacetic acids do not evidence a lanthanide contraction effect: they are MREE downward concave, mimicking both those obtained by Yamamoto et al. (2005) for SRFA and through this study for HA.

The argument used by Sonke and Salters (2006) that a lanthanide contraction effect is observed in the constant pattern of many organic compounds is questionable. Indeed, their demonstration was built on the fact that a positive correlation exists when $\Delta_L \beta_{Lu-La}$ of organic compounds is plotted against the average REE constant (β_{ave}). REE stability constant is not always a simple function of atomic number. As suggested by Byrne and Li (1995), REE are best viewed as two series of elements corresponding to the LREE and HREE groups. The pattern shape of complexation constants for REE with many organic ligands (Wood, 1993; Byrne and Li, 1995) or some inorganic ligands like NO₃⁻ (Wood, 1990; Millero, 1992) are characterized by patterns that exhibit a downward concavity centred on MREE. This shape corresponds to a (La/Sm) ratio below 1 and (Gd/Yb) ratio above 1 (Fig. 2.3a). Thus, such shapes are best viewed when REE are considered as two subgroups. Indeed, $\Delta_L \beta_{Lu-La}$ value does not give an accurate description of the constants pattern. Let us for example consider a $\Delta_L \beta_{Lu-La} > 1$. Such a value may actually reflect a pattern showing a continuous increase of the constant values from La to Lu, and thus a real HREE enrichment. However, it may also reflect a REE pattern showing an increase of log β values only from La to Sm or Eu and then constant values from Gd to Lu (no real HREE enrichment). It may even reflect a MREE downward concave pattern, the only required feature in that case being $\log \beta_{La} < \log \beta_{Lu}$. To test this possibility $\Delta_L \beta_{Lu-Sm}$ (i.e. shape of the MREE and HREE part of the constant pattern) values for the same 101 organic compounds were calculated

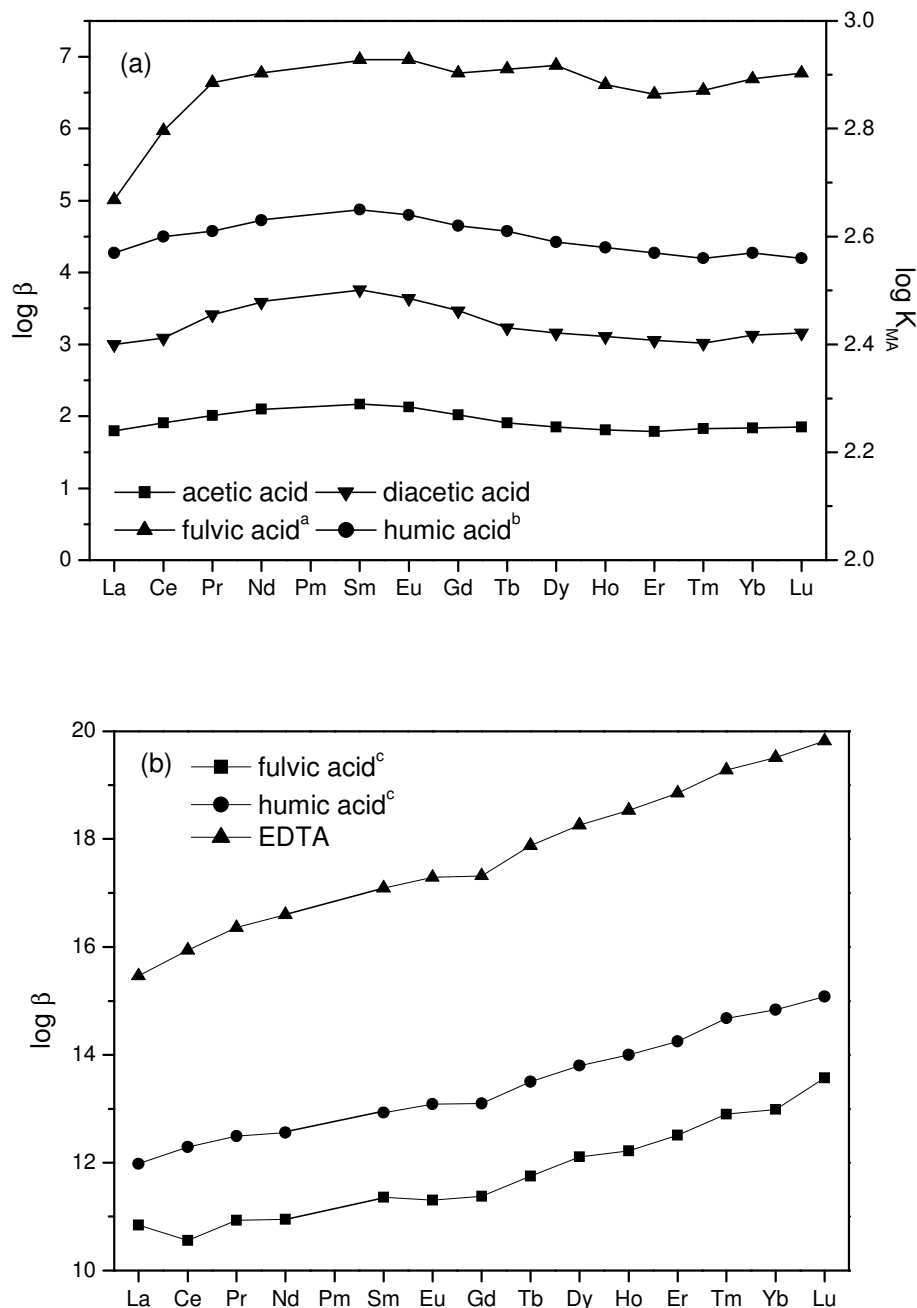


Fig. 2.3. REE patterns for a) $\log \beta$ (REE-acetic acid), $\log \beta$ (REE-diacetic acid), $\log \beta$ (REE-fulvic acid)^a and $\log K_{MA}$ (REE-humic acid)^b and b) $\log \beta$ (REE-EDTA), $\log \beta$ (REE-fulvic acid)^c and $\log \beta$ (REE-humic acid)^c.

^a Yamamoto et al. (2005); ^b this study; ^c Sonke and Salters (2006).

and compared with $\Delta_L \beta_{Lu-La}$ and β_{ave} of these compounds. As shown in Fig. 2.4, the comparison shows that the positive correlation reported by Sonke and Salters (2006) when reporting $\Delta_L \beta_{Lu-La}$ values of 101 compounds against their β_{ave} is lost when $\Delta_L \beta_{Lu-Sm}$ is substituted to $\Delta_L \beta_{Lu-La}$ values. Quite clearly, several strongly REE-complexing organic components ($\log \beta_{ave} > 15$) do have $\Delta_L \beta_{Lu-Sm}$ values close to 0, i.e. flat or concave downward MREE constant pattern. For the purpose comparison Yamamoto et al. data for SRFA (Yamamoto et al., 2005) and Sonke and Salters' data for SRFA and LHA (2006) were included in Fig. 2.4. In the present study, only $\log K_{MA}$ were

determined (and not $\log \beta$). Consequently, only a field of possible β_{ave} (delimited by extremum literature β_{ave} values) can be compared with the $\Delta_L \beta_{\text{Lu-Sm}}$ calculated from $\log K_{\text{MA}}$ (dotted line in Fig. 2.4b). The lower part of this field includes Yamamoto's $\log \beta$ for SRFA. However, the understanding of this fractionation is not obvious and such a MREE downward concavity remains to be explained.

While Yamamoto's $\log \beta$ for SRFA are in the field of carboxylic and phenolic acids (Fig. 2.4), Sonke and Salters' $\log \beta$ for SRFA and LHA are in the field of synthetic iminoacetic acids such as EDTA (Fig. 2.4). $\log \beta$ (REE-HA) patterns reported by Sonke and Salters mimic those of $\log \beta$ (REE-EDTA). Indeed, (Gd/Yb) ratios vary from 0.90 to 0.94 and a "Gd break" can be observed in Sonke and Salters' dataset reflecting an octad effect similar to $\log \beta$ (REE-EDTA) pattern (Fig. 2.3b). Thus, competition experiments between REE, LHA and EDTA do mostly reflect an REE-EDTA pattern. In a ligand-ligand competition technique the requirement is that there should be an equitable distribution of the cation between the two competing ligands (Wu and Horrocks Jr., 1996). However, in their experiments REE-EDTA species are strongly predominant (> 85 % for Eu-EDTA) in the 6-9 pH range (see Fig. 4 in Sonke and Salters, 2006). The HREE-enrichment observed on the $\log \beta$ pattern determined by these authors (Sonke and Salters, 2006) has thus to be considered as an experimental artefact.

However, the similar MREE downward concavity patterns observed for REE complexation with HA (present study), with FA (Yamamoto et al., 2005) and with model molecule of carboxylic sites (acetic acid) (Wood, 1993), evidence that this type of fractionation could be expected in natural systems. Endly, the comparison of Sonke and Salters (2006), Yamamoto et al. (2005), and present datasets allow validating the new $\log K_{\text{MA}}$ (REE-HA) dataset presented in this study which could be then used to predict REE speciation in natural waters.

2.4.2. REE speciation in natural river and soil waters

Several authors confer a major role to the colloidal fraction in the transport of REE by rivers (Hoyle et al., 1984; Goldstein and Jacobsen, 1988; Cantrell and Byrne, 1987; Elderfield et al., 1990; Sholkovitz, 1992). Elderfield et al. (1990) proposed for example the existence of two REE compartments in river waters (Fig. 2.5): (i) a "truly" dissolved pool, LREE depleted, but HREE enriched (Fig. 2.5a) and (ii) a "colloidal" pool LREE enriched and HREE flat, i.e. close to UCC (Fig. 2.5b) (Taylor and McLennan, 1985). Several studies have suggested that the HREE enrichment of the dissolved pool may be due to the greater solubility of HREE carbonate complexes as compared to LREE carbonate ones (Goldstein and Jacobsen, 1988; Elderfield et al., 1990; Sholkovitz, 1992). However, one of the characteristics of some river waters is that $(\text{La/Sm})_{\text{N}}$ and $(\text{Gd/Yb})_{\text{N}}$ ratios are commonly lower than and higher than 1, respectively, producing a concave REE pattern (Fig. 2.5b) (Goldstein and Jacobsen, 1988; Elderfield et al., 1990; Sholkovitz, 1995; Viers et al., 1997; Deberdt et al., 2002). Such a characteristic is also well evidenced in organic rich groundwaters (Viers et al., 1997; Dia et al., 2000; Deberdt et al., 2002; Gruau et al., 2004). As shown on Fig. 2.6, $(\text{Gd/Yb})_{\text{N}}$ ratios increase while DOC content increases (Goldstein and Jacobsen, 1988; Elderfield et al., 1990; Sholkovitz, 1995; Viers et al., 1997; Deberdt et al., 2002). These features are further illustrated by ultrafiltration studies of organic rich river- and ground-water samples. They indicate the absence of fractionation of HREE relative to LREE with decreasing pore-size in the wide range of investigated pH (from 5.6 to 7.7) (Sholkovitz, 1995; Viers et al., 1997; Douglas et al., 1999; Dupré et al., 1999; Dia et al., 2000; Ingri et al., 2000; Deberdt et al., 2002), they even evidence for some of them a MREE downward concavity fractionation (e.g., Fig. 15 in Sholkovitz, 1995). However, such a fractionation alone could not explain the whole REE pattern fractionation. Indeed, Johannesson et al. (1996a) suggested that MREE enrichment in hypersaline waters is the result of mineral weathering due to

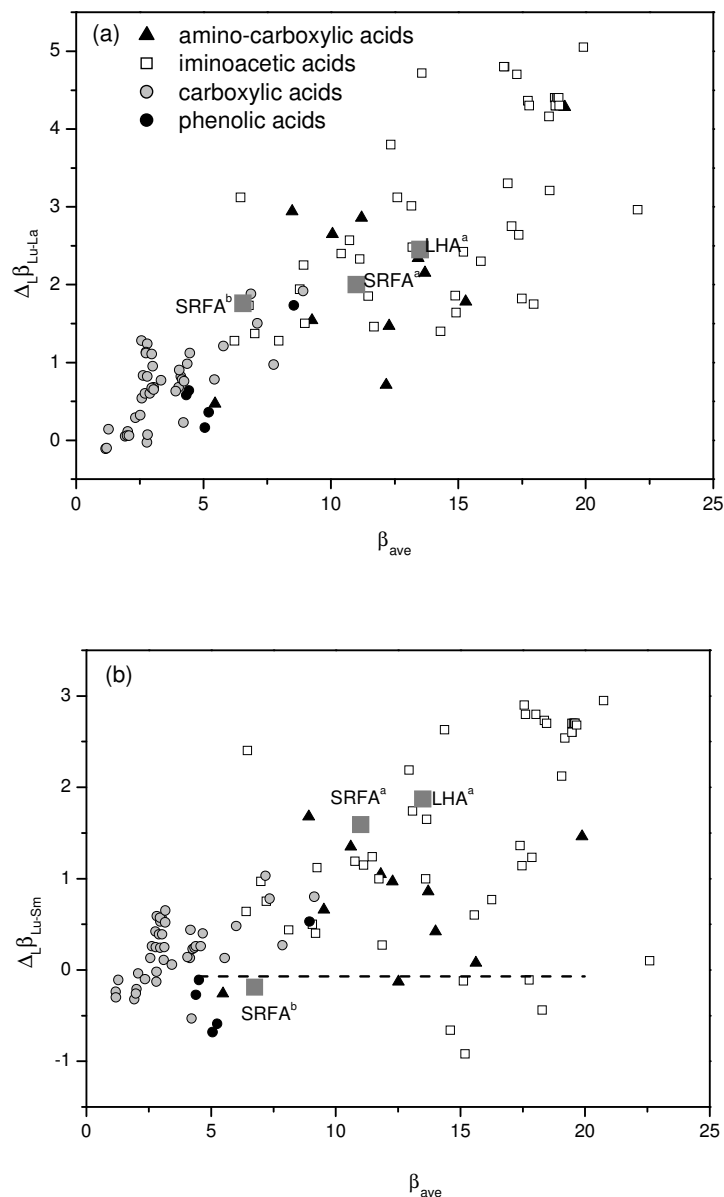


Fig. 2.4. Literature compilation of REE-organic ligand constants (Byrne and Li, 1995).

^a Sonke and Salters (2006); ^b Yamamoto et al. (2005).

dissolution of MREE-enriched Fe- and Mn-rich particulates or surface coatings. Hannigan and Sholkovitz (2001) also proposed that MREE enrichment has to be related to the weathering of co-precipitated phosphates minerals. The present study demonstrates that organic substances plays a major control onto REE speciation and thus onto REE pattern shape. Based on this ability of HA to preferentially complex MREE, REE fractionation patterns at the Earth's surface can be revisited. DOC-rich river- and ground-waters REE pattern may reflect a mixing between (i) dissolved fraction of DOC-rich soil solutions, surface runoff and river waters which display MREE downward concavity patterns (Viers et al., 1997; Dia et al., 2000; Deberdt et al., 2002; Gruau et al., 2004); and (ii) river suspended particles which are slightly HREE depleted (Sholkovitz, 1995) inherited from preferential adsorption of LREE over suspended particle.

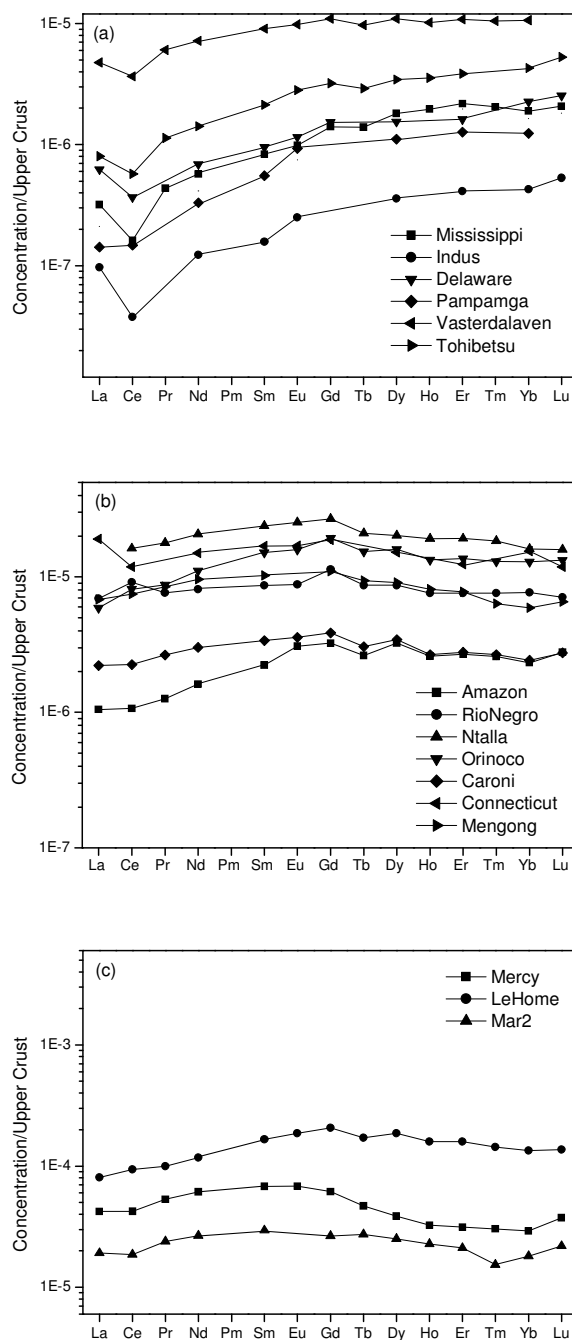


Fig. 2.5. REE normalized (to UCC) (Taylor and McLennan, 1985) patterns of river waters showing a) HREE enrichment and b) MREE enrichment (Goldstein and Jacobsen, 1988; Elderfield et al., 1990; Sholkovitz, 1995; Deberdt et al., 2002), and c) soil waters showing MREE enrichment (Viers et al., 1997; Dia et al., 2000; Gruau et al., 2004).

Up to now investigations of REE speciation in natural river and soil waters were performed using Model V and Model VI only with extrapolated constants obtained from Linear Free-Energy Relationships (LFER) (Tang and Johannesson, 2003; Pourret et al., 2006b). Using the new determined $\log K_{MA}$ dataset, REE speciation calculations - as a function of pH - were performed for the World Average River Water (Tang and Johannesson, 2003) in order to validate the results obtained with extrapolated constants. Major ions such as Fe and Al were adopted for re-calculating the REE speciation of the modelled World Average River Water (see Table 11 in

Tang and Johannesson, 2003). The same value of 5 mg L^{-1} for DOC was used. It was assumed that 80 % and 20 % of DOM are made up of FA and HA, respectively. Since pH is a key parameter to REE speciation, the REE speciation calculations were performed in the same way of these authors (op. cit.), i.e. holding the major solute composition constant (except HCO_3^- and CO_3^{2-}) and varying pH. Moreover, a fair degree of similarity between the model constants obtained for fulvic and humic acids exists as previously stated (Tipping and Hurley, 1992; Tipping, 1998) so $\log K_{\text{MA}}(\text{FA})$ were calculated from $\log K_{\text{MA}}(\text{HA})$, obtained in section 2.3, using Eqn. 19 in Tipping (Tipping, 1998).

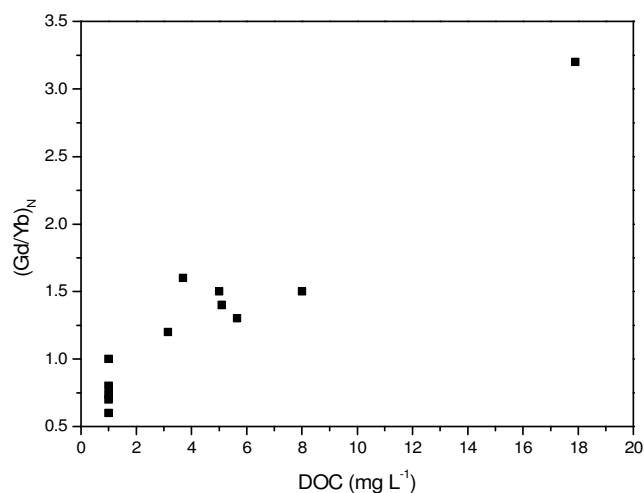


Fig. 2.6. DOC concentrations as a function of $(\text{Gd}/\text{Yb})_N$ ratios; data are from river waters presented in Fig. 2.5 (when no DOC concentrations available a concentration of 1 was assumed for comparison purpose (Thurman, 1985)).

The obtained results are shown for La, Eu, and Lu in Fig. 2.7. The REE-HM species represent the proportion of each REE complexed with humic substances. The Model VI results are consistent with earlier investigations performed using Model V and Model VI with extrapolated constants from LFER (Tang and Johannesson, 2003; Pourret et al., 2006b). Model VI predicts that (i) REE occur predominantly as organic complexes ($\text{REE-HM} \geq 60\%$) in the pH range between 5-5.5 and 7-8.5 (i.e. circumneutral pH waters), (ii) REE-HM complexes become progressively less important with increasing atomic number across the REE series, and (iii) pH at which proportion of REE-HM species is maximum decreases from La to Lu. The only noticeable difference is that the new fitted constants allow Model VI to calculate significantly higher proportions of REE complexed with organic matter at high pH conditions than with extrapolated constants. As an example, with the fitted constants Model VI predicts La-HM $\sim 85\%$ at pH 9, while with extrapolated constants it only predicts 60 % of La-HM. However, these new calculations are also a validation of the LFER method (Tang and Johannesson, 2003; Pourret et al., 2006b). Moreover, these results are coherent with simple speciation calculations performed by Takahashi and co-workers (Takahashi et al., 1997; Takahashi et al., 1999) which led them to speculate that humate complexes should be the dominant species of REE(III) dissolved in natural aquifers where DOM occurs significantly.

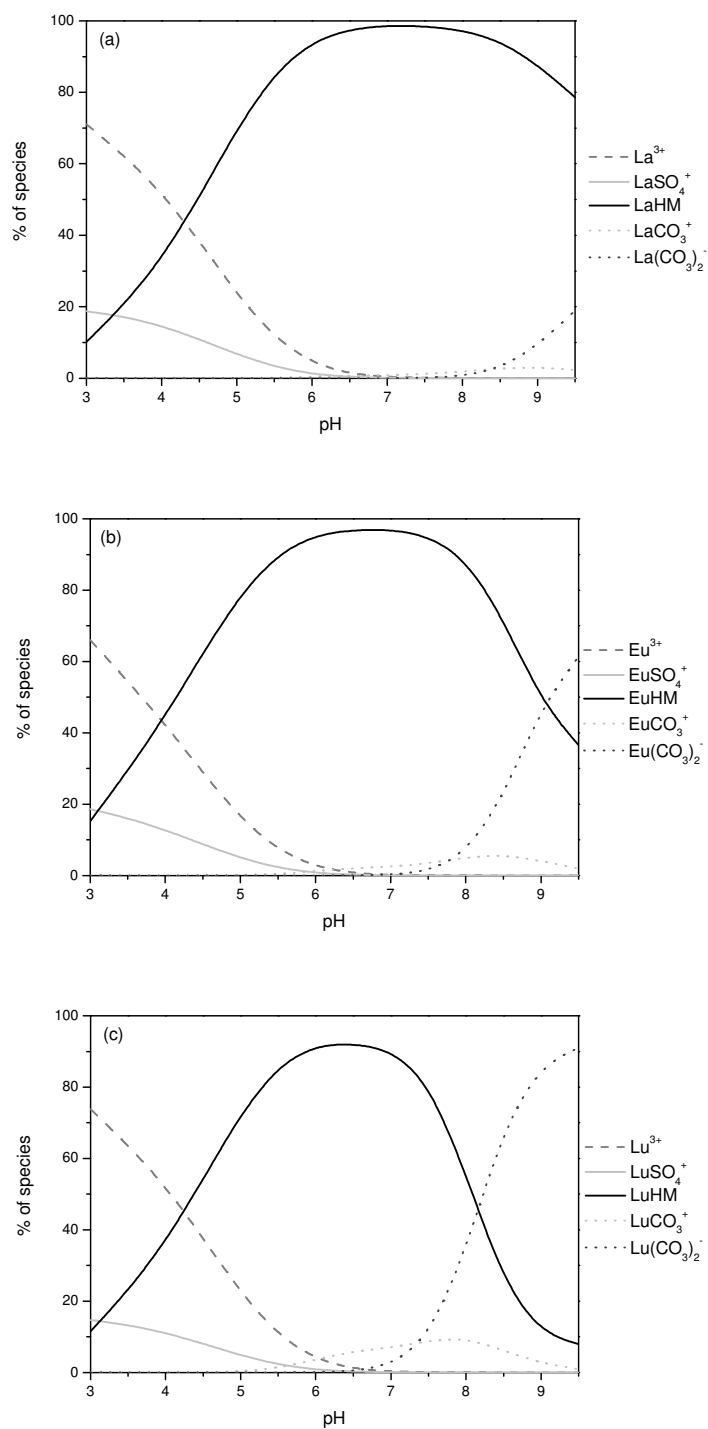


Fig. 2.7. Model VI speciation calculations for (a) La, (b) Eu and (c) Lu in World Average River Water as a function of pH.

2.5. Conclusions

Experimental studies of REE-HA binding were carried out using an ultrafiltration method. A strong pH dependence resulting in a significant increase in the proportion of REE-HA with increasing pH and a MREE downward concavity fractionation at acidic pH were observed. Moreover, modelling was performed using Humic Ion Binding Model VI. Experimental results

were fitted to obtain a set of constants ($\log K_{MA}$). Those constants are in good agreement with some literature constants. However, they are in contradiction with a recent study (Sonke and Salters, 2006) which evidences a lanthanide contraction effect. Model VI constants in this study indicate that REE-HA complexation involved a fractionation similar to the REE complexation with simple carboxylic groups such as acetates. The similar MREE downward concavity pattern observed for REE complexation with HA (this study), with FA (Yamamoto et al., 2005) and with simple organic acid such as acetic acid (Wood, 1993; Byrne and Li, 1995), illustrates that this type of fractionation could be expected in natural systems. These observations led us to rebut that the lanthanide contraction effect proposed by Sonke and Salters (2006) is specific to REE complexation with organic matter. All these observations allow validating the present $\log K_{MA}$ (REE-HA) dataset that can be, therefore, used with confidence to predict REE speciation in natural waters.

Moreover, the results of the present study shed more light on the REE cycle at the Earth's surface. They evidence that organic REE speciation plays a major role onto REE fractionation in natural organic-rich river- and groundwaters. Dissolved fractions of DOC-rich soil solutions, surface runoff, and river waters display MREE downward concavity patterns. The new $\log K_{MA}$ were additionally introduced in WHAM 6 to predict speciation of the World Average River Water. REE occur predominantly as organic complexes ($REE-HM \geq 60\%$) in circumneutral pH waters (pH range between 5-5.5 and 7.5-8). New fitted constants allow Model VI to calculate high proportions of LREE complexed with organic matter under alkaline pH conditions. Overall, the results of this study suggest that further considerations about organic matter should be taken into account to model and thus better understand global continent-ocean trace metal cycles.

Troisième Partie
Complexation compétitive entre acides humiques et
carbonate vis-à-vis des terres rares

1. Competition between humic acid and carbonates for rare earth elements complexation

Cette partie est extraite d'un article soumis à Journal of Colloid and Interface Science, Pourret O., Davranche M., Gruau G. and Dia A. (2006) Competition between Humic Acid and Carbonates for Rare Earth Elements Complexation

Résumé- La complexation compétitive des terres rares (REE) par des acides humiques (HA) et des carbonates a été étudiée expérimentalement pour différents pH et différentes alcalinité en combinant des 'ultrafiltrations et des analyses ICP-MS. Les résultats montrent que les REE sont à la fois sous forme de complexes humiques et carbonatés. Cependant, aucun complexe ternaire n'a été mis en évidence au contraire d'études antérieures. Cette compétition est fortement dépendante du pH et de l'alcalinité. Un fractionnement systématique au sein de la série des REE se produit également. La complexation aux carbonates est maximum à pH 10, celle-ci augmentant avec l'augmentation de l'alcalinité et avec le numéro atomique ($\text{LuCO}_3 \gg \text{LaCO}_3$). La modélisation des données par Model VI et les constantes de complexation terres rares acides - humiques récemment publiées, reproduit les données expérimentales. La capacité de Model VI à déterminer avec précision la spéciation des REE dans les eaux naturelles est donc confirmée. De plus, cette modélisation prouve une nouvelle fois la fiabilité des constantes de complexation récemment proposées. Ce travail met en exergue non seulement la compétition entre carbonates et HA pour la complexation des REE mais également la fiabilité de WHAM 6 et Model VI à prédire la spéciation des REE avec la matière organique dans des eaux organiques alcalines.

Abstract. The competitive binding of rare earth elements (REE) to humic acid (HA) and carbonates was studied experimentally at various pH and alkalinity by combining Ultrafiltration and Inductively Coupled Plasma Mass Spectrometry techniques. The results show that the REE species occur as binary humate or carbonate complexes but not as ternary REE-carbonate-Humate as previously proposed by some authors. They also reveal the strong pH and alkalinity dependence of the competition as well as the existence of a systematic fractionation across the REE series. Specifically, carbonate complexation is maximum at pH 10 and increase with increasing alkalinity and with the atomic number of the REE ($\text{LuCO}_3 \gg \text{LaCO}_3$). Modelling of the data using Model VI and recently published stability constants for complexation of REE by humic acid well reproduced the experimental data, confirming the ability of Model VI to accurately determine REE speciation in natural waters. This modelling is also confirmation of the reliability of recently published stability constants. This work shed more light not only on the competition between carbonates and HA for REE complexation but also on the reliability of WHAM 6 and Model VI in calculating the speciation of REE with organic matter in alkaline organic rich-water.

1.1. Introduction

The hydrochemical behavior of Rare Earth Elements (REE) is strongly influenced by their solution speciation (Wood, 1990; Byrne and Sholkovitz, 1996). Due to the complexation of REE by a large variety of ligands, only a small fraction of each REE occurs as free hydrated ions (Ln^{3+} - Ln as lanthanide) in circumneutral waters. In circumneutral waters, REE are mostly bound to humic substances (HM) such as fulvic acids (FA) and humic acids (HA) (Viers et al, 1997; Dia et al., 2000; Tang and Johannesson, 2003). By contrast, in alkaline waters with high carbonates concentrations, REE complexation is generally dominated by carbonates complexes as LnCO_3^+ and $\text{Ln}(\text{CO}_3)_2^-$ (Byrne and Sholkovitz, 1996; Tang and Johannesson, 2003). However, competition reactions between carbonates and organic matter for REE complexation have not been experimentally constrained. At present, accurate models of REE chemistry in natural waters are only dependent on experimentally determined (i) REE carbonates complexation constants (Cantrell and Byrne, 1987; Millero, 1992; Lee and Byrne, 1993; Liu and Byrne, 1998; Ohta and Kawabe, 2000; Luo and Byrne, 2004; Quinn et al., 2004) and (ii) REE humic substances constants (Yamamoto et al., 2005; Sonke et al., 2006; Pourret et al., 2006c). However, since there is no experimental data about competition between carbonates and organic matter for REE complexation, an important piece of the puzzle is missing.

Previous studies (Wood, 1993; Fairhurst et al., 1995; Lead et al., 1998; Tang and Johannesson, 2003) based on speciation calculation of some REE (e.g., La^{3+} , Eu^{3+} , Lu^{3+}) concluded that organic complexes dominate for intermediate pH range (from pH 4 to 8) whereas carbonate complexes ($\text{Ln}(\text{CO}_3)_2^-$) are the predominant species at alkaline pH (> 8). However, as discussed by these authors themselves, speciation calculation may underestimate the LnHM complexes, especially at alkaline pH (> 8). They suggest that this could have significant effects on ternary inorganic-colloid-HM-Ln interactions (Dierckx et al., 1994; Fairhurst et al., 1995; Moulin et al., 1999). They also suggested that Ln speciation would be dominated by interactions with humic material. The lack of experimental data regarding to the LnHM interactions at neutral-to-alkaline pH leads to important extrapolations and the speciation results on alkaline waters should be regarded with caution (Lead et al., 1998). Takahashi et al. (1999) calculated speciation of Ce^{3+} , Eu^{3+} and Lu^{3+} in solution in the presence of humic acid. Hydroxide carbonates and humate complexes were considered. Unlike above studies, their results suggest that LnHA complexes should be predominant in a large pH range (from pH 3 to 10.5), and even more at higher HA concentrations. $\text{Ln}(\text{CO}_3)_2^-$ should be dominant at pH higher than 10.5. These observations are further illustrated by a new study considering Model VI fitted complexation constants between REE and HA. Model VI calculated high proportions of light REE (LREE) complexed with organic matter under alkaline pH conditions (Pourret et al., 2006c). Comparison of REE speciation model calculations taking into account organic ligands shows thus strong differences between each model regarding the competition between humic substances and carbonates for REE complexation.

In order to assess humic acid and carbonates competition for REE at alkaline pH, batch equilibration experiments with REE, Aldrich HA and carbonates were performed for the 14 naturally occurring REE, simultaneously. This new dataset was obtained using an experimental method which combines an ultrafiltration technique and the Inductively Coupled Plasma Mass Spectrometry method. These experiments are designed to elucidate the pH range where REE-humate complexes could be dominant in natural organic-rich waters for various alkalinity concentrations and test whether significant formation of ternary complexes can take place in such conditions or not. Moreover, Humic Ion Binding Model VI included in WHAM 6 - a model that does not considered ternary surface complexes - was used to model the binding of lanthanides to humic substances (Tipping, 1998). This study should also bring evidence on the ability of the newly determined HA-REE binding constants (Pourret et al., 2006c) to accurately predict the speciation of REE in alkaline waters.

1.2. Materials and Methods

1.2.1. Experimental Binding of Rare Earth Elements by Humic Acid and Carbonates

All chemicals used were of analytical grade, and all the experimental solutions were prepared with doubly deionized water (MilliQ system, Millipore™). Complexes were prepared in polyethylene containers previously soaked in 10 % Ultrapure HNO_3 for 48 h at 60 °C, then rinsed with MilliQ water for 24 h at 60 °C to remove all possible REE contamination sources. Synthetic REE solutions were prepared from nitrate REE standards (10 ppm, Accu Trace™ Reference Standard). All experiments were carried out at room temperature, i.e. 20 °C ± 2.

1.2.1.1. Humic acid

Purified humate, referred to below as HA (humic acid), was obtained from synthetic Aldrich™ humic acid (Aldrich™, H1, 675-2) following the protocol described by Vermeer et al. (1998). HA sample was freeze-dried and stored in a glass container at room temperature. HA obtained was ash free and in its protonated form, with the following elemental composition (in

weight percent): C = 55.8 %, O = 38.9 %, H = 4.6 %, N = 0.6 %. REE concentrations REE in HA were below the detection limit of ICP-MS measurement (i.e. below 1 ppt). HA has a mean molecular weight of 23 kDa (Vermeer et al., 1998). Prior to use, the freeze-dried humate was resuspended overnight in an 0.001 mol L⁻¹ NaCl electrolyte solution at pH = 10, to ensure complete dissolution of the sample (Davranche et al., 2004; 2005).

1.2.1.2. Experimental set-up

REE complexation with HA and carbonates was investigated using a standard batch equilibration technique. 100 mL of solutions were prepared with 50 ppb of each REE (e.g., 360 nmol L⁻¹ La to 286 nmol L⁻¹ Lu), 5 mg L⁻¹ of HA and various concentration of NaHCO₃ (from 10⁻³ to 10⁻² mol L⁻¹) in a 10⁻³ mol L⁻¹ NaCl-solution. Prior to addition of NaHCO₃, pH-solution was about 4. The initial hydroxide concentration was thus negligible and concentration of LnOH²⁺ was therefore minimal. After addition of NaHCO₃, pH was adjusted to the tested pH range, between 6 and 11 by adding NaOH (4 mol L⁻¹). The pH was measured with a combined Radiometer Red Rod electrode. The electrode was calibrated with WTW standard solutions (pH 4, 7 and 10). The accuracy of the pH measurement was ± 0.05 pH unit. Experimental solutions were stirred for 48 h (equilibrium time determined from preliminary kinetic experiments) to allow equilibration and partitioning of REE between the aqueous solution and the humate suspension. Aliquots of 10 mL were sampled twice: at the beginning of the experiment; and after 48 h at equilibrium state. REE complexed by the HA were separated from the remaining inorganic REE by ultrafiltration. Ultrafiltrations were carried out by centrifugating the 10 mL solution samples through 15 mL centrifugal tubes equipped with permeable membranes of 5 kDa pore size (Millipore Amicon Ultra-15). All centrifugal filter devices used were washed and rinsed with 0.1 mol L⁻¹ HCl and MilliQ water two times before use in order to minimize contamination. Centrifugations were performed using a Jouan G4.12 centrifuge with swinging bucket rotor at 3000 g for 30 minutes. This allowed the REE-HA complexes to be quantitatively separated from inorganic REE species. The selectivity of the 5 kDa membrane regards to the REE-HA complexes was verified by monitoring the Dissolved Organic Carbon (DOC) contents of the ultrafiltrates. Results show that the latter were systematically lower or equal to blank values (below 1 ppm). Possible adsorption of inorganic REE species onto the membrane or onto cell walls was also monitored. Inorganic REE solutions of given REE concentration were ultrafiltered several times. Results showed that 100 % of the REE present in solution were recovered in the ultrafiltrates, demonstrating that none REE were adsorbed either on the membranes or on the walls of the cell devices.

Amount of REE complexed with HA correspond to the difference between the initial REE concentration and the remaining REE concentration into the < 5 kDa ultrafiltrates. REE concentrations were determined at Rennes 1 University using an Agilent TechnologiesTM HP4500 ICP-MS instrument. Quantitative analyses were performed using a conventional external calibration procedure. Three external standard solutions with REE concentrations similar to the analyzed samples were prepared from a multi-REE standard solution (Accu TraceTM Reference, 10 mg L⁻¹, USA). Indium was added to all samples as an internal standard at a concentration of 0.87 μmol L⁻¹ (100 ppb) to correct for instrumental drift and possible matrix effects. Indium was also added to the external standard solutions. Calibration curves were calculated from measured REE/indium intensity ratios. The instrumental error on REE analysis in our laboratory as established from repeated analyses of multi-REE standard solution (Accu TraceTM Reference, USA) and of the SLRS-4 water standard is below ± 2 % (Dia et al., 2000; Davranche et al., 2005). Chemical blanks of individual REE were all lower than detection limit (1 ppt), which is negligible since they are three to four orders of magnitude lower than the concentrations measured in the synthetic solutions used for the complexation experiments.

DOC concentrations were determined at Rennes 1 University using a Shimadzu 5000 TOC analyzer. The accuracy of DOC concentration measurements is estimated at $\pm 5\%$ as determined by repeated analyses of freshly prepared standard solutions (potassium biphtalate).

Carbonates concentrations were determined by potentiometric titrations ($\text{HCl } 0.1 \text{ mol L}^{-1}$), with Gran method analysis. The uncertainty is better than 5% .

In order to check that no retention of REE or carbonates occurs inside the membrane during ultrafiltration, mass balance calculations were performed. The initial concentration of each element is compared with the sum of each element concentration in the ultrafiltrate and in the retentate. In the presented experiments, mass balanced calculations show that $> 98\%$ of the REE and $> 95\%$ of the carbonates and DOC were recovered. Moreover, in order to verify that no precipitation occurs, samples were filtrated at $0.2 \mu\text{m}$ before ultrafiltration. Concentrations of REE, HA and carbonates were systematically identical within analytical uncertainties in the $0.2 \mu\text{m}$ filtrates and the raw samples.

1.2.2. WHAM 6 and Humic Ion Binding Model VI

WHAM 6 (version 6.0.10), incorporating Humic Ion Binding Model VI (Model VI), was used to calculate REE speciation in the batch experiments. Model VI has been described in detail by Tipping (1998). The model is a discrete binding site model in which binding is modified by electrostatic interactions. There is an empirical relation between net humic charge and an electrostatic interaction factor. The discrete binding sites are represented by two types of sites (types A and B), and within each type of site there are four different sites present in equal amounts. The two types of sites are described by intrinsic proton binding constants (pK_A and pK_B) and spreads of the values (ΔpK_A and ΔpK_B) within each type of sites. There are n_A (mol g^{-1}) A-type sites (associated with carboxylic type groups) and $n_B = n_A/2$ (mol g^{-1}) B-type of sites (often associated with phenolic type groups). Metal binding occurs at single proton binding sites or by bidentate complexation between pairs of sites depending on a proximity factor that defines whether pairs of proton binding groups are close enough to form bidentate sites. Type A and Type B sites have separate intrinsic binding constants ($\log K_{MA}$ and $\log K_{MB}$), together associated with a parameter, ΔLK_1 , defining the spreads of values around the medians. A further parameter, ΔLK_2 , takes into account a small number of stronger sites (bidentate and tridentate sites). By considering results from many datasets, a universal average value of ΔLK_1 is obtained, and a correlation established between $\log K_{MB}$ and $\log K_{MA}$ (Tipping, 1998). Then, a single adjustable parameter ($\log K_{MA}$) is necessary to fully describe metal binding. In Model VI that the variation in the binding affinities of the proton and metal ions on monodentate sites are perfectly correlated, i.e., a high proton affinity site also does have a high affinity to all metal ions. However, the introduction of bidentate sites reduces the correlation between the proton affinity distribution and the metal ion affinity distribution. Generic parameters for HA are presented in Table 1.1. WHAM 6 databases were modified and included new $\log K_{MA}$ for REE complexation with humic acid (Pourret et al., 2006c) and well-accepted, infinite dilution (25°C) stability constants for REE carbonates complexes (Luo and Byrne, 2004).

1.3. Experimental Results

Experimental data are reported for three REE (La, Eu and Lu) in Table 1.2 and illustrated in Fig. 1.1. Competition between HA and carbonates for REE complexation is examined by considering the mass fraction inorganic REE species as a function of pH. The complementary fraction is under organic complexes. Based on speciation calculation of the inorganic fraction using WHAM 6, inorganic REE were then shown to consist solely of carbonates complexes. In the experimental conditions (see section 1.2.1), neither hydroxide nor free species are thus present.

Parameter	Description	Values
n_A	Amount of type A sites (mol g ⁻¹)	$3.3 \cdot 10^{-3}$
n_B	Amount of type B sites (mol g ⁻¹)	$0.5 \times n_A$
pK_A	Intrinsic proton dissociation constant for type A sites	4.1
pK_B	Intrinsic proton dissociation constant for type B sites	8.8
ΔpK_A	Distribution terms that modifies pK_A	2.1
ΔpK_B	Distribution terms that modifies pK_B	3.6
$\log K_{MA}$	Intrinsic equilibrium constant for metal binding at type A sites	Fitted from experimental data ¹
$\log K_{MB}$	Intrinsic equilibrium constant for metal binding at type B sites	$3.39 \log K_{MA} - 1.15$
ΔLK_1	Distribution term that modifies $\log K_{MA}$	2.8 (REE)
ΔLK_2	Distribution term that modifies the strengths of bidentate and tridentate sites	$0.55 \log K_{NH3} = 0.29$ (REE)
P	Electrostatic parameter	-330
K_{sel}	Selectivity coefficient for counterion accumulation	1
M	Molecular weight	15000 Da
r	Molecular radius	1.72 nm

 Table 1.1. Model VI parameters for humic acid (Tipping, 1998). (¹ Pourret et al., 2006c)

Two REE-carbonate complexations are considered in Fig. 1.1 and described by the following equations:



whereas humic complexation are described by the following equation:



Alkalinity: 10^{-3} mol L ⁻¹				Alkalinity: $5 \cdot 10^{-3}$ mol L ⁻¹				Alkalinity: 10^{-2} mol L ⁻¹			
pH	La	Eu	Lu	pH	La	Eu	Lu	pH	La	Eu	Lu
6.64	0.36	0.44	0.67	6.81	2.83	3.55	6.02	7.00	3.55	6.81	21.76
7.02	0.37	0.50	0.68	7.37	3.92	5.28	10.95	7.48	7.25	11.70	30.89
7.09	0.53	0.64	0.85	8.05	5.71	8.17	14.80	8.11	6.29	11.93	31.63
7.45	0.43	0.51	0.70	8.60	3.68	6.95	18.42	8.71	5.61	15.73	42.77
8.26	0.50	0.57	0.71	9.10	5.41	10.58	26.16	9.03	8.39	21.35	50.42
9.03	0.43	0.47	0.55	9.58	10.86	18.04	33.13	9.53	11.37	27.21	57.76
9.84	0.29	0.25	0.25	10.04	5.46	13.43	31.58	10.04	13.56	30.77	59.50
10.49	0.55	0.62	0.77	10.57	5.08	6.86	10.81	10.50	12.01	23.98	51.16

Table 1.2. Proportion of Ln species in the ultrafiltrate.

As shown in Fig. 1.1, LnCO_3^+ and $\text{Ln}(\text{CO}_3)_2^-$ concentrations depend strongly on the pH and the carbonate concentration-content. LnCO_3^+ concentrations decrease with pH increase whereas $\text{Ln}(\text{CO}_3)_2^-$ concentrations increase while pH increases. Moreover, $\text{Ln}(\text{CO}_3)_2^-$ and LnCO_3^+ concentrations increase with the solution alkalinity. The slight "bump" in the pH range 8-8.5 corresponds to the competitive reaction between mono- (Eqn. 1.1) and di- (Eqn. 1.2) carbonate-complexation reactions. This "bump" is more important for LREE than for HREE, a result consistent with the difference in complexation constants of LREE- and HREE-carbonate complexes (Luo and Byrne, 2004). Thus, a fractionation is apparent between LREE and HREE regarding their complexation to carbonate. Let us as an example consider a pH 10 value of alkalinity 10^{-2} mol L⁻¹ and the results observed for. Only 15 % of La are bound to carbonate whereas 30 % of Eu and up to 60 % of Lu are bound to carbonate. Moreover, carbonate concentrations were systematically identical in the ultrafiltrates and in the initial batches (within the uncertainty of the measures). This demonstrates that no carbonate was bound to HA in our

experiments. Consequently, no additional interactions between metal (Ln^{3+}), ligand (CO_3^{2-}) and surface (HA) occurred demonstrating that ternary surface complexes did not develop.

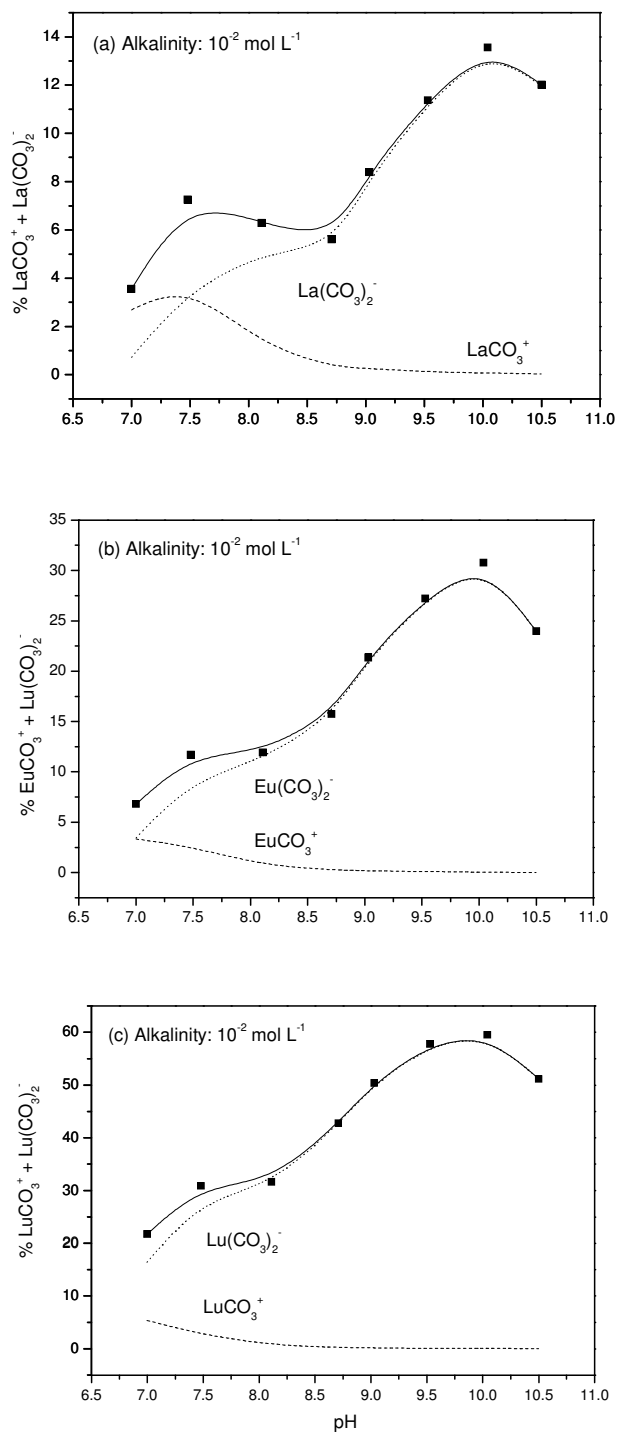


Fig. 1.1. Proportion of inorganic species for (a) La and (b) Lu (alkalinity = $10^{-2} \text{ mol L}^{-1}$). Squares represent experimental data points, whereas solid lines represent total inorganic species, dash lines LnCO_3^+ and dot lines $\text{Ln}(\text{CO}_3)_2^-$.

1.4. Discussion

1.4.1. Lack of evidence of ternary complexe formation

An often arisen question when dealing with metal (M) speciation in systems containing humic substances (HS) such as HA and inorganic ligands (L) such as carbonate is, whether or not, ternary complex (M-HA-L_m with m corresponding to the ligand stoichiometry), can form.

Information about the genesis of ternary complexes in the literature is scarce, especially concerning REE. Even if such a mechanism was suggested for REE (e.g., Fairhurst, 1995), only a few experimental studies brought evidence for possible formation of such complex (Dierckx et al., 1994; Moulin et al., 1999). Dierckx et al. (1994) provided evidence for mixed-ligand complex formation of Eu³⁺ with humic acid and inorganic ligands (i.e., CO₃²⁻). However, the interpretation of Dierckx et al. (1994) left some open questions, as they observed formation of either M-HA or M-HA-L₂ complexes formed across the whole range of L concentrations without observing the formation of M-HA-L₁ complexes. These observations are unusual with respect to common experiences found with inorganic ligands and oxide-based surfaces (e.g., Schindler, 1990). Moreover, Glaus et al. (1995; 2000) have shown that the formation of mixed-ligand-humic complexes is rather weak as compared to the formation of simple ligand-complexes with inorganic ligands. Ternary-humic complexes appear thus less important than predicted by the data of Dierckx et al. (1994).

A possible explanation for the absence of ternary complex formation in the present work might be the electrostatic repulsion between the negatively charged HA and Ln-CO₃. Due to the polyelectrolyte character of HA, this repulsion is stronger than that occurring between low-molecular weight ligands. Schindler (1990) reported that ternary complexes with SiO₂ and TiO₂ surfaces are rather weak. Both surfaces are negatively charged at the pH of Schindler's experiments and can therefore be considered as analogues to HS. Ternary surface complexes are thus not as important as previously stated and do not need to be considered in REE speciation calculation in systems dominated by organic and alkaline water.

1.4.2. Competition between humic acid and carbonates for REE complexation

In order to further constrain the competition between humic acid and carbonates for REE complexation, calculation using Model VI in WHAM 6 were performed. Calculations were conducted using Model VI in which a new determined log K_{MA} dataset for HA-REE complexation was integrated (Pourret et al., 2006c). These calculations only considered trivalent REE species. Speciation calculations are illustrated on Figs. 1.2a, b and c for La, Eu and Lu, respectively, for the three experimental conditions (i.e. increasing alkalinity and pH). In particular, Model VI reproduced quite well the observed dependence of the proportion of carbonate complexes with pH and alkalinity. However, the observed experimental "bump" is not modelled by Model VI. This is due to the fact that only Ln complexation with two CO₃²⁻ is predicted whereas Ln complexation with a single CO₃²⁻ is overwhelmed by competition with HA (Fig. 1.2). Comparison between experimental and calculated values evidences that Model VI slightly underpredicts (0 to 11 %) REE complexation by carbonate (Figs. 1.2a, b and c). Root mean square error (rmse) values represent the sum of the squares of the difference between observed and calculated values. As indicated by the rmse systematically behind 0.06 (Fig. 1.2), fits can be considered of good quality, even if rmse values increase when competition between HA and carbonates is more developed (i.e., for alkalinity of 10⁻² mol L⁻¹). Overall, it is clear that LREE to MREE are strongly bound to HA whereas HREE are more shared between HA and carbonate fractions.

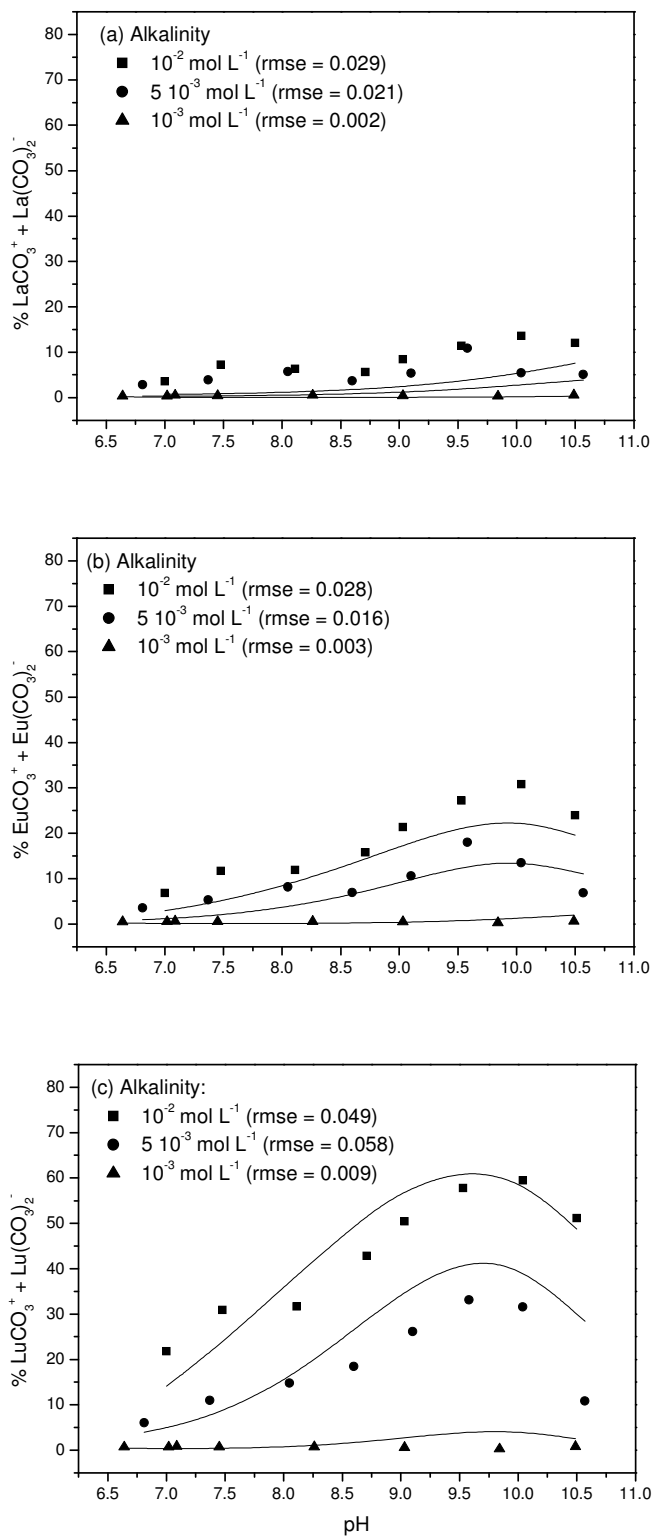


Fig. 1.2. Comparison between Model VI calculations and experiments. Proportion of lanthanides bound to carbonates as a function of pH for various alkalinities: (a) La, (b) Eu and (c) Lu.

More in detail, pH is a crucial parameter affecting binding, since it regulates competition between Ln and carbonates. Carbonate complexation mostly affects REE speciation in alkaline waters (pH above 8.5). These observations validate both the use of Model VI (Tipping, 1998) and of the $\log K_{MA}$ (REE-HA) dataset determined by Pourret et al. (2006c) to confidently predict REE speciation in natural alkaline waters. As stated by Tipping (1998), an important issue in increasing WHAM and Model VI capacity to perform chemical speciation calculations for field situations is whether significant formation of ternary complexes takes place. Simulations on some trace metals may indeed significantly underestimated the extent of metal binding as compared to observation especially when binding occurs through the formation of ternary complexes (Lofts and Tipping, 1999). As evidenced by experimental results, none ternary surface complexation occurs between REE, HA and carbonate. WHAM 6 is thus applicable to calculate REE speciation in natural water even if it does not take into account ternary surface complexation. This study combined with a previous one (Pourret et al., 2006b) now covers a wide range of natural conditions and shows that WHAM and Model VI are reliable in calculating the speciation of REE with organic matter in acidic and circumneutral DOC-rich ground- and river waters (Pourret et al., 2006b) and in alkaline organic rich-water (this study). These results suggest that dissolved organic complexes of the REE are more important than carbonates complexes for LREE to MREE and as important for HREE in World Rivers. As previously suggested by Tang and Johannesson (2003), the role played by organic material to complex REE increases our understanding of REE cycling in the hydrosphere. This also calls into question the fact that carbonate complexes dominate the REE cycle in fresh waters.

1.5. Conclusions

Experimental studies of HA and carbonate competition for REE complexation were carried out for the 14 naturally REE simultaneously. Experimental method combines an ultrafiltration technique and the Inductively Coupled Plasma Mass Spectrometry to determine REE concentrations in the different pools. Competition between HA and carbonates towards REE complexation is pH- and carbonate concentration-dependent. There is no evidence of any ternary surface complex as previously proposed (e.g., Dierckx et al., 1994). These experiments elucidate the pH range where humate complexes could be the dominant species of REE(III) in natural organic-rich waters, for various alkalinity concentrations. Carbonates are only the REE predominant species for HREE at higher alkalinity concentrations for pH above 8.5. A fractionation develops between LREE and HREE relative to REE complexation to carbonates, especially at higher alkalinity. Modelling calculations were performed with Model VI (Tipping, 1998). Calculations reproduced well experimental result, namely the pH- and carbonate concentration-dependence. The results show the influence of the competitive reactions between carbonates and HA for REE complexation at alkaline pH. All these observations allow validating the $\log K_{MA}$ (REE-HA) dataset (Pourret et al., 2006c) that can be, therefore, used with confidence to predict REE speciation in natural alkaline waters. They also evidence the reliability of WHAM 6 and Model VI in calculating the speciation of REE with organic matter in alkaline organic rich-water, as ternary surface complexes do not need to be modelled. Overall, the results of this study suggest that further considerations about organic matter should be taken into account especially at alkaline pH in organic-rich waters.

2. A new insight of cerium anomaly

Cette partie est extraite d'un article soumis à Geochimica et Cosmochimica Acta, Pourret O., Davranche M., Gruau G. and Dia A. (2006) A new insight of cerium anomaly.

Résumé– La compétition entre acides humiques (HA) et carbonates vis-à-vis de la complexation des terres rares (REE) a été étudiée en combinant des ultrafiltrations et une technique ICP-MS. Les expériences de complexation compétitive ont été réalisées à différents pH (6.5 à 10.5) et différentes alcalinités (10^{-2} à 10^{-3} mol L⁻¹) pour les 14 REE simultanément. Les résultats montrent que la compétition entre HA et carbonate vis à vis de la complexation des REE est dépendante du pH et de la concentration en carbonate. Un fractionnement entre les phases inorganiques et organiques est observé. Les spectres de REE de la fraction inorganique montrent un enrichissement en REE lourdes (HREE) qui pourrait être comparé à l'enrichissement en HREE des spectres de REE de l'eau de mer. De plus, une anomalie négative de Ce se développe sur la fraction de REE liée aux carbonates. Un nouveau mécanisme menant au développement d'une anomalie de cérium est ainsi proposé. Au-dessus de pH 8.25, 8.6 et 8.75 (selon l'alcalinité de la solution) le cérium est aisément oxydé en Ce^{IV} par formation d'un complexe pentacarbonaté. Ce complexe est lui-même facilement détruit par complexation du Ce^{IV} par l'acide humique. Il en résulte un pompage du Ce^{IV} de la fraction inorganique par les substances humiques. Une anomalie négative de cérium se développe dans la fraction inorganique. Une anomalie positive complémentaire de Ce se forme dans la fraction organique. Cependant, une telle information est masquée dans le spectre global de REE, qui représente en effet la somme des deux spectres. Cette étude expérimentale démontre que l'anomalie de cérium ne peut pas être employée comme témoin fiable des conditions redox dans des eaux organiques alcalines. D'un point de vue plus général, ce nouveau mécanisme suggère que les spectres de REE de l'eau de mer pourraient résulter d'une séparation physique entre deux phases coexistantes ayant développées des spectres de REE fractionnés dans les eaux de rivière.

Abstract - Competitive binding of rare earth elements (REE) to humic acid (HA) and carbonates was studied by combining Ultrafiltration and Inductively Coupled Plasma Mass Spectrometry techniques. REE-HA and REE-carbonate complexation experiments were performed at various pH (ranging from 6.5 to 10.5) and alkalinity (from 10^{-2} to 10^{-3} mol L⁻¹) for the 14 naturally occurring REE simultaneously. Results show that competition between HA and carbonate towards REE complexation is carbonates-dependent. Fractionation is observed between inorganic and organic phases. Inorganic REE patterns display HREE enrichment which could be compared to HREE enrichment of seawater REE patterns. Moreover, a negative Ce anomaly is developed on the REE fraction bound to carbonates. These experiments elucidate the pH range where humate complexes should be the dominant species of REE(III) in organic-rich waters for various alkalinity concentrations. This allows let to propose a new mechanism for cerium anomaly development in carbonate and organic rich waters. Above pH 8.25, 8.6 and 8.75 (depending on alkalinity of the solution) cerium is readily oxidized to Ce^{IV}, which is easily removed from solution by preferential adsorption. It results in an uptake of Ce^{IV} species from the "truly" dissolved part of solution by humic substances, and thus a negative cerium anomaly is developed in the inorganic fraction. A complementary positive Ce anomaly develops onto the organic fraction. However, such information is screened as REE pattern in solution results from the sum of the two "opposite" pattern complexes. This experimental study demonstrates that cerium anomaly cannot be used as a reliable proxy of redox conditions in alkaline, carbonate and organic rich waters. At a more global scale, this implies that seawater REE pattern shape could result from a physical separation between two coexisting phases having already fractionated REE pattern in river water.

2.1. Introduction

Rare-earth elements exhibit a trivalent (+III) oxidation state in natural waters. However, among the REE, Ce is the only element that can be oxidized to the (+IV) state. Negative cerium anomalies have been extensively observed in seawater (e.g., Elderfield and Greaves, 1982; De

Baar et al., 1985; Elderfield, 1988; German et al., 1991; German et al., 1995) and in groundwaters (e.g., Smedley, 1991; Braun et al., 1998; Dia et al., 2000; Leybourne et al., 2000). However, the mechanism whereby Ce is fractionated from its trivalent neighbors in the aquatic environment remains somewhat controversial.

Moffett (1990 and 1994) demonstrated that biologically mediated oxidations of Ce can lead to the negative Ce anomalies. Ce oxidation can either occur abiotically through oxidation/scavenging of dissolved Ce^{III} by Mn and Fe oxyhydroxides (Koeppenkastrop and De Carlo, 1992; De Carlo et al., 1998; Bau, 1999; Ohta and Kawabe, 2001). This provided evidence that oxidative scavenging of Ce at this mineral surface can occur in absence of bacterial activity. Thus, Ce oxidation in seawater represents another example of competing biotic and abiotic processes. Since Ce^{IV} is adsorbed more strongly than the other trivalent REE do, the Ce oxidation/scavenging reaction may result in solutions displaying a negative Ce anomaly, whereas solids exhibit positive Ce anomalies. In fact, negative Ce anomalies are widespread in both oceanic and fresh waters. Seawater, for example, shows a strong negative Ce anomaly mirrored by a positive anomaly in hydrogenic ferromanganese nodules (Piper, 1974; Elderfield et al., 1981; De Carlo and McMurtry, 1992). By contrast, Möller and Bau (1993) reported positive Ce anomalies in REE patterns of alkaline natural waters. These anomalies result from the stabilization of carbonate- Ce^{IV} -complexes in solution leading to enhanced abundances of Ce in comparison with its trivalent REE neighbors. Positive Ce anomalies may be general features of alkaline, carbonate-rich and aerobic waters. Moreover, in recent papers, Davranche et al. (2004, 2005) demonstrated experimentally that the complexation of REE by dissolved humic substances prevents any Ce anomaly development during REE partitioning between Fe- and Mn-oxyhydroxides and solution. Hoyle et al. (1984) and Sholkovitz (1995) data show concomitant REE and iron oxide-organic complex removal from solution. Organic complexation may also be an influent parameter for REE behaviour.

Considering that Ce oxidation can occurred by carbonates complexation (Möller and Bau, 1993) and by analogy with the mechanisms described in presence of Fe and Mn oxyhydroxide and organic matter, what will be the impact of organic matter on the Ce anomaly development in a carbonate-rich system? Organic matter is both a REE competitor as regards to carbonates and a scavenging surface likely to adsorb Ce^{IV} . Will the dominating mechanism be the complexation with carbonates or the adsorption by organic matter? Does REE fractionation between both phases be balanced? Which will be the impact of organic matter on the REE pattern shape and on the Ce anomaly amplitude?

In order to assess humic acid and carbonate competition for REE as well as impact on Ce redox behavior at alkaline pH, batch equilibration experiments with REE, Aldrich HA and carbonates were performed for the 14 naturally occurring REE simultaneously. This experimental method combines ultrafiltration and Inductively Coupled Plasma Mass Spectrometry.

2.2. Experimental Binding of Rare Earth Elements by Humic Acid and Carbonates

All chemicals used were of analytical grade, and all the experimental solutions were prepared with doubly deionized water (MilliQ system, Millipore™). Complexes were prepared in polyethylene containers previously soaked in 10 % Ultrapure HNO_3 for 48 h at 60 °C, then rinsed with MilliQ water for 24 h at 60 °C to remove all possible REE contamination sources. Synthetic REE solutions were prepared from nitrate REE standards (10 ppm, Accu Trace™ Reference Standard). All experiments were carried out at room temperature, i.e. 20 °C ± 2.

2.2.1. Humic acid

Purified humate, referred to below as HA (humic acid), was obtained from synthetic Aldrich™ humic acid (Aldrich™, H1, 675-2) following the protocol described by Vermeer et al. (1998). HA sample was freeze-dried and stored in a glass container at room temperature. HA obtained was ash free and in its protonated form, with the following elemental composition (in weight percent): C = 55.8 %, O = 38.9 %, H = 4.6 %, N = 0.6 %. REE concentrations REE in HA were below the detection limit of ICP-MS measurement (i.e. below 1 ppt). HA has a mean molecular weight of 23 kDa (Vermeer et al., 1998). Prior to use, the freeze-dried humate was resuspended overnight in an 0.001 mol L⁻¹ NaCl electrolyte solution at pH = 10, to ensure complete dissolution of the sample (Davranche et al., 2004; 2005).

2.2.2. Experimental set-up description

REE complexation with HA and carbonates was investigated using a standard batch equilibration technique. 100 mL of solutions were prepared with 50 ppb of each REE (e.g., 360 nmol L⁻¹ La to 286 nmol L⁻¹ Lu), 5 mg L⁻¹ of HA and various concentration of NaHCO₃ (from 10⁻³ to 10⁻² mol L⁻¹) in a 10⁻³ mol L⁻¹ NaCl-solution. Prior to addition of NaHCO₃, pH-solution was 4. The initial hydroxide concentration was thus negligible and concentration of LnOH²⁺ was therefore very small. After addition of NaHCO₃, pH was adjusted to the needed pH in a range of 6 to 11 by adding NaOH (4 mol L⁻¹). The pH was measured with a combined Radiometer Red Rod electrode. The electrode was calibrated with WTW standard solutions (pH 4, 7 and 10). The accuracy of the pH measurement was ± 0.05 pH unit. The redox potential was measured with a Mettler combined Pt electrode (Eh varies between 350 and 450 mV). The accuracy of Eh measurement was ± 5 mV. Experimental solutions were stirred for 48 h (equilibrium time determined from preliminary kinetic experiments) to allow equilibration and partitioning of REE between the aqueous solution and the humate suspension. Aliquots of 10 mL were sampled twice: at the beginning of the experiment; and after 48 h at equilibrium state. REE complexed by the HA were separated from the remaining inorganic REE by ultrafiltration. Ultrafiltrations were carried out by centrifugating the 10 mL solution samples through 15 mL centrifugal tubes equipped with permeable membranes of 5 kDa pore size (Millipore Amicon Ultra-15). All centrifugal filter devices used were washed and rinsed with 0.1 mol L⁻¹ HCl and MilliQ water two times before use in order to minimize contamination. Centrifugations were performed using a Jouan G4.12 centrifuge with swinging bucket rotor at 3000 g for 30 minutes. This allowed the REE-HA complexes to be quantitatively separated from inorganic REE species. The selectivity of the 5 kDa membrane regards to the REE-HA complexes was verified by monitoring the Dissolved Organic Carbon (DOC) contents of the ultrafiltrates. Results show that the latter were systematically lower or equal to blank values (below 1 ppm). Possible adsorption of inorganic REE species onto the membrane or onto cell walls was also monitored. Inorganic REE solutions of given REE concentration were ultrafiltrated several times. Results showed that 100 % of the REE present in solution was recovered in the ultrafiltrates, demonstrating that none REE was adsorbed neither on the membranes nor on the walls of the cell devices.

Concentrations of REE complexed with HA correspond to the difference between the initial REE concentration and the remaining REE concentration into the < 5 kDa ultrafiltrates. REE concentrations were determined at Rennes 1 University using an Agilent Technologies™ HP4500 ICP-MS instrument. Quantitative analyses were performed using a conventional external calibration procedure. Three external standard solutions with REE concentrations similar to the analyzed samples were prepared from a multi-REE standard solution (Accu Trace™ Reference, 10 mg L⁻¹, USA). Indium was added to all samples as an internal standard at a concentration of 0.87 μmol L⁻¹ (100 ppb) to correct for instrumental drift and possible matrix effects. Indium was also added to the external standard solutions. Calibration curves were calculated from measured

REE/indium intensity ratios. The instrumental error on REE analysis in our laboratory as established from repeated analyses of multi-REE standard solution (Accu Trace™ Reference, USA) and of the SLRS-4 water standard is below $\pm 2 \%$ (Dia et al., 2000; Davranche et al., 2005). Chemical blanks of individual REE were all lower than detection limit (1 ppt), which is negligible since they are three to four orders of magnitude lower than the concentrations measured in the synthetic solutions used for the complexation experiments.

DOC concentrations were determined at Rennes 1 University using a Shimadzu 5000 TOC analyzer. The accuracy of DOC concentration measurements is estimated at $\pm 5 \%$ as determined by repeated analyses of freshly prepared standard solutions (potassium biphtalate).

Carbonate concentrations were determined by potentiometric titrations ($\text{HCl } 0.1 \text{ mol L}^{-1}$), with Gran method analysis. The uncertainty is better than 5% .

In order to check that none retention of REE or carbonates occurs inside the membrane during ultrafiltration, mass balance calculations were performed. The initial concentration of each element is compared with the sum of each element concentration in the ultrafiltrate and in the retentate. The element sum measured from the ultrafiltrate and the retentate differs from the initial content less than 2% for REE and less than 5% for carbonates and DOC. In order to ensure that no precipitation occurs, samples were filtrated at $0.2 \mu\text{m}$ before ultrafiltration. None difference was found (within the uncertainty of the measures) between the $0.2 \mu\text{m}$ filtrate and the raw sample for REE, HA and carbonates.

2.3. Experimental results

Experimental results are reported in Table 2.1. Competition between HA and carbonates for REE complexation is examined by considering the inorganic REE species as a function of pH. The complementary fraction occurs as organic complexes form. In the experimental conditions (see section 2.2.1), neither hydroxide nor free species are present. As evidenced in a companion paper (Pourret et al., 2006d), REE carbonates complexations are described by the following equations:



whereas humic complexation are described by the following equation:



Inorganic fraction REE patterns (Fig. 2.1a, 2.1b and 2.1c) are shown for the three experimental conditions. They displayed more important HREE enrichment for strong carbonate concentrations. Moreover, at alkaline pH (i.e., above 8.5), REE patterns exhibit a negative cerium anomaly. In addition, organic REE patterns (Fig. 2.1d, 2.1e and 2.1f) are shown for the same three experimental conditions. They displayed more significant LREE enrichment for strong carbonates concentrations. Moreover, at alkaline pH (i.e., above 8.5), REE patterns exhibit a positive cerium anomaly. Overall, REE pattern shape is thus controlled by carbonate complexes.

Cerium is redox sensitive, and even if the solution chemistry of Ce^{III} is similar to that of other REE, Ce^{IV} is generally preferentially adsorbed on surface in natural water (De Baar et al., 1988). The influence of redox processes on its distribution can be evaluated by measuring Ce fractionation from strictly trivalent neighbors, La and Pr (e.g., Elderfield, 1988). By this definition, Ce anomaly values greater than or less than one represent preferential enrichment or removal of Ce, respectively. Cerium anomalies are quantified as follows:

$$Ce/Ce^* = \frac{2.(Ce)}{(La) + (Pr)} \quad (2.4)$$

Ce/Ce^* is shown on Fig. 2.2a as a function of pH. The development of a negative Ce anomaly is observed for pH above 8.25, 8.6 and 8.75, for the three increasing alkalinity, respectively. The negative Ce anomaly increases with pH from 1 to 0.05 (Fig. 2.2a). Ce/Ce^* is also shown on Fig. 2.2b as a function of carbonate concentrations. The development of a negative Ce anomaly is observed for various carbonates concentrations, it develops for a CO_3^{2-} concentration above 10^{-5} , 10^{-4} and $4 \cdot 10^{-4}$ mol L⁻¹, for the three increasing alkalinity, respectively (Fig. 2.2b).

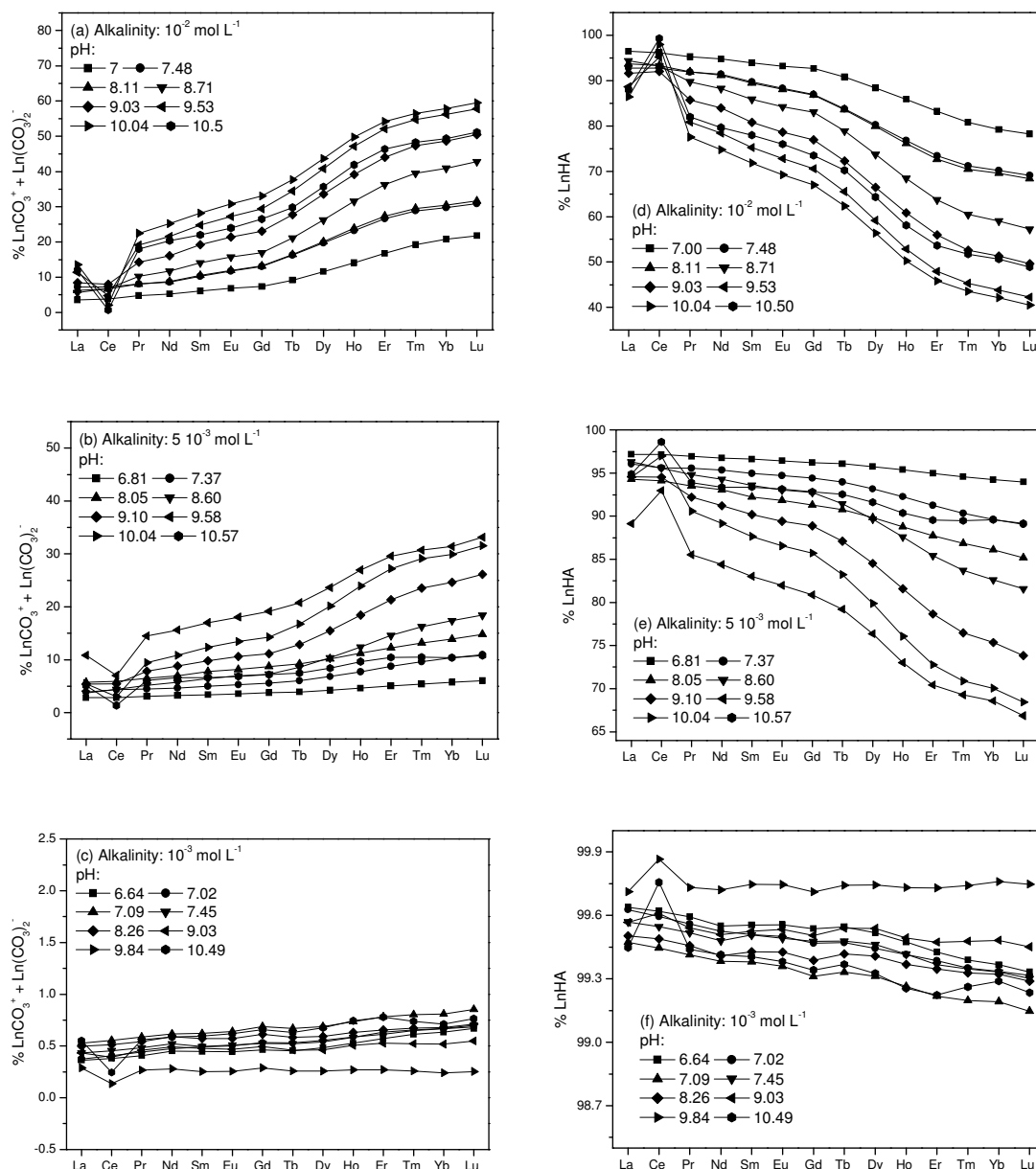


Fig. 2.1. Proportion of REE complexed to carbonates as a function of pH for various alkalinity conditions (a) 10^{-2} mol L⁻¹, (b) $5 \cdot 10^{-3}$ mol L⁻¹ and (c) 10^{-3} mol L⁻¹ and proportion of REE complexed to HA as a function of pH for various alkalinity conditions (d) 10^{-2} mol L⁻¹, (e) $5 \cdot 10^{-3}$ mol L⁻¹ and (f) 10^{-3} mol L⁻¹.

Alkalinity: 10^{-3} mol L ⁻¹								
pH	6.64	7.02	7.09	7.45	8.26	9.03	9.84	10.49
La	0.36	0.37	0.53	0.43	0.50	0.43	0.29	0.55
Ce	0.38	0.41	0.55	0.45	0.51	0.39	0.14	0.24
Pr	0.41	0.44	0.59	0.48	0.54	0.46	0.27	0.56
Nd	0.45	0.47	0.62	0.52	0.59	0.49	0.28	0.59
Sm	0.45	0.49	0.62	0.49	0.57	0.48	0.25	0.59
Eu	0.44	0.50	0.64	0.51	0.57	0.47	0.25	0.62
Gd	0.46	0.53	0.69	0.52	0.61	0.50	0.29	0.66
Tb	0.45	0.53	0.67	0.52	0.58	0.46	0.26	0.63
Dy	0.48	0.56	0.69	0.54	0.59	0.46	0.26	0.67
Ho	0.53	0.58	0.74	0.58	0.63	0.51	0.27	0.75
Er	0.57	0.61	0.78	0.63	0.65	0.53	0.27	0.78
Tm	0.61	0.65	0.80	0.65	0.67	0.52	0.26	0.74
Yb	0.63	0.67	0.81	0.67	0.68	0.52	0.24	0.71
Lu	0.67	0.68	0.85	0.70	0.71	0.55	0.25	0.77
Alkalinity: $5 \cdot 10^{-3}$ mol L ⁻¹								
pH	6.81	7.37	8.05	8.60	9.10	9.58	10.04	10.57
La	2.83	3.92	5.71	3.68	5.41	10.86	5.46	5.08
Ce	2.85	4.38	5.91	4.41	5.47	7.03	3.02	1.37
Pr	3.06	4.44	6.48	5.18	7.79	14.47	9.41	6.12
Nd	3.25	4.64	6.94	5.70	8.77	15.62	10.83	6.64
Sm	3.37	5.02	7.76	6.41	9.79	16.98	12.34	6.63
Eu	3.55	5.28	8.17	6.95	10.58	18.04	13.43	6.86
Gd	3.77	5.58	8.70	7.25	11.11	19.14	14.27	7.18
Tb	3.90	6.03	9.22	8.58	12.89	20.79	16.76	7.46
Dy	4.24	6.82	10.16	10.33	15.46	23.64	20.12	8.39
Ho	4.60	7.71	11.23	12.41	18.42	26.98	23.93	9.64
Er	5.04	8.74	12.25	14.58	21.33	29.57	27.21	10.43
Tm	5.40	9.65	13.16	16.26	23.53	30.72	29.13	10.50
Yb	5.75	10.36	13.87	17.37	24.64	31.41	29.94	10.40
Lu	6.02	10.95	14.80	18.42	26.16	33.13	31.58	10.81
Alkalinity: 10^{-2} mol L ⁻¹								
pH	7.00	7.48	8.11	8.71	9.03	9.53	10.04	10.50
La	3.55	7.25	6.29	5.61	8.39	11.37	13.56	12.01
Ce	3.87	7.20	6.65	6.76	7.99	4.77	2.07	0.68
Pr	4.74	8.13	8.06	10.27	14.24	19.11	22.46	18.01
Nd	5.23	8.57	8.81	11.73	16.04	21.55	25.25	20.34
Sm	6.08	10.27	10.56	14.09	19.23	24.77	28.14	22.01
Eu	6.81	11.70	11.93	15.73	21.35	27.21	30.77	23.98
Gd	7.34	13.07	13.18	16.96	23.06	29.44	33.03	26.51
Tb	9.18	16.25	16.41	21.12	27.74	34.48	37.65	29.79
Dy	11.61	19.75	20.09	26.25	33.56	40.85	43.65	35.67
Ho	14.11	23.23	23.89	31.53	39.18	47.14	49.73	41.88
Er	16.76	26.61	27.34	36.28	44.05	52.11	54.18	46.34
Tm	19.23	28.83	29.52	39.50	47.37	54.70	56.45	48.27
Yb	20.79	29.81	30.43	40.93	48.65	56.20	57.85	49.38
Lu	21.76	30.89	31.63	42.77	50.42	57.76	59.50	51.16

Table 2.1. Proportion of Ln species in the ultrafiltrate.

2.4. Discussion

2.4.1. Cerium Anomaly

In this work, a negative cerium anomaly was evidenced in the inorganic fraction whereas a positive cerium anomaly was developed on the organic fraction. Dolezal and Novak (1959) have shown that strong carbonato-Ce-complexes may be formed following the reaction:

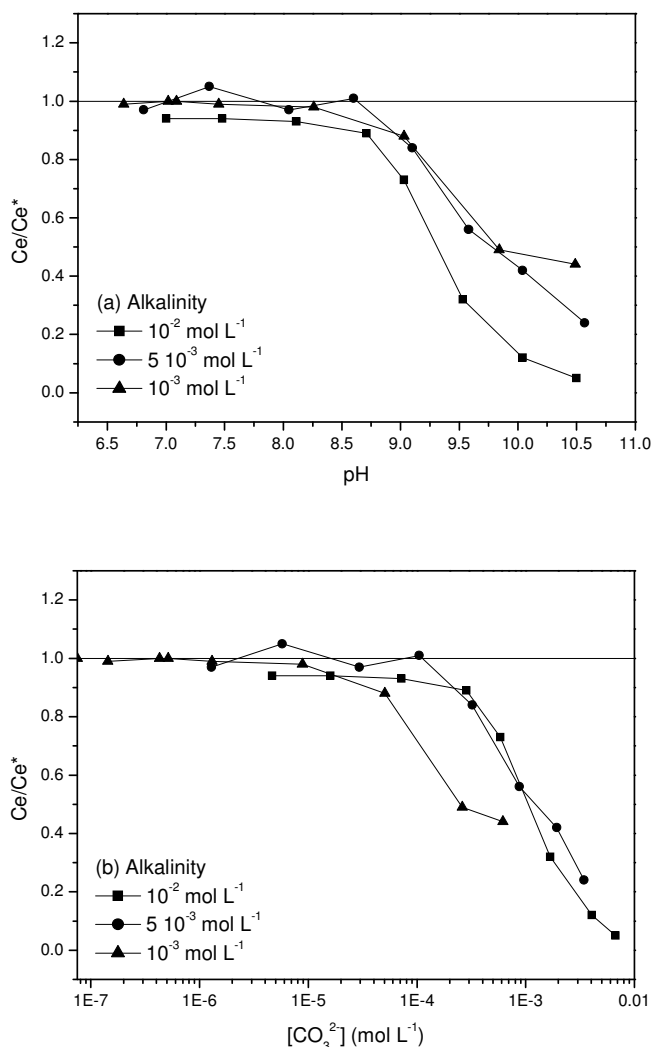
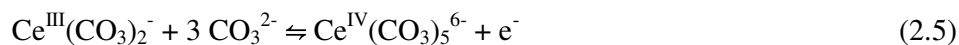


Fig. 2.2. (a) Cerium anomaly (Ce/Ce^*) as a function of pH and (b) Ce/Ce^* as a function of carbonate concentrations for variable alkalinity.

Using this reaction a pe-pH diagram for the system Ce-C-O-H for $a(\text{Ce}) = 3.6 \cdot 10^{-7} \text{ mol L}^{-1}$ and alkalinity of $10^{-2} \text{ mol L}^{-1}$, Fig. 2.3a was constructed (data compiled from Dolezal and Novak, 1959; De Baar et al., 1988; Möller and Bau, 1993). Due to complexation with carbonate species and HA, Ce are prevented from as $\text{Ce}(\text{OH})_3$ at low pe values (see section 2.2.1) and are thus not considered in this construction. Stable relationships are indicated by continuous lines and metastable relationship by dashed lines. Because of the uncertainty of the exact value of the

activity coefficient γ of the pentacarbonato-Ce^{IV}-complex, values were assumed for $Q = \gamma(\text{Ce}^{\text{III}}(\text{CO}_3)^{2-}) / \gamma(\text{Ce}^{\text{IV}}(\text{CO}_3)_5^{6-})$. A variety of equilibrium curves are then used to construct the diagram. They place the experimental conditions between $4 < \log Q < 6$. As stated by Möller and Bau (1993), these values seem rather high. However, considering the extended Debye-Hückel equation for calculation of γ of the Ce^{IV} complex, γ should (i) be proportional to the square of the ionic charge (i.e., 6) and (ii) be dependent on a rather large ionic Debye-Hückel parameter, which may be as high as 9 for lanthanides (Stumm and Morgan, 1996). Thus, $\log Q$ between 4 and 6 is not unlikely. The resulting shifting pH of 8 to 9 within the pe range ca. 7 moves the $a(\text{Ce}^{\text{III}}(\text{CO}_3)^{2-}) / a(\text{Ce}^{\text{IV}}(\text{CO}_3)_5^{6-})$ equilibrium close to the $a(\text{Ce}^{\text{III}}(\text{CO}_3)^{2-}) / a(\text{Ce}^{\text{IV}}\text{O}_2)$ equilibrium. Therefore, Ce does not form CeO₂ but Ce^{IV}(CO₃)₅⁶⁻, under the conditions prevailing in the experiments. Subsequently, Ce as Ce(IV) form is preferentially adsorbed by humic substances following the reaction :



Ce^{IV}(CO₃)₅⁶⁻ could then be considered as a precursor complex for the Ce^{IV} adsorption to HA. Ce^{IV} complexation by HA result from an uptake of Ce^{IV} species from the "truly" dissolved part of solution, and involves the development of negative cerium anomaly in the inorganic fraction. A complementary positive Ce anomaly will thus develop onto HA. However, such information is masked if the whole solution REE pattern is considered since it results from the sum of the two patterns.

Fig. 2.3b illustrates the pH- and carbonate concentrations- dependence of the pentacarbonato-Ce^{IV}-complex range formation. As explain previously, Ce^{IV}(CO₃)₅⁶⁻ can be formed only if CeO₂ not precipitates, in other words when $(\text{Ce}^{\text{III}}(\text{CO}_3)^{2-}) / a(\text{Ce}^{\text{IV}}(\text{CO}_3)_5^{6-})$ equilibrium is superior to the $a(\text{Ce}^{\text{III}}(\text{CO}_3)^{2-}) / a(\text{Ce}^{\text{IV}}\text{O}_2)$ equilibrium. Fig. 2.3b provided evidence that the intercept of both equilibrium moves towards more acidic pH when alkalinity and consequently CO₃²⁻ concentrations decrease. Therefore, Ce^{IV}(CO₃)₅⁶⁻ can developed at low carbonate concentration and circumneutral pH. Moreover, when DOC/Alkalinity ratio is high only a small part of the REE is complexed by carbonates (i.e. > 1 %) and thus, the amount of HA necessary to break the precursor complex is relatively small. When DOC/Alkalinity ratio is low, the amount of precursor complex is higher and the extent of HA needed is bigger. A higher pH is thus needed to achieve this conditions, as the electro-negativity of HA increases with pH (e.g., Milne et al., 2001).

2.4.2. Inferences on the understanding of Ce anomaly in natural waters

Shallow organic-rich waters from several continental areas have been reported to display small negative Ce anomalies - or no anomaly at all - despite the occurrence of strongly oxidizing conditions (Viers et al., 1997; Braun et al., 1998; Dia et al., 2000; Gruau et al., 2004). In such organic-rich, shallow groundwaters, the so-called "dissolved" REE pool generally occurs as REE(III)-humate complexes (Sholkovitz, 1995; Viers et al., 1997). Considering that Ce and REE occur predominantly as dissolved and colloidal organic complexes, Dia et al. (2000) put forward two hypotheses to account for this lack of Ce anomalies: (i) either Ce precipitation and oxidation become impossible because of the complexation of Ce^{III} by organic matter or, (ii) CeO₂ are precipitated onto colloids then considered as part of the solution. Experimental data reported by Davranche et al. (2004; 2005) favour the first hypothesis. In complement, a third hypothesis not previously stated could be that the preferential Ce^{IV} sorption is screened rather than inhibited as evidenced by new experimental results presented in this contribution. Indeed, an uptake of Ce^{IV} species from the "truly" dissolved part of solution, and thus a development of negative cerium anomaly in the inorganic fraction could occur. However, as a complementary positive Ce anomaly develops on HA, considering the whole REE pattern will led to hide part of information. As previously sketched on Fig. 2.3b, Ce^{IV}(CO₃)₅⁶⁻ can be formed at circumneutral pH conditions

for pe values higher than 10. Such a phenomenon could thus occur in circumneutral highly oxidized natural waters.

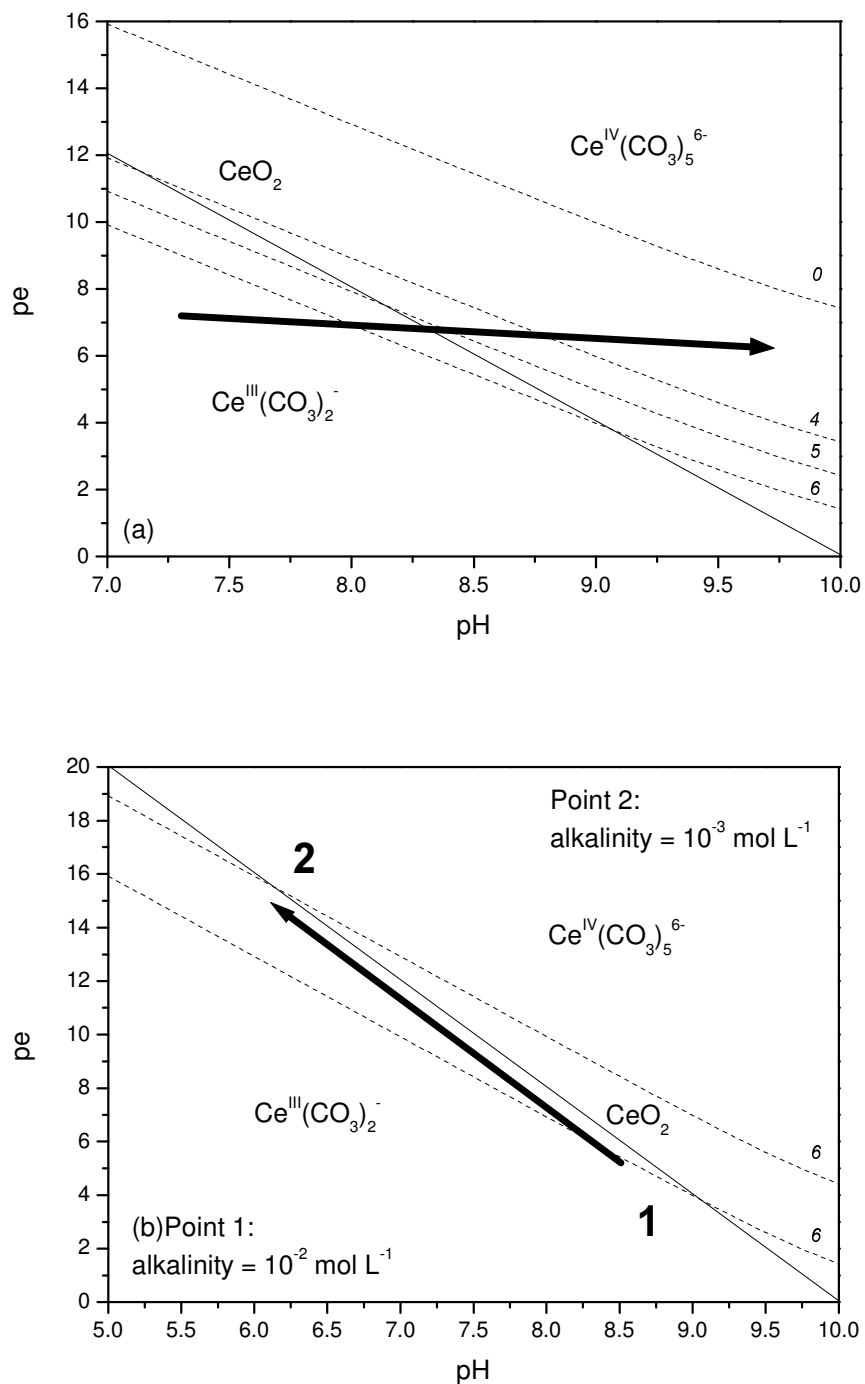


Fig. 2.3. (a) pe - pH diagram for the system Ce-C-O-H at 25 °C and $I = 0$. Solid lines correspond to stable relationship and dashed lines to metastable relationships, while black arrow indicates redox potential evolution of experimental conditions and numbers in *italics* indicate assumed $\log Q$ (see text for further details). Thermodynamic data are from Dolezal and Novak, 1959; De Baar et al., 1988; Möller and Bau, 1993. (b) pe - pH diagram for the system Ce-C-O-H at 25 °C and $I = 0$: sketch of decreasing carbonate concentrations.

2.4.3. Implications on the understanding of cerium anomaly in natural water

Generally, the absolute and relative concentrations of REE in the ocean waters reflect (i) their input from rivers, from aeolian transport and from hydrothermal vents as well as (ii) their interactions with the biogeochemical cycle involving removal from surface waters by adsorption at particle surfaces. The depletion of Ce in the oceans and river waters were attributed to its redox chemistry (e.g., Elderfield, 1988). Nevertheless, different processes may lead to Ce removal from solution. (i) The most often discussed is that chemical fractionation which take place during estuarine mixing enhanced by extremely high particle reactivity (e.g., MnO_2) with a preferential HREE enrichment. (ii) Removal of REE from solution could also take place by a removal of some or all of the colloidal REE pool by coagulation as previously showed for dissolved humic acids and iron during estuarine mixing (Sholkovitz et al., 1978).

Input to the ocean from rivers displays relatively flat REE pattern (Sholkovitz, 1995) without cerium anomaly whereas oceanic REE patterns used to display large negative Ce anomaly and HREE enrichment. Results from this study led us to favour REE removal by colloidal coagulation. In this case, REE fractionation occurs since colloidal and dissolved pools have different REE patterns. Such a scenario could explain why, Schijf et al. (1994), did not evidence any oxidative scavenging of Ce, whereas reductive dissolution of metal oxide carrier phases was found to be important in the cycling of all REE across the oxic/anoxic interface in the Black Sea. Indeed, both organic and inorganic REE pools coexist in solution, and the only way to verify such a hypothesis would be to perform ultrafiltration on such water samples.

2.5. Conclusions

Experimental studies of HA and carbonate competition for REE complexation were carried out for the 14 naturally REE simultaneously. Experimental method combines an ultrafiltration technique and the Inductively Coupled Plasma Mass Spectrometry method. Competition between HA and carbonates towards REE complexation is pH and carbonates-dependent. Fractionation is observed between organic phase (LnHA) and inorganic phases (Ln-carbonate). In the inorganic phase, REE patterns display HREE enrichment typical of seawater REE patterns. A negative Ce anomaly is developed in the REE fraction bound to carbonates at pH above 8.25, 8.6 and 8.75 (depending on alkalinity of the solution) whereas a positive Ce anomaly is developed in the organic fraction. These experiments shed more light not only on a new way to develop Ce anomaly but also on the understanding of cerium anomaly cycle in natural water. Indeed, these results evidence a new mechanism for cerium anomaly development. In presence of carbonate, cerium is readily oxidized in Ce^{IV} , which is easily removed from solution by preferential adsorption. Humic substances take up Ce^{IV} from the "truly" dissolved part of solution, and a negative cerium anomaly thus developed in the inorganic fraction. A complementary positive Ce anomaly appeared on the organic fraction. The preferential Ce^{IV} sorption is screened. Ce anomaly cannot thus be used anymore as a reliable proxy of redox conditions in organic-rich waters or in precipitates formed at equilibrium with organic-rich waters. Moreover, in seawater REE removal from solution, and thus separation of already two fractionated phases, should occur by the removal of some or all of the colloidal REE pool by coagulation. This process has been previously invoked rather than REE fractionation during estuarine mixing. Reactions involved during estuarine mixing seem to be a secondary phenomenon responsible for only a minor proportion of the negative cerium anomaly being present on oceanic REE pattern. Overall, the results of this study suggest that further considerations about organic matter should be taken into account especially at alkaline pH in organic-rich water.

Conclusions et Perspectives

1. CONCLUSIONS

Cette étude avait pour but de décrire et de comprendre l'impact de la matière organique sur le comportement des terres rares en solution. A ce titre, ce travail a permis des avancées scientifiques significatives dans la compréhension de l'expression des mécanismes responsables de la spéciation des terres rares dans les eaux naturelles riches en matière organique. Cette étude a permis de:

(i) montrer pourquoi le développement d'anomalie de cérium négative dans des eaux organiques oxydantes ne se produit pas systématiquement;

(ii) tester la capacité de deux modèles thermodynamiques spécifiques à la matière organique à prédire la distribution des terres rares dans les eaux organiques de manière fiable et précise;

(iii) fournir un jeu de constantes terres rares - acides humiques spécifiques à Model VI (Tipping, 1998);

(iv) tester l'impact des réactions de compétition entre des ligands organiques (acide humique) et inorganiques (carbonates) forts pour la complexation des terres rares sur leur distribution;

(v) mettre en évidence un nouveau processus chimique capable de produire une anomalie négative de Ce dans les eaux organiques naturelles.

Les principaux résultats obtenus sont résumés ci-dessous:

Expériences d'adsorption/oxydation. Les expériences d'adsorption des complexes terres rares-acides humiques à la surface d'oxyhydroxydes de fer et de manganèse ont montré que la complexation des terres rares par la matière organique inhibait à la fois, l'oxydation du Ce(III) en Ce(IV) et le développement d'un effet tetrad au niveau des spectres de terres rares des eaux. Cette inhibition est due au développement d'un écran organique entre les terres rares et les surfaces oxydantes/adsorbantes que représentent les oxydes de fer et de manganèse (Fig. 1).

Modélisation. La comparaison entre les résultats calculés et les expériences d'ultrafiltration a permis de valider Model VI (Tipping, 1998) dans sa capacité à prédire la spéciation des terres rares dans les eaux organiques. Par contre, la divergence entre les résultats obtenus avec SHM (Gustafsson, 2001a) et les résultats expérimentaux indique que SHM, dans l'état actuel du programme, n'est pas apte à décrire précisément la spéciation des terres rares dans une eau naturelle.

Les expériences de complexation terres rares - acides humiques ont montré une forte dépendance au pH. La proportion de complexe organique de terres rares augmente significativement avec les forts pH. Une complexation plus marquée des terres rares intermédiaires a également été observée sur les différents spectres obtenus (Fig. 2). Ces données ont été modélisées avec Model VI, ce qui a permis d'obtenir une série de constantes de complexation terres rares acides humiques, spécifiques à ce modèle ($\log K_{MA}(\text{REE-HA})$). Les constantes obtenues pour Model VI montrent un fractionnement des terres rares similaire à celui obtenu avec des groupements carboxyliques simples comme les acides acétiques. Cependant, aucun effet "contraction des lanthanides" n'a été observé au contraire de certains auteurs (Sonke et Salters, 2006).

La détermination de la spéciation des terres rares dans les eaux organiques par l'approche combinée de codes de calculs (Stockholm Humic Model et Humic Ion Binding Model VI) et d'une technique physique de fractionnement (i.e. ultrafiltration), a permis de caractériser la spéciation des terres rares dans des eaux de rivières (Fig. 3) et dans des eaux de nappes superficielles (Fig. 4). Les calculs de spéciation, utilisant des constantes de complexation

extrapolées, montrent une forte complexation des terres rares à la matière organique (i.e. > 60 % pour $5 < \text{pH} < 8.5$) dans les eaux de rivières moyennes mondiales (Fig. 2).

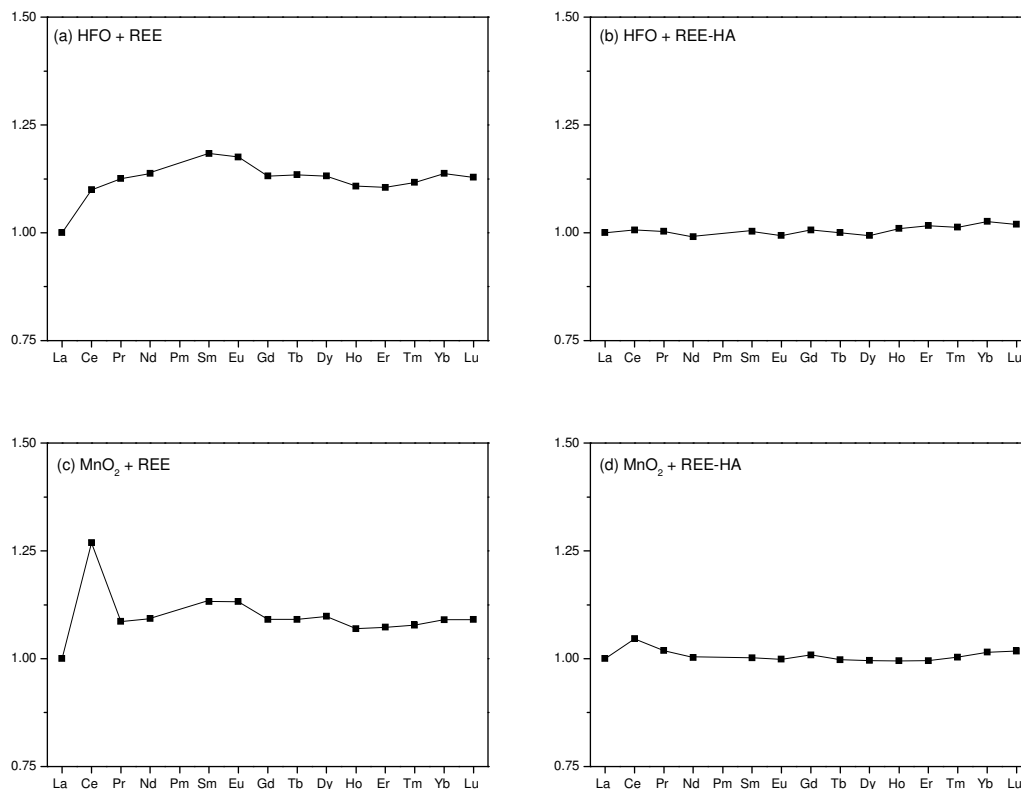


Fig. 1. Spectres des coefficients de partage des terres rares (normalisation au La) adsorbés sur des oxydes de fer et de manganèse si les terres rares se trouvent sous forme (a et c) d'ions libre ou (b et d) de complexes organiques.

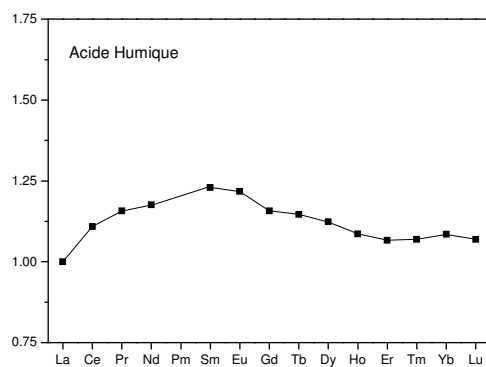


Fig. 2. Spectre des coefficients de partage des terres rares complexées aux acides humiques à pH 5 pour une concentration en acides humiques de 5 mg L^{-1} (normalisation par rapport au La).

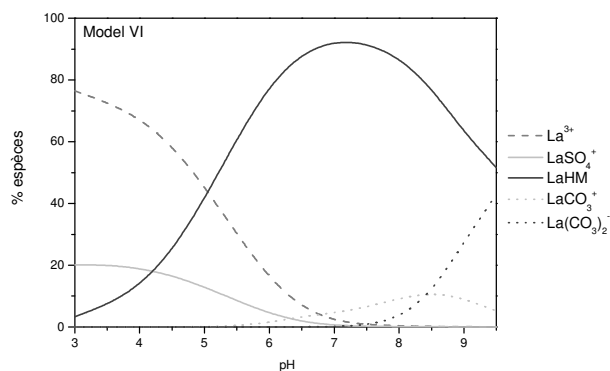


Fig. 3. Répartition des différentes espèces de Lanthane (La) dans une eau de rivière moyenne en fonction du pH, calculée avec Model VI (Tipping, 1998).

Les expériences d'ultrafiltration d'eau de sols riches en matières organiques ont montré un fractionnement des terres rares entre les différentes tailles de matières organiques (~ 90 %) et la phase inorganique (~ 10 %) (Fig. 3). Une relation linéaire est observée entre la concentration en terres rares et la concentration en carbone organique dissous.

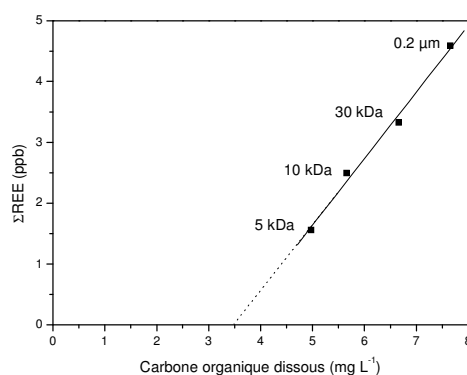


Fig. 4. Somme des terres rares fonction du carbone organique dissous pour les différents seuils de coupure d'ultrafiltration.

Compétition acides humiques/carbonates. Les expériences de complexation compétitive carbonate/acide humique vis à vis des terres rares ont montré une forte dépendance au pH et à l'alcalinité (Fig. 5). Aucune donnée ne permet de soupçonner la formation de complexe ternaire de surface mettant en jeu des terres rares. Les calculs de spéciations avec Model VI reproduisent quantitativement les dépendances au pH et à la concentration en carbonates des résultats expérimentaux. Ces nouvelles données permettent de valider la série de constantes ($\log K_{MA}$ (REE-HA)) déterminées dans cette thèse, qui peut être utilisée avec confiance pour prédire la spéciation des terres rares dans des eaux alcalines. Ainsi, WHAM 6 et Model VI sont confortés dans leur capacité à calculer de manière fiable la spéciation des terres rares avec la matière organique en conditions alcalines. De plus ces résultats montrent qu'il n'est pas nécessaire d'introduire de complexes ternaires dans le modèle.

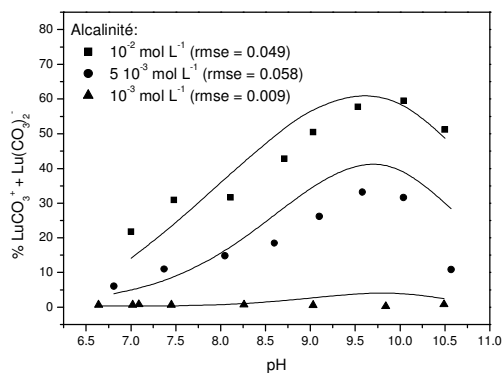


Fig. 5. Proportion de Lu complexé aux carbonates en fonction du pH pour différentes conditions d'alcalinité. Comparaison entre expériences (points) et calculs avec Model VI (lignes continues).

Nouveau processus de formation d'anomalie de Ce. Les expériences de compétition entre carbonates et acides humiques pour la complexation des terres rares ont également mis en évidence un fractionnement des terres rares entre ces complexants (Fig. 6).

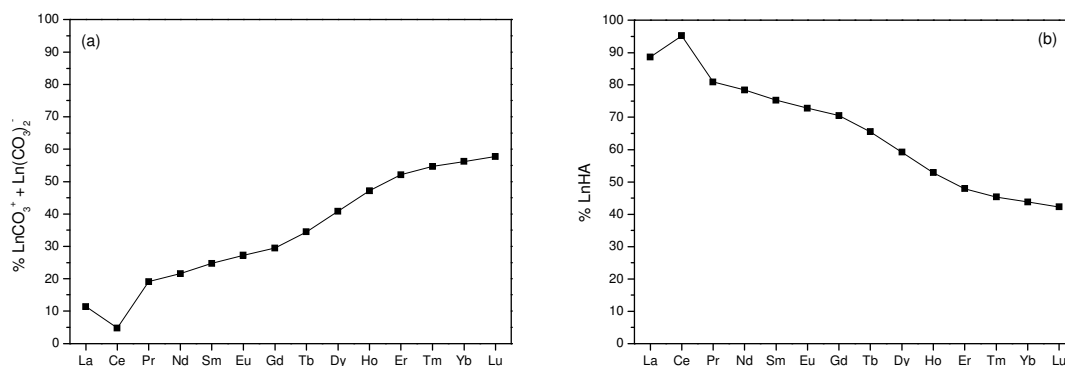


Fig. 6. Spectres de terres rares (a) de la fraction inorganique complexée aux carbonates et (b) de la fraction organique complémentaire complexée aux acides humiques (alcalinité = 10^{-2} mol L⁻¹ et pH = 9.58).

En utilisant une méthode d'ultrafiltration, les phases complexées aux acides humiques et aux carbonates ont pu être séparées. Les résultats ont permis de mettre en évidence le développement d'une anomalie négative de Ce dans la fraction inorganique de la solution pour des pH supérieurs à 8, dont l'amplitude croît avec l'alcalinité. En vis-à-vis, une anomalie de Ce positive se développe sur les colloïdes organiques. Pour des pH > 8, le cérium s'oxyde sous forme Ce^{IV} par formation d'un complexe carbonaté Ce^{IV}(CO₃)₅⁶⁻, qui peut être qualifié de précurseur. Une fois formé ce complexe entre en compétition avec les acides humiques de la solution. Les constantes de complexation terres rares - acides humiques plus fortes que les constantes terres rares - pentacarbonate sont à l'origine de la déstructuration de ce complexe. Le Ce^{IV} ayant plus d'affinité pour les substances humiques que les autres terres rares trivalentes, celui-ci est préférentiellement adsorbé par les acides humiques de plus en plus électronégatifs. Il en résulte le développement d'une anomalie de Ce positive au sein de la fraction organique de la solution, et négative dans la fraction inorganique.

2. IMPLICATIONS

Il ressort de ce travail que la matière organique est un fort complexant des terres rares dans les eaux douces naturelles. La forme organique des terres rares doit donc être systématiquement prise en compte dans les études de transport des ces éléments dans les eaux.

2.1. Spéciation des terres rares dans les eaux douces naturelles.

La détermination de la spéciation des terres rares dans les eaux combinant l'utilisation de codes de calculs et d'une technique d'ultrafiltration a montré que les complexes humiques de terres rares étaient dominants dans les eaux de rivières et dans des eaux de nappes superficielles. D'une façon plus générale, l'importance de la matière organique sur le cycle de terres rares à la surface de la Terre est confirmée (Dupré et al., 1996; Viers et al., 1997; Tang et Johannesson, 2003). Cette forte complexation des terres rares par les colloïdes organiques dans les eaux fait que le comportement de ces éléments est plus assimilable à celui d'une phase particulière qu'à un véritable soluté.

De plus, le spectre de terres rares et le niveau de concentration en terres rares d'une eau seront très dépendants de sa concentration en colloïdes organiques. En effet, la matière organique exerce un fort contrôle sur la forme du spectre de terres rares. Le spectre d'une eau va correspondre à la transformation du spectre de terres rares de la source solide en un spectre "colloïdal" de la source solide. Les fractions dissoutes (i.e. $< 0.2 \mu\text{m}$) des eaux contenant de la matière organique que ce soit dans les sols ou les rivières montrent des spectres de terres rares concaves enrichis en terres rares intermédiaires.

Une meilleure considération de la matière organique doit donc être portée dans les études d'échantillons naturels. Une analyse systématique des concentrations en carbone organique dissous doit être envisagée afin d'intégrer cette spéciation organique dans la compréhension des mécanismes observés. De telles données sont aussi nécessaires à la poursuite de modélisations utilisant des codes de calcul de spéciation.

Les résultats présentés dans cette étude ont aussi montré que Model VI et les constantes déterminées au cours de cette thèse fournissaient de bons éléments de prédiction de la spéciation des terres rares dans les eaux naturelles.

2.2. Remise en cause de l'utilisation de l'anomalie de Cérium comme témoin des conditions d'oxydoréduction.

Ces dernières années, une grande attention a été portée à l'utilisation de l'anomalie de Ce comme indicateur paléo-océanographique de l'anoxie marine, et/ou des conditions redox enregistrées dans les paléosols (Wright et al., 1987; MacLeod et Irving, 1996; Gallet et al., 1996; Holser, 1997; Morad et Felitsyn, 2001; Picard et al., 2002). Cependant, les eaux organiques peu profondes de plusieurs régions continentales montrent peu ou pas d'anomalies négatives de Ce en dépit des conditions fortement oxydantes et de la présence d'oxydes de manganèse dans les horizons de sols associés (Viers et al., 1997; Braun et al., 1998; Dia et al., 2000; Gruau et al., 2004). Dans ces échantillons, les terres rares de la fraction filtrée à $0.2 \mu\text{m}$ se retrouvent en majorité sous forme complexée à la matière organique (Sholkovitz, 1995; Viers et al., 1997). En considérant que le Ce et les terres rares ne sont pas sous formes libres, Dia et al. (2000) ont émis l'hypothèse que l'oxydation et la précipitation du Ce (sous forme cérianite) étaient impossibles en raison de la complexation du Ce^{III} par la matière organique. Les résultats obtenus dans cette thèse semblent favoriser cette hypothèse en expliquant que l'oxydation du Ce est empêchée par la présence d'un écran organique entre les terres rares et les surfaces oxydantes des oxydes de fer et de manganèse.

Il est également possible que la sorption préférentielle du Ce^{IV} par une surface solide soit masquée par la présence de colloïdes organiques. Dans de telles conditions l'information redox

sera portée par la fraction inorganique des eaux qui (i) ne représente qu'une partie très faible du total des terres rares en solution et (ii) de ce fait verra sa signature masquée par la fraction organique dominante qui elle ne montre pas d'anomalie. Additionner ces deux processus, consiste donc à masquer une partie de l'information. Pour accéder à l'information redox il faudra impérativement procéder à des expériences d'ultrafiltration afin d'éliminer la fraction colloïdes organiques.

La complexation des terres rares par les acides humiques (réaction fortement probable lors de la formation de paléosols riches en matière organique) peut donc remettre en cause l'utilisation de l'anomalie de Ce comme proxy puisqu'elle peut inhiber ou masquer son développement. Des conditions redox variables combinées à une spéciation organique des terres rares peuvent ainsi mener à la formation de spectres de terres rares complexes dans les paléosols, ces spectres ne reflétant pas alors les conditions redox et par extrapolation les conditions climatiques régnant au moment de la genèse de ces sols. Il est cependant difficile d'établir un lien direct entre les conditions redox régnant dans une solution et l'enregistrement porté par un solide. En effet, une telle information peut être masquée ou altérée lors de processus tels que la cristallisation ou la diagenèse des constituants d'un sol. Il semble donc nécessaire de déterminer expérimentalement l'impact de tels processus sur l'enregistrement des conditions redox sur des phases solides.

2.3. Conséquences sur le cycle externe des terres rares

La combinaison de tous les résultats obtenus dans ce travail de thèse permet d'établir un schéma de formation des spectres des terres rares dans les eaux naturelles et d'expliquer la chute des concentrations en solution en terres rares depuis les eaux du sol jusqu'à l'océan. Une réinterprétation du cycle externe des terres rares est proposée et illustrée sur la Fig. 7.

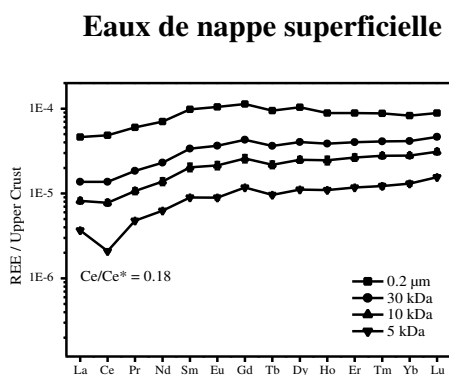
La chute de concentration en solution du Ce dans les océans et les rivières (développement d'une anomalie négative de Ce au niveau des spectres) a été attribuée à sa chimie redox (e.g., Elderfield, 1988). Toutefois les différents processus pouvant mener à cette chute sont mal identifiés. De façon plus générale concernant le fractionnement des terres rares dans leur globalité, le processus le plus souvent discuté est celui qui propose que le fractionnement ait lieu pendant le mélange estuarien favorisé par la réactivité extrêmement élevée de particules (par exemple, MnO_2) et qui aboutit à un enrichissement en terres rares lourdes (Elderfield, 1988; Elderfield et al., 1990; Sholkovitz, 1995). La chute de concentration des terres rares pourrait également avoir lieu par coagulation du "pool" colloïdal de terres rares pendant les mélanges estuariens (Hoyle et al., 1984; Elderfield, 1988; Elderfield et al., 1990; Sholkovitz, 1995). Dans ce cas, le fractionnement des terres rares se produit par séparation des "pools" colloïdaux et "dissous vrai" qui présentent chacun des formes spécifiques de spectres de terres rares (Sholkovitz, 1992; Sholkovitz, 1995).

Les résultats expérimentaux de notre étude montrent que la compétition entre les acides humiques et les carbonates pour la complexation des terres rares peut mener au fractionnement des terres rares. Ces expériences illustrent et confirment le possible contrôle de la chute de concentration des terres rares par coagulation du "pool" colloïdal de terres rares pendant les mélanges estuariens (Elderfield et al., 1990; Sholkovitz, 1995). Lorsque les deux phases sont physiquement séparées, elles présentent deux spectres de terres rares différents: (i) la phase organique montrant un spectre de terres rares relativement plat, (ii) la phase inorganique montre un spectre enrichi en terres rares lourdes proche de celui de l'eau de mer. Or, dans le milieu naturel, la séparation de la phase organique colloïdale du dissous peut tout à fait se produire lors d'une augmentation de salinité qui entraînerait la floculation de colloïdes organiques.

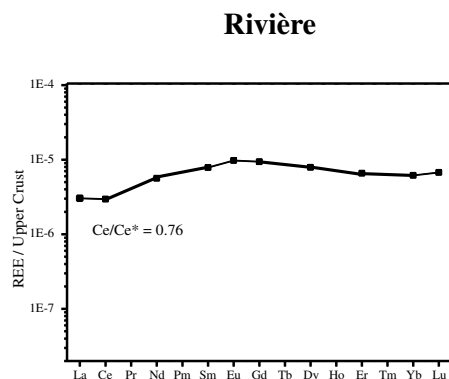
Les expériences d'ultrafiltration sur des eaux de nappe de sol riches en matières organiques indiquent qu'environ 90 % des terres rares sont présentes sous formes organiques. Environ 10 % du pool de terres rares des eaux de nappes superficielles est transféré vers les fleuves où la spéciation est ici considérée constante. Le transfert des fleuves vers les océans

aboutit aux estuaires, où ont lieu des mélanges et où les phases organiques et inorganiques sont séparées. Environ 90 % des terres rares se retrouvent extraites de la solution par floculation du matériel organique. Les terres rares inorganiques restant en solution peuvent également être fractionnées en contact avec des particules fortement réactives (comme les nodules de ferromanganèse) mais cette proportion est minimale (1 % des REE par rapport au retrait de 90 % par floculation organique). Ainsi, les spectres de terres rares des océans semblent refléter les spectres de terres rares de la fraction inorganique des eaux de rivières. Une telle information est donc masquée jusqu'à ce que les phases inorganiques et organiques soient séparées comme pendant un mélange estuarien par exemple.

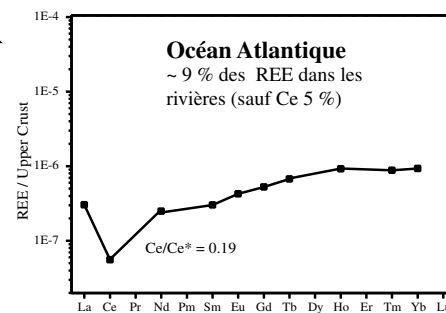
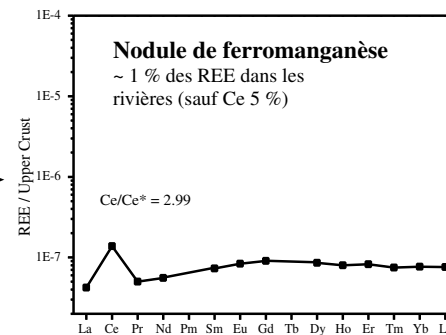
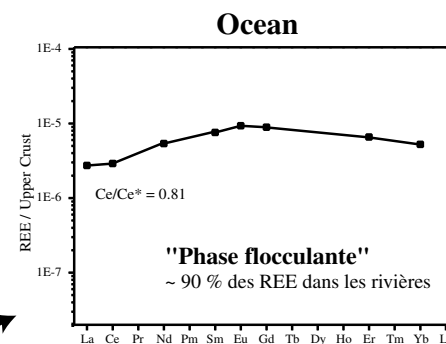
Fig. 7. Cycle des terres rares des eaux souterraines en passant par les rivières jusqu' aux océans. Les données sont extraites de De Baar et al. (1988), Elderfield et al. (1990) et Pourret et al. (2006b).



Spéciation
 > 90 % organique
 < 10 % inorganique



Mélange estuarien



Augmentation de la force ionique et du pH
 Floculation organique et retrait des terres rares de la solution

3. PERSPECTIVES

3.1. Perspectives à court terme

Les résultats présentés dans cette étude ont montré l'impact de la matière organique sur la spéciation des terres rares dans des eaux organiques de forces ioniques faibles typiques de rivières ou d'eaux souterraines. Étendre la gamme de force ionique permettrait de connaître l'impact de cette complexation organique pour des conditions représentatives des eaux marines. Des expérimentations en laboratoire de floculation - coagulation d'échantillons de rivières riches en terres rares et en matières organiques permettraient de comprendre et de modéliser la transition eaux de rivières - océan.

L'impact de la complexation organique sur le fractionnement des terres rares permet de remettre en cause l'utilisation des terres rares en tant que traceurs des conditions redox. Cependant, l'aspect cinétique de la complexation organique n'a pas été pris en compte dans notre étude. Or, si la cinétique de complexation organique est plus lente que la cinétique d'oxydation du Ce et/ou d'adsorption des terres rares, un fractionnement pourrait apparaître. L'aspect cinétique de la réaction de complexation entre terres rares et matière organique pourrait alors minimiser l'impact de la complexation sur le fractionnement des terres rares.

Comme suggéré précédemment, le spectre global de terres rares d'un échantillon d'eau souterraine représente la somme de différentes fractions organiques et inorganiques. La comparaison d'expériences d'ultrafiltration sur deux échantillons d'eaux de sol riches en matières organiques (Fig. 8), l'un en conditions réductrices et l'autre en conditions oxydantes, montre une variation de l'intensité de l'anomalie de Ce de la fraction inorganique (i.e. la fraction < 5 kDa).

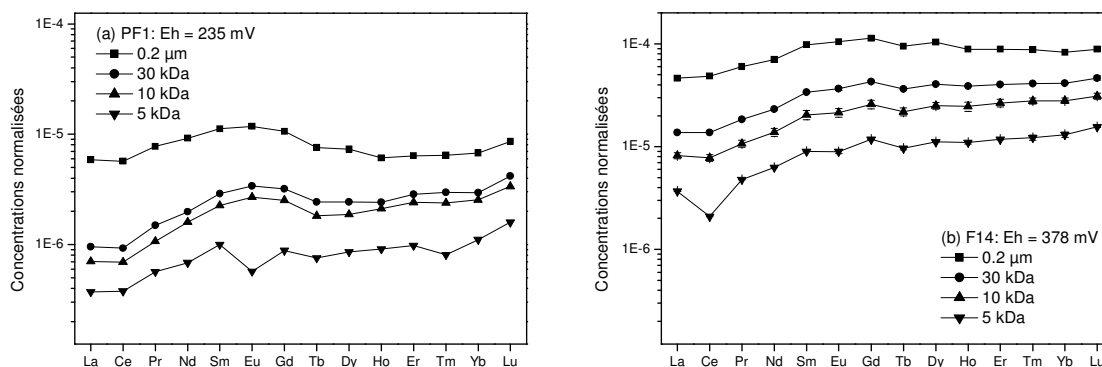


Fig. 8. Spectres de terres rares normalisés à la croûte continentale supérieure pour les différentes ultrafiltrations réalisées pour des échantillons d'eau de zones humides (a) en conditions réductrices ($E_h = 235$ mV) et (b) en conditions oxydantes ($E_h = 378$ mV). Les données sont extraites de Pourret et al., (2006b).

Une étude temporelle d'eau de nappes de sol couplée à des ultrafiltrations permettrait de vérifier que la fraction inorganique est effectivement sensible aux variations des conditions d'oxydo-réduction et climatiques.

Enfin, les données expérimentales de complexation de terres rares aux acides humiques peuvent être utilisées afin de déterminer des constantes de complexations intrinsèques à l'aide du logiciel FITEQL (Herbelin et Westall, 1999). Ceci permettrait d'utiliser les terres rares dans des modèles de spéciation plus généralistes du type PHREEQC (Parkhurst et Appelo, 1999) qui prennent en compte les réactions de précipitation et d'oxydoréduction non considérées dans des modèles du type WHAM.

3.2. Perspectives à moyen et long termes

Aux interfaces sol/solide/solution, il est souvent difficile d'identifier les paramètres les plus influents sur les réactions géochimiques. Les terres rares sont particulièrement intéressantes dans ce cas, certaines réactions chimiques peuvent produire des spectres de terres rares caractéristiques. Les terres rares constituent donc un outil précieux et puissant dans la compréhension et l'identification des processus géochimiques aux interfaces sol/solide/solution. Cependant, les spectres de terres rares d'échantillons naturels reflètent la superposition de plusieurs processus de fractionnement. En effet, la forme des spectres est liée (i) à la nature et à l'abondance des phases solides mises en jeu dans les réactions d'adsorption, (ii) aux compétitions entre surfaces et ligands en solution, (iii) aux paramètres physico-chimiques (e.g., pH, force ionique, alcalinité).

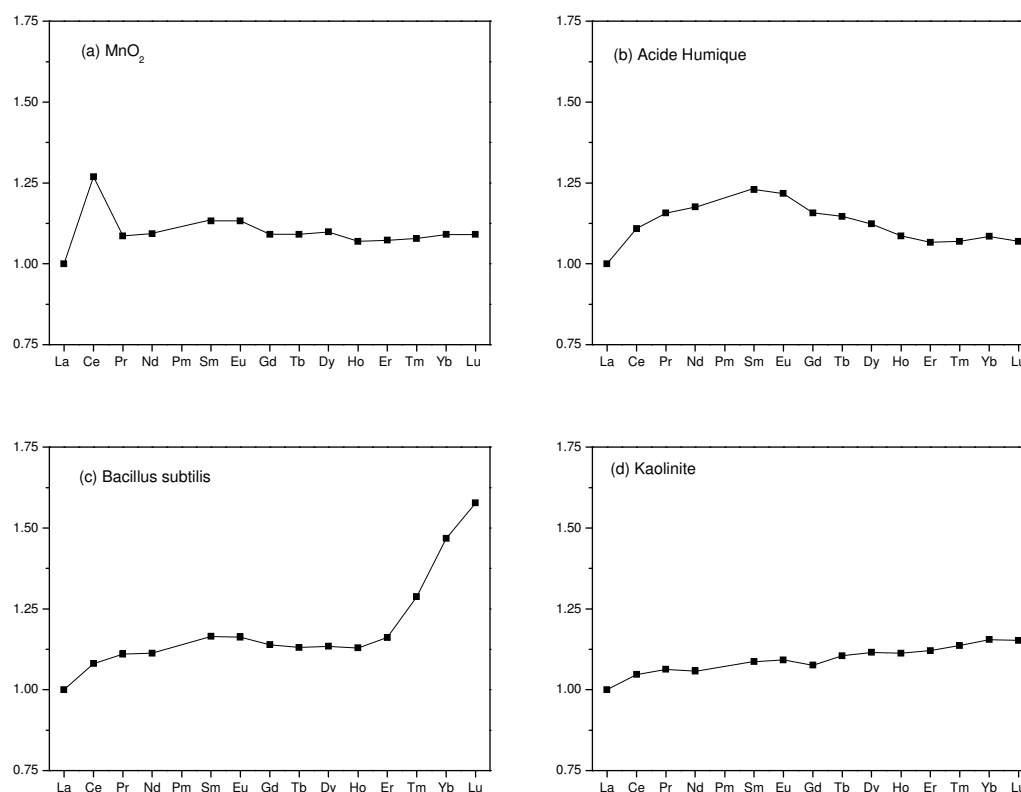


Fig. 9. Spectres des coefficients de partage des terres rares adsorbées sur (a) un oxyde de manganèse (Davranche et al., 2005, cf Partie I.2), (b) un acide humique (Pourret et al., 2006b; cf Partie II.2), (c) une bactérie (Takahashi et al., 2005), (d) une argile (Coppin et al., 2002).

Les surfaces solides impliquées dans les réactions d'adsorption sont les oxyhydroxydes de Fe, Mn (e.g., cette étude; De Carlo et al., 1998; Quinn et al., 2004), les argiles (e.g., Sinitsyn et al., 2000; Coppin et al., 2002), les sables (e.g., Tang et Johannesson, 2006), les matières organiques (e.g., Yamamoto et al., 2005; cette étude) colloïdales ou particulières et les bactéries (e.g., Takahashi et al., 2005). A chaque nature de "solide" correspond un spectre spécifique de terres rares (Fig. 9). D'une manière générale, l'impact des ligands inorganiques sur le fractionnement des terres rares a été plus souvent étudié (e.g. pour les carbonates, Cantrell et Byrne, 1987; Millero, 1992; Ohta et Kawabe, 2000; Luo and Byrne, 2004; e.g. pour les sulfates, Millero, 1992; Astrom, 2001; Schijf et Byrne, 2004). Cependant, peu d'études traitent de la compétition des ces ligands inorganiques avec les surfaces adsorbantes décrites précédemment.

Une étude intégrant l'ensemble de ces surfaces fournirait à la fois des spectres spécifiques aux réactions, et des données expérimentales nécessaires à la détermination de constantes thermodynamiques indispensables à la modélisation. Les spectres de terres rares obtenus représenteront la somme des différents processus chimiques impliqués. De plus, les modèles pourraient tenir compte de tous les équilibres chimiques permettant de modéliser l'ensemble des réactions de complexation, dont les réactions redox pour mieux contraindre le cycle des éléments redox sensibles comme le Ce. Ces spectres de référence pourraient être confrontés aux spectres de terres rares de solutions naturelles et permettraient après déconvolution d'identifier et de hiérarchiser, à la fois, les paramètres physico-chimiques influents (potentiel redox, pH...) et les phases solides jouant un rôle majeur dans un sol ou un aquifère donné dans la mobilisation des terres rares. Les modèles plus globaux couplant les cycles d'éléments traces pourraient ainsi profiter d'une meilleure compréhension des interactions terres rares - colloïdes.

Annexes

Cette partie est extraite d'un article sous presse à Applied Geochemistry, Olivier Pourret, Aline Dia, Mélanie Davranche, Gérard Gruau, Odile Hénin and Maxime Angée (2006) Organo-colloidal control on major- and trace-element partitioning in shallow groundwaters: confronting ultrafiltration and modelling.

Abstract- Ultrafiltration experiments using new small ultracentrifugal filter devices were performed at different pore size cut-offs to allow the study of organo-colloidal control on metal partitioning in water samples. Two shallow, circumneutral pH waters from the Mercy site wetland (western France) were sampled: one dissolved organic carbon (DOC)- and Fe-rich and a second DOC-rich and Fe-poor. Major- and trace-element cations and dissolved organic carbon concentrations were analysed and data treated using an ascendant hierarchical classification method. This reveals the presence of three groups: (i) a "truly" dissolved group (Na, K, Rb, Ca, Mg, Ba, Sr, Si and Ni), (ii) an inorganic colloidal group carrying Fe, Al and Th and (iii) an organic colloidal group enriched in Cr, Mn, Co, Cu and U. However, REE and V have an ambivalent behaviour, being alternatively in the organic pool and in the inorganic pool depending on sample. Moreover, organic speciation calculation using Model VI were performed on both samples for elements for which binding constants were available (Ca, Mg, Ni, Fe, Al, Th, Cr, Cu, Dy, Eu). Calculation shows relatively the same partitioning of these elements as ultrafiltration does. However, some limitations appear such as (i) a direct use of ultrafiltration results which tends to overestimate the fraction of elements bound to humic material in the inorganic pool as regards to model calculations as well as, (ii) a direct use of speciation calculation results which tends to overestimate the fraction of elements bound to humic material in the organic pool regards to ultrafiltration results. Beside these limitations, one can consider that both techniques, ultrafiltration and speciation calculation, give complementary information, especially for more complex samples where inorganic and organic colloids compete.

Keywords: organic matter, colloids, major and trace elements, ultrafiltration, speciation

1. Introduction

Dissolved Organic Matter (DOM) is ubiquitous in aquatic and terrestrial environments and plays a key role in the geochemistry of major and trace elements (Stumm and Morgan, 1996). While DOM represents only a small proportion of the global carbon reservoir, it is instrumental in many reactions and influences environmental chemistry far beyond its mass contribution (Macalady, 1998). DOM acts as a major carrier for many elements through complexation, sorption and dissolution reactions (Buffle, 1988; Cabaniss and Schumann, 1988; Benedetti et al., 1996; Buerge-Weirich et al., 2003).

Since DOM may compete with rock surfaces because of their high sorption capacities (Iler, 1979), sorption and/or complexation of cations onto DOM are major controlling processes for element migration and removal in weathering and aquifer systems (McCarty et al., 1998; Tosiani et al., 2004; Braun et al., 2005). Moreover, speciation, bioavailability and mobility of major and trace elements can be strongly influenced by DOM (Wells and Goldberg, 1991; Tipping and Hurley, 1992; Dahlgvist et al., 2004). Since in natural aquatic systems, metal ions are rarely present as free hydrated ions, DOM provides binding sites influencing both their bioavailability and general transport behaviour. It also interacts with mineral phases modifying the exchange rates with solutions and constrains part of elemental mobility (Bennett and Siegel, 1987; Christensen et al., 1996; Schmitt et al., 2003).

Colloids, ubiquitous in natural waters, either organic or inorganic, are microscopic particles with size in the range 1 μm to 1 nm (Stumm and Morgan, 1996). Because of their small size, they tend not to settle out of suspensions, being influenced by Brownian motion and minor currents in the bulk solutions. The solid-water interface established by these microparticles plays a key role in regulating the concentrations of most reactive elements and of many pollutants in soils and natural waters (Stumm and Morgan, 1996). They adsorb heavy metal ions and waterborne pollutants governing, via their movements in aqueous systems, the fates of reactive elements and/or pollutants.

Recent studies coupled or not with speciation calculations suggested that a large fraction of trace elements are closely associated with DOM including colloidal organic matter in many natural waters (Tanizaki et al., 1992; Viers et al., 1997; Dupré et al., 1999; Dia et al., 2000; Ingri et al., 2000; Gruau et al., 2004; Johannesson et al., 2004). Moreover, redox conditions do control the dynamics and fate of some toxic and/or redox sensitive elements at the soil/water interface. The true respective roles of DOM and Fe-Mn oxyhydroxides as elemental carriers are still poorly understood. As Fe-Mn oxyhydroxides are redox sensitive (Stumm and Morgan, 1996), it is not clear whether trace metals are directly bound to the oxyhydroxides and complexed by DOM when the oxyhydroxides are dissolved during reduction, or whether they are directly bound to DOM and controlled by the organic matter dynamics throughout the entire redox cycle.

Considering that the respective contribution of organic and inorganic element carriers still remains a matter of debate, this work is dedicated to (i) investigate trends in trace element partitioning in size fractionated samples of well water using small ultracentrifugal devices and (ii) compare this field data to geochemical modelling calculations.

2. Samples

2.1. Sample location

The Kervidy/Coët-Dan catchment (5 km²) is located in the Coët-Dan drainage basin, about 100 km southwest of Rennes in Central Brittany, France (Fig. 1). The bedrock is made of fissured and fractured upper Proterozoic schists (Dabard et al., 1996). The soils, developed into a loamy material derived from bedrock weathering and eolian Quaternary deposits, exhibit facies variations, which are locally, dominated by silt, clay or sandstone materials (Pellerin and Van Vliet-Lanoë, 1994). The mineralogical composition of schist was determined from drill cutting analysis and includes (in decreasing relative proportion): quartz, muscovite, chlorite, K-feldspar and plagioclase (Pauwels et al., 1998). The soil horizons comprise a large number of secondary mineral phases including illite, smectite, kaolinite, various Fe-oxides and Fe-oxyhydroxides (hematite, goethite...) and Mn oxides (Pauwels et al., 1998; Curmi et al., 1995).

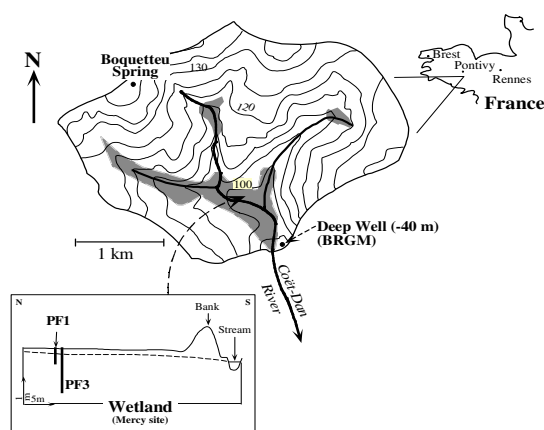


Fig. 1. Sketch showing (a) topography, channel network geometry and geographical location of the Kervidy-Coët Dan subcatchment, and (b) sampling point locations (Wt: wetland samples; Rv: river samples). Discontinuous patterned areas located close to the channel network indicate the location of wetland zones.

Previous hydrochemical studies (Durand and Torres, 1996; Jaffrézic, 1997; Dia et al., 2000; Molénat et al., 2002) showed that the Kervidy/Coët-Dan groundwater can be summarized by the contrast of two spatially-distributed chemical domains. These include: (i) the uppermost

part of the groundwater, sampled below the hillslope, and which is colourless, slightly acidic, always oxidized and nitrate-contaminated (up to $200 \text{ mg L}^{-1} \text{ NO}_3^-$) (Molénat et al., 2002), (ii) the shallow groundwater domain located in the wetlands where the water table reaches the organic-rich upper soil horizons. This second groundwater component is coloured, DOC-rich and exhibits variable nitrate concentrations (Durand and Torres, 1996; Jaffrézic 1997). In addition, these waters are characterized by the development of periodic reducing conditions mostly in late winter and spring, which is a direct consequence of the waterlogging of the uppermost soil horizon (Jaffrézic, 1997).

2.2. Sampling procedure

Two organic-rich groundwater samples were collected from shallow wells (PF1, 0.5-m- and PF3, 0.8-m-deep) located in the Mercy wetland (Fig. 1) in November 2004. Physico-chemical parameters (pH and temperature) were measured directly in the field. The pH was measured with a combined Sentix 50 electrode after a calibration performed with WTW standard solutions (pH = 4.01 and 7.00 at $25 \text{ }^\circ\text{C}$). The accuracy of the pH measurement is ± 0.05 pH unit. Samples used for determination of dissolved ($< 0.2 \text{ }\mu\text{m}$) major-, trace-element and DOC concentrations were pumped using Teflon tubing connected to a polyethylene syringe. The collected waters (about 1 L) were immediately filtered on site using $0.2 \text{ }\mu\text{m}$ cellulose acetate filter capsule (polyether sulfone membrane Sartorius Minisart), and stored in pre-cleaned, acid-washed polyethylene bottles. About 30 mL were used to measure alkalinity, major anions and DOC concentrations. The remaining solution was used to measure major and trace cation concentrations and was then successively filtered through ultracentrifugal devices with decreasing pore size cut-offs in order to allow separation of colloids from "truly" dissolved forms.

3. Experimental

3.1. Ultrafiltration set-up description and chemical analysis

To separate the colloidal bound elements from the non colloid-borne elements ultrafiltration experiments were performed on these samples using 15 mL centrifugal tubes (Millipore Amicon Ultra-15) equipped with permeable membranes of decreasing pore sizes (30 kDa, 10 kDa, and 5 kDa with $1 \text{ Da} = 1 \text{ g mol}^{-1}$). Metal-colloid complexes are retained by the ultrafiltration membrane while free ions and smaller complexes pass into ultrafiltrate. The degree of metal-colloid complexation is usually determined from the metal concentration in the ultrafiltrate relative to the original solution. Each centrifugal filter device was washed and rinsed with HCl 0.1 N and MilliQ water two times before use. The starting filtrate had been passed through $0.2 \text{ }\mu\text{m}$ filter, and then aliquots of these filtrates were passed through membranes of smaller sizes. All ultrafiltrations of the $0.2 \text{ }\mu\text{m}$ filtrates were done in parallel. The centrifugations were performed using a Jouan G4.12 centrifuge equipped with swinging bucket at about 3000 g for 20 minutes and 30 minutes, for 30 kDa and 10 kDa, and 5 kDa devices, respectively (centrifugation times determined from preliminary experiments not shown). All experiments were carried out at room temperature: $20 \pm 2 \text{ }^\circ\text{C}$.

Major cations and trace elements concentrations were determined at Rennes 1 University using an Agilent TechnologiesTM HP4500 ICP-MS instrument. Quantitative analyses were performed using a conventional external calibration procedure. Three external standard solutions with major and trace elements concentrations similar to the analyzed samples were prepared from mono- and multi-elements standard solutions (Accu TraceTM Reference, USA). Indium was added to all samples as an internal standard at a concentration of $0.87 \text{ }\mu\text{mol L}^{-1}$ (100 ppb) to

correct for instrumental drift and possible matrix effects. Indium was also added to the external standard solutions. Calibration curves were calculated from measured major cations and trace elements /indium intensity ratios. The instrumental error on major cations and trace elements analysis in our laboratory as established from repeated analyses of the SLRS-4 water standard is $< \pm 2 \%$. DOC concentrations were determined at Rennes 1 University using a Shimadzu 5000 TOC analyzer. The accuracy of DOC concentration measurements is estimated at $\pm 5 \%$ as determined by repeated analyses of freshly prepared standard solutions (potassium biphtalate). Total alkalinity was determined by potentiometric titration with an automatic titrating device (794 Basic Titrimo Methrom). Major anions (Cl^- , SO_4^{2-} and NO_3^-) concentrations were measured by ionic chromatography (Dionex DX-120): the uncertainty is below $\pm 4 \%$.

The same material was used for all filtrations, molecular size exclusion rather than adsorption onto membranes should control the colloid distributions between ultrafiltrates. The selectivity of the 10 and 5 kDa membranes regards to Aldrich Humic Acid, with a mean molecular weight of 23 kDa, was verified by monitoring the Dissolved Organic Carbon (DOC) contents of the ultrafiltrates (preliminary experiments not shown). Results show that the latter were systematically lower or equal to blank values (≤ 1 ppm). Possible adsorption of inorganic major and trace elements species onto the membrane or onto cell walls was also monitored. Inorganic multi-elements solutions of known concentration were ultrafiltered several times. Results showed that 100 % of the major and trace elements present in solution was recovered in the ultrafiltrates, demonstrating that no major and trace elements was adsorbed neither on the membranes nor on the walls of the cell devices used. All ultrafiltration were performed in duplicate. A good reproducibility is observed for DOC and major and trace elements concentrations. Duplicates are better than 5 % for most elements except for some trace elements in the lower pore size cut-off fraction (i.e. in the < 5 kDa fraction, about 10 %).

All procedures (sampling, filtration, storing and analysis) were carried out in order to minimize contamination. Samples were stored in acid-washed Nalgene polypropylene containers before analyses. Chemical blank concentrations of individual major cations and trace elements were all better than 2 % for all studied elements except for DOC, Al and Cu ($< 8 \%$, 10% and 11% , respectively).

3.2. Speciation calculation

The aqueous speciation of some major (Al, Ca, Fe, Mg) and trace elements (Cu, Eu, Dy, Th) was calculated using the computer program WHAM 6 (Version 6.0.13). It includes Model VI which has been described in detail by Tipping (1998). The model is a discrete binding site model in which binding is modified by electrostatic interactions. There is an empirical relation between net humic charge and an electrostatic interaction factor. In this study the computation is performed using only the default parameters values and the generic $\log K_{MA}$ values (see Tipping, 1998). Humic substances were the only colloidal phases considered in this calculation, none colloidal oxide phase was considered.

3.4. Data treatment

The ascending hierarchical classification using Ward criterion was performed through SPAD 4.5 routines (DECISIA, France) so as to implement sample classification (Dillon and Goldstein, 1984). This method is based on squared Euclidian distances between individuals in the space formed by the available variables. The initial sample is partitioned into several classes of individuals so as to maximise interclass inertia (i.e. to maximise variability between groups) and minimise intraclass inertia (i.e. to maximise homogeneity in each group). As for factor analysis, the raw data matrix was introduced in principal component analysis, without any rotation. The input data are the whole set of ultrafiltrates after each cut-off for all considered elements.

	PF1							PF3						
	0.2 µm	30 kDa	30 kDa	10 kDa	10 kDa	5 kDa	5 kDa	0.2 µm	30 kDa	30 kDa	10 kDa	10 kDa	5 kDa	5 kDa
T (°C)	10.6							10.7						
pH	7.08							6.93						
Cl	47							37						
SO4	10							9						
NO3	2							46						
Alkalinity	1867							385						
DOC	17.3	15.7	15.8	13.9	14.6	13.9	13.0	7.66	6.73	6.60	5.60	5.72	5.13	4.82
Na	17130	17480	17300	16850	16580	15797	16187	16150	14950	15310	15400	15550	13015	13466
Mg	21550	21690	21850	21170	21110	19801	20039	15710	14980	14850	15220	15220	13363	13705
Al	25	12	12	11	10	6	7	72.6	18.4	17.7	15.8	15.0	10.8	10.3
Si	4027	4013	4042	3903	3882	3751	3781	4234	3922	3946	4007	4048	3656	3679
K	564	546	555	546	537	501	510	468	426	434	441	435	400	403
Ca	10310	10050	10190	9717	9218	8915	9033	7437	7088	7539	7371	7151	6686	6719
V	0.34	0.18	0.19	0.18	0.17	0.11	0.12	0.27	0.16	0.16	0.16	0.16	0.16	0.15
Cr	1.36	1.16	1.15	1.08	1.00	0.61	0.67	0.87	0.69	0.68	0.67	0.69	0.59	0.54
Mn	31.16	25.40	25.27	24.87	24.63	9.55	9.66	9.77	9.40	9.41	9.34	9.49	2.65	2.67
Fe	955	35	34	21	25	6	7	98.5	12.1	11.6	8.0	n.a.	0.0	0.0
Co	3.75	3.10	3.10	2.85	2.78	1.16	1.23	1.13	1.07	1.07	1.04	1.10	0.20	0.20
Ni	5.52	5.15	5.44	4.90	4.97	3.80	4.03	6.45	5.94	5.91	5.75	n.a.	4.59	4.57
Cu	1.94	1.70	1.72	1.39	1.37	1.20	1.25	5.68	4.84	4.88	3.91	3.90	3.12	3.12
Zn	5.69	cntd	cntd	cntd	cntd	cntd	cntd	11.74	cntd	cntd	cntd	cntd	cntd	cntd
Rb	2.83	2.77	2.76	2.75	2.73	2.67	2.67	0.45	0.40	0.40	0.41	0.40	0.40	0.40
Sr	57.18	55.87	55.75	55.07	54.60	53.43	53.56	51.56	50.82	50.61	50.39	50.34	49.98	50.27
Ba	7.28	6.65	6.72	6.58	6.51	6.32	6.26	10.71	10.48	10.39	10.35	10.26	10.18	10.18

Table 1. (to be continued)

	PF1							PF3						
	0.2 μm	30 kDa	30 kDa	10 kDa	10 kDa	5 kDa	5 kDa	0.2 μm	30 kDa	30 kDa	10 kDa	10 kDa	5 kDa	5 kDa
La	0.176	0.029	0.029	0.021	0.021	0.010	0.012	0.804	0.580	0.571	0.436	0.430	0.284	0.274
Ce	0.365	0.059	0.060	0.045	0.044	0.019	0.029	1.889	1.352	1.347	1.027	0.996	0.600	0.578
Pr	0.055	0.011	0.011	0.007	0.008	0.004	0.004	0.255	0.184	0.185	0.140	0.138	0.095	0.091
Nd	0.239	0.053	0.050	0.041	0.042	0.016	0.019	1.105	0.833	0.819	0.630	0.618	0.417	0.404
Sm	0.050	0.012	0.014	0.010	0.010	0.005	0.004	0.194	0.144	0.140	0.104	0.100	0.070	0.067
Eu	0.010	0.003	0.003	0.003	0.002	0.000	0.001	0.037	0.027	0.026	0.019	0.019	0.012	0.012
Gd	0.040	0.012	0.012	0.010	0.009	0.003	0.004	0.135	0.096	0.095	0.075	0.071	0.046	0.044
Tb	0.005	0.001	0.002	0.001	0.001	0.000	0.001	0.013	0.010	0.009	0.007	0.007	0.004	0.004
Dy	0.026	0.009	0.008	0.007	0.007	0.003	0.003	0.067	0.049	0.047	0.035	0.037	0.022	0.021
Ho	0.005	0.002	0.002	0.002	0.002	0.001	0.001	0.013	0.009	0.010	0.007	0.007	0.004	0.004
Er	0.015	0.006	0.007	0.006	0.005	0.002	0.002	0.035	0.027	0.026	0.019	0.020	0.012	0.013
Tm	0.002	0.001	0.001	0.001	0.001	0.000	0.000	0.005	0.004	0.004	0.003	0.003	0.002	0.002
Yb	0.015	0.006	0.007	0.006	0.005	0.002	0.003	0.030	0.025	0.023	0.018	0.018	0.012	0.012
Lu	0.003	0.001	0.001	0.001	0.001	0.000	0.001	0.005	0.004	0.004	0.003	0.003	0.002	0.002
ΣREE	1.005	0.205	0.206	0.161	0.158	0.067	0.083	4.587	3.344	3.307	2.524	2.468	1.584	1.527
Pb	0.784	cntd	cntd	cntd	cntd	cntd	cntd	0.128	cntd	cntd	cntd	cntd	cntd	cntd
Th	0.045	0.027	0.027	0.023	0.019	0.003	0.005	0.063	0.025	0.024	0.016	0.014	0.008	0.006
U	0.046	0.035	0.036	0.030	0.028	0.022	0.023	0.049	0.035	0.034	0.024	0.024	0.014	0.012

Table 1. Ultrafiltration results, all concentrations are expressed in ppb, except Cl^- , NO_3^- , SO_4^{2-} and DOC in mg L^{-1} , and alkalinity in $\mu\text{mol L}^{-1}$.

4. Results

4.1. Ultrafiltrations

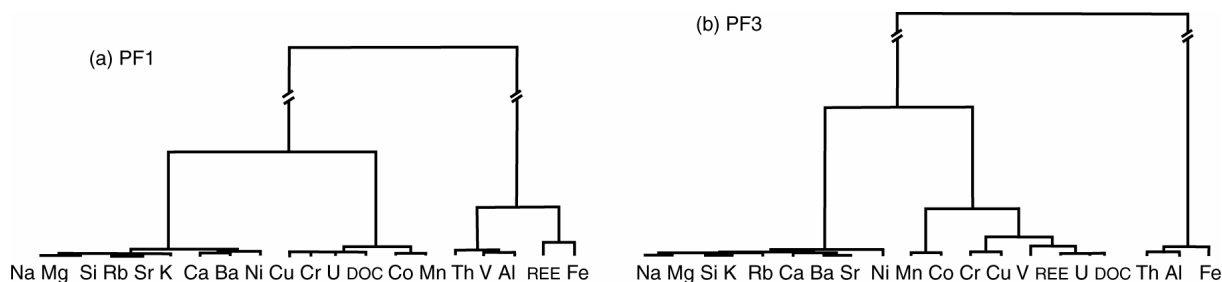


Fig. 2. Dendrograms of samples (a) PF1 and (b) PF3 showing the hierarchical classification of the elements in three clusters.

In the following sections the behaviour of major, trace, and DOC concentrations obtained for successive ultrafiltrations will be discussed. Major, trace element, and DOC concentrations are reported in Table 1. Major anions are not considered in this part of the study. Ultrafiltration data are presented following the hierarchical classification described in the hereabove "data treatment" paragraph. The results of cluster analysis are presented as a dendrogram, where the similarity of two elements is conversely proportional to the linkage distance (Fig. 2). This graph reveals three clusters: (i) cluster I includes alkalis (Na, K, Rb), alkaline earth metals (Ca, Mg, Ba, Sr) as well as Si and Ni, (ii) cluster II contains Cr, Mn, Co, Cu and U and (iii) cluster III includes Al, Fe and Th. REE and V are either, in cluster II or, in cluster III for PF1 and PF3 samples, respectively.

As stated previously, colloids span a wide range from about 1 nm to a few μm ; successive ultrafiltrations through decreasing pore size membranes, DOC concentrations decrease in the ultrafiltrates (Fig. 3). These successive ultrafiltrations allow further consideration about various molecular weight humic substances. To determine whether metals are bound or not to humic substances, metal concentrations will be systematically plot as a function of DOC concentrations.

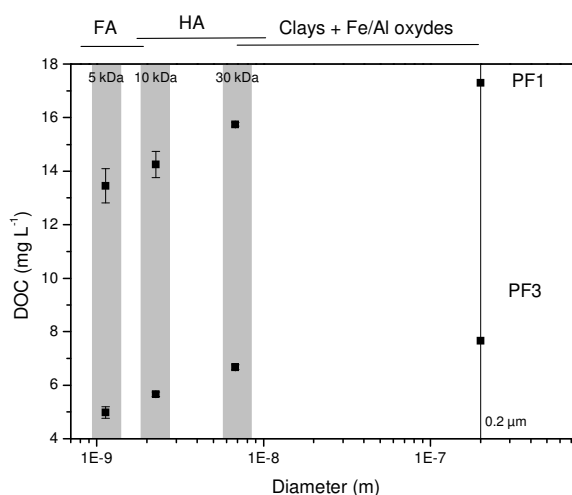


Fig. 3. DOC concentrations versus Molecular Weight Cut-Offs. Values for molecular weight are approximated, since the spatial extension of macromolecules such as humic substances is depending on molecular structure and surrounding conditions. FA: Fulvic Acid; HA: Humic Acid.

4.1.1. Common elemental distribution in the two samples

(i) cluster I : "truly" dissolved behaviour

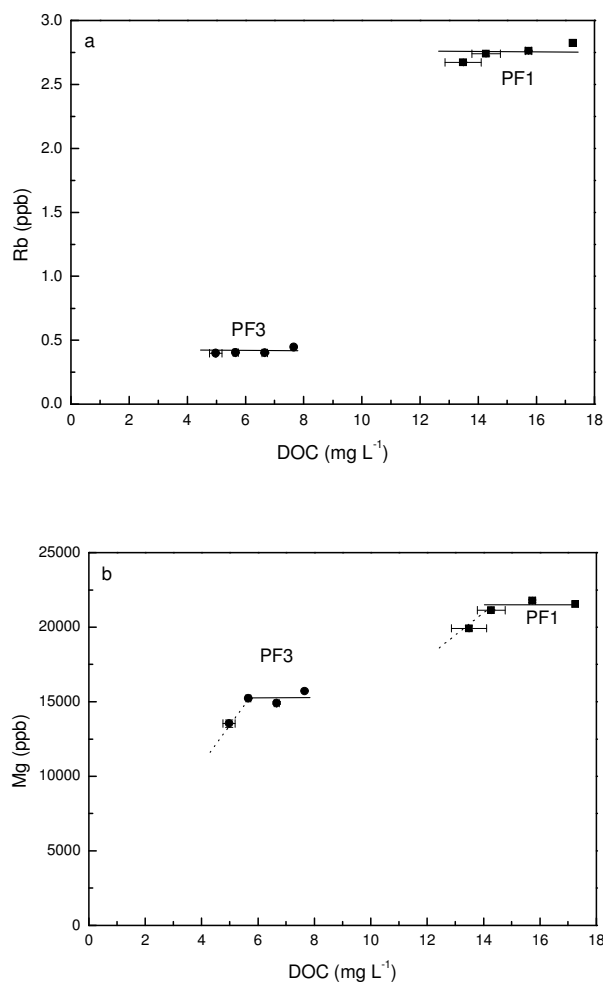


Fig. 4. Variations of (a) Rb and (b) Mg concentrations versus DOC concentrations in the different filtrates. Errors bars correspond to standard deviation for two replicates, some errors bars are within the symbol size.

Concentrations of Rb and other alkalis such as Na and K, are not affected by ultrafiltrations since no fractionation occurs when following the decreasing pore sizes or the DOC concentrations (Fig. 4a). Alkaline elements behave as "truly" dissolved in the form of inorganic species as often reported in the literature (Pokrovsky and Schott, 2002 and references therein).

Major and trace alkaline earth (Ca, Mg, Sr and Ba) concentrations do not change significantly during filtration except for the smallest pore size (5 kDa). The small drop between 5 kDa and 10 kDa filtrates (Fig. 4b) can suggest that part of these elements (about 10 %) could be associated with low-molecular weight organic colloids as reported elsewhere where complexes of Ca and Mg with natural fulvic acids have been identified (Shapiro, 1964).

Si concentrations display no significant variations in the successive filtrates. This suggests that aqueous silica is not trapped by organic colloids (Pokrovski and Schott, 1998) and/or by small-size clay minerals or phytolites. Ni concentrations do not exhibit large variations through the different decreasing pore size cut-offs suggesting that this transition metal has to be mostly present as "truly" dissolved species or small size inorganic complexes.

(ii) cluster II: organic colloidal pool-borne elements

Both Cu and U concentrations display extremely regular linear relationship as reported versus DOC concentrations for both samples (Figs. 5a, 5b ; Table 1). The linear relationships suggests that these two trace elements are strongly bound to organic matter and probably complexed to very low molecular weight organic ligands such as extracellular ligands as well as, larger size colloids such as fulvic and/or humic acids, cell fragments or bacteria as elsewhere reported (Xue et al., 1995; Sigg et al., 2000). Since Cu and U concentrations tend to zero before DOC ones do, one can suggest that no fraction of Cu and U occurs as free species in solutions and that a fraction of DOM is unable to complex these two elements. However, organic matter remains the major carrier of Cu and U as often previously stated (Stumm and Morgan, 1996).

Cr, Mn and Co concentrations (Table 1) also display linear positive correlations when reported versus DOC concentrations for both samples. Organic matter is thus also a major carrier of these elements.

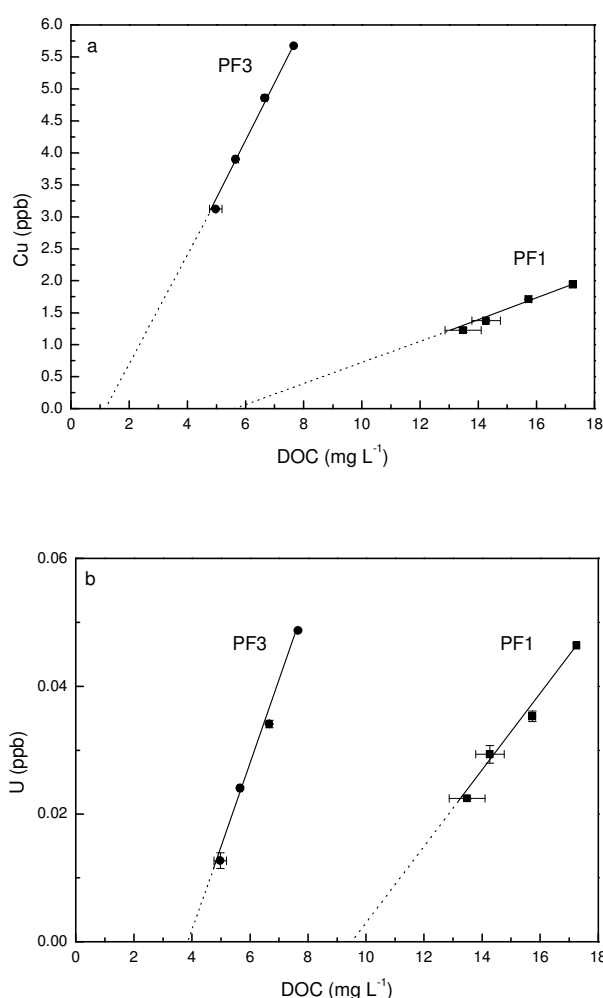


Fig. 5. Variations of (a) Cu and (b) U concentrations versus DOC concentrations in the different filtrates. Errors bars correspond to standard deviation for two replicates, some errors bars are within the symbol size.

(iii) cluster III: inorganic colloidal pool-borne elements

Al and Fe concentration variations through successive filtrations (Fig. 6a and 6b) suggest that these elements do not occur as free species in solution, and that two types of colloids can

carry these metals (i.e. Al-, Fe- rich inorganic colloids or organic-, Al-, Fe- complexing colloids). Al and Fe concentrations vary following the same trend (Table 1) both strongly affected by a large drop of concentrations between 0.2 μm and 30 kDa filtrations. Up to 96 % and 75 % for Fe and Al, respectively, are removed by the first ultrafiltration step. This indicates a major control of Al by inorganic mixed Fe/Al oxyhydroxides as already reported (Pokrovsky and Schott, 2002; Geckeis et al., 2003). This is particularly true for Al-rich PF3 sample as compared to PF1 where Fe dominates regards to Al. However, a small part of Al and Fe could be partially bound to low-molecular weight organic-rich colloids. Al concentration tends to zero before DOC does for both samples. This is not the case for Fe, since Fe disappears before DOC does. This suggests that the Fe budget between organic and inorganic carrier phases has to be different from that of Al, depending also which sample is considered. Furthermore, Al could be carried by another low-molecular weight DOC-poor phase which does not trap Fe in PF1 sample, but not in PF3. Al cannot be present as clay colloids since Si occurs at "truly" dissolved state.

Thorium concentrations regularly decrease through the successive decreasing pore size cut-offs with a large drop (up to 40 %) between 0.2 μm and 30 kDa (Fig. 6c). This suggests that this fraction of Th has to be associated to large size organic colloids while about 60 % of Th appears to be carried by colloids smaller than 30 kDa. Th concentrations decrease quicker than do DOC concentrations suggesting that Th is probably mostly carried in solution by high-molecular weight organic-rich colloids. Th concentration versus Al concentration diagram (Fig. 6d) suggests that Th might be also partly carried by Al-rich phases as well as DOC-rich ones. Clays and clay-organic complexes could be possible Th carriers in these waters.

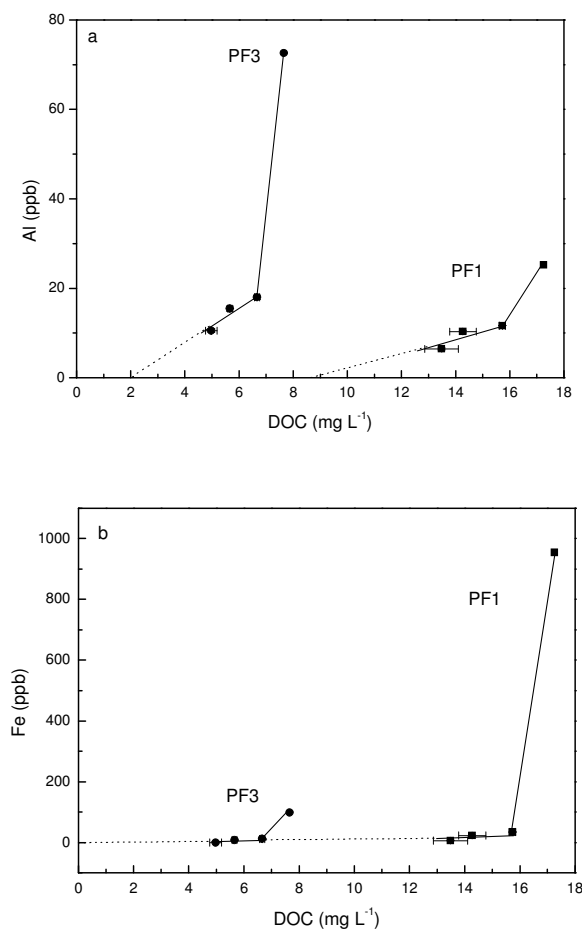


Fig. 6. (to be continued).

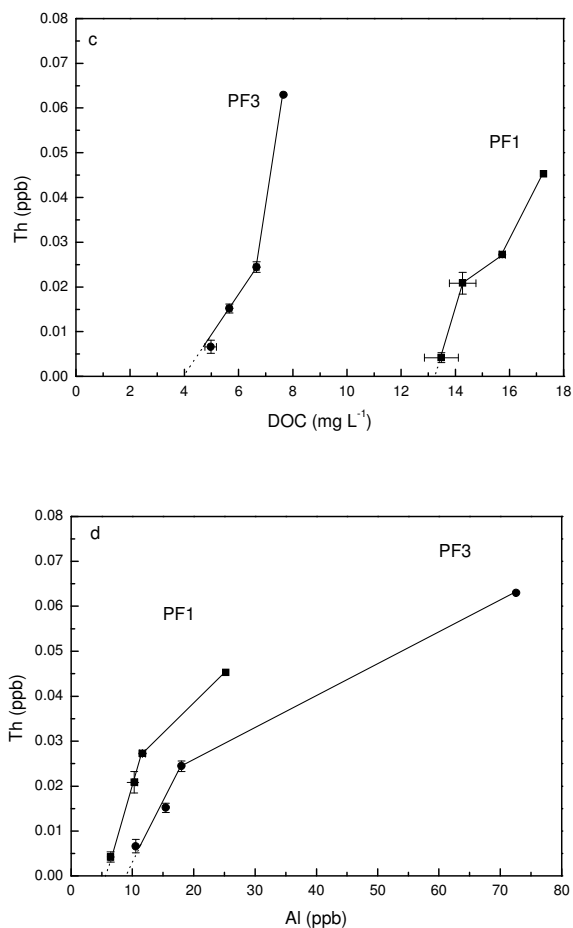


Fig. 6. Variations of (a) Al, (b) Fe, (c) Th concentrations versus DOC concentrations and (d) Th concentrations versus Al concentrations in the different filtrates. Errors bars correspond to standard deviation for two replicates, some errors bars are within the symbol size.

4.1.2. Peculiar elemental distribution in the DOC-depleted sample

REE and V display an ambivalent behaviour regards to sample considered. Plot of Σ REE concentrations versus DOC concentrations for the successive ultrafiltrations (Fig. 7a) show a general decreasing tendency going through zero REE that illustrates the removing of REE jointly to DOC. However, there is still DOC left in solution as REE concentrations are close to zero, which allows us to extrapolate that not all the organic pool is able to complex REE. The REE appear to be strongly complexed by high-molecular weight organic matter as previously stated in other ultrafiltration studies (Sholkovitz, 1995; Viers et al., 1997; Dia et al., 2000). However, a recurrent problem of ultrafiltration studies is that Fe and Mn oxyhydroxides can be present in the waters along with organic colloids, some of them being potentially strong competitors of organic matter for REE complexation (Bau, 1999; Dupré et al., 1999). PF1 sample presents a significant decrease in its Fe content upon ultrafiltration at the 30 kDa ultrafiltration step. This decrease corresponds to a marked change in the slope of the REE-DOC linear relationships otherwise observed in the REE versus DOC variation diagrams (Fig. 7a). About 80 % of the REE and 96 % of the Fe, but only 9 % of the DOC, are removed during the first ultrafiltration step of this sample. Such a relationship strongly suggests that the "colloidal" REE budget of PF1 samples is controlled, in part, by REE-bearing Fe colloids as suspected by looking at Fig. 7b. By contrast for PF3 sample, REE concentrations display a strong correlation as reported versus DOC

concentrations irrespective of the cut-off. The linear relationship suggests that in this sample REE are strongly bound to organic matter.

Vanadium concentrations reported versus DOC concentrations display a large drop between 0.2 μm and 30 kDa filtrations in the two samples (Fig. 7c). This suggests that a significant fraction (about 40 %) of V has to be carried by large size organic colloids. By contrast, when looking at lower cut-off the V concentrations behave differently in the two samples. On one side for the uppermost sample (PF1) a three step-shape decrease following DOC concentrations lowering suggesting that V remains carried by the organic phase (low- and high-molecular weight). Whereas on the other side, the decrease of V concentrations follows that of Al. This suggests that as do Th concentrations regards to DOC and Al concentrations, V concentrations follow the same trend (Fig. 7d). Both V and Th concentrations in organic-rich upper level seem to be controlled by mixed DOC/Al-rich phases, whatever may be the pore size cut-off.

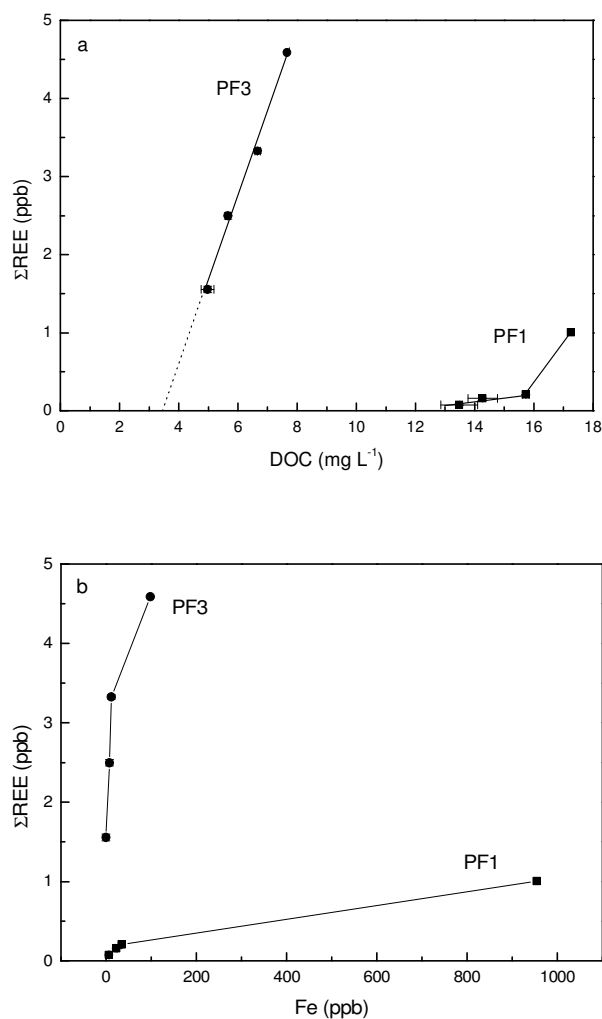


Fig. 7. (to be continued).

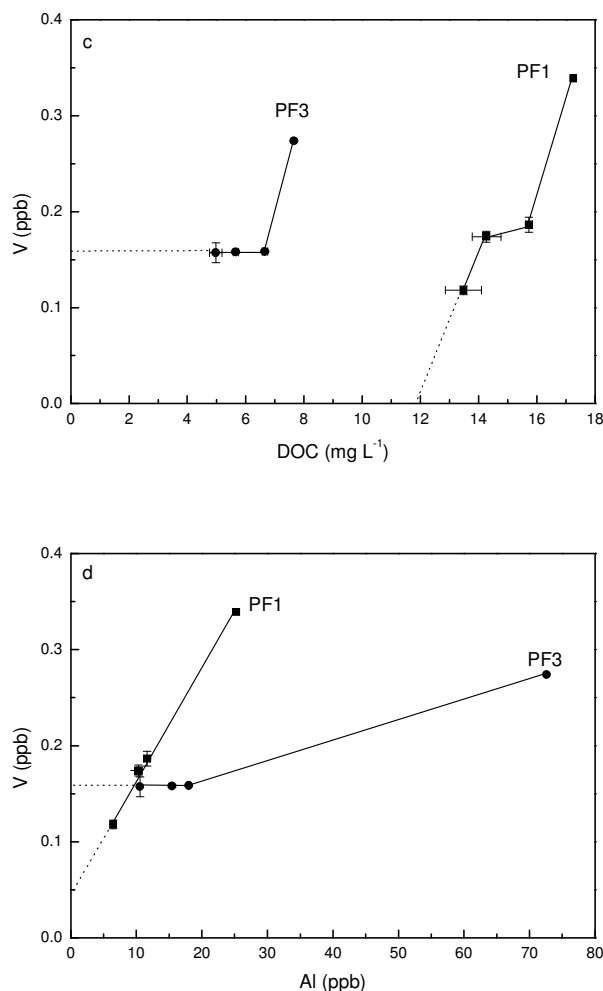


Fig. 7. Variations of REE concentrations versus (a) DOC and (b) Fe concentrations, and V concentrations versus (c) DOC and (d) Al concentrations in the different filtrates. Errors bars correspond to standard deviation for two replicates, some errors bars are within the symbol size.

Moreover, the large decrease of V concentrations following that of Fe between 0.2 μm and 30 kDa suggests that Fe-rich phases exert as well an important control on the speciation of V at this cut-off as earlier reported (Pokrovsky and Schott, 2002). At lower filtration sizes, V concentrations tends to zero, suggesting that V has also to be carried by a mixed Al/Fe/DOC-rich phase. The lower sample (PF3) displays a strong decrease in the first filtration step which implies that V is strongly bound to high-molecular weight organic material, and a constant V concentration after the 30 kDa filtration which implies that V behaves independently of DOC. However, the V concentration pattern is different in the DOC-depleted sample with no variation versus Al concentrations after the 30 kDa filtration. This suggests that V is not carried by an Al-rich phase, but mostly occurs as "truly" dissolved species as free hydrated ion.

4.2. Speciation calculations

The aqueous speciation of some major (Ca, Mg, Al, Fe) and trace elements (Cr, Ni, Cu, Eu, Dy, Th) in the two samples are calculated using Model VI (Tipping, 1998). The pH values were fixed at 7.08 and 6.93, for PF1 and PF3 samples, respectively. The DOC concentrations as well as major and trace elements concentrations input in the model were those displayed in Table

1. The Humic Acid (HA) and Fulvic Acid (FA) contents necessary to run both models are assumed to be equal to the difference between the DOC content of the $< 0.2 \mu\text{m}$ fraction and that of the $< 5 \text{ kDa}$ fraction for HA, and to the DOC content of the $< 5 \text{ kDa}$ fraction for FA. Fractions of elements complexed to humic substances samples are reported in Table 2. As for the ultrafiltrations experiments three distinct groups appear from the calculations: (i) Mg, Ca, Ni appear to be mainly present as "truly" dissolved species in the solution, $< 8 \%$ of elements are complexed to humic substances. (ii) Fe and Al are partly complexed to organic matter; between 16 and 81 % of these elements are bound to humic substances. Al is more strongly bound to humic substances than Fe does. (iii) According to calculations Cr, Cu, Eu, Dy and Th exhibit comparable speciation : $> 86 \%$ (except Cu for PF1 sample) of elements are complexed by humic substances.

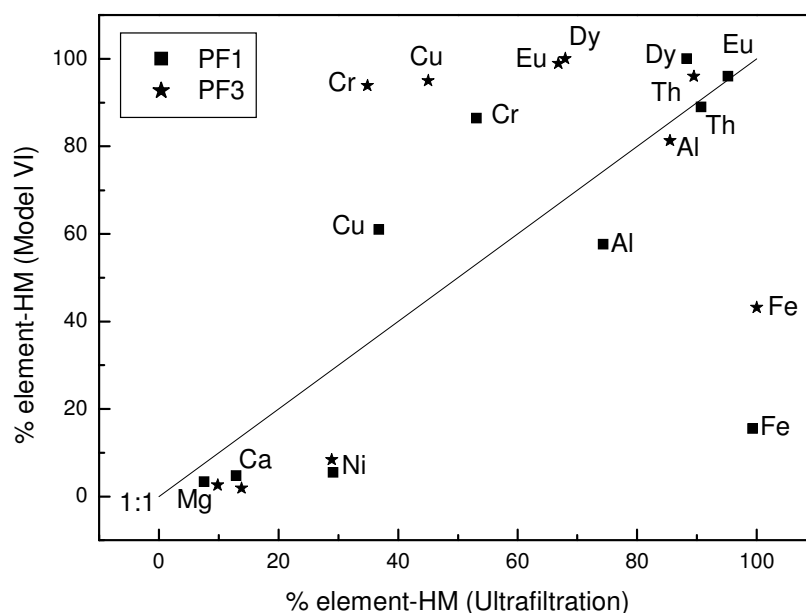


Fig. 8. Proportion of elements complexed with humic substances calculated (with Model VI) versus proportion of elements complexed with humic substances observed (by ultrafiltration).

	Mg	Al	Ca	Cr	Fe	Ni	Cu	Eu	Dy	Th
PF1	3	58	5	86	16	6	61	96	100	89
PF3	2	81	3	94	43	8	95	99	100	96

Table 2. Speciation calculations results: proportion of elements complexed with humic substances.

5. Confronting speciation calculations with ultrafiltration data

The need for the knowledge of "truly" dissolved and colloidal concentrations includes several points such as (i) an understanding of element geochemical cycles and partitioning, (ii) a better prediction of element fate in polluted environments, or (iii) the relevance to bioavailability issues. The comparison between results obtained by ultrafiltration and by speciation calculation leads to some comments. Three groups can be considered.

For Mg and Ca the results of speciation calculation are in good agreement with the ultrafiltration data. These elements behave as "free" ions in the dissolved pool in the form of inorganic species. Speciation calculations performed for Cr, Cu, Dy, Eu and Th give a higher proportion of elements bound to humic substances than those recovered from ultrafiltration data. By contrast, for Al, Fe and Ni speciation calculations give a slightly lower proportion of elements

bound to humic substances as compared to those obtained from ultrafiltration data. Even if there are slight differences between ultrafiltration and speciation calculations, trends are relatively similar for Al, Dy, Eu and Th. Major differences evidenced for Cr, Cu, Fe and Ni could be explain by the fact models need improvement as already stated for Cu and Ni (Unsworth, 2006).

Since the binding constants with humic substances are not available for the whole set of studied elements, the speciation calculations were performed for part of them. However, the calculations were achieved for one or several elements belonging to each of the three groups, allowing these elements to be considered as a "pilot study" for each group. In the following, the discussion will be focused on these "pilot study" elements considering that these latter are representative of the elements within the different groups.

5.1. "Truly" dissolved elements

Concentrations of alkalis and alkaline earth elements (major and trace ones) appear to be not significantly affected by ultrafiltrations suggesting that they are part of the dissolved pool. Since there is no clear relationship between DOC or Fe and these elemental concentrations, one can consider that these species do not occur as small-size organic or inorganic complexes in the dissolved pool. The speciation calculations performed during this study for alkalis and alkaline earth metals agree with ultrafiltration data. The occurrence of these metals in the dissolved pool was predictable since these elements belong to the class A ion group following the Nieboer and Richardson (1980) classification of elements. The so-called A group corresponds to metals with spherical symmetry and low polarizability. Aside from the metallic form, they always have a single oxidation state (+1) or (+2) for alkalis and alkaline earth elements, respectively (Ahrland et al., 1958; Nieboer and Richardson, 1980). This implies that they are not directly influenced by the redox status of the water and that they display the lowest stability complexes. Si, which also belongs to the type A group following Nieboer and Richardson classification, displays no significant variation of concentrations throughout the ultrafiltration procedure. This suggests that Si has also to be considered as a "truly" dissolved element. Although not part of the A class group, but part of the so-called "borderline" group (Nieboer and Richardson, 1980), Ni and Co behave also as "truly" dissolved ions as do alkalis and alkaline earth metals.

5.2. Complexed metals

It is now widely accepted that colloidal material plays a significant role in the transport and cycling of trace metals in waters. However, as often debated elsewhere (Lyven et al., 2003 and references therein) the key question is which is the true competition between Fe- and C-based colloidal carriers for trace metals?

5.2.1. *The inorganic colloidal pool as a metal carrier*

Fe, unlike DOC is strongly affected by the first ultrafiltration step (i.e. 30 kDa). Fe is present as large-size colloids and is almost completely removed from solution after this first step. Fe and DOC behave independently during the ultrafiltration. Al, like Fe, is strongly affected by the first ultrafiltration step. Fe oxyhydroxides are though much more soluble than Al ones do (Stumm and Morgan, 1996). PF1 sample displays a strong dominance of Fe over Al, with a Fe/Al molar ratio as high as 20. In PF3 sample the Fe/Al molar ratio is smaller with Fe and Al concentration being present in equal proportion. Moreover, Al concentration is well correlated with that of Fe and is only weakly dependent on DOC. This indicates a control of Al by inorganic mixed Fe/Al oxyhydroxides colloids. However, the major controlling parameter remains pH which governs solubility of Fe oxyhydroxides and therefore the release and trapping of associated trace metals.

Thorium follows closely aluminum, being mostly controlled by Fe/Al oxyhydroxides. Its concentration strongly decreases with the decrease of Al and Fe concentrations in the filtrate whereas it does not depend on DOC concentrations. Th is generally known to be immobile during weathering, accumulating in residual phases. However, his migration is possible in organic- and Fe/Al-rich waters (Pokrovsky and Schott, 2002). Mixed Fe/Al colloids are essentially responsible for these concentrations as already observed elsewhere (Pokrovsky and Schott, 2002; Geckeis et al., 2003). However, this result is different from those already published by Viers et al. (1997) where this element appears to be exclusively controlled by DOC. Even if adsorption of organic matter would result in a negative surface charge on the iron colloid surface, the negative surface charge density would be significantly less than that at purely humic colloids so that a significant difference in electrostatic binding would still be expected. Thus, Fe/Al oxyhydroxides remain the major complexing agent of Th and in this case Th is mostly controlled by Fe/Al oxyhydroxides colloids.

Model VI tends to underestimate the proportion of metal bound to humic substances as compared to ultrafiltration data (Fig. 8). It is important to note that the < 5 kDa fraction is considered as free species, which is not true as fulvic acids are characterized by lower molecular weight. Thus, if the fraction > 5 kDa is considered to be the humic bound fraction and as the correlation between DOC and Fe and Al shows no common behaviour, ultrafiltration experiments should be taken into account carefully. Such a direct use of ultrafiltration results led to an overestimation of elements bound to humic substances regards to Model VI calculations.

5.2.2. *The organic colloidal pool as a metal carrier*

REE and (+2) cations (V, Cr, Mn, Co, Cu) of the first transition series show strong correlation with DOC. These cations are all A-Type (Nieboer and Richardson, 1980), where electrostatic binding dominates over covalent one. It is therefore more expected for the smaller cations in each series to be associated with strongly negatively charged organic (humic) colloids than with iron colloids with small positive charge for circumneutral pH samples (Stumm and Morgan, 1996). Among the transition metals, the sequence of complex stability is known to be $Mn^{2+} < Co^{2+} < Ni^{2+} < Cu^{2+}$, a sequence known as the Irving-Williams Series. As expected Cu appears to be the most strongly bound to organic ligands as evidenced elsewhere (Buerge-Weirich et al., 2003). Xue and Sigg (1993) and Tipping et al. (2002) suggested that such strong binding has to be related to highly selective organic ligands, released by phytoplankton in order to control metal levels in their immediate environment. Pronounced differences are observed in this study as compared to what is expected for the other transition metals (Eyrolle et al., 1993) with for example Ni occurring in the "truly" dissolved pool. This may be caused by the fact that organic molecules can often be characterized by more than one functional group and hence can coordinate a metal at several positions (Stumm and Morgan, 1996). Moreover, data are consistent with dominance of organic matter complexation of REE (Johannesson et al., 2004), even if REE in the high-molecular weight fraction (i.e. > 30 kDa) of PF1 sample seem to be complexed with Fe oxyhydroxides. These results are also consistent with evaluation made on models calculations onto REE speciation (Pourret et al., 2006b).

In contrast, uranium may form oxocation UO^{2+} at equilibrium in oxic waters. This cation is known to have a very strong affinity for carbonate ions. While carbonate concentrations are very low in the circumneutral pH groundwaters, binding to carboxylate and/or phenolate groups, which represent major functional group in humic substances (Aiken et al., 1985), may contribute to the observed association of U with organic colloids.

Model VI tends to overestimate the proportion of metals (Cu, Cr and REE) bound to humic substances (Fig. 8). It is important to note that the < 5 kDa fraction is considered as free species, which is not true as fulvic acids are characterized by lower molecular weight. Thus, if all these elements (Cu, Cr and REE) are considered to be bound to organic ligands due to the good

correlation they formed with DOC, model calculation results are in good agreement for these elements.

5.3. Limitations of Model VI speciation calculations

Although the 5 kDa cut-off allow very small colloids to stay in solution, the lack of integration of adsorption processes onto inorganic species, as well as coprecipitation of inorganic species appear to be the major causes of disagreement between ultrafiltration data and speciation calculations for V and REE. It is then important to be aware that such model does not take into account any uptake of metals resulting from competitive reactions between Fe- and DOC-rich colloids. Moreover as stated by Unsworth et al. (2006) model predictions of free ions activities generally did not agree with measurement (e.g. for Cd, Cu, Ni and Zn), highlighting the need for further work and difficulties in obtaining appropriate data.

The studied samples are organic-rich groundwaters with an organic pool that seems to be in excess regards to the metals available for complexation: in such samples the speciation appears to be constrained only by organic species. But, what does happen when the samples are organic-poor? Oxides, hydroxides, clay minerals, and organic matter present in the natural system become all potential sites for adsorption. Scavenging between oxyhydroxides and organic matter will occur and form ternary surface complex (surface/ligand/metal). However, such a competition is still difficult to interpret from ultrafiltration data. As evidenced by previously experimental data and calculations, it appears that the competitive reactions and the formation of ternary surface complexes on oxyhydroxides represent the major interferences of the organic ligands on metal adsorption (Buerge-Weirich et al., 2003). Cation ligand complexes can adsorb onto solid to form ternary surface complexes either, as cation linked to the mineral surface over the ligand or as ligand linked to the surface over the cation. As an example, recently published experimental REE data (Davranche et al., 2004; 2005) show the impact of ternary surface complexes (humates/oxyhydroxides/REE) on metal speciation. Thus, it appears absolutely necessary to take into account in such speciation models, processes such as adsorption onto Mn and Fe oxyhydroxides, considering that the lack of such reaction precludes any true speciation to be assessed, the competition between Fe and C-based colloidal carriers being required for constraining element geochemical cycles or element fate in polluted environments.

6. Conclusions

An ultracentrifugation method that allows the study of DOM-trace metal distribution at different pore size cut-offs was tested on two shallow, circumneutral pH waters: one dissolved DOC- and Fe-rich and a second DOC-rich and Fe-poor. Data were analyzed using an ascendant hierarchical classification. Three groups of elements were identified regards to their affinity for DOM, which implies several consequences regards to their respective bioavailability or fate in the environment: (i) a "truly" dissolved behaviour group (Na, K, Rb, Ca, Mg, Ba, Sr, Si and Ni), (ii) an inorganic colloidal pool (Fe, Al and Th) and (iii) an organic colloidal pool (Cr, Mn, Co, Cu and U). However, REE and V have an ambivalent behaviour, being alternatively in the organic pool and in the inorganic pool depending on sample. Moreover, speciation calculation using Model VI were performed on both samples on some elements (Ca, Mg, Ni, Fe, Al, Th, Cr, Cu, Dy, Eu). Calculation shows relatively comparable elemental distribution with regards to ultrafiltration. Although some limitations appear: a direct use of ultrafiltration results tends to overestimate the fraction of elements bound to humic material in the inorganic pool as well as, a direct use of speciation calculation results tends to overestimate the fraction of elements bound to humic material in the organic pool with regards to ultrafiltration data. Both techniques, ultrafiltration and speciation calculation, give complementary information, especially for more complex samples where inorganic and organic colloids compete. The formation of water-soluble

complexes between humic materials and metal ions (radioactive, toxic or none) can increase the concentrations of these species in natural water to higher levels than expected from their thermodynamic solubilities. Since the retention, transport and fate of trace metals mediated by organic matter has still to be better constrained to understand the functional role played by DOM at the soil-water interface regards to trace metal dynamics, further studies dedicated to space- and time-linked variations of the joined colloidal pool and trace element partitioning has to be now undertaken in waters from different DOM-rich environments.

Bibliographie

- AFNOR. (1994) *Qualité des Sols*. AFNOR.
- Ahrland S., Chatt S.J., and Davies N.R. (1958) The relative affinities of ligand atoms for acceptor molecules and ions. *Q. Rev. Chem. Soc. London* **12**, 265-276.
- Aiken G.R., McKnight D.M., Wershaw R.L., and MacCarthy P. (1985) Humic substances in soil, sediment and water: Geochemistry, isolation and characterization. John Wiley and Sons, New York.
- Alibert C. and McCulloch M. T. (1993) Rare earth element and neodymium isotopic compositions of the banded iron-formations and associated shales from Hamersley, Western Australia. *Geochim. Cosmochim. Acta* **57**, 187-204.
- Andersson K., Dahlqvist R., Turner D., Stolpe B., Larsson T., Ingri J., and Andersson P. (2006) Colloidal rare earth elements in boreal river: Changing sources and distributions during the spring flood. *Geochim. Cosmochim. Acta in press*.
- Astrom A. (2001) Abundance and fractionation patterns of rare earth elements in streams affected by acid sulphate soils. *Chem. Geol.* **175**, 249-258.
- Aubert D., Stille P., and Probst A. (2001) REE fractionation during granite weathering and removal by waters and suspended loads: Sr and Nd isotopic evidence. *Geochim. Cosmochim. Acta* **65**, 387-406.
- Aubert D., Stille P., Probst A., Gauthier-Lafaye F., Pourcelot L., and Del Nero M. (2002) Characterization and migration of atmospheric REE in soils and surface waters. *Geochim. Cosmochim. Acta* **66**, 3339-3350.
- Avena M. J. and Koopal L. K. (1999) Kinetics of humic acid adsorption at solid-water interfaces. *Environ. Sci. Technol.* **33**, 2739-2744.
- Bau M. (1991) Rare-earth element mobility during hydrothermal and metamorphic fluid-rock interaction and the significance of the oxidation state of europium. *Chem. Geol.* **93**, 219-230.
- Bau M. (1996) Controls on the fractionation of isoivalent trace elements in magmatic and aqueous systems: evidence from Y/Ho, Zr/Hf, and lanthanide tetrad effect. *Contrib. Mineral. Petrol.* **123**, 323-333.
- Bau M. (1999) Scavenging of dissolved yttrium and rare earths by precipitating iron oxyhydroxide: Experimental evidence for Ce oxidation, Y-Ho fractionation, and lanthanide tetrad effect. *Geochim. Cosmochim. Acta* **63**, 67-77.
- Bau M. and Dulski P. (1996) Anthropogenic origin of positive gadolinium anomalies in river waters. *Earth Planet. Sci. Lett.* **143**, 245-255.
- Bau M., Koschinsky A., Dulski P., and Hein J. R. (1996) Comparison of the partitioning behaviours of yttrium, rare earth elements, and titanium between hydrogenetic marine ferromanganese crusts and seawater. *Geochim. Cosmochim. Acta* **60**, 1709-1725.
- Bau M., Möller P., and Dulski P. (1997) Yttrium and lanthanides in eastern Mediterranean seawater and their fractionation during redox-cycling. *Mar. Chem.* **56**, 123-131.
- Benedetti M.F., Van Riemsdijk W.H., Koopal L.K., Kinniburgh D.G., and Milne C.J. (1996) Metal ion binding to natural organic matter: from the model to the field. *Geochim. Cosmochim. Acta* **60**, 2503-2513.
- Bennett P. and Siegel D.I. (1987) Increased solubility of quartz in water due to complexing by organic compounds. *Nature* **326**, 684-686.
- Biddau R., Cidu R., and Frau F. (2002) Rare earth elements in waters from the albitite-bearing granodiorites of Central Sardinia, Italy. *Chem. Geol.* **182**, 1-14.
- Bidoglio G., Grenthe I., Qi P., Robouch P., and Omenetto N. (1991) Complexation of Eu and Tb with fulvic acids as studied by time-resolved laser induced fluorescence. *Talanta* **38**, 999-1008.
- Braun J. J., Viers J., Dupré B., Polvé M., Ndam J., and Muller J. P. (1998) Solid/liquid REE fractionation in the lateritic system of Goyoum, East Cameroon: the implication for the present dynamics of the soil covers of the humid tropical regions. *Geochim. Cosmochim. Acta* **62**, 273-299.
- Braun J.J., Ndam Ngoupayou J.R., Viers J., Dupré B., Bedimo Bedimo J.P., Boeglin J.L., Robain H., Nyeck B., Freyrier R., Sigha Nkamdjou L., Rouiller J., and Müller J.P. (2005) Present weathering rates in a humid tropical watershed: Nsimi, South Cameroon. *Geochim. Cosmochim. Acta* **69**, 357-387.
- Brownlow A. H. (1996) *Geochemistry*. Prentice Hall, Englewood Cliffs, NJ.
- Buerge-Weirich D., Behra P., and Sigg L. (2003) Adsorption of copper, nickel, and cadmium on goethite in the presence of organic ligands. *Aquat. Chem.* **9**, 65-85.
- Buffle J. (1988) *Complexation reactions in aquatic systems: an analytical approach*. Ellis Norwood, Chichester.
- Byrne R. H. and Kim K.-H. (1990) Rare earth element scavenging in seawater. *Geochim. Cosmochim. Acta* **54**, 2645-2656.
- Byrne R. H. and Li B. (1995) Comparative complexation behavior of the rare earths. *Geochim. Cosmochim. Acta* **59**, 4575-4589.
- Byrne R. H. and Sholkovitz E. R. (1996) Marine chemistry and geochemistry of the lanthanides. In *Handbook on the Physics and Chemistry of Rare Earths*, Vol. 23 (ed. K.A. Gschneidner Jr. and L.R. Eyring), pp. 497-593. Elsevier Sciences B.V.
- Cabaniss S.E. and Schumann M. (1988) Copper binding by dissolved organic matter. I; Suwannee river fulvic acid equilibria. *Geochim. Cosmochim. Acta* **52**, 185-193.
- Cantrell K. J. and Byrne R. H. (1987) Rare earth element complexation by carbonate and oxalate ions. *Geochim. Cosmochim. Acta* **51**, 597-605.

- Christensen J.B., Jensen D.L., and Christensen T.H. (1996) Effect of dissolved organic carbon on the mobility of cadmium, nickel, and zinc in leachate polluted groundwater. *Wat. Res.* **30**, 3067-3049.
- Coppin F., Berger G., Bauer A., Castet S., and Loubet M. (2002) Sorption of lanthanides on smectite and kaolinite. *Chem. Geol.* **182**, 57-68.
- Cory N. and Andr en C. (2004) Modelling of aluminium speciation as a complement to laboratory-based analysis, pp. 1-14. Sveriges Lantbruksuniversitet.
- Crawford M. B. (1996) PHREEQEV: the incorporation of a version of Model V for organic complexation in aqueous solutions into the speciation code PHREEQE. *Comput. Geosci.* **22**, 109-116.
- Curmi P., Durand P., Gascuel-Oudou C., Hallaire V., M erot P., Robin P., Trolard F., Walter C., and Bourri  G. (1995) Le programme CORMORAN-INRA: de l'importance du milieu physique dans la r gulation biog ochimique de la teneur en nitrate des eaux superficielles. *J. Europ. Hydrol.* **26**, 37-56.
- Dabard M.P., Loi A., and Peucat J.J. (1996) Zircon typology combined with Sm-Nd whole rock isotope analysis to study Brioverian sediments from the Armorican Massif. *Sedim. Geol.* **101**, 243-260.
- Dahlqvist R., Benedetti M.F., Andersson K., Turner D., Larsson T., Stolpe B., and Ingri J. (2004) Association of calcium with colloidal particles and speciation of calcium in the Kalix and amazon rivers. *Geochim. Cosmochim. Acta* **68**, 4059-4075.
- Davis J. A. and Kent D. B. (1990) Surface complexation modeling in aqueous geochemistry. In *Mineral-Water Interface Geochemistry*, Vol. 23 (ed. M. F. Hochella and A. F. White), pp. 177-260. Mineralogical Society of America.
- Davranche M., Lacour S., Bordas F., and Bollinger J.-C. (2003) An easy determination of the surface chemical properties of simple and natural solids. *J. Chem. Educ.* **80**, 76-78.
- Davranche M., Pourret O., Gruau G., and Dia A. (2004) Impact of humate complexation on the adsorption of REE onto Fe oxyhydroxide. *J. Colloid Interface Sci.* **277**, 271-279.
- Davranche M., Pourret O., Gruau G., Dia A., and Le Coz-Bouhnik M. (2005) Adsorption of REE(III)-humate complexes onto MnO₂: Experimental evidence for cerium anomaly and lanthanide tetrad effect suppression. *Geochim. Cosmochim. Acta* **69**, 4825-4835.
- De Baar H. J. W., Bacon M. P., and Brewer P. G. (1983) Rare-earth distributions with a positive Ce anomaly in the Western North Atlantic Ocean. *Nature* **301**, 324-327.
- De Baar H. J. W., Bacon M. P., Brewer P. G., and Bruland K. W. (1985) Rare earth elements in the Pacific and Atlantic Oceans. *Geochim. Cosmochim. Acta* **49**, 1943-1959.
- De Baar H. J. W., German C. R., Elderfield H., and van Gaans P. (1988) Rare earth element distributions in anoxic waters of the Cariaco Trench. *Geochim. Cosmochim. Acta* **52**, 1203-1219.
- De Baar H. J. W., Schijf J., and Byrne R. H. (1991) Solution chemistry of the rare earth elements in seawater. *Eur. J. Solid State Inorg. Chem.* **28**, 357-373.
- De Carlo E. H. and Green W. J. (2002) Rare earth elements in the water column of Lake Vanda, McMurdo Dry Valleys, Antarctica. *Geochim. Cosmochim. Acta* **66**, 1323-1333.
- De Carlo E. H. and McMurtry G. M. (1992) Rare-earth element geochemistry of ferromanganese crusts from the Hawaiian Archipelago, central Pacific. *Chem. Geol.* **95**, 235-250.
- De Carlo E. H., Wen X. Y., and Coven J. P. (2000) Rare earth element fractionation in hydrogenetic Fe-Mn crusts: The influence of carbonate complexation and phosphatization on Sm/Yb ratios. In *Marine Authigenesis: From Global to Microbial*, Vol. SEPM Special No. 64 (ed. C.R. Glenn, L. Prevot-Lucas, and J. Lucas), pp. 271-285.
- De Carlo E. H., Wen X.-Y., and Irving M. (1998) The influence of redox reactions on the uptake of dissolved Ce by suspended Fe and Mn oxide particles. *Aquat. Geochem.* **3**, 357-389.
- Deberdt S., Viers J., and Dupr  B. (2002) New insights about the rare earth elements (REE) mobility in river waters. *Bull. Soc. Geol. Fr.* **173**, 147-160.
- Dia A., Gruau G., Olivi -Lauquet G., Riou C., Mol nat J., and Curmi P. (2000) The distribution of rare earth elements in groundwaters: assessing the role of source-rock composition, redox changes and colloidal particle. *Geochim. Cosmochim. Acta* **64**, 4131-4151.
- Dierckx A., Maes A., and Vancluysen J. (1994) Mixed complex formation of Eu³⁺ with humic acid and a competing ligand. *Radiochim. Acta* **66/67**, 149-156.
- Dillon W.R. and Goldstein M. (1984) Multivariate analysis: Methods and applications. Wiley, New-York.
- Dolezal J. and Novak J. (1959) Beitrag zum polarographischen Verhalten von drei- und vierwertigem Cer. *Collect. Czech. Chem. Commun.* **24**, 2182-2189.
- Douglas G. B., Hart B. T., Beckett R., Gray C. M., and Oliver R. L. (1999) Geochemistry of suspended particulate matter (SPM) in the Murray-Darling River system: a conceptual isotopic/geochemical model for the fractionation of major, trace and rare earth elements. *Aquat. Geochem.* **5**, 167-194.
- Duncan T. and Shaw T. J. (2004) The mobility of rare earth elements and redox sensitive elements in the groundwater/seawater mixing zone of a shallow coastal aquifer. *Aquat. Geochem.* **9**, 223-255.
- Dupr  B., Gaillardet J., Rousseau D., and All gre C. J. (1996) Major and trace elements of river-borne material: The Congo Basin. *Geochim. Cosmochim. Acta* **60**, 1301-1321.

- Dupré B., Viers J., Dandurand J.-L., Polvé M., Bénézeth P., Vervier P., and Braun J.-J. (1999) Major and trace elements associated with colloids in organic-rich river waters: ultrafiltration of natural and spiked solutions. *Chem. Geol.* **160**, 63-80.
- Durand P. and Juan Torres J.L. (1996) Solute transfer in agricultural catchments: the interest and limits of mixing models. *J. Hydrol.* **181**, 1-22.
- Dzombak D. A. and Morel F. M. M. (1990) *Surface complexation modeling-Hydrous ferric oxide*. Wiley Intersciences.
- Elbaz-Poulichet F. and Dupuy C. (1999) Behaviour of rare earth elements at the freshwater-seawater interface of two acid mine rivers: the Tinto and Odiel (Andalucia, Spain). *Appl. Geochem.* **14**, 1063-1072.
- Elderfield H. (1988) The oceanic chemistry of the rare earth elements in seawater. *Phil. Trans. R. Soc. Lond. A* **325**, 105-126.
- Elderfield H. and Greaves M. J. (1982) The rare earth elements in seawater. *Nature* **296**, 214-219.
- Elderfield H., Hawkesworth C. J., Greaves M. J., and Calvert S. E. (1981) Rare earth element geochemistry of oceanic ferromanganese nodules and associated sediments. *Geochim. Cosmochim. Acta* **45**, 513-528.
- Elderfield H., Upstill-Goddard R., and Sholkovitz E. R. (1990) The rare earth elements in rivers, estuaries, and coastal seas and their significance to the composition of ocean waters. *Geochim. Cosmochim. Acta* **54**, 971-991.
- Eyrolle F., Benedetti M.F., Benaim J.Y., and Février D. (1996) The distributions of colloidal and dissolved organic carbon, major elements, and trace elements in small tropical catchments. *Geochim. Cosmochim. Acta* **60**, 3643-3656.
- Fairhurst A. J., Warwick P., and Richardson S. (1995) The influence of humic acid on the adsorption of europium onto inorganic colloids as a function of pH. *Colloids Surf. A* **99**, 187-199.
- Fee J. A., Gaudette H. E., Lyons W. B., and Long D. T. (1992) Rare-earth element distribution in Lake Tyrrell groundwaters, Victoria, Australia. *Chem. Geol.* **96**, 67-93.
- Franz C., Herrmann G., and Trautmann N. (1997) Complexation of Samarium(III) and Americium(III) with humic acid at very low metal concentrations. *Radiochim. Acta* **77**, 177-181.
- Gaillardet J., Dupré B., Allègre C. J., and Négrel P. (1997) Chemical and physical denudation in the Amazon River Basin. *Chem. Geol.* **142**, 141-173.
- Gaillardet J., Viers J., and Dupré B. (2004) Elements in River Waters. In *Treatise on Geochemistry*, Vol. 5 (ed. E. D. Holland, Turekian, K.K.), pp. 225-263. Elsevier-Pergamon.
- Gallet S., Jahn B.-M., and Torii M. (1996) Geochemical characterization of the Luochuan loess-paleosol sequence, China, and paleoclimatic implications. *Chem. Geol.* **133**, 67-88.
- Gammons C. H., Wood S. A., Ponas J. P., and Madison J. P. (2003) Geochemistry of the rare-earth elements and uranium in the acidic Berkeley Pit Lake, Butte, Montana. *Chem. Geol.* **198**, 269-288.
- Geckeis H., Ngo Mahn Th., Bouby M., and Kim J.I. (2003) Aquatic colloids relevant to radionuclide migration/characterization by size fractionation and ICP-mass spectrometric detection. *Colloids and Surface A: Physicochem. Eng. Aspects* **00**, 1-8.
- Gerard M., Seyler P., Benedetti M. F., Alves V. P., Boaventura G. R., and Sondag F. (2003) Rare earth elements in the Amazon basin. *Hydrol. Proc.* **17**, 1379-1392.
- German C. R. and Elderfield H. (1990) Application of the Ce anomaly as a paleoredox indicator: the ground rules. *Paleoceanography* **5**(5), 823-833.
- German C. R., Holiday B. P., and Elderfield H. (1991) Redox cycling of rare earth elements in the suboxic zone of the Black Sea. *Geochim. Cosmochim. Acta* **55**, 3553-3558.
- German C. R., Masuzawa T., Greaves M. J., Elderfield H., and Edmond J. M. (1995) Dissolved rare earth elements in the Southern Ocean: Cerium oxidation and the influence of hydrography. *Geochim. Cosmochim. Acta* **59**, 1551-1558.
- Glaus M. A., Hummel W., and Van Loon L. R. (1995) Stability of mixed-ligand complexes of metal ions with humic substances and low molecular weight ligands. *Environ. Sci. Technol.* **29**, 2150-2153.
- Glaus M. A., Hummel W., and Van Loon L. R. (2000) Trace metal-humate interactions. I. Experimental determination of conditional stability constants. *Appl. Geochem.* **15**, 953-973.
- Goldberg E. D., Koide M., Schmitt R. A., and Smith R. H. (1963) Rare earth distribution in the marine environment. *J. Geophys. Res.* **68**, 4209-4217.
- Goldstein S. J. and Jacobsen S. B. (1988) Rare earth elements in river waters. *Earth Planet. Sci. Lett.* **89**, 35-47.
- Gosselin D. C., Smith M. R., Lepel E. A., and Laul J. C. (1992) Rare earth elements in chloride-rich groundwater, Palo Duro Basin, Texas, USA. *Geochim. Cosmochim. Acta* **56**, 1495-1505.
- Gruau G., Dia A., Olivie-Lauquet G., Davranche M., and Pinay G. (2004) Controls on the distribution of rare earth elements in shallow groundwaters. *Wat. Res.* **38**, 3576-3586.
- Gustafsson J. P. (2001a) Modeling the acid-base properties and metal complexation of humic substances with the Stockholm Humic Model. *J. Colloid Interface Sci.* **244**, 102-112.
- Gustafsson J. P. (2001b) <http://www.lwr.kth.se/english/OurSoftware/vminteq/index.htm>.

- Gustafsson J. P. and van Schaik J. W. J. (2003) Cation binding in a mor layer: batch experiments and modelling. *Eur. J. Soil Sci.* **54**, 295-310.
- Gustafsson J. P., Pechova P., and Berggren D. (2003) Modeling metal binding to soils: the role of natural organic matter. *Environ. Sci. Technol.* **37**, 2767-2774.
- Hannigan R. E. and Sholkovitz E. (2001) The development of middle rare earth element enrichments in freshwaters: weathering of phosphate minerals. *Chem. Geol.* **175**, 495-508.
- Haskin L. A., Haskin M. A., Frey F. A., and Wilderman T. R. (1968) Relative and absolute terrestrial abundances of the rare earths. In *Origin and distributions of the elements*, Vol. 30 (ed. A. L.H.), pp. 889-912.
- Henderson P. (1984) *Rare earth element geochemistry*. Elsevier.
- Herbelin A. L. and Westall J. C. (1999) FITEQL A computer program for determination of chemical equilibrium constants from experimental data. Department of Chemistry - Oregon State University.
- Holser W. T. (1997) Evaluation of the application of rare-earth elements to paleoceanography. *Paleogeol. Paleoclim. Paleocol.* **132**, 309-323.
- Hoyle J., Elderfield H., Gledhill A., and Greaves M. (1984) The behaviour of rare earth elements during mixing of river and sea waters. *Geochim. Cosmochim. Acta* **48**, 143-149.
- Iler R.K. (1979) The geochemistry of colloid systems for earth scientists. By S. Yariv & H. Cross. Springer-Verlag, Berlin, Heidelberg and New York. 1979 Book review. *J. Colloid. Interf. Sci.* **72**, 177-178.
- Ingri J., Widerlund A., Land M., Gustafsson O., Andersson P., and Ohlander B. (2000) Temporal variations in the fractionation of the rare earth elements in a boreal river; the role of colloidal particles. *Chem. Geol.* **166**, 23-45.
- Jaffrézic A. (1997) Géochimie des éléments métalliques, des nitrates et du carbone organique dissous dans les eaux et les sols hydromorphes. Agriculture intensive et qualité des eaux dans les zones humides en Bretagne. Ph.D. dissertation, University Rennes I (France).
- Jahn B.-M., Gallet S., and Han J. (2001) Geochemistry of the Xining, Xifeng and Jixian sections, Loess Plateau of China: eolian dust provenance and paleosol evolution during the last 140 ka. *Chem. Geol.* **178**, 71-94.
- Janssen R. P. T. and Verweij W. (2003) Geochemistry of some rare earth elements in groundwater, Vierlingsbeek, The Netherlands. *Wat. Res.* **37**, 1320-1350.
- Johannesson K. H. and Lyons W. B. (1994) The rare earth element geochemistry of Mono Lake water and the importance of carbonate complexing. *Limn. Oceanogr.* **39**, 1141-1154.
- Johannesson K. H. and Lyons W. B. (1995) Rare-earth element geochemistry of Colour Lake, an acidic freshwater lake on Axel Heiberg Island, Northwest Territories, Canada. *Chem. Geol.* **119**, 209-223.
- Johannesson K. H. and Zhou X. (1999) Origin of middle rare earth element enrichments in acid waters of a Canadian High Arctic lake. *Geochim. Cosmochim. Acta* **63**, 153-165.
- Johannesson K. H. and Hendry M. J. (2000) Rare earth element geochemistry of groundwaters from a thick till and clay-rich aquitard sequence, Saskatchewan, Canada. *Geochim. Cosmochim. Acta* **64**, 1493-1509.
- Johannesson K. H., Stetzenbach K. J., and Hodge V. F. (1995) Speciation of the rare earth element neodymium in groundwaters of the Nevada Test Site and Yucca Mountain and implications for actinide solubility. *Appl. Geochem.* **10**, 565-572.
- Johannesson K. H., Lyons W. B., Yelken M. A., Gaudette H. E., and Stetzenbach K. J. (1996a) Geochemistry of the rare earth elements in hypersaline and dilute acidic natural terrestrial waters: complexation behavior and middle rare-earth element enrichments. *Chem. Geol.* **133**, 125-144.
- Johannesson K. H., Stetzenbach K. J., Hodge V. F., and Lyons W. B. (1996b) Rare earth element complexation behavior in circumneutral pH groundwaters: Assessing the role of carbonate and phosphate ions. *Earth Planet. Sci. Lett.* **139**, 305-319.
- Johannesson K. H., Stetzenbach K. J., and Hodge V. F. (1997) Rare earth elements as geochemical tracers of regional groundwater mixing. *Geochim. Cosmochim. Acta* **61**, 3605-3618.
- Johannesson K. H., Farnham I. M., Guo C., and Stetzenbach K. J. (1999) Rare earth element fractionation and concentration variations along a groundwater flow path within a shallow, basin-fill aquifer, southern Nevada, USA. *Geochim. Cosmochim. Acta* **63**, 2697-2708.
- Johannesson K. H., Zhou X., Guo C., Stetzenbach K. J., and Hodge V. F. (2000) Origin of rare earth element signatures in groundwaters of circumneutral pH from southern Nevada and eastern California, USA. *Chem. Geol.* **164**, 239-257.
- Johannesson K. H., Tang J., Daniels J. M., Bounds W. J., and Burdige D. J. (2004) Rare earth element concentrations and speciation in organic-rich blackwaters of the Great Dismal Swamp, Virginia, USA. *Chem. Geol.* **209**, 271-294.
- Kawabe I., Ohta A., and Miura N. (1999) Distribution coefficients of REE between Fe oxyhydroxide precipitates and NaCl solutions affected by REE-carbonate complexation. *Geochem. J.* **33**, 181-197.
- Klungness G. D. and Byrne R. H. (2000) Comparative hydrolysis behavior of the rare earths and yttrium: the influence of temperature and ionic strength. *Polyhedron* **19**, 99-107.
- Koeppenkastrop D. and De Carlo E. H. (1992) Sorption of rare-earth elements from seawater onto synthetic mineral particles: An experimental approach. *Chem. Geol.* **95**, 251-263.

- Koeppenkastrop D. and De Carlo E. H. (1993) Uptake of rare earth elements from solution by metal oxides. *Environ. Sci. Technol.* **27**, 1796-1802.
- Koeppenkastrop D., De Carlo E. H., and Roth M. (1991) A method to investigate the interaction of rare earth elements in aqueous solution with metal oxides. *J. Radioanal. Nucl. Chem.* **152**, 337-346.
- Kuss J., Garbe-Schönberg C.-D., and Kremling K. (2001) Rare earth elements in suspended particulate material of North Atlantic surface waters. *Geochim. Cosmochim. Acta* **65**, 187-199.
- Langmuir D. (1997) *Aqueous Environmental Geochemistry*. Prentice Hall.
- Lawrence M. G. and Kamber B. S. (2006) The behaviour of the rare earth elements during estuarine mixing - revisited. *Mar. Chem.* **100**, 147-161.
- Lead J. R., Hamilton-Taylor J., Peters A., Reiner S., and Tipping E. (1998) Europium binding by fulvic acids. *Anal. Chim. Acta* **369**, 171-180.
- Lee J. H. and Byrne R. H. (1992) Examination of comparative rare earth element complexation behavior using linear free-energy relationships. *Geochim. Cosmochim. Acta* **56**, 1127-1137.
- Lee J. H. and Byrne R. H. (1993) Complexation of trivalent rare earth elements (Ce, Eu, Gd, Tb, Yb) by carbonate ions. *Geochim. Cosmochim. Acta* **57**, 295-302.
- Leybourne M. I., Goodfellow W. D., Boyle D. R., and Hall G. M. (2000) Rapid development of negative Ce anomalies in surface waters and contrasting REE patterns in groundwaters associated with Zn-Pb massive sulphide deposits. *Appl. Geochem.* **15**, 695-723.
- Lippold H., Müller N., and Kupsch H. (2005) Effect of humic acid on the pH-dependent adsorption of terbium(III) onto geological materials. *Appl. Geochem.* **20**, 1209-1217.
- Liu X. and Byrne R. H. (1998) Comprehensive investigation of yttrium and rare earth element complexation by carbonate using ICP-Mass Spectrometry. *J. Solution Chem.* **9**, 803-815.
- Lofts S. and Tipping E. (1999) Modelling the solid-solution partitioning of metals in environmental systems. *Environ. Geochem. Health* **21**, 299-304.
- Luo Y.-R. and Byrne R. H. (2004) Carbonate complexation of yttrium and the rare earth elements in natural rivers. *Geochim. Cosmochim. Acta* **68**, 691-699.
- Lyven B., Hassellöv M., Turner D.R., Haraldsson C., and Andersson K. (2003) Competition between iron- and carbon-based colloidal carriers for trace metals in a freshwater assessed using flow field-flow fractionation coupled to ICP-MS. *Geochim. Cosmochim. Acta* **67**, 3791-3802.
- Macalady D.L. (1998) *Perspectives in environmental chemistry*. Oxford University Press.
- MacLeod K. G. and Irving A. J. (1996) Correlation of cerium anomalies with indicators of paleoenvironment. *J. Sedim. Res.* **66**, 948-955.
- Maes A., De Brabandere J., and Cremers A. (1988) A modified Schubert method for the measurement of the stability of europium humic acid complexes in alkaline conditions. *Radiochim. Acta* **44/45**, 51-57.
- Martell A. E. and Smith R. M. (1998) *NIST Critical Selected Stability Constants of Metal Complexes Database*.
- Martin J.-M., Hogdahl O., and Philippot J. C. (1976) Rare earth element supply to the ocean. *J. Geophys. Res.* **81**, 3119-3124.
- McCarty J.F., Sanford W.E., and Stafford P.L. (1998) Lanthanide field tracers demonstrate enhanced transport of transuranic radionuclides by natural organic matter. *Environ. Sci. Technol.* **32**, 3901-3906.
- McLennan S. M. (1989) Rare earth element geochemistry in sedimentary rocks: influence of provenance and sedimentary processes. In *Geochemistry and mineralogy of rare earth elements*, Vol. 21 (ed. Lipin B.R. and Mc Kay G.A.), pp. 169-200.
- McLennan S. M. (1994) Rare earth element geochemistry and the "tetrad" effect. *Geochim. Cosmochim. Acta* **58**, 2025-2033.
- Millero F. J. (1992) Stability constants for the formation of rare earth inorganic complexes as a function of ionic strength. *Geochim. Cosmochim. Acta* **56**, 3123-3132.
- Milne C. J., Kinniburgh D. G., and Tipping E. (2001) Generic NICA-Donnan Model parameters for proton binding by humic substances. *Environ. Sci. Technol.* **35**, 2049-2059.
- Milne C. J., Kinniburgh D. G., Van Riemsdijk W. H., and Tipping E. (2003) Generic NICA-Donnan Model parameters for metal-ion binding by humic substances. *Environ. Sci. Technol.* **37**, 958-971.
- Moffett J. W. (1990) Microbially mediated cerium oxidation in sea water. *Nature* **345**, 421-423.
- Moffett J. W. (1994) A radiotracer study of cerium and manganese uptake onto suspended particle in Chesapeake Bay. *Geochim. Cosmochim. Acta* **58**, 695-703.
- Molénat J., Durand P., Gascuel-Oudoux C., Davy P., and Gruau G. (2002) Mechanisms of nitrate transfer from soil to stream in an agricultural watershed of French Brittany. *Water, Air and Soil Pollution* **133**, 161-183.
- Möller P. and Bau M. (1993) Rare-earth patterns with positive cerium anomaly in alkaline waters from Lake Van, Turkey. *Earth Planet. Sci. Lett.* **117**, 671-676.
- Möller P., Paces T., Dulski P., and Morteani G. (2002) Anthropogenic Gd in surface water, drainage system, and the water supply of the city of Prague, Czech Republic. *Environ. Sci. Technol.* **36**, 2387-2394.
- Morad S. and Felitsyn S. (2001) Identification of primary Ce-anomaly signatures in fossil biogenic apatite: implication for the Cambrian oceanic anoxia and phosphogenesis. *Sed. Geol.* **143**, 259-269.

- Moulin C., Wei J., Van Iseghem P., Laszak I., Plancque G., and Moulin V. (1999) Europium complexes investigations in natural waters by time-resolved laser-induced fluorescence. *Anal. Chim. Acta* **396**, 253-261.
- Moulin V., Tits J., Moulin C., Decambox P., Mauchien P., and de Ruty O. (1992) Complexation behaviour of humic substances towards actinides and lanthanides studied by Time-Resolved Laser-Induced Spectrofluometry. *Radiochim. Acta* **58/59**, 121-128.
- Nelson B. J., Wood S. A., and Osiensky J. L. (2004) Rare earth element geochemistry of groundwater in the Palouse Basin, northern Idaho-eastern Washington. *Geochem. Explor. Environ. Anal.* **4**, 227-241.
- Nieboer E. and Richardson D.H.S. (1980) The replacement of the nondescript term "heavy metals" by a biologically and chemically significant classification of metal ions. *Environ. Pollut. Ser.B* **1**, 3-26.
- Nowack B. and Sigg L. (1996) Adsorption of EDTA and metal-EDTA complexes onto goethite. *J. Colloid Interface Sci.* **177**, 106-121.
- Ohta A., Ishii S., Sakakibara M., Mizuno A., and Kawabe I. (1999) Systematic correlation of the Ce anomaly with Co/(Ni+Cu) ratio and Y fractionation from Ho in distinct types of Pacific deep-sea nodules. *Geochem. J.* **33**, 399-417.
- Ohta A. and Kawabe I. (2000) Rare earth element partitioning between Fe oxyhydroxide precipitates and aqueous NaCl solutions doped with NaHCO₃: Determinations of rare earth element complexation constants with carbonate ions. *Geochem. J.* **34**, 439-454.
- Ohta A. and Kawabe I. (2001) REE(III) adsorption onto Mn dioxide and Fe oxyhydroxide: Ce(III) oxidation by Mn dioxide. *Geochim. Cosmochim. Acta* **65**, 695-703.
- Olivié-Lauquet G., Gruau G., Dia A., Riou C., Jaffrezic A., and Henin O. (2001) Release of trace elements in wetlands: role of seasonal variability. *Wat. Res.* **35**, 943-952.
- Parkhurst D. L. and Appelo C. A. J. (1999) User's guide to PHREEQC (Version 2) - A computer program for speciation, batch-reaction, one-dimensional transport, and inverse geochemical calculations, pp. 309. U.S. Geological Survey Water-Resources Investigations Report.
- Pauwels H., Kloppmann W., Foucher J. C., Martelat A., and Fritsche V. (1998) Field tracer test for denitrification in a pyrite-bearing schist aquifer. *Applied Geochem.* **13**, 767-778.
- Pellerin J. and Van Vliet-Lanoë B. (1994) Cadre géomorphologique du bassin du Coët-Dan et du Haut Evel (Morbihan): Rapport sur les travaux de cartographie et de stratigraphie. Unpublished Ph-D Thesis. Brest University, France.
- Peppard D. F., Mason G. W., and Lewey S. (1969) A tetrad effect in the liquid-liquid extraction ordering of lanthanide(III). *J. Inorg. Nucl. Chem.* **31**, 2271-2272.
- Picard S., Lécuyer C., Barrat J.-A., Garcia J.-P., Dromart G., and Sheppard S. M. F. (2002) Rare earth element contents of Jurassic fish and reptile teeth and their potential relation to seawater composition (Anglo-Paris Basin, France and England). *Chem. Geol.* **186**, 1-16.
- Piper D. Z. (1974) Rare earth elements in ferromanganese nodules and other marine phases. *Geochim. Cosmochim. Acta* **38**, 1007-1022.
- Pokrovski G.S. and Schott, J. (1998) Experimental study of the complexation of silicon and germanium with aqueous organic species: implications for germanium and silicon transport and Ge/Si ratio in natural waters. *Geochim. Cosmochim. Acta* **62**, 3413-3428.
- Pokrovsky O.S and Schott J. (2002) Iron colloids/organic matter associated transport of major and trace elements in small boreal rivers and their estuaries (NW Russia). *Chem. Geol.* **190**, 141-179.
- Pourret O., Dia A., Davranche M., Gruau G., Hénin O., and Angée M. (2006a) Organo-colloidal control on major- and trace-element partitioning in shallow groundwaters: confronting ultrafiltration and modelling. *Appl. Geochem.* **In press**.
- Pourret O., Davranche M., Gruau G., and Dia A. (2006b) Organic complexation of rare earth elements in natural waters: Evaluating model calculations from ultrafiltration data. *Geochim. Cosmochim. Acta* **In review**.
- Pourret O., Davranche M., Gruau G., and Dia A. (2006c) Rare Earth Elements complexation with humic acid. *Chem. Geol.* **In review**.
- Pourret O., Davranche M., Gruau G., and Dia A. (2006d) Competition between humic acid and carbonates for rare earth elements complexation. *J. Colloid Interface Sci.* **In press**.
- Quinn K. A., Byrne R. H., and Schif J. (2004) Comparative scavenging of yttrium and the rare earth elements in seawater: competitive influences of solution and surface chemistry. *Aquat. Geochem.* **10**, 59-80.
- Ramsey J. B. (1969) Tests for specification errors in classical linear least-squares regression analysis. *Journal of the Royal Statistical Society, Series B* **XXXI**(Part 2), 350.
- Rankin P. C. and Childs C. W. (1976) Rare-earth elements in iron-manganese concretions from some New Zealand soils. *Chem. Geol.* **18**, 55-64.
- Shapiro J. (1964) Effect of yellow organic acids on iron and other metals in water. *Am. Water Works Assoc. J.* **55**, 1062-1082.

- Schijf J. and Byrne R. H. (2004) Determination of $\text{SO}_4\beta_1$ for yttrium and the rare earth elements at $I = 0.66$ m and $t = 25$ °C- Implications for YREE solution speciation in sulfate-rich waters. *Geochim. Cosmochim. Acta* **68**, 2825-2837.
- Schijf J., De Baar H. J. W., and Millero F. J. (1994) Kinetics of Ce and Nd scavenging in Black Sea waters. *Mar. Chem.* **46**, 345-359.
- Schindler P. W. (1990) Co-adsorption of metal ions and organic ligands: formation of ternary surface complexes. In *Mineral-Water Interface Geochemistry*, Vol. 23 (ed. M. F. Hochella and A. F. White), pp. 281-307. Mineralogical Society of America.
- Schmitt D., Saravia F., Frimmel F.H., and Schuessler W. (2003) NOM-facilitated transport of metal ions in aquifers: importance of complex-dissociation kinetics and colloid formation. *Wat. Res.* **37**, 3541-3550.
- Schwertmann U. and Cornell R. M. (1996) *Iron Oxides in the Laboratory, Preparation and Characterization*. VCH Verlag.
- Shacat J. A., Green W. J., De Carlo E. H., and Newell S. (2004) The geochemistry of Lake Joyce, McMurdo Dry Valleys, Antarctica. *Aquat. Geochem.* **10**, 325-352.
- Shiller A. M. (2002) Seasonality of dissolved rare earth elements in the Lower Mississippi River. *Geochem. Geophys. Geosyst.* **3**, 1068.
- Shimizu H., Umemoto N., Masuda A., and Appel P. W. U. (1990) Sources of iron-formations in the archeinusia and malene supracrustals, West Greenland: Evidence from La-Ce and Sm-Nd isotopic data and REE abundances. *Geochim. Cosmochim. Acta* **54**, 1147-1154.
- Sholkovitz E. R. (1993) The geochemistry of rare earth elements in the Amazon River estuary. *Geochim. Cosmochim. Acta* **57**, 2181-2190.
- Sholkovitz E. R. (1995) The aquatic chemistry of rare earth elements in rivers and estuaries. *Aquat. Geochem.* **1**, 1-34.
- Sigg L., Xue H., Kistler D., and Schönenberger R. (2000) Size fractionation (dissolved, colloidal and particulate) of trace metals in Thur river, Switzerland. *Aquat. Geochem.* **6**, 413-434.
- Smedley P. L. (1991) The geochemistry of rare earth elements in groundwater from the Cammenellis area, southwest England. *Geochim. Cosmochim. Acta* **55**, 2767-2779.
- Sonke J. E. and Salters V. J. M. (2006) Lanthanide-humic substances complexation. I. Experimental evidence for a lanthanide contraction effect. *Geochim. Cosmochim. Acta* **70**, 1495-1506.
- Stumm W. and Morgan J. J. (1996) *Aquatic Chemistry*. Wiley Intersciences.
- Sverjensky D. A. (1984) Europium redox equilibria in aqueous solution. *Earth Planet. Sci. Lett.* **67**, 70-78.
- Takahashi Y., Minai Y., Ambe S., Makide Y., Ambe F., and Tominaga T. (1997) Simultaneous determination of stability constants of humate complexes with various metal ions using multitracer technique. *Sci. Tot. Environ.* **198**, 61-71.
- Takahashi Y., Minai Y., Ambe S., Makide Y., and Ambe F. (1999) Comparison of adsorption behavior of multiple inorganic ions on kaolinite and silica in the presence of humic acid using the multitracer technique. *Geochim. Cosmochim. Acta* **63**, 815-836.
- Takahashi Y., Kimura T., and Minai Y. (2002) Direct observation of Cm(III)-fulvate species on fulvic acid-montmorillonite hybrid by laser-induced fluorescence spectroscopy. *Geochim. Cosmochim. Acta* **66**, 1-12.
- Takahashi Y., Châtellier X., Hattori K. H., Kato K., and Fortin D. (2005) Adsorption of rare earth elements onto bacterial cell walls and its implication for REE sorption onto natural microbial mats. *Chem. Geol.* **219**, 53-67.
- Tang J. and Johannesson K. H. (2003) Speciation of rare earth elements in natural terrestrial waters: Assessing the role of dissolved organic matter from the modeling approach. *Geochim. Cosmochim. Acta* **67**, 2321-2339.
- Tanikazi Y., Shimokawa T., and Nakamura M. (1992) Physicochemical speciation of trace elements in river waters by size fractionation. *Environ. Sci. Technol.* **26**, 1433-1444.
- Taylor S. R. and McLennan S. M. (1985) The Continental Crust: Its composition and evolution, pp. 312. Blackwell.
- Thurman E. M. (1985) *Organic Geochemistry of Natural Waters*.
- Tipping E. (1994) WHAM - A chemical equilibrium model and computer code for waters, sediments, and soils incorporating a discrete site/electrostatic model of ion-binding by humic substances. *Comput. Geosci.* **20**, 973-1023.
- Tipping E. (1998) Humic Ion-Binding Model VI: an improved description of the interactions of protons and metal ions with humic substances. *Aquat. Geochem.* **4**, 3-48.
- Tipping E. and Hurley M. A. (1992) A unifying model of cation binding by humic substances. *Geochim. Cosmochim. Acta* **56**, 3627-3641.
- Tipping E., Rey-Castro C., Bryan S. E., and Hamilton-Taylor J. (2002) Al(III) and Fe(III) binding by humic substances in freshwaters, and implication for trace metal speciation. *Geochim. Cosmochim. Acta* **66**(18), 3211-3224.
- Tosiani T., Loubet M., Viers J., Valladon M., Tapia J., Marrero S., Yanes C., Ramirez A., and Dupré B. (2004) Major and trace elements in river-borne materials from the Cuyuni basin (southern Venezuela): evidence for organo-colloidal control on the dissolved load and element redistribution between the suspended and dissolved load. *Chem. Geol.* **211**, 305-334.

- Tricca A., Stille P., Steinmann M., Kiefel B., Samuel J., and Eikenberg J. (1999) Rare earth elements and Sr and Nd isotopic compositions of dissolved and suspended loads from small river systems in the Vosges mountains (France), the river Rhine and groundwater. *Chem. Geol.* **160**, 139-158.
- Unsworth E. R., Warnken K. W., Zhang H., Davison W., Black F., Buffle J., Cao J., Cleven R., Galceran J., Gunkel P., Kalis E., Kistler D., Van Leeuwen H. P., Martin M., Noël S., Nur Y., Odzak N., Puy J., Van Riemsdijk W., Sigg L., Temminghoff E., Tercier-Webber M.-L., Toepperwien S., Town R. M., Weng L., and Xue H. (2006) Model predictions of metal speciation in freshwaters compared to measurements by in situ techniques. *Environ. Sci. Technol.* **40**, 1942-1949.
- van Middlesworth P. E. and Wood S. A. (1998) The aqueous geochemistry of the rare earth elements and yttrium. Part 7. REE, Th and U contents in thermal springs associated with the Idaho batholith. *Appl. Geochem.* **13**, 861-884.
- Vermeer A. W. P., Van Riemsdijk W. H., and Koopal L. K. (1998) Adsorption of humic acid to mineral particles. 1. Specific and electrostatic interactions. *Langmuir* **14**, 2810-2819.
- Viers J., Dupré B., Polvé M., Schott J., Dandurand J.-L., and Braun J. J. (1997) Chemical weathering in the drainage basin of a tropical watershed (Nsimi-Zoetele site, Cameroon): comparison between organic-poor and organic-rich waters. *Chem. Geol.* **140**, 181-206.
- Wells M.L. and Goldberg E.D. (1991) Occurrence of small colloids in sea water. *Nature* **353**, 342-346.
- Wood S. A. (1990) The aqueous geochemistry of the rare-earth elements and yttrium. 1. Review of the available low-temperature data for inorganic complexes and inorganic REE speciation in natural waters. *Chem. Geol.* **82**, 159-186.
- Wood S. A. (1993) The aqueous geochemistry of the rare-earth elements: Critical stability constants for complexes with simple carboxylic acids at 25°C and 1 bar and their application to nuclear waste management. *Eng. Geol.* **34**, 229-259.
- Wright J., Schrader H., and Holser W. T. (1987) Paleoredox variations in ancient oceans recorded by rare earth elements in fossil apatite. *Geochim. Cosmochim. Acta* **51**, 631-644.
- Wu S. L. and Horrocks Jr. W. D. (1996) General method for the determination of stability constants of lanthanide ion chelates by ligand-ligand competition: laser-excited Eu³⁺ luminescence excitation spectroscopy. *Anal. Chem.* **68**, 394-401.
- Xue H. and Sigg L. (1993) Free cupric ion concentration and Cu(II) speciation in eutrophic lake. *Limnol. Oceanogr.* **38**, 1200-1213.
- Xue H., Kistler D., and Sigg L. (1995) Competition of copper and zinc for strong ligands in a eutrophic lake. *Limnol. Oceanogr.* **40**, 1142-1152.
- Yamamoto Y., Takahashi Y., and Shimizu H. (2005) Systematics of stability constants of fulvate complexes with rare earth ions. *Chem. Lett.* **34**, 880-881.
- Yan X.-P., Kerrich R., and Hendry M. J. (2001) Distribution of the rare earth elements in porewaters from a clay-rich aquitard sequence, Saskatchewan, Canada. *Chem. Geol.* **176**, 151-172.
- Yeghicheyan D., Carignan J., Valladon M., Bouhnik Le Coz M., Le Cornec F., Castrec-Rouelle M., Robert M., Aquilina L., Aubry E., Churlaud C., Dia A., Deberdt S., Dupré B., Freyrier R., Gruau G., Hénin O., de Kersabiec A.-M., Macé J., Marin L., Morin N., Petitjean P., and Serrat E. (2002) Compilation of silicon and thirty one trace elements measured in the natural river water reference material SLRS-4 (NRC-CNRC). *Geostand. Newslett.* **25**, 465-474.